# Nutritional Interactions in the Cnidarian-Dinoflagellate Symbiosis and their Role in Symbiosis Establishment

Ashley E. Sproles

A thesis submitted to
Victoria University of Wellington
in fulfilment of the requirements for the degree of
Doctor of Philosophy in Science

**Victoria University of Wellington**

**2017**

## Abstract

Mass bleaching events induced by climate change are threatening coral reef ecosystems worldwide. Elevated seawater temperatures cause breakdown of the coral's endosymbiotic relationship with dinoflagellate algae from the genus *Symbiodinium*. Corals rely on these symbionts for the majority of their metabolic carbon (provided by photosynthetic products) and for efficient nitrogen cycling in the reef ecosystem. Researchers have predicted that corals may potentially adapt to higher ocean temperatures according to the Adaptive Bleaching Hypothesis (ABH), which states that bleaching can facilitate a change in symbiont communities, allowing more thermally tolerant symbionts to become dominant. Hosting thermally tolerant symbionts thus grants the coral a higher resistance to bleaching. However, confidence in this adaptation method has wavered due to the nutritional impairments of hosts harbouring thermally tolerant symbionts under normal environmental conditions. It is also unknown if coral species that do not currently associate with thermally tolerant symbionts would be able to successfully switch their symbiont communities. Here, I explore the mechanisms driving nutritional exchange in the symbiosis and determine the effect of establishing a non-native (heterologous) association with a thermally tolerant symbiont. A combined approach of bioinformatic analysis with proteomic and isotopic labelling experiments is used to uncover a link between host-symbiont cellular integration, the potential for nutrient exchange, and the success of establishing a symbiosis.

In Chapter 2, I characterized membrane protein sequences discovered in publicly available cnidarian and *Symbiodinium* transcriptomes and genomes to identify potential transporters of sugars into cnidarian cells and nitrogen products into *Symbiodinium* cells. I examined the facilitated glucose transporters (GLUT), sodium/glucose cotransporters (SGLT), and aquaporin (AQP) channels in the cnidarian host as mechanisms for sugar uptake, and the ammonium and high-affinity nitrate transporters (AMT and NRT2, respectively) in the algal symbionts as mechanisms for nitrogen uptake. Homologous protein sequences were used for phylogenetic analysis and tertiary structure deductions. In cnidarians, I identified putative glucose transporters of the GLUT family and glycerol transporting AQP proteins, as well as sodium monocarboxylate transporters and sodium myo-inositol cotransporters homologous to SGLT proteins. I predict that cnidarians use GLUT proteins as the primary mechanism for glucose uptake, while glycerol moves into cells by passive diffusion. I also identified putative

AMT proteins in several *Symbiodinium* clades and putative NRT2 proteins only in a single clade. I further observed a high expression of putative AMT proteins in *Symbiodinium*, which may have resulted from adaptations to conditions experienced inside the host cell. This study is the first to identify transporter sequences from a diversity of cnidarian species and *Symbiodinium* clades.

The phylogenetic patterns seen in chapter 2 led to the hypothesis that symbiont types may have different influences on host-symbiont cellular integration. In chapter 3, I explored this notion using the model cnidarian *Aiptasia*. A population of anemones was rendered aposymbiotic using a menthol-bleaching method developed by my colleagues and I, and anemones then experimentally infected with either the native (homologous) symbiont (*Symbiodinium minutum*, clade B1) or a thermally tolerant heterologous symbiont (*Symbiodinium trenchii*, clade D1a). The response of the host proteome to these associations was examined by analysing the extracted host proteins with liquid chromatography-nano-electrospray-tandem mass spectrometry (LC-nano-ESI-MS/MS), and identifying resulting peptides against a cnidarian database. Proteins were compared between B1-colonised anemones, D1a-colonised anemones, and aposymbiotic anemones to determine which proteins were affected by the different treatments. Overall, I found that the response of D1a-colonised anemones mimicked that of aposymbiotic anemones to some degree, and showed signs of less efficient carbon and nitrogen pathways. Additionally, I discovered that the symbiosome protein NPC2 was upregulated only in B1-colonised anemones and could therefore be an important determinant of symbiont success.

I further investigated the apparent inadequacy of carbon and nitrogen pathways in hosts harbouring *Symbiodinium* D in chapter 4, using isotope labelling and sub-cellular imaging. Carbon and nitrogen fluxes between experimentally infected *Aiptasia* with both homologous (*Symbiodinium* B1) and heterologous (*Symbiodinium* D1a) symbionts were compared over multiple time points during symbiosis establishment. This was accomplished by incubating anemones in $^{13}C$- and $^{15}N$-labelled seawater to measure metabolite transfer to the host, and anemones were also fed $^{13}C$- and $^{15}N$-labelled *Artemia* to measure reverse translocation to the symbiont. Carbon and nitrogen enrichment in host tissues and symbiont cells were imaged using nanoscale secondary ion mass spectrometry (nanoSIMS). In both the earlier stages of

symbiosis establishment (2 days post-inoculation) and later stages of symbiont proliferation (14 days post-inoculation), *Symbiodinium* B1 reached significantly higher population densities (> 300%) than *Symbiodinium* D1a. Differences in symbiont nitrogen uptake from host tissues were detectable, however they were likely due to nitrogen limitation imposed by the comparatively high densities of the homologous symbiont. While *Symbiodinium* B1 cells maintained a high degree of carbon fixation throughout symbiosis establishment, less than 50% of *Symbiodinium* D1a cells were found to be fixing carbon in the later stages of establishment, despite still receiving substantial amounts of host-derived nitrogen. These findings support my previous prediction that *Symbiodinium* D1a affects the host's carbon and nitrogen pathways, acting as a less mutually beneficial symbiont.

Overall, my results provide new insights into the underlying factors determining the success of symbiotic interactions. The results indicate that cnidarian hosts and their dinoflagellate symbionts have adapted to the symbiotic life-style by cellular integration, thereby making compatibility of certain biological processes a key factor in determining symbiosis success. Furthermore, the findings presented here show how the potential for nutritional exchange may be linked to host-symbiont compatibility and hence specificity. This information is relevant when making predictions about which corals may successfully adapt to climate change *via* the ABH.

**Acknowledgements**

I owe much gratitude to the many brilliant scientists I have met during my life that have inspired me to continue pursuing academic research. I have incredible appreciation for my undergraduate professors from Florida Institute of Technology, Dr. Ralph Turingan, Dr. Richard Turner, and Dr. Rob van Woesik, who provided me with exceptional instruction during my undergraduate studies and motivated me to continue exploring the marine environment. Additionally, I thank Dr. Joshua Voss from Harbor Branch Oceanographic Institute for being a mentor during my first experience in coral reef research, and the entire Voss lab for their valued knowledge and friendship. I am also grateful to Dr. Clay Cook for sharing with me his infinite wisdom on the cnidarian-dinoflagellate symbiosis, and for encouraging me to participate in this project. Of course, this thesis would not have been possible without the help of my supervisor, Dr. Simon Davy, whom I thank for believing in me and providing me with much helpful advice and opportunities for academic collaboration. I would also like to thank my secondary supervisor, Dr. Clint Oakley, for his assistance with my proteomics work and perseverance with working out any technical difficulties we faced. A big thank you also goes out to the rest of the Davy lab members for providing a positive and intellectually stimulating work environment.

This research was possible thanks to the financial support of the Royal Society of New Zealand's Marsden Fund, and many thanks are also due to the VUW Faculty of Science for awarding me a Faculty Strategic Research Grant that allowed me to present my research at the 2016 International Coral Reef Symposium. I was lucky to be afforded collaborative research trips to Hawaii, Oregon, and Switzerland throughout my study, where those at the hosting institutions helped in making my research goals possible. Thank you to Nathan Kirk and Sheila Kitchen (Oregon State University) for teaching me bioinformatics and phylogenetics, Thomas Krueger and Anders Miebom (École Polytechnique Fédérale de Lausanne) for hosting me in their lab and allowing me to use the nanoSIMS, also thanks to Ruth Gates, Hollie Putnam, and the rest of the Gates lab (Hawaii Institute of Marine Biology) for their assistance with my field work in Hawaii, to Tina Carvalho (University of Hawaii at Manoa) for allowing me to book out the only bench space in the microscopy lab for an entire two weeks, and to St. John Wakefield and Jane Anderson (University of Otago) for allowing me the use of their facilities to process an excessive amount of samples in a very short time frame. Special

acknowledgements are also due for Arthur Grossman (The Carnegie Institute), for critiquing my work to the highest standards and providing excellent suggestions to my experimental designs, and for Virginia Weis (OSU), for acting almost as an additional supervisor by investing a considerable amount of time and effort into helping design, execute, and edit my work.

Throughout my time at Victoria University I have been lucky to acquire many friends that have provided valuable moral support. I would like to especially thank my fellow Davy lab member, Jennifer Matthews, for being an incredible friend and constant source of advice and support throughout the past four years. I would also like to thank Grace Paske, Emily McGrath, Megan Schaffer, Becky Focht, Steph Price, Kirsty Yule, Amanda Taylor, and Katie Hillyer for keeping me sane with many fun-filled evenings and adventures away from the lab.

I sincerely thank my parents, Karen and Bud, for teaching me to be ambitious in all my life endeavours and supporting me unconditionally throughout my academic journey. I also thank my brother, Dan, for graciously letting me attempt to claim the Dr. Sproles title before him. Lastly, many thanks to Josh for his willingness to move 8,000 miles away from our home country to support me during my studies, and for having much patience and sense of adventure along the way.

## List of Abbreviations

| | |
|---|---|
| **$^{13}C$** | Isotopically-labelled carbon |
| **$^{15}N$** | Isotopically-labelled nitrogen |
| **3D** | Three dimensional |
| **AA** | Amino acids |
| **AB** | Accumulation body |
| **ABC** | ATP-binding cassette |
| **ABH** | Adaptive bleaching hypothesis |
| **AMT** | Ammonium transporter |
| **ANOVA** | Analysis of Variance |
| **APC** | Acid-polyamine-organocation |
| **ATP** | Adenosine triphosphate |
| **AQP** | Aquaporin |
| **BHMT** | Betaine-Homocysteine S-Methyltransferase |
| **BLAST** | Basic local alignment search tool |
| **BSA** | Bovine serum albumin |
| **C** | Carbon |
| **CA** | Carbonic anhydrase |
| **CCM** | Carbon concentrating mechanism |
| **Chl** | Chloroplast |
| **CHT** | Choline transporter |
| **$CO_2$** | Carbon dioxide |
| **COACH** | Consensus approach |
| **CS** | Circumsporozoite |
| **CZAR** | Carbon contribution of algae to animal respiration |
| **DCMU** | 3-(3,4-dichlorophenyl)-1,1-dimethylurea |
| **df** | Degrees of freedom |
| **DIC** | Dissolved inorganic carbon |
| **DIN** | Dissolved inorganic nitrogen |
| **DMSO** | Dimethyl sulfoxide |
| **DNA** | Deoxyribonucleic acid |
| **EM** | Electron microscopy |

| | |
|---|---|
| **ER** | Endoplasmic reticulum |
| **FDR** | False discovery rate |
| **FSW** | Filtered seawater |
| **GLM** | Generalized linear model |
| **GLUT** | Facilitated glucose transporter |
| **GO** | Gene ontology |
| **G-protein** | Guanine nucleotide binding protein |
| **h** | Hour(s) |
| **$H_2O$** | Water |
| **HCl** | Hydrochloric acid |
| **$HCO_3^-$** | Bicarbonate ion |
| **HMIT** | Proton/*myo*-inositol cotransporter |
| **HPLC** | High performance liquid chromatography |
| **HRF** | Host release factors |
| **I-TASSER** | Iterative threading assembly refinement |
| **IRMS** | Isotope-ratio mass spectrometry |
| **ITS2** | Internal transcriber spacer 2 |
| **$K^{15}NO_3$** | Potassium nitrate |
| **LC-nano-ESI-MS/MS** | Liquid chromatography-nano electrospray-tandem mass spectrometry |
| **LD** | Lipid droplets |
| **MAFFT** | Multiple alignment using fast fourier transform |
| **Mep** | Methylammonium permease |
| **MFI** | Mean fluorescence index |
| **MFS** | Major facilitator superfamily |
| **min** | Minute(s) |
| **MS** | Mass spectrometry |
| **MS/MS** | Tandem mass spectrometry |
| **N** | Nitrogen |
| **$NaHCO_3$** | Sodium bicarbonate |
| **$NaNO_3$** | Sodium nitrate |
| **NanoSIMS** | Nanoscale secondary ion mass spectrometry |
| **NCBI** | National Center for Biotechnology Information |
| **NIP** | Nodulin-26-like proteins |

| | |
|---|---|
| **NMDS** | Non-metric multidimensional scaling |
| **NPC2** | Niemann-Pick type C |
| **NRT2** | High-affinity nitrate transporter 2 |
| **OCT** | Organic cation transporters |
| **$OsO_4$** | Osmium tetroxide |
| **P:R** | Ratio of maximum gross photosynthesis to respiration |
| **PCR** | Polymerase chain reaction |
| **$P_{gross}$** | Maximum gross photosynthesis |
| **PI** | Precursor intensity |
| **PPM** | Parts per million |
| **Pyr** | Pyrenoid |
| **qPCR** | Quantitative real-time PCR |
| **RNA** | Ribonucleic acid |
| **ROI** | Region of interest |
| **ROS** | Reactive oxygen species |
| **SGLT** | Sodium/glucose cotransporter |
| **SLC** | Solute carrier |
| **SMCT** | Sodium-coupled monocarboxylate transporters |
| **SMIT** | Sodium/*myo*-inositol cotransporter |
| **Symb** | Symbiosome |
| **TM** | Transmembrane |
| **TP1** | Time point 1 |
| **TP2** | Time point 2 |
| **UA** | Uric acid crystals |
| **UniProtKB** | UniProt knowledgebase |

## List of Figures

## List of Tables

## Table of Contents

# Chapter 1: General Introduction

## 1.1 Endosymbiosis as a Basis for Entire Ecosystems

Symbiosis is defined as the close interaction between different species living together over a long period of time (Freedman 2014). The term as we know it today was first coined in 1877 by German botanist Heinrich Anton de Bary, who observed that lichens were two organisms, a fungus and an alga, living essentially as one (cited in Sapp 2004). The remainder of the nineteenth century was a pinnacle of exploration into the complexities of symbiotic associations. In 1881, Karl Andreas Heinrich Brandt concluded from his observations, that photosynthetic pigments found in animals were due to symbiotic plant invaders within the animal cells (Krueger 2016). Nearly a century thereafter, 'The Endosymbiont Theory' was first formulated to describe the origin of all plant and animal cells. The theory postulated that chloroplasts and mitochondria originated from symbiotic prokaryotes which evolved into the fully integrated organelles of eukaryotes that we see today (Margulis 1971; Werner 1992).

Symbiotic interactions can take a variety of forms, which are described by the following three categories: (1) parasitism, where one partner benefits at a cost to the other; (2) commensalism, where neither partner benefits nor is harmed; and (3) mutualism, where both partners benefit from the relationship (Roossinck 2005). To date, numerous microorganisms have been described as endosymbionts that form complex mutualisms with plants and animals. These symbioses involve cellular integration of the symbiont into the host's cells, and can become the basis of entire ecosystems by facilitating nutrient cycling. For instance, legume plants harbour populations of nitrogen-fixing soil bacteria (rhizobia) within their root nodules that facilitate nitrogen-carbon exchange with the host (Werner 1992; Udvardi & Day 1997). Many plants outside the legume family also utilize nitrogen-fixing symbionts in various plant organelles (Santi *et al.* 2013). This mechanism is essential to many terrestrial ecosystems, since nitrogen is a limiting factor for plant growth and nitrogen gas cannot be fixed by plants alone (Santi *et al.* 2013). A range of marine invertebrates also forms ecologically significant endosymbioses. In particular, the relationship between sulphur-oxidizing chemoautotrophic bacteria and deep-sea marine invertebrates involves an exchange of nutrients that is so efficient the animals completely lack a mouth and gut (Cavanaugh 1994). Symbiotic associations with photosynthetic algae and bacteria are common among poriferans and cnidarians, primarily because the relationships allows these animals to adopt features which help them survive in

otherwise uninhabitable locations, and in particular nutrient-poor seas (Venn *et al.* 2008). Studies of the symbiosis between the freshwater Hydra and green alga *Chlorella* have discovered an intimate integration of host and symbiont metabolism that likely occurred as a result of co-evolution between the two partners (Muscatine 1965; Muscatine & Lenhoff 1965; Cook 1972; Kovačević *et al.* 2010). With functional similarities to the Hydra-*Chlorella* association is the most well-known and ecologically important marine symbiosis of all, is that between cnidarians and dinoflagellate algae of the genus *Symbiodinium*, which will be the focus of the research described here.

## 1.2 Cnidarian-Dinoflagellate Symbiosis

### *1.2.1 Structure of the cnidarian-dinoflagellate symbiosis*

The algal symbionts reside within the cnidarian host's gastrodermal cells, which can contain up to six cells each (Muscatine *et al.* 1998). Surrounding each algal cell is a multilayer series of membranes called the symbiosome membrane complex (Fig. 1.1; Wakefield et al. 2000; Wakefield and Kempf 2001). The complex consists of an outer, host-derived membrane that is formed by a phagosome undergoing early arrest (Palincsar *et al.* 1988; Rands *et al.* 1993; Mohamed *et al.* 2016), and multiple symbiont-derived inner layers (Taylor 1971; Trench & Winsor 1987). The inner membranes are thought to be sloughed-off layers of symbiont theca (Taylor 1968; Trench & Blank 1987; Schwarz *et al.* 1999; Wakefield *et al.* 2000; Wakefield & Kempf 2001). The symbiosome serves as the interface for all molecular exchanges between host and symbiont and is also key to avoiding host digestion of the algal cells (Fitt & Trench 1983; Barott *et al.* 2015). It is still unknown exactly how and when during symbiosis establishment the symbiosome is formed; however, a crucial component in symbiosome biogenesis might be the retention of certain membrane proteins which regulate membrane fusion with host endocytic vesicles, such as ApRab4 in the symbiont (Hong *et al.* 2009) and sym32 in the host (Reynolds *et al.* 2000; Schwarz & Weis 2003).

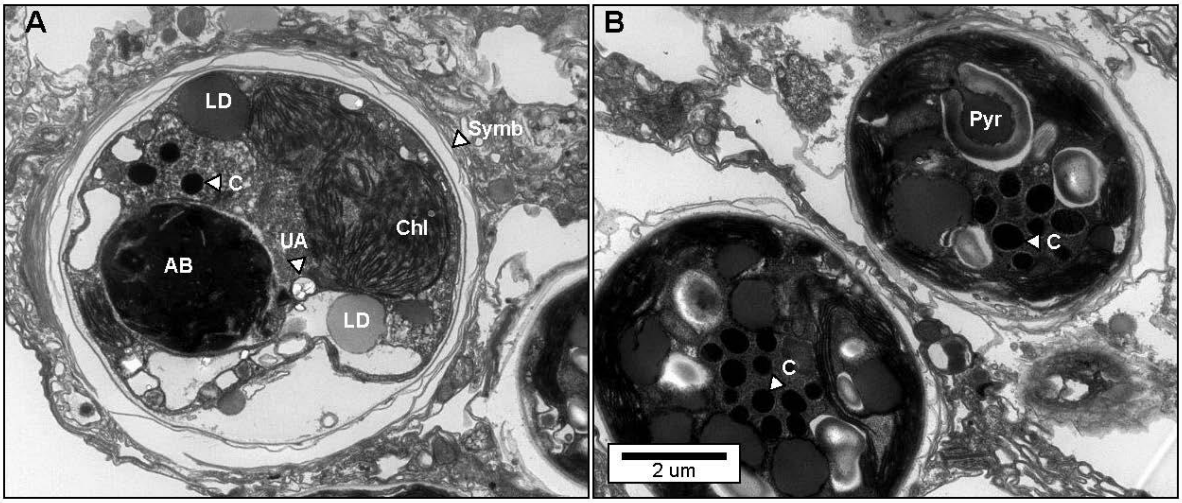


**Figure 1.1** Transmission electron micrographs of *Symbiodinium* cells within *Aiptasia* gastrodermal tissue. (A) *Symbiodinium* cell housed inside a multi-layered membrane complex (Symb, symbiosome), containing photosynthetic organelles (Chl, chloroplasts), a nucleus with chromosomes (C), lipid droplets (LD), uric acid crystals (UA), and an accumulation body (AB). (B) Detail of the *Symbiodinium* pyrenoid (Pyr), emerging from the chloroplast. Micrographs by A. Sproles.

*Symbiodinium* cells contain uric acid crystals (Fig. 1.1), which are produced as nitrogen stores that can be readily utilized when environmental conditions become nitrogen-depleted (Clode *et al.* 2009; Kopp *et al.* 2013). Cells also may contain a single-stalked pyrenoid capped by a starch granule emerging from the chloroplast, as well as lipid droplets and accumulation bodies (Fig. 1.1; Wakefield *et al.* 2000). Pyrenoids act as starch reserves in most algae, and may facilitate the distribution of photosynthetic products from the chloroplast to other organelles (Griffiths 1970). Lipid droplet formation in *Symbiodinium* is enhanced by environmental stressors such as elevated temperatures and nitrogen starvation (Jiang *et al.* 2014; Pasaribu *et al.* 2016), and is thought to play a key role in the exchange of compounds between partners (Kellogg & Patton 1983; Patton & Burris 1983; Pasaribu *et al.* 2014). Accumulation bodies are poorly understood, but most likely act similarly to lysosomes, in being a 'trash dump' for the cell (Taylor 1968; Wakefield *et al.* 2000). Interestingly, they are also enriched in the symbiosis-related protein Sym32, a cell adhesion protein (Schwarz & Weis 2003).

*1.2.2 Uptake, recognition, and regulation of symbionts*

Cnidarian hosts can obtain endosymbiotic *Symbiodinium* by either horizontal or vertical transmission. Horizontal transmission involves acquisition of symbionts from the surrounding environment, while vertical transmission involves the host parent passing symbionts to its offspring (Stat *et al.* 2006)). Species that use horizontal transmission have the benefit of potentially being able to form associations with a wide variety of symbiont types, while vertical transmission guarantees the host a symbiont that has already been selected for as successful in their species (Douglas 1998; Loh *et al.* 2001; Barneah *et al.* 2004). Most scleractinian coral species produce aposymbiotic larvae, requiring them to acquire symbionts *via* horizontal transmission (Babcock & Heyward 1986; Richmond & Hunter 1990; Abrego *et al.* 2009). Cnidarian larvae are only able to acquire symbionts from their environment once they have formed a mouth, and usually do so while feeding (Schwarz *et al.* 1999; Bucher *et al.* 2016). *Symbiodinium* cells are attracted to the cnidarians by chemical cues, such as ammonia, that are given off as they are feeding (Fitt 1984). In order to avoid digestion by the animal, a host-symbiont recognition phase must occur during initial contact of algal and host cells (Fig 1.2). *Symbiodinium* cells release species-specific glycoconjugates that act as a form of inter-partner signalling to the host (Markell *et al.* 1992; Markell & Trench 1993; Markell & Wood-Charlson 2010). Additionally, the algal cell walls are lined with an assemblage of glycoproteins that can serve as recognition factors during symbiosis establishment, by binding to lectins on the animal cells surface (Lin *et al.* 2000; Wood-Charlson *et al.* 2006; Wood-Charlson & Weis 2009; Logan *et al.* 2010; Neubauer *et al.* 2016). These glycan/lectin interactions are part of an innate immune response that, in vertebrates, is used to recognize and destroy pathogenic invaders (Mcguinness *et al.* 2003). The signalling pathways of this response may play a role in both recognition and maintenance of accepted symbionts (Poole *et al.* 2016; Bay *et al.* 2011). Certain genes have also been hypothesized to play a role in symbiont recognition, such as scavenger receptors, Sym32, carbonic anhydrase, and Niemann-Pick type C (NPC2) genes (Rodriguez-Lanetty *et al.* 2006; Ganot *et al.* 2011; Dani *et al.* 2014).

As algal cells make contact with the host, they are phagocytosed (Smith 1979; Fitt & Trench 1983). After the recognition and phagocytosis phases, sorting occurs as the host decides whether to reject or accept each newly acquired symbiont (Fig. 1.2). Although initial symbiont uptake in new coral recruits may be fairly unspecific, as larvae mature they begin to exhibit

more specificity for certain symbiont types (Weis *et al.* 2001; Little *et al.* 2004; Thornhill *et al.* 2006). During this sorting phase, rejected cells are destroyed *via* host cell apoptosis (programmed cell death; Dunn and Weis 2009), while the accepted cells proliferate within the host *via* cell division (Wilkerson *et al.* 1983, 1988).

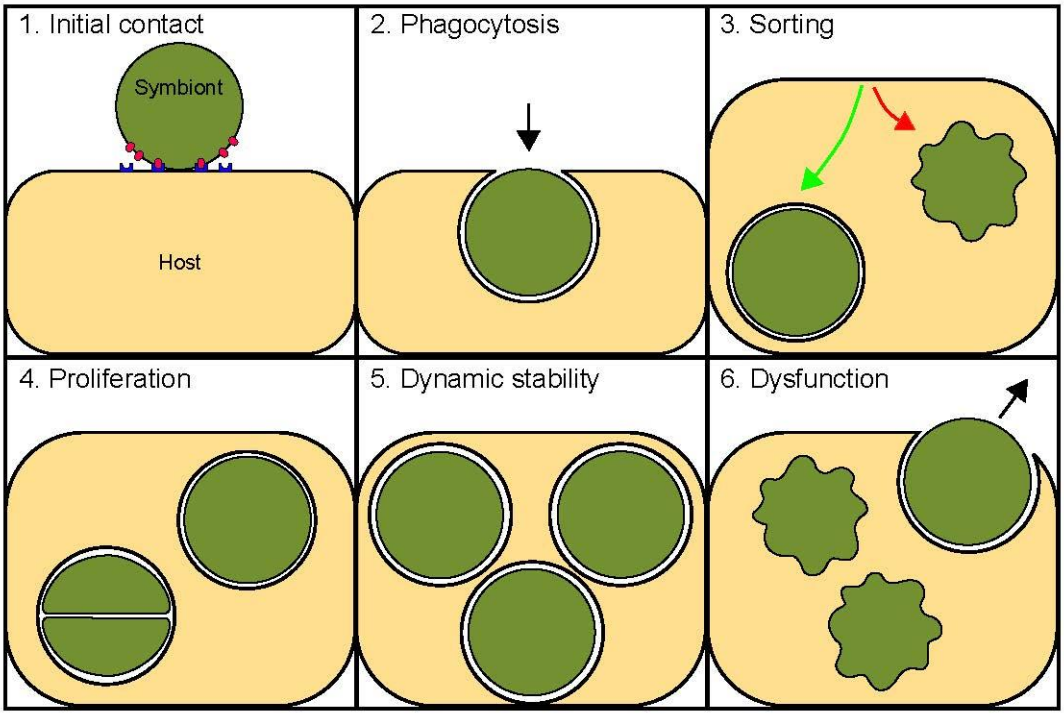


**Figure 1.2** The six phases of symbiosis establishment (according to description in Davy *et al.* 2012). 1) Initial contact between *Symbiodinium* and host cells, where recognition is facilitated by cell surface molecules from each partner. 2) Phagocytosis of algal cell by the host cell. 3) Sorting of algal cells into accepted symbionts (green arrow) to be housed in symbiosome membranes, and rejected cells (red arrow) which are removed via apoptosis, autophagy, or exocytosis. 4) Proliferation of symbiont population by cell division. 5) Dynamic stability of symbiont population. 6) Dysfunction of symbiont cells due to natural degradation or stress. Image credit: A. Sproles.

The accepted cells then transition into a haploid vegetative state and are stored in the host's endodermal cells (Davy & Turner 2003; Santos & Coffroth 2003). Regulatory mechanisms are enforced to keep symbiont density at a relatively constant level, achieving dynamic stability by balancing population numbers through nutrient limitation and removal of excess algae (Muscatine & Pool 1979; Jones & Yellowlees 1997; Koike *et al.* 2004). Symbiont proliferation is slowed while *in hospite* by controlling the amount of nutrient flux from the host (Miller & Yellowlees 1989; Leletkin 2000), or by reducing rates of cell division (reviewed in Davy et al. 2012). Surplus algae are removed through apoptosis, autophagy (digestion of cells), or exocytosis (expulsion of symbiont into environment) (Titlyanov *et al.* 1996; Dunn *et al.* 2004, 2007b; Ainsworth *et al.* 2007; Weis 2008; Paxton *et al.* 2013; Hawkins *et al.* 2013, 2014).

Inter-partner signalling pathways are also important to the regulation of symbiont populations (Rodriguez-Lanetty *et al.* 2006; Detournay & Weis 2011). In particular, the sphingosine rheostat pathway acts using a complement of two molecular signals: one that promotes apoptosis of the symbiotic cells and one that inhibits it, allowing control over symbiont population numbers (Detournay & Weis 2011). Another, called the transforming growth factor beta (TGFβ) pathway, also functions as part of the immune response to allow tolerance of the symbiont (Detournay *et al.* 2012). The last phase of symbiosis, dysfunction, is the breakdown of the association due to senescence (natural cell degradation) or stress (Sawyer & Muscatine 2001; Hanes & Kempf 2013; Tolleter *et al.* 2013; Dani *et al.* 2016), and involves removal of algal cells through one of the previously mentioned mechanisms.

## 1.3 Significance of Coral Reefs

### *1.3.1 Ecological importance*

The cnidarian-dinoflagellate symbiosis is widespread throughout the world's oceans, acting as a foundation for the construction of vast coral reef ecosystems (Fig. 1.3). Coral reefs serve as biodiversity hot spots in waters with very low nutrient availability and plankton abundance (Muscatine & Porter 1977). Additionally, they support a high diversity of marine fauna while providing a home for millions of endemic species and act as a nursery for many juvenile fish (Reaka-Kudla 1997; Knowlton 2001). The endosymbiotic algae are critical to the existence of the reef system, since they provide the animal with the majority of its required metabolic carbon (Lasker 1981; Muscatine *et al.* 1981; Richmond 1993). The algae are also proficient at nitrogen cycling, which allows reef systems to have such high productivity within oligotrophic waters (Suzuki *et al.* 1995). Nitrogen recycling occurs when nitrogenous products (ammonium and nitrate) are obtained by the algae from either host excretions or dissolved inorganic material in the seawater, and then used to assimilate amino acids, some of which are translocated back to the host (Wang & Douglas 1999; Tanaka *et al.* 2006; O'Neil & Capone 2008). However, the assimilated amino acids are also used for the algae's own cellular processes with sometimes only small amounts of nitrogen products being returned to the host

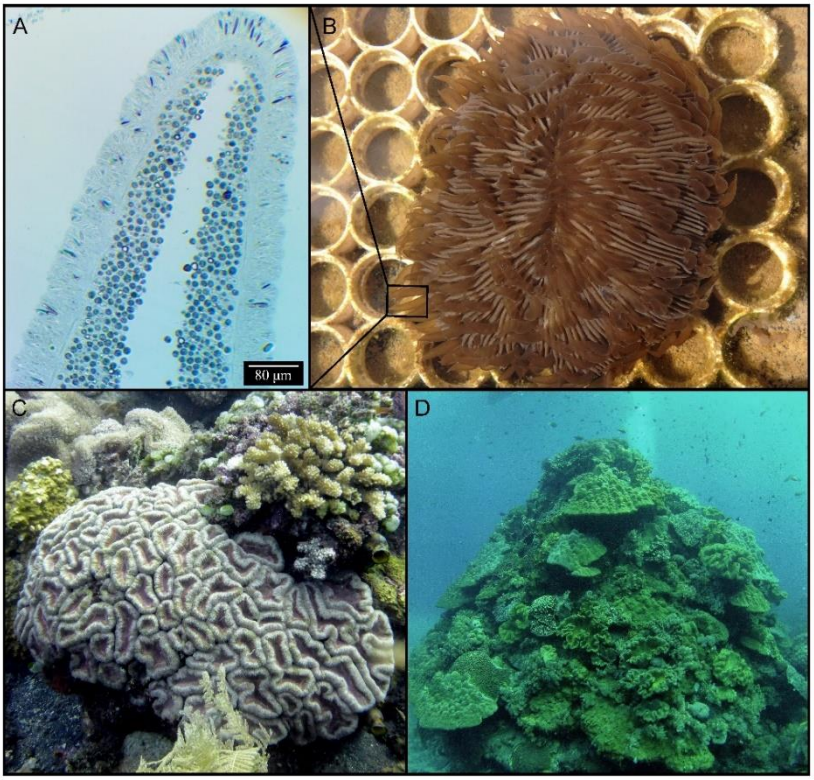


**Figure 1.3** The cnidarian-dinoflagellate symbiosis supports coral reef ecosystems. (A) Histological section of a cnidarian tentacle showing Symbiodinium cells within host gastrodermal tissue (20x mag). (B) Detail of tentacles on the mushroom coral *Fungia scutaria*. (C) Individual coral colonies of different morphologies. (D) Coral reef with high coral diversity in Bali, Indonesia. Micrographs and photographs by A. Sproles.

(Wang & Douglas 1998; Lipschultz & Cook 2002). Photosynthetic products transferred to the host also enhance coral calcification rates (Colombo-Pallotta *et al.* 2010; Holcomb *et al.* 2014; Bertucci *et al.* 2015), which aids in building the reef. The complex reef structure is thereby able to act as a safe haven against turbulent waters and predation for millions of marine fauna (Pearse & Muscatine 1971).

Unfortunately, coral reefs worldwide are threatened by climate change. Incidents of bleaching have been increasing dramatically since the 1980s, and are causing degradation of many of the world's coral reefs ecosystems (Hoegh-Guldberg 1999). In most cases, bleaching (i.e. the loss of the symbiotic algae and/or their photosynthetic pigments) causes mortality of the coral unless it is able to quickly re-establish its symbiont population (Jokiel 2004). Current predictions show that reefs across the globe are amidst the longest bleaching event on record (2014 – present) with extended summer-like temperatures each season that are expected to continue (Heron *et al.* 2016).

## 1.4 Symbiont Diversity and Specificity

### *1.4.1 Genetic diversity within Symbiodinium*

The species *Symbiodinium microadriaticum* was first described in 1962 to describe the symbionts of the jellyfish *Cassiopeia* sp. (Freudenthal 1962). This was thought to be the only member of this genus until Trench and Blank (1987) introduced three new species: *S. goreauii* from a sea anemone, *S. kawagutii* from a coral, and *S. pilosum* from a zoanthid. Later researchers began to use molecular techniques to examine the DNA of the small ribosomal subunit of *Symbiodinium* within reef corals. This revealed large genetic diversity within the species, and further physiological differences between genotypes led to suggestions that many more species might be present (Rowan & Powers 1991). Six additional *Symbiodinium* species were then identified from a bivalve, corals, and sea anemones (McNally 1994; Trench 1997). As diversity studies continued to use ribosomal subunit DNA, genetically distinct clades of *Symbiodinium* were designated as A, B, C, and D (Carlos *et al.* 1999). Further developments came with the discovery that the ribosomal internal transcribed spacer (ITS) regions from *Symbiodinium* could be used as a marker since it had a better molecular resolution than previous techniques (LaJeunesse 2001; Rodriguez-Lanetty 2003). This, coupled with other methods such as denaturing gradient gel electrophoresis (DGGE), allowed further classification into

sub-clades or ‘types’ (e.g. A3, B1, D1a) to better reflect the physiological and ecological differences within each clade (van Oppen *et al.* 2001; LaJeunesse & T. 2002; LaJeunesse *et al.* 2004; Sampayo *et al.* 2009; Finney *et al.* 2010). Currently, around 70 different types within nine divergent clades (A-I) and 22 species of *Symbiodinium* have been described, although about half of these clades (F-I) associate primarily with foraminiferans rather than metazoans, or are free-living (LaJeunesse 2001; Stat *et al.* 2006; Pochon & Gates 2010; LaJeunesse *et al.* 2012; Jeong *et al.* 2014; Hume *et al.* 2015; LaJeunesse *et al.* 2015; Lee *et al.* 2015).

Physiology and tolerance to environmental stress vary widely between different types of *Symbiodinium*. Some, such as those from clade A and clade D, are more tolerant to thermal stress and therefore relay a higher resistance of bleaching to the host (Thornhill *et al.* 2006; Loram *et al.* 2007; LaJeunesse *et al.* 2009; Stat & Gates 2011; Ladner *et al.* 2012; Barshis *et al.* 2014; Lee *et al.* 2015). Some *Symbiodinium* types have evolved tolerances of, are oxidative stress in some members of clade C (Hawkins & Davy 2012), cold stress in some clade B types (Thornhill *et al.* 2008), and high light stress in some clade A and D types (Reynolds *et al.* 2008; Hennige *et al.* 2008; Yuyama *et al.* 2016). Attributes like respiration rate, photosynthetic efficiency and production, and nitrogen assimilation can also differ between symbiont types (Baker *et al.* 2013; Starzak *et al.* 2014; Hawkins *et al.* 2016; McIlroy *et al.* 2016). The large genetic and functional diversity of cnidarian symbionts is now clearer, thanks to the constant development of new identification techniques. Further study of functional differences within *Symbiodinium* will allow more accurate predictions of how coral reefs might respond to the stressors of climate change.

### *1.4.2 Host-symbiont specificity*

Host-symbiont specificity is defined as a clearly non-random pattern of association where the ratio of observed host-symbiont combinations compared with the range of possible combinations is very small (Baker 2003). An early hypothesis as to why specificity occurs was posed by Trench (1997), who concluded that specificity was likely due to the co-adaptation of the host and symbiont to environmental conditions. Early experiments on infectivity of aposymbiotic (i.e. lacking symbionts) hosts with different algal strains observed these non-random patterns of symbiont uptake in gorgonians and sea anemones (Kinzie 1974; Kinzie & Chee 1979), followed by the finding of different algal cell surface antigens (Kinzie & Chee

1982). It is now known that metazoans possess lectins with a glycan-binding function (as explained in section 1.2.2), which is known to be used in cell-cell adhesion and recognition (Wood-Charlson & Weis 2009; Logan *et al.* 2010). Experiments show that some cnidarian lectins have a specificity for binding mannose (Vidal-Dupiol *et al.* 2009) and galactose side-chains (Koike *et al.* 2004), the latter of which were also found to be present on the cell surface of the symbionts (Fig 1.3). This suggests that glycan-lectin binding may be a major determinant of host-symbiont specificity (Bay *et al.* 2011).

Molecular approaches have revealed patterns of host-symbiont specificity in nature, where hosts exhibit strong selectivity for some symbiont types over others (van Oppen *et al.* 2001; Santos *et al.* 2003; LaJeunesse *et al.* 2004; Stat *et al.* 2009; Mieog *et al.* 2009; Abrego *et al.* 2009; Xiang *et al.* 2013). Usually, this entails a symbiont assemblage of one dominant type existing with one or more 'background' symbiont type(s) that exist in only low population densities (Héloïse *et al.* 2017; Ziegler *et al.* 2017). Experimental methods have found heterologous (i.e. non-native) algae to infect hosts less successfully than homologous (i.e. native) algal types (Weis *et al.* 2001; Belda-Baillie *et al.* 2002; Dunn & Weis 2009; Starzak *et al.* 2014), illustrating the specificity for some symbionts over others. However, over longer periods of time, heterologous algal types may be able to establish long-term associations with host corals, as demonstrated by the invasion of clade D *Symbiodinium* in Caribbean corals (Pettay *et al.* 2015), and a newly discovered association of clade B *Symbiodinium* in corals from French Polynesia (Héloïse *et al.* 2017). Specificity may also be caused by symbiont transmission method, since horizontal transmission allows more interactions with generalist algae (Fabina *et al.* 2012), or host depth (Frade *et al.* 2008) due to the fact that some types may be more or less sensitive to light. Quality of metabolic exchange and energetic costs for the host could also be an underlying factor that contributes to specificity (Cooper *et al.* 2011; Starzak *et al.* 2014), but this has been rarely studied at the cellular level.

*1.4.3 Thermally tolerant symbionts as a mechanism of adaptation*

Although many cnidarians have high specificity for one symbiont type (Santos *et al.* 2004; Thornhill *et al.* 2009), many have the advantage of being able to harbour multiple algal types (Baker 2003; Silverstein *et al.* 2012). This feature can prove essential during times of stress when changing symbiont population composition allows the more tolerant algae to become dominant (Jones *et al.* 2008; Abrego & Ulstrup 2008; LaJeunesse *et al.* 2009, 2010; Thomas *et al.* 2014). This phenomenon has been defined as the Adaptive Bleaching Hypothesis (Fig. 1.4), which proposes that bleaching provides the opportunity for the host to be repopulated with a different symbiont assemblage (Buddemeier & Fautin 1993; Fautin & Buddemeier 2004). Baker (2003) has described the two methods of symbiont community change that may arise after such an event as: 'symbiont shuffling', a quantitative change in the relative abundance of existing symbiont communities within colonies (Fig. 1.4A); and 'symbiont switching', a qualitative change by recombination with symbionts acquired from the environment (Fig. 1.4B). Symbiont shuffling occurs in many instances after bleaching events, often with symbionts from clade D becoming dominant (LaJeunesse *et al.* 2009; Kemp *et al.* 2014). Algae from *Symbiodinium* clade D (primarily *Symbiodinium trenchii*, type D1a) act as opportunists by existing as background symbionts until the dominant population is removed by thermally-induced bleaching, at which point clade D symbionts proliferate to high densities that increase coral survival (Stat & Gates 2011; Kemp *et al.* 2014; Bay *et al.* 2016). The ability to successfully function under thermal stress, and its identity as a host-generalist, make D1a an ideal candidate for coral adaptation through symbiont shuffling (Berkelmans & van Oppen 2006; LaJeunesse *et al.* 2014). It has been questioned whether symbiont switching is possible, considering that observations of this phenomenon in the field are rare. Nevertheless, switching

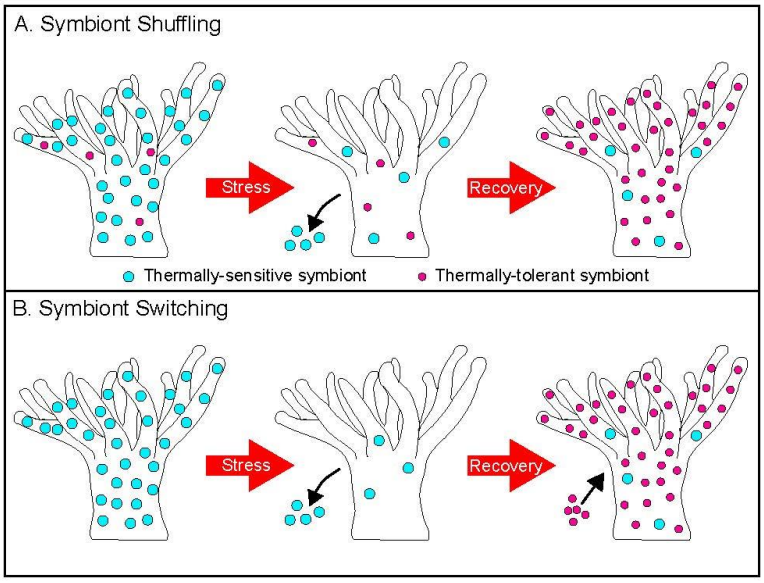


**Figure 1.4** Depiction of the two methods of symbiont community change (as described by Baker *et al.* (2003) under the adaptive bleaching hypothesis. (A) Symbiont shuffling, a quantitative change in existing symbiont communities. (B) Symbiont switching, a qualitative change by recombination with symbionts acquired from the environment. Image credit: A. Sproles.

to a clade D symbiont has been demonstrated experimentally (Boulotte *et al.* 2016), illustrating that it is fundamentally possible. However, the overall potential for clade D symbionts is hindered by their sub-optimal functioning under normal environmental conditions (Little *et al.* 2004; Jones & Berkelmans 2011; Baker *et al.* 2013; Pernice *et al.* 2014), and the potential combined effects of other environmental factors induced by climate change (Hoadley *et al.* 2016).

## 1.5 Metabolite Exchange between Partners

### *1.5.1 Translocation of photosynthetic products*

One of the most widely studied aspects of cnidarian-dinoflagellate symbiosis is the nutrient exchange between symbiont and host. The algal endosymbionts capture light to produce fixed carbon *via* photosynthesis, of which up to 99% is translocated to the host in the form of essential sugars, lipids, amino acids, and glycoproteins (Muscatine & Cernichiari 1969; Davies 1984; Muscatine 1984; Davy *et al.* 2012). The photosynthate can satisfy from 50-100% of the host's daily carbon requirements for respiration, growth, and maintenance (Muscatine *et al.* 1981; Edmunds and Davies 1986; Davies 1991), depending on the light regime and species concerned. (Falkowski *et al.* 1984; Davies 1991). Early studies on photosynthate transport to the host focused on glycerol, as it was thought to be incorporated into cnidarian lipid pools or used as metabolic fuel (Muscatine 1967; Schmitz & Kremer 1977; Hofmann & Kremer 1981; Battey & Patton 1984; Colombo-Pallotta *et al.* 2010). It is now known that glycerol is exuded as a stress response from *Symbiodinium* cells, and also may be translocated to the host as a minor metabolite (Lewis & Smith 1971; Whitehead & Douglas 2003; Burriesci *et al.* 2012; Suescun-Bolivar *et al.* 2016). Fixed carbon for animal metabolism is now primarily thought to be translocated to the host in the form of glucose (Muscatine *et al.* 1967; Ishikura *et al.* 1999; Burriesci *et al.* 2012; Hillyer *et al.* 2016). Lipids are also translocated from the symbiont to host, as storage molecules like wax esters and triacylglycerol, and as sterols and fatty acids such as palmitic, stearic, and oleic acid (von Holt & von Holt 1968a; Yamashiro *et al.* 1999; Hillyer *et al.* 2016). Fatty acids and phospholipids may also have a role in the recognition, proliferation, and overall success of symbiotic associations, since inhibition of these compounds impairs symbiont infection rates (Wang *et al.* 2013b). Additional products released by the symbiont are organic acids (von Holt & von Holt 1968a; b, Trench 1971a; b; Whitehead

& Douglas 2003), glycolic acid (Cernichiari *et al.* 1969), and amino acids (von Holt & von Holt 1968a; b; Lewis & Smith 1971). Overall, translocation of fixed carbon is the central feature of the symbiosis, as it is incorporated into all host tissues (Tremblay *et al.* 2012; Kopp *et al.* 2015; Freeman *et al.* 2016). The potential for carbon translocation could be an underlying cause of symbiont selectivity, since some *Symbiodinium* types do not translocate as much carbon to hosts as others (Starzak *et al.* 2014; Pernice *et al.* 2014).

### *1.5.2 Reverse translocation*

The reverse translocation of inorganic and organic compounds from within the host's gastrodermal cells provides essential nutrients to the symbionts. The symbionts utilize $CO_2$ derived from host respiration as well as dissolved inorganic carbon (DIC) from the seawater, transported in the form of bicarbonate ions through the host epithelial cells (Allemand *et al.* 1998). Inorganic carbon is necessary for both algal photosynthesis and host calcification, therefore carbonic anhydrase proteins are essential as they work in the carbon-concentrating mechanism of the symbiosis to catalyse the absorption of carbon for these processes (Furla *et al.* 2000; Bertucci *et al.* 2013; Barott *et al.* 2015). Two of the other major nutrients that the algae require are phosphorus and nitrogen, both of which are known to be essential macronutrients for all organisms (Cook *et al.* 1988). Phosphate uptake for symbiont nutrition has been demonstrated both in the dark (Cates & McLaughlin 1979; Deane & O'Brien 1981) and in the light, where it is said to be enhanced by photosynthesis (Jackson & Yellowlees 1990). Nitrogen may be obtained by the algal symbionts from several sources: nitrogen fixed by bacterial colonies within the holobiont (Lesser *et al.* 2007; Freeman *et al.* 2016), dissolved inorganic nitrogen from the seawater (O'Neil & Capone 2008; Kopp *et al.* 2013, 2015), or nitrogen excreted by the host as waste from heterotrophic feeding on zooplankton (Porter 1974; Steen 1986; Anthony & Fabricius 2000; Houlbrèque *et al.* 2004). Nitrogenous compounds from these sources are taken up by the symbiont in the forms of both ammonium (Muller-Parker *et al.* 1994; Pernice *et al.* 2012) and nitrate (D'Elia *et al.* 1983; Miller & Yellowlees 1989; Grover *et al.* 2003). The symbiont uses these compounds for amino acid assimilation, some of which are used for building algal proteins, and others are recycled back to the host (Lewis & Smith 1971; Tanaka *et al.* 2006). Additionally, host-derived fatty acids, lipids, and the amino acid glycine are translocated to the symbionts (von Holt 1968; Wang & Douglas 1999; Imbs *et al.* 2014).

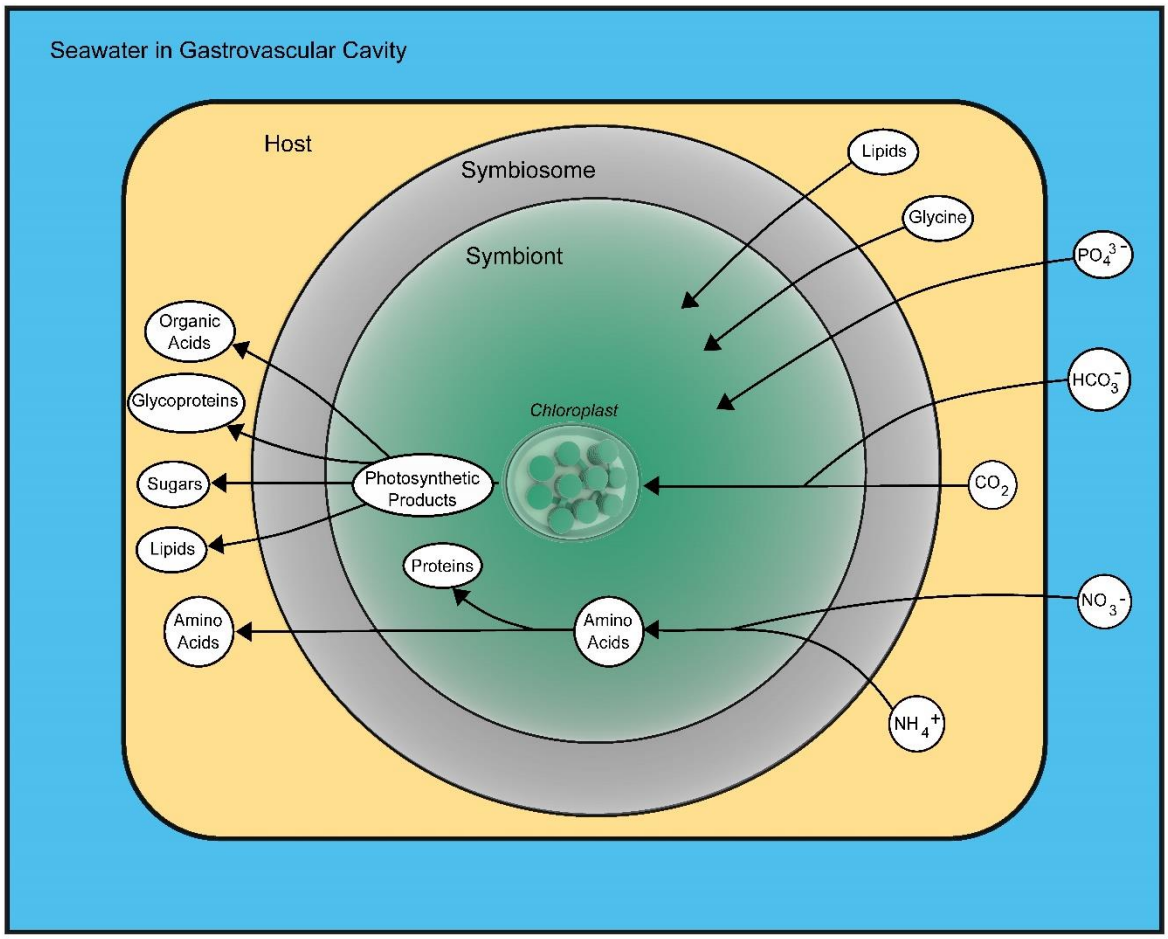


**Figure 1.5** Summary of intercellular metabolite exchange within cnidarian-dinoflagellate associations. Phosphate, bicarbonate, and nitrate ions are acquired from the seawater and passed through the host cells, then through the symbiosome membrane for utilization by *Symbiodinium* cells. Host-derived carbon dioxide, ammonium, lipids, and glycine are also translocated to the symbiont. The symbiont uses the carbon and nitrogen compounds to photosynthesize and assimilate amino acids, respectively. Photosynthetic products and amino acids are then translocated to the host. Image credit: A. Sproles.

Modern technology may hold the key to deeper understanding of nutritional transport between cnidarians and *Symbiodinium*. Nanoscale secondary ion mass spectrometry (nanoSIMS) has been successfully used to quantify and localize carbon and nitrogen pools within coral and symbiont cells using $^{13}C$ and $^{15}N$ isotope tracers (Clode *et al.* 2007; Pernice *et al.* 2012; Kopp *et al.* 2013, 2015). This technique has been applied to measure carbon and nitrogen exchange between a coral that can harbour two different symbiont types, finding that those from clade C were able to fix and pass more carbon to the host than those from clade D (Pernice et al. 2014). So far the studies have mainly focused on nitrogen assimilation and are only just starting to include carbon fixation and the differences in translocation between symbiont types (Clode *et al.* 2007; Pernice *et al.* 2012, 2014, Kopp *et al.* 2013, 2014). However, characterization of

nutritional fluxes between different host-symbiont pairs during symbiosis establishment could uncover more details about the mechanisms that underlie host-symbiont specificity.

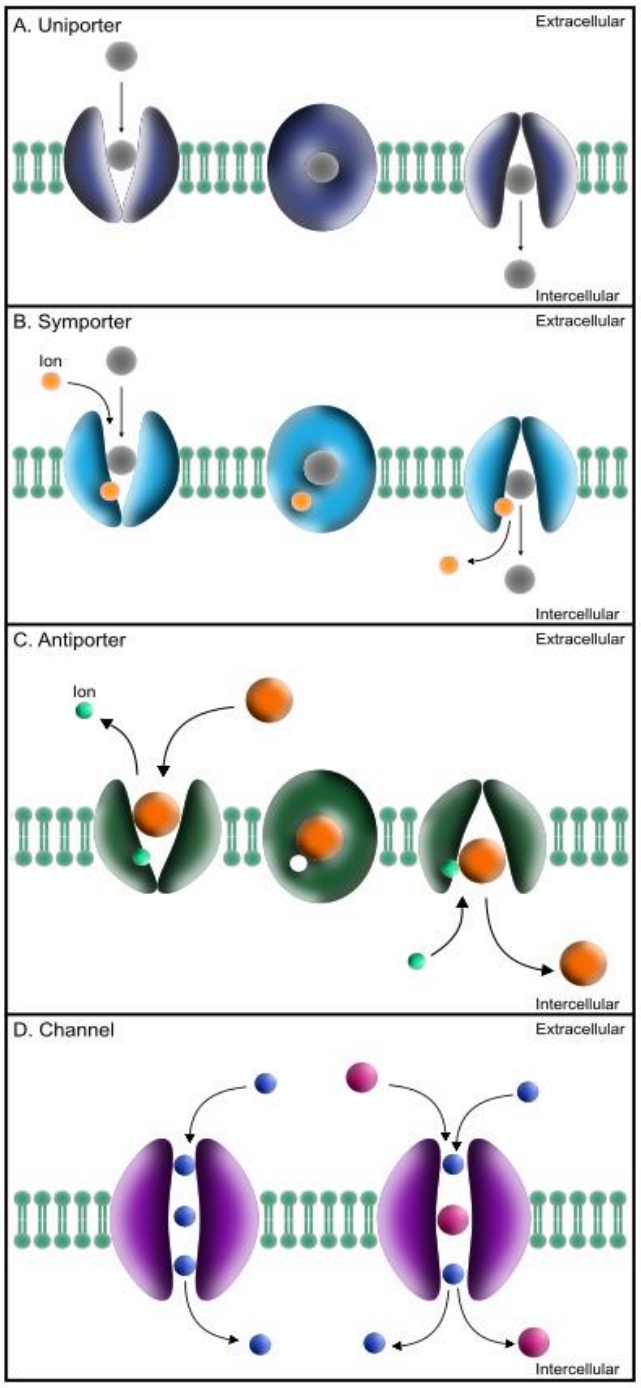


**Figure 1.6** Functional diagrams of secondary active transport proteins (A-C) and channel proteins (D). A) Uniporter, a solute is transported along its concentration gradient. B) Symporter, a solute is transported against its concentration gradient with an ion along its concentration gradient. C) Antiporter, a solute and an ion are transported along their concentration gradients together. D) Channel, solutes flow passively along their concentration gradient. Image credit: A. Sproles

### *1.5.3 Mechanisms of inter-partner transport*

The exact mechanisms of transport between host and symbiont are still not entirely known, however exchanged molecules would certainly need to traverse the symbiosome membrane (Fig. 1.5). While little is known about the identity of symbiosome transporters, predictions can be made based on information from related systems and overall cell biology. Passive diffusion is only able to account for a small percentage of membrane transport, with polar molecules such as amino acids and carbohydrates unable to pass through the cell membrane without facilitation by active transporter proteins (Vander Heiden *et al.* 2009). For example, only about 15% of DIC necessary for symbiont photosynthesis can be obtained by cellular diffusion, meaning that carbon is likely transported actively by either bicarbonate and $CO_2$ pumps, or symport and antiport mechanisms (Allemand *et al.* 1998). Almost all of the metabolites described in section 1.5.1-1.5.2 can be transported across the plasma membrane by either secondary active transporters in the major facilitator superfamily (MFS) or passively

through channel proteins (Fig 1.6). The MFS are secondary carriers that occur ubiquitously throughout life and transport small molecules using energy from a chemiosmotic ion gradient (Pao *et al.* 1998); it is the largest superfamily of secondary active transporters, encompassing 29 protein families that transport sugars, drugs, organophosphates, Krebs cycle intermediates, inorganic anions (such as nitrate/nitrite, phosphate, and cyanate), nucleosides, and monocarboxylic acids (Saier *et al.* 1999). Each protein family in the MFS has individually defined motifs, but they all share one highly conserved five-residue motif and thirteen-residue motif characteristic for MFS transporters (Pao *et al.* 1998). The structure of MFS proteins is the same regardless of whether they are a symporter, uniporter, or antiporter: 12 transmembrane α-helices (TMs) joined by hydrophilic loops with both the N and C terminus inside the cytoplasm (Law *et al.* 2008). Other transporter families that could possibly be involved in nutrient transport include: outer membrane porins (channels that non-selectively allow passage of solutes; Fig. 1.6), ABC transporters, ligand-gated ion channels, amino acid-polyamine-choline transporters, and the ATPases P type, F type, V type, and A type; however, transporters from these families are much less diverse and abundant than those from the MFS superfamilies (Saier 1994). Nutrient transporters are highly conserved macromolecules throughout all domains of life, so the known proteins within these families could very likely have orthologous counterparts within the cnidarian-dinoflagellate symbiosis.

## 1.6 "Omics" Investigations of Nutritional Transport

### *1.6.1 Transcriptomics and genomics*

With publicly available transcriptome and genome sequences for both partners, the potential for bioinformatics as an effective tool for elucidating proteins involved in these symbiotic associations has never been greater. There are currently 29 cnidarian transcriptomes and four genomes available, including those of *Aiptasia* (Lehnert *et al.* 2012; Baumgarten *et al.* 2015). In addition, there are at least nine transcriptomes and three genomes available for different *Symbiodinium* types (Appendix A, Table A1). Reviewed transporter protein sequences are also freely available through NCBI, UniProtKB, and various other databases, providing opportunities for investigative searches of interesting proteins within these genetic resources. Identification of C-type lectins within the cnidarian *Nematostella* was accomplished using the genomic database, which greatly influenced information on cell-surface recognition

mechanisms (Wood-Charlson & Weis 2009). Additionally, sequences from symbiotic *vs*. aposymbiotic samples of the same cnidarian species have been compared in order to successfully detect changes due to symbiosis. Interestingly, while few transcriptional changes happen in larvae newly engaged in symbiosis (Yuyama *et al.* 2005; Deboer *et al.* 2007; Voolstra *et al.* 2009), many genes are up-regulated – including several that encode for transporters of glucose, fatty acids, sterols, amino acids, ammonium, carbonic-anhydrase, phosphate, sulphate, and zinc – in adult symbiotic anemones compared with aposymbiotic counterparts (Rodriguez-Lanetty *et al.* 2006; Lehnert *et al.* 2014). This method has also allowed identification of genes involved in light-enhanced calcification (Bertucci *et al.* 2015) and symbiont selectivity (Wolfowicz *et al.* 2016). Transcriptomic studies have also been used to identify evolving proteins (Voolstra *et al.* 2011; Kitchen *et al.* 2015; Bellis *et al.* 2016), such as those that are linked to thermal sensitivity in corals and their symbionts (Barshis *et al.* 2014; Howells *et al.* 2016; Levin *et al.* 2016). Additionally, these resources have helped to detect conserved genes and metabolic pathways in *Symbiodinium*, and describe genetically unique areas between the clades (Rosic *et al.* 2014), as well as identify symbiont proteins involved in nutrient uptake (Leggat *et al.* 2007; Aranda *et al.* 2016). Bioinformatics has the potential to detect membrane transport proteins that exchange metabolites between different host-symbiont pairs, yet a comprehensive analysis of this kind has not yet been done.

### *1.6.2 Identification of symbiosis-associated proteins*

Although identification of genes involved in the symbiosis provides useful information, it is important to use this alongside proteomic analysis in the laboratory to yield the most conclusive results. Previous methods to assess symbiosis-associated proteins have used 2D gel electrophoresis (Weis & Levine 1996), but recent techniques allow for more specific protein identification. Liquid chromatography tandem mass spectrometry (LC-MS/MS) is able to analyse cnidarian peptides that are identified using databases generated from cnidarian and *Symbiodinium* genetic resources (Peng *et al.* 2010; Oakley *et al.* 2016). Immunocytochemistry can then be used to localize proteins to tissues within the symbiotic association (Yuyama & Watanabe 2008; Dani *et al.* 2014; Barott *et al.* 2015). These techniques have led to discovery of a few likely symbiosome membrane proteins (Peng *et al.* 2010; Dani *et al.* 2014; Barott *et al.* 2015), proteins associated with coral disease (Garcia *et al.* 2016), and a full characterization of the proteomic changes in *Aiptasia* that take place in response to establishment of symbiosis

(Oakley *et al.* 2016). Finding these proteins has allowed better predictions of the cellular processes at work during these interactions. For instance, these results have revealed the sterol-transporting NPC2 protein to be of potential significance in the cnidarian-dinoflagellate symbiosis, as it is upregulated in symbiotic anemones and is localized to symbiosome membranes (Dani *et al.* 2014; Oakley *et al.* 2016). Another finding shows that an ion pump (vacuolar $H^+$-ATPase) is located in the symbiosome and helps to acidify the algal environment (Barott *et al.* 2015). Many other functional implications can be drawn from the few studies that have successfully executed proteomic identifications in the cnidarian-dinoflagellate symbiosis, and continuation of this type of work will hopefully be able to uncover some of the mysteries that still persist in the field.

### *1.6.3* Aiptasia *as a model organism*

The sea anemone *Aiptasia* sp. ( = *ExAiptasia*) has become a globally-adopted, tractable model for studies of the cnidarian-*Symbiodinium* symbiosis, as it is easily kept under laboratory conditions and can be experimentally bleached and re-infected with different strains of *Symbiodinium* (Belda-Baillie *et al.* 2002; Xiang *et al.* 2013; Starzak *et al.* 2014; Hambleton *et al.* 2014; Matthews *et al.* 2016). Access to this model cnidarian overcomes some of the difficulties of working with live corals, and allows more in-depth investigations of the processes behind symbiosis establishment and persistence. Like many corals, *Aiptasia* produces non-symbiotic larvae that acquire symbionts from their environment, and undergo the same phases of symbiosis establishment described above (Bucher *et al.* 2016). In fact, the sea anemone has the same symbiont selection patterns during the larval stage as two different *Acropora* coral species (Wolfowicz *et al.* 2016). The genome of *Aiptasia* has been assembled along with the transcriptomes of the anemone in symbiotic and aposymbiotic states (Lehnert *et al.* 2014; Baumgarten *et al.* 2015), leaving great potential for bioinformatics-based studies. So far, the sea anemone has provided an ideal model system for examining gene expression (Kuo *et al.* 2004; Dunn *et al.* 2007a; Lehnert *et al.* 2014), bleaching mechanisms (Sawyer & Muscatine 2001; Hanes & Kempf 2013; Fransolet *et al.* 2013; Paxton *et al.* 2013; Bieri *et al.* 2016), carbon and nitrogen metabolism (Swanson *et al.* 1998; Smith *et al.* 2004; Clode *et al.* 2009; Dunn *et al.* 2012; Hillyer *et al.* 2016), protein expression (Oakley *et al.* 2016), symbiont selectivity (Hambleton *et al.* 2014; Bellis *et al.* 2016; Wolfowicz *et al.* 2016), ocean acidification (Gibbin & Davy 2014), bacterial associations (Palincsar *et al.* 1989; Röthig *et al.*

2016), and immune pathways (Hawkins *et al.* 2013; Poole *et al.* 2016) in the cnidarian-dinoflagellate symbiosis, although this list is not exhaustive. The usage of *Aiptasia* allows the biological systems within coral reefs to be examined without having to compromise any corals themselves, making it a valuable research tool in the field of cnidarian-dinoflagellate symbiosis. The combination of "omics" research with other isotopic labelling experiments could be powerful in studying this model cnidarian system.

### 1.7 Aims and Objectives

The primary aim of this research was to identify whether carbon and nitrogen exchange in the cnidarian-dinoflagellate symbiosis is impacted by symbiont type, and infer how any difference may influence the potential of corals to adapt to warming oceans under climate change. This was addressed using a combination of bioinformatic analysis and experimental investigations using proteomics and nanoSIMS techniques. The mechanisms of nutritional exchange across the symbiotic interface are largely unknown, so these were first explored to characterize evolutionary patterns leading to the integration of host-symbiont metabolite exchange; next, the functional implications of cnidarians associating with a thermally-tolerant, opportunistic *Symbiodinium* type were assessed. My specific objectives were therefore to:

1. Identify and characterize the membrane transporter sequences of the major exchanged metabolites (glucose, glycerol, ammonium, and nitrate) in the cnidarian-dinoflagellate symbiosis, across a range of cnidarian species and *Symbiodinium* clades.

    Hypothesis: Cnidarians will possess sequences homologous to human GLUT, SGLT, and AQP proteins for the uptake of glucose and glycerol from symbionts, while *Symbiodinium* will possess sequences homologous to plant AMT and NRT2 proteins for the uptake of ammonium and nitrate from the host.

2. Construct phylogenies of the characterized transporters, to determine how conserved nutrient transport is within the symbiotic associations and if diversification due to symbiosis has occurred during protein evolution.

    Hypothesis: Transporter proteins will be highly conserved from humans to cnidarians, and from *Arabidopsis* to *Symbiodinium,* since they provide an essential cellular

function. Furthermore, diversification of protein sequences is likely to have occurred during the evolution of symbiosis.

3. Use the model system of *Aiptasia*, to identify the response of a host proteome to a heterologous, thermally-tolerant symbiont type (*Symbiodinium trenchii*, type D1a) compared to a homologous symbiont type under normal environmental conditions.

Hypothesis: The heterologous symbiont will elicit proteins indicative of a less successful carbon and nitrogen metabolism then those of a host with homologous symbionts. Moreover, proteins involved in other important symbiotic processes will be down-regulated in heterologous symbionts.

4. Compare intercellular carbon and nitrogen translocation from symbiont to host, as well as carbon and nitrogen 'reverse translocation' between a heterologous, thermally-tolerant symbiont type (*Symbiodinium trenchii*, type D1a) with that of a homologous symbiont type (*Symbiodinium minutum*, type B1) in *Aiptasia* hosts under normal environmental conditions.

Hypothesis: The bi-directional translocation of both carbon and nitrogen will be lower when the host associates with *Symbiodinium* D1a than B1 at non-stressful temperatures, due to poorer integration of the novel symbiosis.

5. Determine whether nutrient (C and N) exchange changes with time during the colonization of the host by different symbiont types (homologous and heterologous).

Hypothesis: Nutritional exchange will increase with time, from the early to latter stages of symbiosis establishment, but to a greater extent when infected by a homologous rather than heterologous symbiont type.

The research comprising this thesis has been written as a series of stand-alone manuscripts, therefore some degree of overlap in the introduction of each chapter may be present. All laboratory and fieldwork, statistical analyses, and writing were completed by the author, with further assistance from others as follows:

**Chapter 2**: This chapter is formatted as an individual manuscript with combined results and discussion, as this improves the clarity and interpretation of the very complex data sets included. It has been submitted for publication in the journal *Molecular Phylogenetics and Evolution* and is currently 'under review': Sproles, A. E., Kirk, N. L., Kitchen, S. A., Oakley, C. A., Grossman, A. R., Weis, V. M., Davy, S. K. Phylogenetic characterization of transporter proteins in the cnidarian-dinoflagellate symbiosis. N. L. Kirk and S. A. Kitchen assisted with study design, data analysis and writing. C. A. Oakley, A. R. Grossman, V. M. Weis, and S. K. Davy assisted with study design and writing.

**Chapter 3**: This chapter is formatted as an individual manuscript in preparation for publication: Sproles, A. E., Matthews, J. M., Oakley, C. A., Grossman, A. R., Weis, V. M., Davy, S. K. Proteomic changes show that thermally-tolerant *Symbiodinium* may impair host cellular processes. Experimental infection of *Aiptasia* and infection success measurements were conducted equally with J. M. Matthews. C. A. Oakley assisted with protein preparations, experimental design, and writing. V. M. Weis and A. R. Grossman assisted with experimental design. S. K. Davy assisted with experimental design and writing.

**Chapter 4**: This chapter is formatted as an individual manuscript in preparation for publication: Sproles, A. E., Krueger, T., Oakley, C. A., Grossman, A. R., Weis, V. M., Miebom, A., Davy, S. K. *Symbiodinium* type effects nutrient exchange and symbiont success in *Aiptasia*. T. Krueger assisted with experimental design and nanoSIMS preparation and analysis. C. A. Oakley, A. R. Grossman, V. M Weis and A. Miebom assisted with experimental design, and S. K. Davy assisted with experimental design and writing.

# Chapter 2: Phylogenetic characterization of transporter proteins in the cnidarian-dinoflagellate symbiosis

## 2.1. Introduction

The cnidarian-dinoflagellate symbiosis is an endosymbiotic relationship involving intercellular exchange of many compounds. Dinoflagellates of the genus *Symbiodinium* reside within cnidarian endodermal cells and provide the host with the majority of its fixed carbon as photosynthetic products, with sugars being the major trafficked metabolites (Gordon & Leggat 2010; Davy *et al.* 2012; Kopp *et al.* 2015). In exchange, the cnidarian provides nitrogenous compounds, generated as by-products from heterotrophic feeding, to the algal symbionts (Allemand *et al.* 1998; Houlbrèque *et al.* 2004; Davy *et al.* 2012). Successful metabolite exchange between the host and symbiont is key to the health and survival of reef-building corals, as it allows the partners to obtain necessary nutrients that are often limiting in oligotrophic oceans (Muscatine *et al.* 1981; O'Neil & Capone 2008).

Characterization of transported metabolites has long been a focus of cnidarian-dinoflagellate research. Glucose is now considered to be the primary carbon product translocated to the host from the symbiont (Burriesci *et al.* 2012; Hillyer *et al.* 2016), although evidence from early studies pointed to glycerol (Muscatine 1967; Lewis & Smith 1971; Schmitz & Kremer 1977). It is now thought that glycerol is primarily released by *Symbiodinium* cells in isolation (e.g. in culture), while glucose is the major photosynthetic product translocated from the symbiont to the host *in hospite* (Ishikura *et al.* 1999; Whitehead & Douglas 2003; Burriesci *et al.* 2012; Hillyer *et al.* 2016). High levels of glycerol are also released as an osmolyte in response to stress (Suescún-Bolívar *et al.* 2012). In the opposite direction, the major nitrogen metabolite transported to the symbiont by the host is thought to be ammonium, while nitrate is an important nutrient obtained from seawater (Muller-Parker *et al.* 1994; Pernice *et al.* 2012; Kopp *et al.* 2013). Nitrogenous compounds are used for the synthesis of amino acids that are then incorporated into symbiont proteins (Wang & Douglas 1998) or translocated back to the animal (Wang & Douglas 1999; Tanaka *et al.* 2006).

Although these carbon and nitrogen metabolites are an important source of energy and nutrition in the symbiosis, the transport mechanisms are still poorly understood. All molecules entering or leaving a cell must traverse the plasma membrane, most either by active transport or passive diffusion through transporter or channel proteins (Lodish *et al.* 2000). In the cnidarian-dinoflagellate symbiosis, *Symbiodinium* cells are housed within a host-derived vacuole called the symbiosome, which acts as the interface between host and symbiont (Fitt & Trench 1983; Wakefield *et al.* 2000; Wakefield & Kempf 2001). Therefore, the exchange of compounds must be facilitated by proteins in the cellular membranes of each of the partners as well as in the symbiosome interface (Fig. 1.5).

Insights on nutrient transport can be gained from studies of other systems. Glucose primarily enters eukaryotic cells through transporters in two families of compounds: facilitated glucose transporters (GLUT) and sodium-coupled glucose transporters (SGLT) (Wood & Trayhurn 2003; Scheepers *et al.* 2015). Members of both families have been extensively characterized in humans and other animals (Escher & Rasmuson-Lestander 1999; Doege *et al.* 2000, 2001; Joost *et al.* 2002; Wright 2013). While few invertebrate GLUT and SGLT homologs have been described (Escher & Rasmuson-Lestander 1999; Feng *et al.* 2013), proteins from both of these families are encoded by genes of the cnidarian *Aiptasia pallida (*also known as *ExAiptasia pallida)* (Baumgarten *et al.* 2015). Previous studies have used proteomics (Peng *et al.* 2010; Oakley *et al.* 2016) and transcriptomics (Lehnert *et al.* 2014) to identify proteins involved in the symbiosis; however, transporters specific to the symbiosome membrane have not been firmly established. Glycerol can be trafficked by aquaporin (AQP) channels, which are intrinsic water channels that transport small molecules (Hara-Chikuma & Verkman 2006; Rojek *et al.* 2008). Since most eukaryotes already use AQP to facilitate the diffusion of water, I predict that cnidarians likely have AQP members capable of glycerol transport as well.

Currently, three genes encoding ammonium transporters (AMT proteins) and two encoding high-affinity nitrate transporters (NRT proteins) have been identified in *Symbiodinium* transcriptomes (Mayfield *et al.* 2010; Brown *et al.* 2011; Van Den Heuvel 2012). The recent genome assembly of *Symbiodinium kawagutii* (Clade F) has also revealed genes encoding AMT and NRT family members (Lin *et al.* 2015). However, these studies have only focused on a single *Symbiodinium* type and did not consider the large genetic diversity within the genus.

Currently, the *Symbiodinium* genus is classified into nine divergent clades (A–I), with each (except clade E) further divided into sub-clades or "types" (e.g., A3, B1, D1a) and some described species (Coffroth & Santos 2005; Pochon & Gates 2010; LaJeunesse *et al.* 2012). Genetic distances between these clades were found to be greater than the distances separating different species of free-living dinoflagellates (Santos *et al.* 2002; Takabayashi *et al.* 2004; Sampayo *et al.* 2009; Krueger *et al.* 2015). Therefore, analysis of these proteins from a diversity of *Symbiodinium* types may reveal differences in their conservation.

The goal of this study was to identify and characterize potential membrane transport mechanisms employed by both partners of the cnidarian-dinoflagellate symbiosis by performing informatics/phylogenetic investigations of well-described sugar and nitrogen transport proteins that are highly conserved among eukaryotes. I investigated five protein families: three families of secondary active transporters, GLUT, SGLT, and NRT2, and two families of channel proteins, AQP and AMT. I used a phylogenetic approach to identify cnidarian homologs to GLUT, SGLT, and AQP, and *Symbiodinium* homologs to AMT and NRT2. I then performed protein structural predictions, conservation analyses, and structural domain identifications to help establish whether or not these proteins function in metabolite exchange within the cnidarian-dinoflagellate symbiosis. Insights gained from these analyses will help inform further functional investigations of the symbiosome membrane and enhance our understanding of nutrient exchange in the cnidarian-dinoflagellate symbiosis.

## 2.2. Methods

### *2.2.1 Identification of cnidarian and* Symbiodinium *transporter proteins*

Separate analyses were completed to categorize the major transporters of the cnidarian host and *Symbiodinium* symbiont. Cnidarian and *Symbiodinium* transcriptomes and genomes were downloaded from publically available sources (Appendix A, Table A1), and each was formatted into a searchable database. Reference sequences for each protein family were obtained from UniProt (Appendix A, Table A2); these included *Homo sapiens* GLUT, SGLT, and AQP, and *Arabidopsis thaliana* AMT and NRT2 (Appendix A, Table A2). Putative orthologues to the reference sequences were identified in the cnidarian and *Symbiodinium*

databases by reciprocal BLAST (Telford 2007; Voolstra *et al.* 2011) with a bit-score cut-off of 80 for any given alignment. To identify cnidarian sugar transporters, *H. sapiens* reference proteins (Appendix A, Table A2) were used as BLAST input queries to search cnidarian databases and identify *Symbiodinium* nitrate and ammonium transporters; *A. thaliana* reference proteins (Appendix A, Table A2) were similarly used as BLAST input queries for searching the *Symbiodinium* databases. The best scoring matches were then converted to predicted proteins using custom Perl scripts (obtained from Eli Meyer, https://github.com/Eli-Meyer).

### *2.2.2 Retrieval of protein homologs*

Sequences from the cnidarian and *Symbiodinium* databases with high sequence similarity to the reference proteins were retrieved and used for phylogenetic analyses. Those protein sequences were also used to search the NCBI non-redundant (nr) database using BLASTp, retrieving sequences with an E value cut-off of $\leq 1 \times 10^{-5}$ and excluding hypothetical proteins (Appendix A, Datasheets A1–A5). The top five annotated BLAST hits for each sequence were used as additional homologs in the phylogenetic analyses (Appendix A, Datasheets A1–A5).

### *2.2.3 Sequence alignment and phylogenetic analysis*

Protein family sequences were aligned using MAFFT v. 7.017 (default parameters) (Katoh & Standley 2013). Alignments were manually edited in Aliview (Larsson 2014) to eliminate false positive matches (Bucka-Lassen *et al.* 1999) by removing protein fragments (sequences of < 150 amino acids) and sequences that did not align with any of the defined motifs. Motifs used were: the GLUT GR, GRR, and PETK motifs (Appendix A, Fig. A1), all of which are considered necessary for sugar transport function (Joost & Thorens 2001); the SGLT Y, GG, and D motifs (Appendix A, Fig. A2), which are the most conserved (≥77%) between all pro- and eukaryotic taxa (Wright & Turk 2004); the two NPA motifs and one D residue of AQP (Appendix A, Fig. A3), since NPA motifs form the aqueous pore and represent the AQP signature while the D residue is present in aquaglyceroporins and widens the pore opening allowing the transfer of larger solutes (Agre *et al.* 2002); the AMT D, AG, VH, and G motifs (Appendix A, Fig. A4), which are responsible for ammonium recognition and transport

function (Marini *et al.* 2006); the NRT2 conserved F residue along with the proposed NNP signature A/G-G-W-G/A-N/D-M/L-G and the structurally important GG and GAGG glycine clusters (Appendix A, Fig. A5) (Trueman *et al.* 1996; Forde 2000).

Phylogenetic analysis of each protein family was conducted using maximum-likelihood inference in RAxML v8.0.26 (Stamatakis 2014). The PROTGAMMAAUTO function was used to empirically determine the best substitution model for each dataset (highest likelihood score of starting parsimony tree); all datasets in this study were best suited to using the AUTO model. The topology with the highest likelihood score for each protein tree was selected from 100 replicate trees, and then branch support was calculated using 100 bootstraps. Trees were rooted to the most ancestral protein recovered by BLAST homology searches, where ancestry was determined in previous studies. Phylogenetic inference was then used to draw conclusions on the protein identities of novel cnidarian and *Symbiodinium* sequences (Eisen *et al.* 1997; Eisen 1998; Zmasek & Eddy 2001; Sjölander 2004).

### *2.2.4 Structural predictions and characterization of proteins*

Additional sequence analyses were conducted to further characterize the identified cnidarian and *Symbiodinium* proteins. The number of transmembrane (TM) helices and subcellular localization for each protein were predicted using the MemPype webserver, which outperforms other localization methods with an accuracy rate of 70% (Pierleoni *et al.* 2011), and protein domains were determined using the InterProScan (Quevillon *et al.* 2005) in Geneious v. 7.1.9. One protein sequence *per* gene family was also selected for protein structural analysis. Sequences from the cnidarian *Nematostella vectensis* with high similarity to the reference sequences were used for analysis of the cnidarian proteins because they were closest in amino acid length and had the highest similarity to the reference proteins. Furthermore, the *N. vectensis* genome had the most complete annotations. A sequence from *Symbiodinium* clade C was used for AMT structural analysis to further examine the sequences within the observed protein expansion, and a sequence from *Symbiodinium* clade A was chosen for NRT2 structural analysis since it was the only clade with sequences retrieved for this protein family. The three-dimensional structure and protein function were predicted using I-TASSER (Zhang 2008; Roy *et al.* 2010). I-TASSER aligns predictions with the most similar protein structures from the

Protein Data Bank (http://www.rcsb.org/pdb) and evaluates the structural similarity using a TM-score ranging from 0 – 1, where 1 indicates a perfect match. Ligands and ligand-binding sites are also predicted as part of I-TASSER using the COACH algorithm (Yang *et al.* 2013), which evaluates the confidence of the prediction using a C-score ranging from 0 – 1, where 1 indicates 100% confidence in the prediction. To determine the degree of structural conservation within each cnidarian and *Symbiodinium* protein family, all newly identified sequences were aligned within their family using MAFFT v. 7.017 and submitted to the ConSurf server (Ashkenazy *et al.* 2010) along with the corresponding predicted 3D structure. Conservation scores for each residue were calculated using the Bayesian method with the best evolutionary substitution model determined empirically as WAG (Mayrose *et al.*, 2004), and scores were subsequently depicted onto the protein structures using Polyview 3D (Porollo & Meller 2007).

## 2.3. Results and Discussion

### *2.3.1 Cnidarian GLUT proteins*

A total of 23 cnidarian sequences were identified as GLUT homologs, representing putative glucose transporters (Appendix A, Table A1). Sequence lengths were highly variable, with some sequences containing fewer than the 12 TM domains that are typical of proteins within the major facilitator superfamily (MFS), which includes GLUT proteins (Reddy *et al.* 2012). These sequences may represent incomplete proteins that were not excluded from our analysis because they contain the conserved protein motifs (Appendix A, Table A1). Only cnidarian sequences from GLUT classes 1 and 2 were identified. All sequences include domains for MFS sugar transporters, while some also contain domains associated with specific GLUT members.

Our phylogenetic analysis of the GLUT proteins resolved the sequences into four main clades of solute transporters (Fig. 2.1): (1) organic cation transporters (OCT); (2) class 1 and 2 GLUT proteins; (3) GLUT6 and GLUT8; and (4) GLUT10, GLUT12, and HMIT (proton/myo-inositol transporter). One divergent protein from *Porites australiensis* (Fig. 2.1) branches from near the root of the tree rather than clustering with any of the four main clades. This protein shares the highest sequence similarity with the yeast glucose transporter RGT2 (Appendix A, Table A1).

Since the *P. australiensis* transcriptome was generated from RNA derived from the entire holobiont rather than just host material, it is likely that this deduced protein represents RNA contamination from the algal symbiont or bacteria (Shinzato *et al.* 2014). Robust support is only observed for the OCT clade, with the other major clades being less well resolved. OCT is another MFS protein family that is closely related to the sugar porter family (Saier *et al.* 1999) (Fig. 2.1, clade 1). These proteins facilitate diffusion of organic cations such as neurotransmitters, amino and fatty acids, and nucleotides in vertebrates, but they have not been well studied in invertebrate systems (Eraly *et al.* 2004; Ciarimboli 2008).

The clustering of the GLUT sequences resulted in a branching order that follows previously constructed metazoan GLUT phylogenies (Wilson-O'Brien *et al.* 2010). Class 3 GLUT proteins are ancestral to the other GLUTs, and they have diverged into three well supported sub-clades (GLUT6 and GLUT8; GLUT10 and GLUT12; and HMIT), while class 1 and 2 proteins form a well-supported clade as sister groups that evolved more recently (Wilson-O'Brien *et al.* 2010; Scheepers *et al.* 2015). Overall, I identified cnidarian homologs to all class 1 and class 3 GLUT members, except for GLUT6 (Appendix A, Table A1).

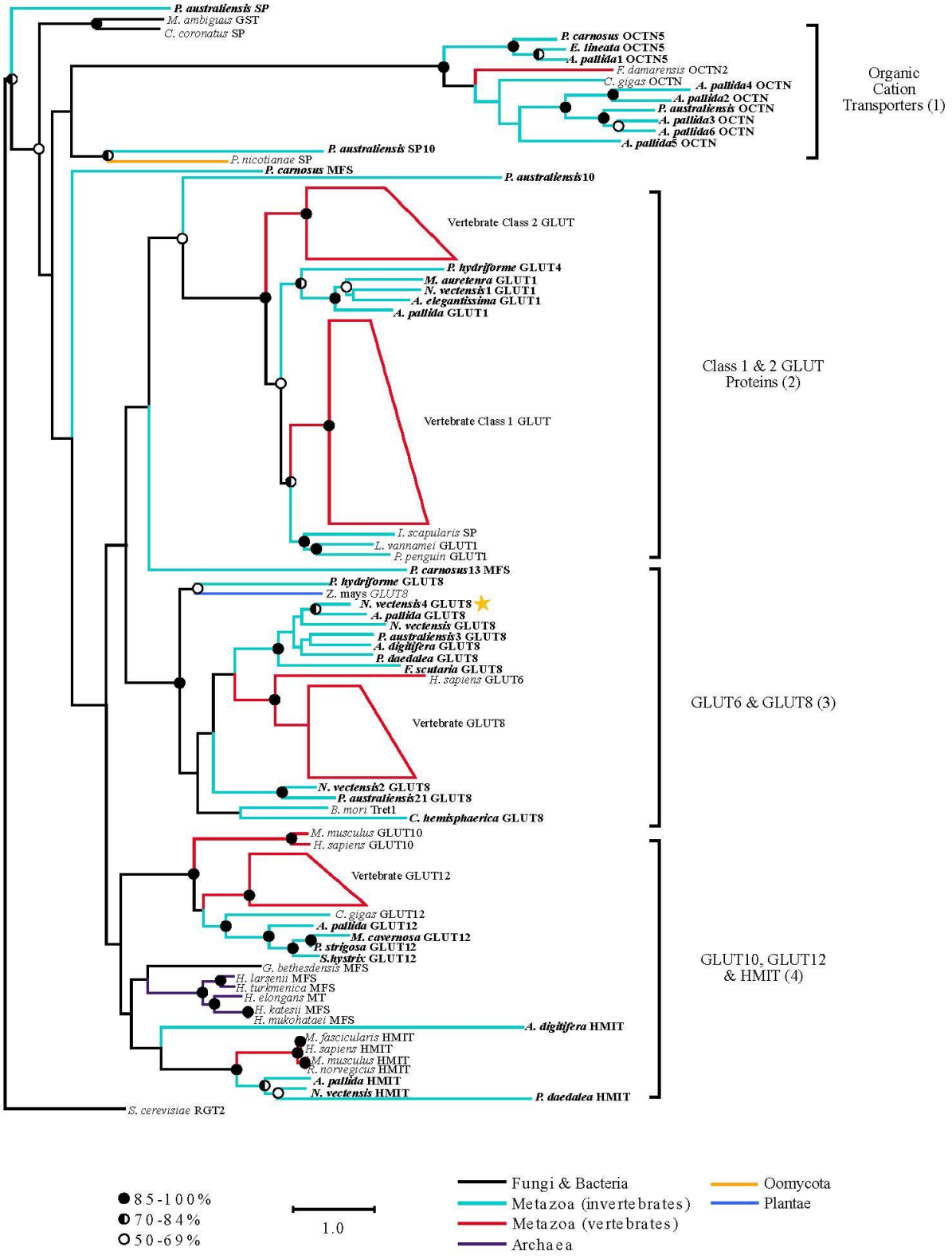


**Figure 2.1** Maximum likelihood phylogenetic inference of GLUT sequences. The clustering of the GLUT sequences resulted in a branching order that follows previously constructed metazoan GLUT phylogenies (Wilson-O'Brien *et al.*, 2010). Class 3 GLUT proteins are ancestral to the other GLUTs, and they have diverged into three well supported sub-clades (GLUT6 and GLUT8; GLUT10 and GLUT12; and HMIT), while class 1 and 2 proteins form a well-supported clade as sister groups that evolved more recently (Scheepers *et al.*, 2015; Wilson-O'Brien *et al.*, 2010). Overall, I identified cnidarian homologs to all class 1 and class 3 GLUT members, except for GLUT6 (Appendix A, Table A1).

Ten cnidarian putative GLUT8 proteins were identified (Fig. 2.1). GLUT8 is of particular interest in the cnidarian-dinoflagellate symbiosis because it has a high affinity for glucose (Uldry & Thorens 2004) and exhibits increased mRNA levels in symbiotic *A. pallida* relative to those in aposymbiotic anemones of the same species (Lehnert *et al.* 2014). As it is localized to endosomal compartments in mice, GLUT8 is predicted to function as a hexose transporter in intracellular membranes (Augustin *et al.* 2005). Four of the identified cnidarian GLUT8 proteins in this study were predicted to be localized to internal membranes, while six were predicted to exist in the plasma membrane (Appendix A, Table A1). Internal GLUT proteins may reside in the symbiosome membrane, which is an internal vacuolar membrane of host origin that is derived from an early endosome (Fitt & Trench 1983; Rands *et al.* 1993; Wakefield & Kempf 2001). Three GLUT8 proteins were expressed in *N. vectensis* and two in *P. australiensis*. All proteins in the non-symbiotic cnidarian *N. vectensis* were predicted to be localized to the plasma membrane. The two GLUT8 proteins in the symbiotic cnidarian, *P. australiensis*, had different predicted localizations based on the MemLoci algorithm; one is likely in the plasma membrane while the other appears to reside in internal membranes. These analyses raise the possibility that symbiotic cnidarians have a distinct GLUT8 that is associated with the symbiosome membrane where it facilitates movement of glucose from the symbiont to the host.

The deduced 3D structure of the cnidarian GLUT8 protein closely resembles the crystal structure of human GLUT1 (TM score = 0.89, Fig. 2.2). All ten structural hits from the Protein Data Bank were GLUT proteins from other species ranging from bacteria to vertebrates (Appendix A, Datasheet A1, Tab C). Among the cnidarian GLUT sequences, conservation was highest for residues on the inner surface of the translocation pore, where the active binding sites are presumably located (Fig. 2.2). The predicted ligand was maltose (Fig. 2.2), a disaccharide composed of two glucose molecules (Berg *et al.* 2002). However, confidence of this prediction was low (C-score = 0.11), so I cannot make definitive conclusions about the solutes transported by the cnidarian GLUT protein. Overall, the results of the structural analysis support the hypothesis that the identified cnidarian proteins shared a common ancestor with human GLUT proteins.

### *2.3.2 Cnidarian SGLT proteins*

A total of 23 cnidarian predicted sequences are homologs to SGLT proteins. While most sequences contain the 12 TM helices indicative of the amino acid-polyamine- organocation superfamily (APC), to which the SGLTs belong (Saier 2000), three sequences appear to be protein fragments (Appendix A, Datasheet A2). Only one cnidarian sequence was identified as likely to be a true SGLT (*N. vectensis* SLGT4). This sequence clustered with two other cnidarian SGLT sequences that were previously identified in *A. pallida*. Similarly, one cnidarian sequence was identified as a choline transporter (CHT) with high similarity to the *A. pallida* CHT protein. The majority of cnidarian sequences were identified as putative sodium myo-inositol transporters (SMIT) or sodium-coupled monocarboxylate transporters (SMCT) (Fig. 2.3). All of the identified SGLT homologs were predicted to be localized to either the plasma membrane or internal membranes and contained the sodium solute symporter domain (Appendix A, Datasheet A2).

All proteins in the three main clades (CHT, SMCT, and SGLT) are part of the *SLC5* gene family and function as sodium ion symporters. Recovered cnidarian proteins did not share high sequence similarity to the SGLT1-5 reference proteins, but they were closely related to SMCT or SMIT proteins (Fig. 2.3). The SMCT1 protein (encoded by *SLC5A8*) can transport fatty acids, carboxylic acids, and vitamins; it also functions as a tumour suppressor factor in humans by allowing the uptake of the fatty acid butyrate, which induces apoptosis (Gupta *et al.* 2006; Ganapathy *et al.* 2008).

Cnidarian SMCT proteins were primarily predicted to be localized to internal membranes, with fewer in the plasma membrane. Additionally, multiple SMCT sequences were found in two of the symbiotic coral species, *Fungia scutaria* and *P. australiensis* (Appendix A, Datasheet A2, Tab D). Symbiotic cnidarians are thought to regulate internal algal populations through apoptosis of symbiont-containing gastrodermal cells (Muscatine & Pool 1979; Dunn *et al.* 2007b; Dunn & Weis 2009). If this is the case, the SMCT proteins could be located in the symbiosome membrane to illicit this regulatory response by inducing host cell degradation.

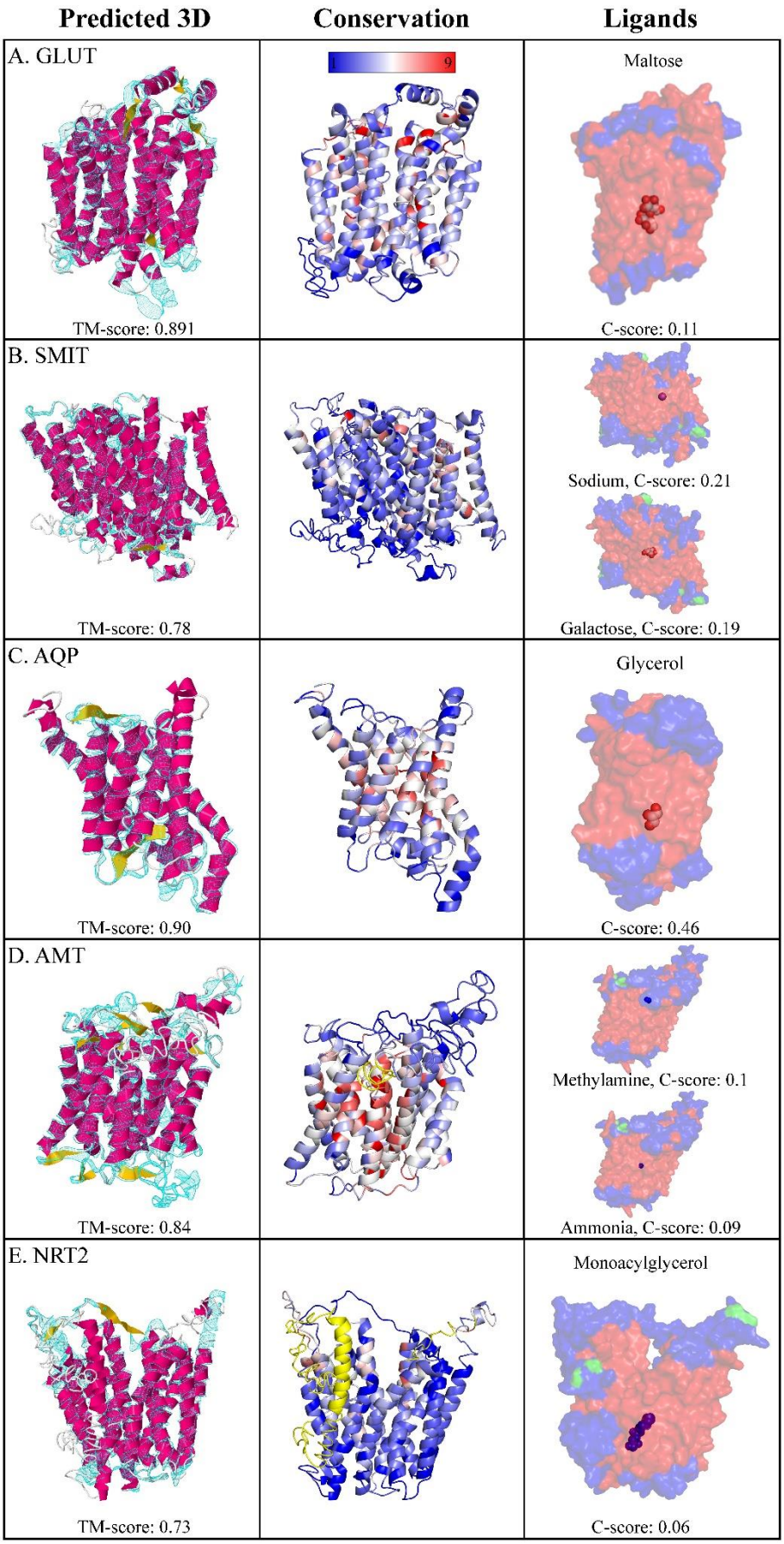


**Figure 2.2** Protein structural analysis of selected sequences from each gene family. Predicted 3D structures (left), conservation analysis (middle), and predicted ligands (right) of cnidarian proteins (A-C) and *Symbiodinium* proteins (D-E): (A) GLUT, as deduced from the amino acid sequence of *N. vectensis*_4 GLUT8 and aligned with the human GLUT1 protein (PDB ID = 4pyp), (B) SMIT, as deduced from the *N. vectensis*_5 SMIT sequence and aligned with the K294A mutant of VSGLT (PDB ID = 2xq2), (C) AQP, as deduced from the *N. vectensis*_4 AQP3 sequence and aligned with the *E. coli* glycerol facilitator GLPF (PDB ID = 1fx8).

(D) AMT, as deduced from *Symbiodinium* C1_25 AMT sequence and aligned with the *S. cerevisiae* methylammonium permease Mep2 (PDB ID = 5aexA), and (E) NRT2, as deduced from the *Symbiodinium*A_24 NRT2 sequence and aligned with the *E. coli* glycerol-3-phosphate transporter GlpT (PDB ID = 1pw4). Predicted structures of each protein are coloured by structure (alpha helix = pink, coil = white, with yellow arrows ribbons showing sequence direction) and aligned with the top matching structure from the Protein Data Bank, depicted by a cyan mesh ribbon. Conservation scores are rendered onto the protein models using a colour gradient, from blue (low conservation, score = 1) to red (high conservation, score = 9), with yellow regions indicating insufficient data for analysis. Ligand predictions show the ligand at the predicted binding sites with transparent protein models coloured by secondary structure (helices = red, coils = blue).

The SGLT protein clade has high bootstrap support, and the tree shows SGLT and SMIT sequences clustering together within vertebrate and invertebrate sub-clades, with one sub-clade consisting entirely of cnidarian proteins (Fig. 2.3). Nine cnidarian proteins in this clade were identified as SMITs, which are closely related to SGLTs of the *SLC5* gene family. These proteins function similarly to proton myo-inositol transporters (HMIT), primarily transporting myo-inositol (Bourgeois *et al.* 2005). SMIT1 can also transport a variety of sugars, including glucose, although it does so with low affinity (Wright 2013), while SMIT2 can transport D-*chiro*-inositol (Coady *et al.* 2002). Myo-inositol is important for the growth of mammalian cells and is a key component in phospholipid biosynthesis and eukaryotic signalling pathways (Holub 1986). The identification of both HMIT and SMIT transporters in cnidarians suggests an uncharacterized role for myo-inositol in cnidarian metabolism or cell structure.

A SMIT protein sequence from *N. vectensis* (*N. vectensis*_5 SMIT) was used for 3D structural analysis (Fig. 2.2). The predicted tertiary structure of the protein most closely resembles that of the K294A mutant of the VSGLT protein from *Escherichia coli* (TM score = 0.78). Overall residue conservation was low, with the most conserved residues lining the protein pore (Fig. 2.2). The ligands were predicted to be sodium (C-score = 0.21) and galactose (C-score = 0.19), which only weakly supports the idea that this protein functions as a sodium-coupled sugar transporter (Fig. 2.2). Proteins in the SGLT family are known to transport galactose, some with a high affinity (Zhao & Keating 2007); however, experimental analysis is needed to confirm this function in cnidarians.

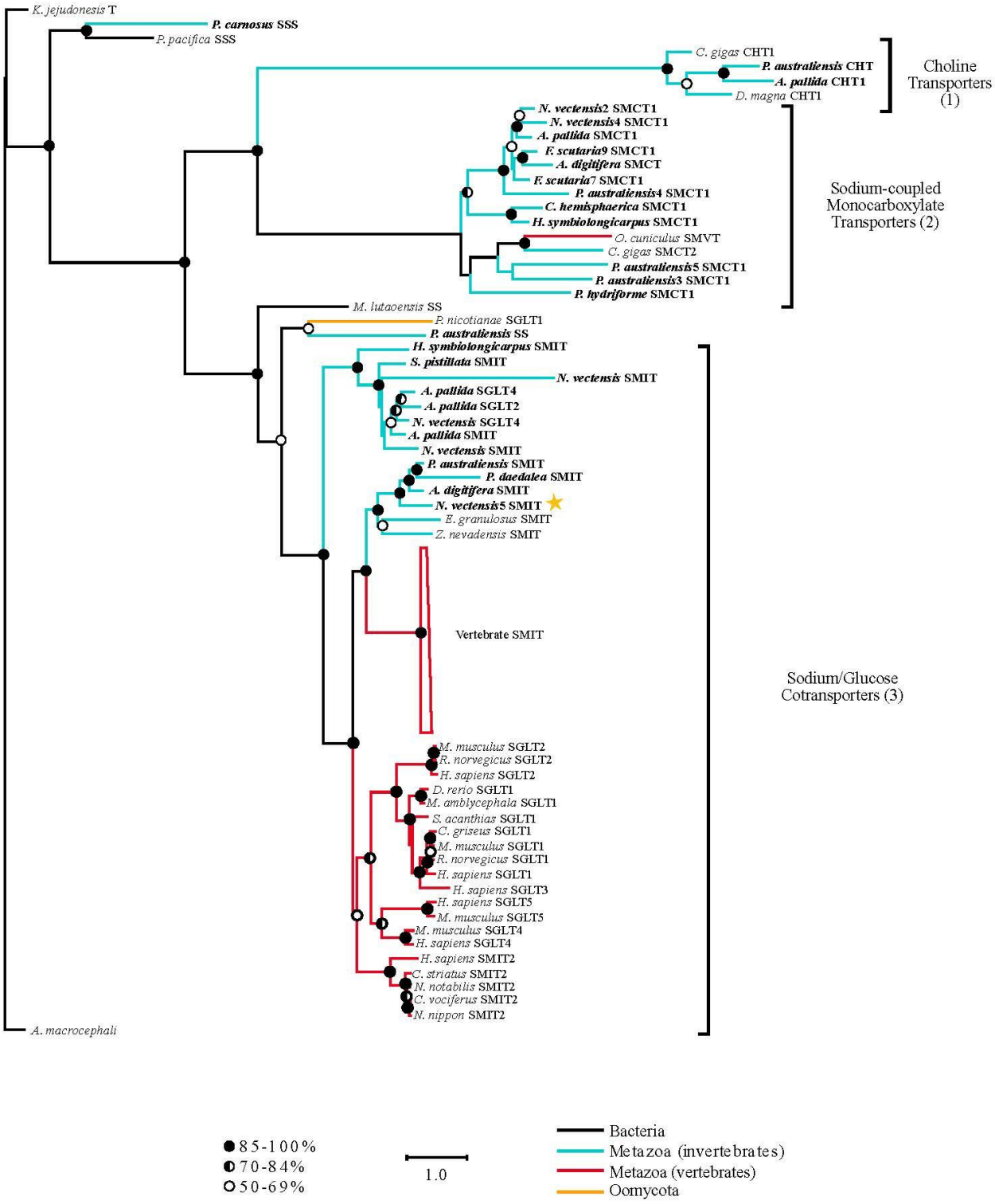


**Figure 2.3** Maximum likelihood phylogenetic inference of SGLT sequences. The tree was rooted by the bacterial sodium solute symporter (SSS) homolog from *Acanthamoeba castellanii*. The number of amino acid substitutions is indicated by the scale bar, and bootstrap support for nodes >50% is represented by shaded circles. Three main clades were resolved: (1) choline transporters (CHT), (2) sodium-coupled monocarboxylate transporters (SMCT), and (3) sodium/glucose cotransporters (SGLT and SMIT). The cluster of vertebrate SMIT proteins is collapsed to enhance tree clarity. The sequence used for structural analysis is marked by a yellow star (*N. vectensis*_5 SMIT).

### *2.3.3 Metazoan AQP proteins*

A total of 16 cnidarian sequences were identified as AQP homologs, all with at least five TM domains typical of AQPs (Appendix A, Datasheet A3). In cnidarians, the majority of the AQP homologs were predicted to be localized to internal membranes (Appendix A, Datasheet A3). All sequences contained domains present in members of the major intrinsic protein family and in AQP transporters, while some also had domains associated with specific AQPs (Appendix A, Datasheet A3). Our phylogenetic analysis resulted in the emergence of two sister clades: (1) aquaglyceroporins; and (2) classical aquaporins (Fig. 2.4). All sequences identified as aquaglyceroporins contained the conserved aspartate (D) residue that signifies a larger protein pore (Agre *et al.* 2002).

Aquaglyceroporin proteins all share a common ancestor, but these proteins were shown to have diverged into vertebrate and invertebrate lineages before the emergence of the different protein members. The cnidarian aquaglyceroporin sequences were identified as either AQP3 or AQP9. These sub-clades of exclusively cnidarian sequences are highly supported and include two previously identified AQP3 sequences from *A. pallida*, suggesting that the other cnidarian sequences are also AQP3 proteins. In mammals, aquaglyceroporins can transport a diversity of solutes other than glycerol, including urea and water (Rojek *et al.* 2008). AQP3 primarily transports water and glycerol, while AQP9 can also transport larger molecules, such as lactate, purines, and pyrimidines (Ishibashi *et al.* 2011). Experimental evidence is needed to confirm which of these small solutes the cnidarian AQP proteins transport.

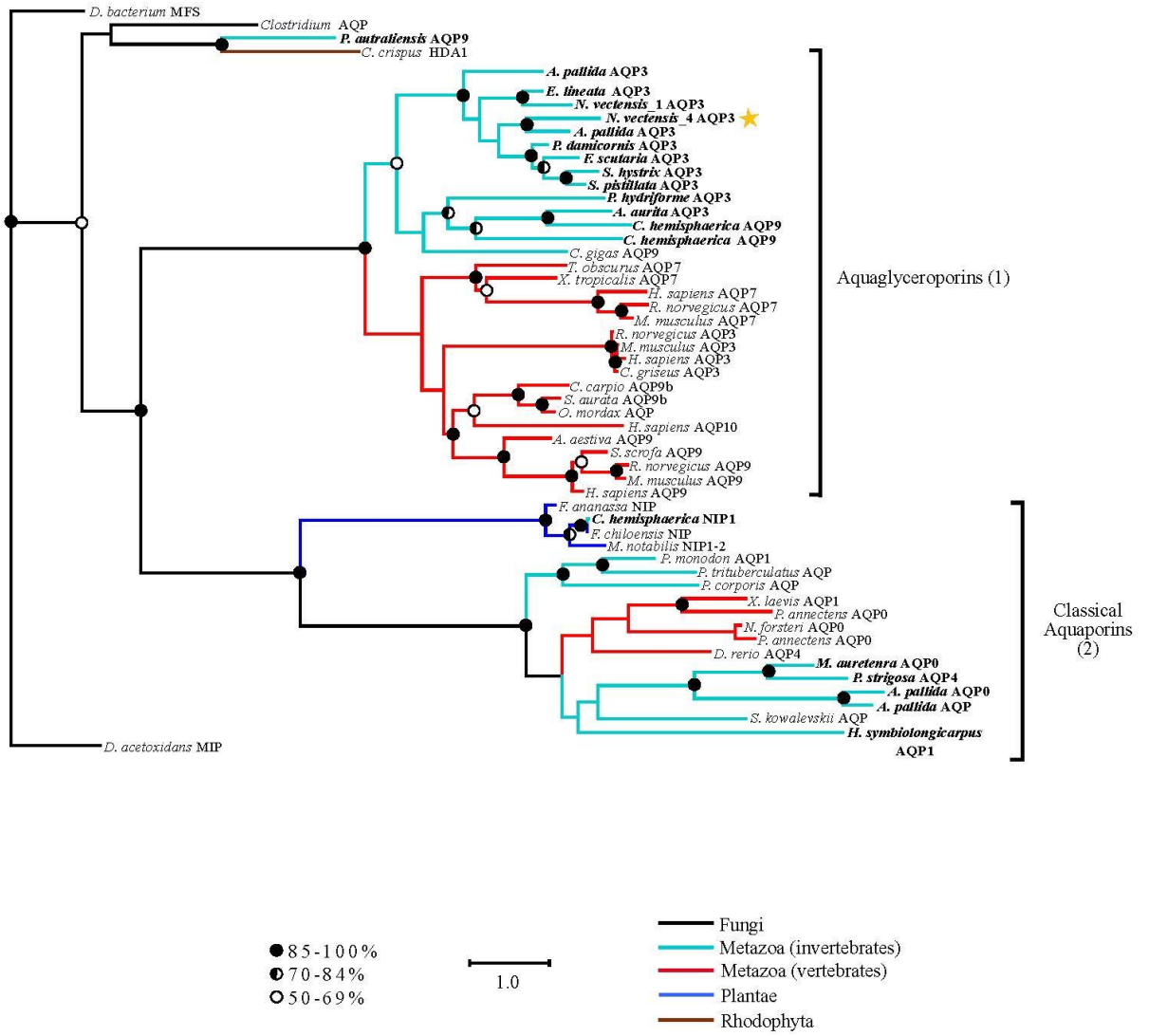


**Figure 2.4** Maximum likelihood phylogenetic inference of AQP sequences. The tree was rooted by the bacterial homolog from *Desulfuromonas acetoxidans*. The number of amino acid substitutions is indicated by the scale bar, and bootstrap support for nodes >50% is represented by shaded circles. The proteins resolved into two main clades: (1) aquaglyceroporins and (2) classical aquaporins. The sequence used for structural analysis is marked by a yellow star (*N. vectensis*_4 AQP3).

The clade of classical aquaporins diverges into a sub-clade of nodulin 26-like proteins (NIP) and a sub-clade of metazoan proteins. The NIP clade is highly supported and contains mostly proteins from vascular plants, along with one cnidarian NIP (Fig. 2.4). The identification of a cnidarian NIP is surprising since these proteins are known as plant-specific water channels that function similarly to aquaglyceroporins (Ishibashi *et al.* 2011). Nodulin 26 is an integral symbiosome membrane protein in nitrogen-fixing soybean nodules that acts as both an ion channel and a water channel (Fortin *et al.* 1986; Weaver *et al.* 1994); however, the cnidarian NIP in this study was present in a non-symbiotic species and may be representative of contamination from the cnidarian's environment.

The sub-clade of metazoan classical aquaporins contains cnidarian sequences sharing a common ancestor with vertebrate and invertebrate AQP1, as well as vertebrate AQP4 and AQP0 (Fig. 2.4). While AQP1 and AQP4 are water-only channels, AQP0 has a variety of functions in other organisms (Agre *et al.* 2002). AQP0 is the lens major intrinsic protein, originally found in lens fibre cells of vertebrate eyes and later discovered to function in increasing the water permeability of animal cells (Gorin *et al.* 1984; Mulders *et al.* 1995). Its suspected structural role in cell adhesion making AQP0 unique in the aquaporin family (Fotiadis *et al.* 2000). Cell adhesion proteins are important in the cnidarian-dinoflagellate symbiosis for cell-cell interactions, such as signalling between partners (Reynolds *et al.* 2000); cnidarian AQP0 may function in this capacity.

One AQP9 sequence from *N. vectensis* (*N. vectensis*_4 AQP3) was used for structural analysis of the cnidarian AQP protein (Fig. 2.2). The deduced structure was very similar to that of the *E. coli* glycerol facilitator, GLPF (Fig. 2.2, TM score = 0.90). Additional hits from the Protein Data Bank were protein structures of aquaglyceroporins from other species (Appendix A, Datasheet A3, Tab C). Furthermore, the predicted ligand (Fig. 2.2) was glycerol (C-score = 0.46), and the most highly conserved residues among all cnidarian AQPs were those lining the protein pore (Fig. 2.2). Overall, the structural analysis supports the prediction that these proteins function as glycerol channels.

### *2.3.4* Symbiodinium *AMT proteins*

A total of 40 *Symbiodinium* sequences were putatively identified as AMT proteins. Most of these sequences contained 10–12 TM domains, which is typical of AMT proteins (Thomas & Mullins 2000; von Wiren *et al.* 2000), while five sequences were shorter, containing only seven to nine TM helices. The sequences were primarily identified as general AMT proteins rather than specific members or isoforms and were predicted to be localized to either the cell membrane or internal membranes (Appendix A, Datasheet A4, Tab D). All sequences contained the domain for ammonium transport (Appendix A, Datasheet A4, Tab D).

Phylogenetic analysis showed the divergence of five main AMT clades: (1) bacterial cyclases; (2) metazoan-like AMT proteins; (3) diaphoretickes AMT proteins; (4) alveolate AMT proteins; and (5) bacterial-like AMT proteins (Fig. 2.5). The clade of bacterial cyclases is not well supported and includes the enzymes adenylate cyclase and guanylate cyclase exclusively from bacterial species.

Several clades of AMT proteins were identified in the phylogenetic analysis. The first clade shows AMT proteins diverging into three sub-clades, although not all are well resolved (Fig. 2.5). Clade 2 has robust support and shows metazoan AMT proteins emerging alongside a cluster of exclusively *Symbiodinium* proteins. This clade includes four *A. pallida* sequences in the metazoan cluster and five of the *Symbiodinium* sequences that contain the domain characteristic of AMT3. The finding of *Symbiodinium* AMTs sharing a common ancestor and sequence similarities with AMTs of the cnidarian host *A. pallida* raises the possibility of horizontal gene transfer between symbiotic partners, which was also found to be the case in the *Aiptasia* genome assembled by Baumgarten *et al.* (2015). Twenty-nine *Aiptasia* gene products within the genome were found to best align with *Symbiodinium* proteins, and formed a distinct clade together after phylogenetic analysis, further supporting the hypothesis of horizontal gene transfer between *Symbiodinium* and cnidarians (Baumgarten *et al.* 2015).

Clade 3 is only weakly supported overall and includes proteins from organisms within the expansive diaphoretickes super-group (Adl *et al.* 2012). Nevertheless, a well-supported sub-clade shows a *Symbiodinium* AMT sequence (*Symbiodinium*C1_12) grouping with vascular plant and red algal proteins. This *Symbiodinium* sequence also had high sequence similarity to the AMT1-3, which in plants has a high affinity for the uptake of both methylammonium and ammonium (von Wiren *et al.* 2000). While clade 4 is also lacking adequate bootstrap support, it contains a highly supported sub-clade that includes a large amount of expressed *Symbiodinium* C1 AMT proteins in relation to other alveolates (Fig. 2.5). While expression of multiple AMT proteins is observed for almost all alveolate species in the analysis, *Symbiodinium* C1 was found to express a total of 28 proteins, while other alveolate species have only one to four expressed AMT proteins.

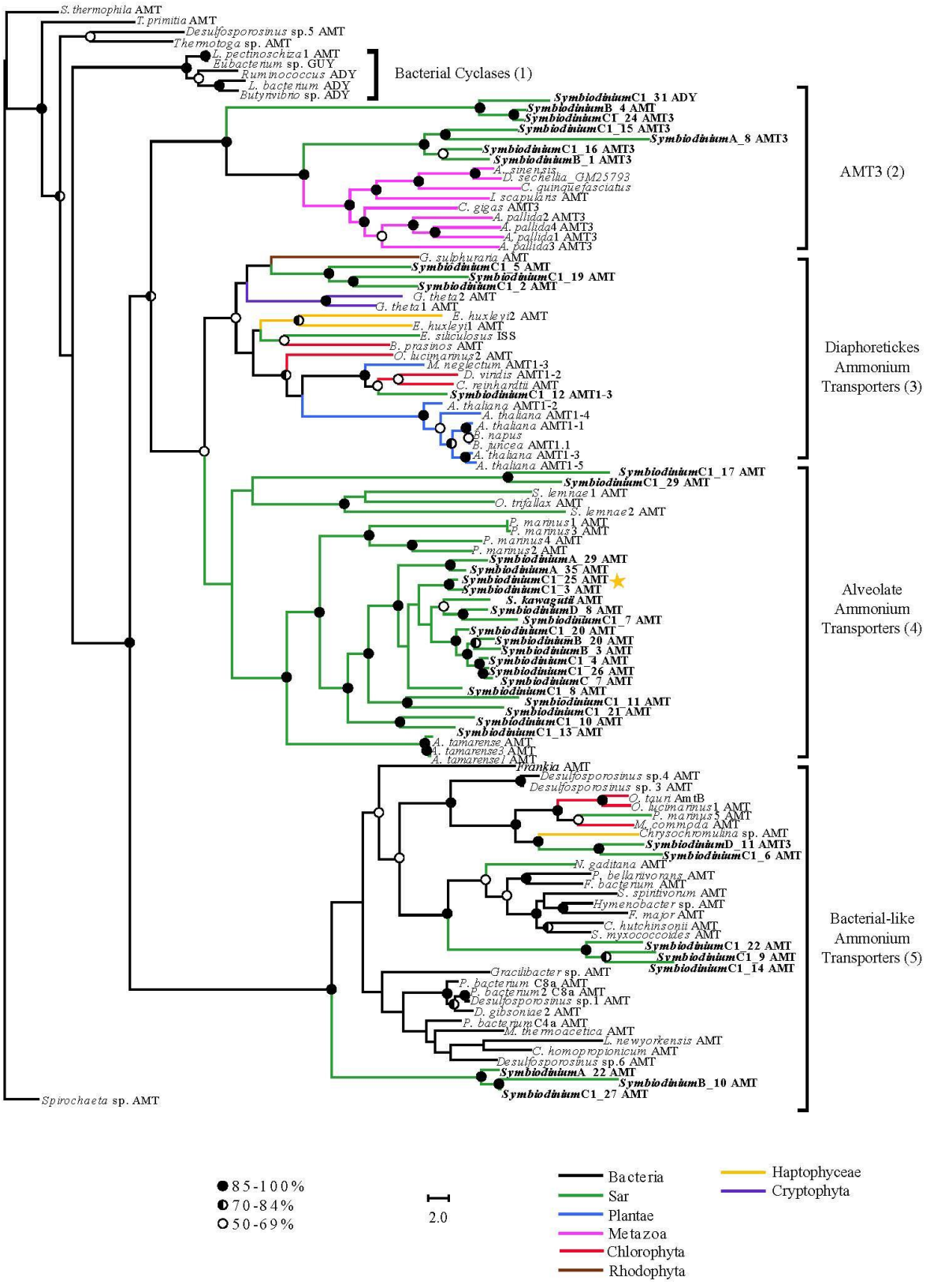


**Figure 2.5** Maximum likelihood phylogenetic inference of AMT sequences. The tree was rooted by the bacterial homolog from a *Spirochaeta* sp. The number of amino acid substitutions is indicated by the scale bar, and bootstrap support for nodes >50% is represented by shaded circles. The proteins resolved into five main clades: (1) bacterial cyclases, (2) metazoan-like ammonium transporters, (3) plant-like ammonium transporters, (4) chromalveolate ammonium transporters, and (5) bacterial-like ammonium transporters. The sequence used for structural analysis is marked by a yellow star (*Symbiodinium* C1_25 AMT).

*Symbiodinium* C1 is known as a generalist symbiont that occurs worldwide, forming associations with a variety of invertebrate hosts (LaJeunesse 2005; Stat *et al.* 2009). Consequently, the upregulation of AMT proteins in this *Symbiodinium* type may have evolved as an adaptation to survive the varying nitrogen conditions experienced in different host cell environments. The second lineage including *Symbiodinium* AMT proteins is a well-supported clade showing divergence from bacterial proteins into alveolate and red algal proteins (Fig. 2.5, clade 5). Overall, our analysis of the *Symbiodinium* AMT proteins and their homologs has revealed a large diversity of these transporters within this dinoflagellate species, which may have arisen through multiple evolutionary events caused by horizontal gene transfer, duplication, or classical evolution.

For structural analysis of the *Symbiodinium* AMT proteins, one sequence from *Symbiodinium* clade C (*Symbiodinium*C1_25) that falls within the alveolate cluster was used. The predicted 3D structure most closely resembles the structure of the *Saccharomyces cerevisiae* methylammonium permease Mep2 (TM score = 0.84, Fig. 2.2). Residues lining the inside of the protein channel are highly conserved (Fig. 2.2), suggesting their importance in transport function. Ligand predictions (Fig. 2.2) had very low confidence scores but favoured methylamine (C-score = 0.1) and ammonia (C-score = 0.09). The information gained from this structural analysis provides preliminary evidence that these highly conserved proteins serve as ammonium channels.

### *2.3.5* Symbiodinium *NRT2 proteins*

Only four sequences in total were identified as *Symbiodinium* NRT2 homologs, all of which were from *Symbiodinium* clade A, although a sequence from clade C and an unspecified *Symbiodinium* sequence within the NCBI database were also related to NRT2. The four sequences had high similarity with one another (74–79%) and ranged in length from 549–613 amino acids with 11–12 TM helices, typical of MFS transporters (Appendix A, Datasheet A5). Half of these NRT2 homologs were predicted to be localized to the plasma membrane and the

other half to internal membranes, while all sequences contained the domains for MFS and were related to high affinity nitrate transporter 2.3 (Appendix A, Datasheet A5, Tab D).

Phylogenetic analysis of the NRT2 proteins showed divergence of: (1) eukaryotic; and (2) bacterial nitrate transporters (Fig. 2.6). Surprisingly, very few NRT sequences were recovered from the *Symbiodinium* databases, and no other alveolate NRT2 sequences were identified (Fig. 2.6). Expression of *NRT2* proteins are highly regulated by environmental nitrate concentrations. As part of the high-affinity uptake system, the proteins are upregulated during nitrogen starvation (< 0.5 mM) and repressed when nitrate levels are high (> 0.5 mM) (Okamoto *et al.* 2003; Lezhneva *et al.* 2014). If the *Symbiodinium* NRT2 protein level is regulated in the same way, then the gene would be repressed when the cells are grown in the commonly used f/2 culture medium, since it contains 0.882 mM nitrate (Guillard 1975). However, as copies of the *NRT2* genes were not discovered in the *Symbiodinium* genomes surveyed, identification of the protein may indicate that this gene has either been lost in some derived species of this genus but retained by the more ancestral *Symbiodinium* clade A, or that the proteins discovered were from contaminants in the clade A transcriptome.

The expression of nitrate transporters in only *Symbiodinium* clade A could be due to the free-living nature of some dinoflagellate types within this clade (Hirose *et al.* 2008; Reimer *et al.* 2010), allowing the cells to more readily utilize nitrate from seawater. Ammonium is excreted by the host, while nitrate is not, and ammonium has been predicted to be the primary nitrogen source for symbiotic *Symbiodinium* cells (Kopp *et al.* 2013; Pernice *et al.* 2014). Many *Symbiodinium* types that have evolved to be strictly symbiotic may have lost the need for high-affinity nitrate transport, while those with a partially or wholly free-living lifestyle may have retained it.

While I had initially hypothesized that the identified *Symbiodinium* NRT2 homologs are nitrate transporters, the structural analysis indicates otherwise. The predicted 3D structure of the putative *Symbiodinium* NRT2 sequence (*Symbiodinium* A-24 NRT) was most similar to that of the glycerol-3-phosphate transporter from *E. coli* (TM score = 0.73, Fig. 2.2), rather than any nitrate transporters. Overall conservation was low, and one of the TM helices was only found

in a single sequence (Fig. 2.2). The ligand was predicted as monoacylglycerol (Fig. 2.2) but with low confidence (C-score = 0.06). While the identified potential NRT2 homologs resemble integral membrane transport proteins, they are very likely MFS transporters with a different function.

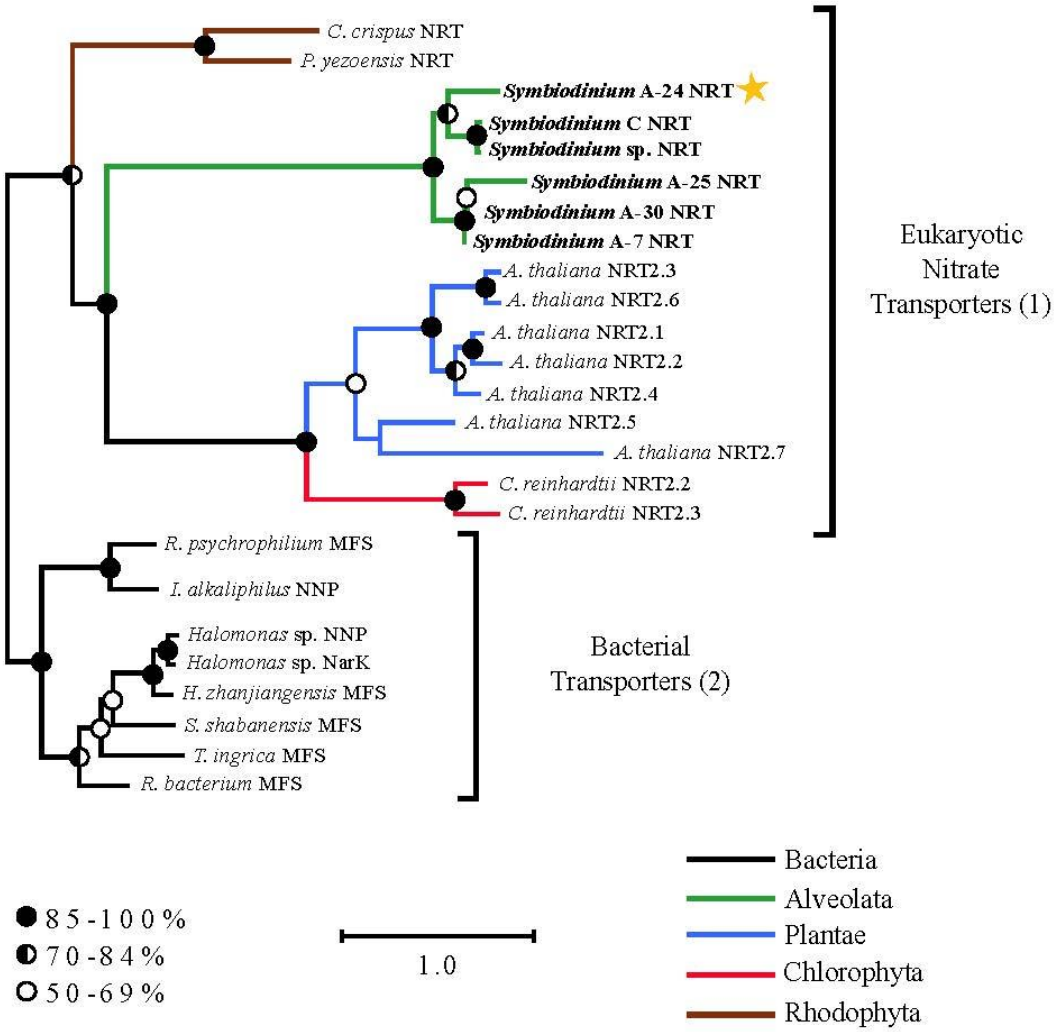


**Figure 2.6** Maximum likelihood phylogenetic inference of NRT2 sequences. The tree was rooted by the clade of bacterial sequences. The number of amino acid substitutions is indicated by the scale bar, and bootstrap support for nodes >50% is represented by shaded circles. Proteins resolved into two clades: (1) eukaryotic and (2) bacterial nitrate transporters. The sequence used for protein structural analysis is marked with a yellow star (*Symbiodinium* A-24 NRT).

## 2.4. Conclusions

This study identified sugar transport proteins from cnidarians and nitrogen transport proteins from their dinoflagellate symbionts. Homology searches identified previously undescribed cnidarian GLUT, SGLT, and AQP homologs and *Symbiodinium* AMT and NRT2 homologs. Phylogenetic and structural analyses demonstrated high conservation of most of the investigated protein families, suggesting that the characterized transport functions of the reference sequences are likely retained in the identified cnidarian and *Symbiodinium* sequences.

Considerably more cnidarian sequences were identified in the GLUT family than in the SGLT family, signifying that GLUT proteins could be involved in the transport of glucose between the symbiont and cnidarian host. Genes encoding for glucose transporters are present in the *Symbiodinium* genome, indicating the ability of the sugar to be exported to the symbiosome space via this mechanism (Lin *et al.* 2015), where cnidarian GLUT proteins could facilitate uptake into the animal cells. Furthermore, potentially related transporters of the *SLC5* gene family known to transport other compounds, such as monocarboxylates and myo-inositol, were identified in the cnidarians. Protein sequences for cnidarian aquaglyceroporins were also discovered, suggesting a potential mechanism for glycerol translocation into cnidarian cells.

Many of the sugar transporters discussed here have predicted localizations to internal membranes, which are defined in the MemPype pipeline as "the endoplasmic reticulum, the nuclear membranes, the Golgi apparatus, the vesicles, the vacuoles, the lysosomes, the peroxisome, the microsomes, and the endosome" (Pierleoni *et al.* 2011). Since the symbiosome is derived from an early endosome (Fitt & Trench 1983; Wakefield & Kempf 2001), I presume that symbiosome-localized proteins would fall into the "internal membrane" category. Transporters predicted as localized to only internal membranes were OCT and AQP9 (Appendix A, Datasheets A2–A3). Investigations of these proteins might identify them as being associated exclusively with the symbiosome, which would be helpful in the establishment of specific marker proteins for identification of symbiosome membranes.

Additionally, more *Symbiodinium* AMT sequences were identified than NRT sequences, which is likely due to ammonium being the primary nitrogen source for symbiotic dinoflagellates (D'Elia *et al.* 1983; Grover *et al.* 2002). Based on our findings, I suggest the use of AMT transporters to investigate the nutritional conditions experienced by symbionts *in hospite*. Since expression of these proteins is known to be regulated by environmental ammonium concentrations, AMT transporter expression patterns by *Symbiodinium* cells *in hospite* could reveal information about the nutrient conditions experienced within symbiotic host cells. It has previously been hypothesized that the host can regulate intracellular symbiont populations by limiting their growth and nutrient supply (Muscatine & Pool 1979; Falkowski *et al.* 1993; Jones & Yellowlees 1997; Wooldridge 2010). In plants and various algal species, AMT isoforms are transcriptionally regulated by environmental conditions, in a manner similar to that for genes encoding NRT2 proteins, where high-affinity isoforms are expressed during nitrogen starvation and low-affinity isoforms are expressed under ample nutrient availability (Gazzarrini *et al.* 1999; González-Ballester *et al.* 2004; Lezhneva *et al.* 2014). Therefore, verification of regulated expression in *Symbiodinium* and analysis of AMT proteins during colonization experiments may help to establish whether or not the host imposes nitrogen limitations on the symbiont population.

The resources used to compile cnidarian and *Symbiodinium* databases in this study included mostly transcriptomic data. Molecular phylogenies conducted on proteins rather than DNA are more accurate at establishing relationships between lineages, since proteins are the molecules on which natural selection acts (Salemi & Vandamme 2003). While transcriptomes contain highly useful information about the proteins being transcribed during the times of sampling, they represent only a snapshot of an organism's genome and not a comprehensive view of its total coding capacity. The results of this study can be interpreted as putative identification of symbiont and host transport proteins, while the absence of any proteins in our datasets does not necessarily indicate their absence from the organism. Absence of proteins indicates that they were not expressed at the time of sampling for the transcriptome, yet the organism may still have the genes for these proteins; only an analysis of the organism's genome would be able to confirm this information. All new protein identifications described here are inferred from homology and require verification through experimental analyses. While the results cannot be used to deduce the full range of cnidarian and *Symbiodinium* proteins from each of these five transporter families, they do give us a previously unseen glimpse of a subset of transporter

proteins that are likely used in the cnidarian-dinoflagellate symbiosis. Using currently available genetic resources, I have taken the first steps towards uncovering mechanisms used in the exchange of carbon and nitrogen between the partner organisms in the cnidarian-*Symbiodinium* symbiosis. With the emergence of new genomic resources and proteomic-based experiments, we are likely to develop a more complete picture of transporter functions and mechanisms in symbiotic associations.

# Chapter 3: Proteomic changes show that thermally-tolerant *Symbiodinium* may impair host cellular processes

## 3.1 Introduction

The cnidarian-dinoflagellate symbiosis allows for the sustainability of biodiverse coral reef ecosystems within nutrient-limited oceans (Muscatine & Porter 1977). A range of cnidarian species can act as the host – such as corals, sea anemones, and jellyfish – while the symbionts are dinoflagellates from the genus *Symbiodinium* (Schoenberg & Trench 1980). Genetic diversity within the genus is extensive; the genus is classified into nine divergent clades, which are further subdivided into sub-clades or 'types', along with a handful of described species (Trench and Blank 1987; Coffroth and Santos 2005; Pochon and Gates 2010; LaJeunesse *et al.* 2012; LaJeunesse *et al.* 2015; Lee *et al.* 2015). Physiology and host specificity vary between *Symbiodinium* types, with a range of thermal tolerances (Rowan *et al.* 1997; Berkelmans & van Oppen 2006) and abilities to form associations with either multiple or just a single host species (van Oppen *et al.* 2001; Baker 2003; Santos *et al.* 2004; Xiang *et al.* 2013). The underlying cause of host-symbiont specificity is still not entirely clear, although it is linked to cellular interactions between partners (Lin *et al.* 2000; Bay *et al.* 2011; Davy *et al.* 2012).

Coral reefs worldwide are threatened by climate change, which is warming the oceans and inducing breakdown of the symbiosis, a process also known as coral bleaching (Hoegh-Guldberg *et al.* 2007). Coral bleaching often leads to host mortality, unless a symbiont population can quickly be re-established (Jokiel 2004). Some *Symbiodinium* types are more tolerant to higher temperatures (such as many members of clades A and D), therefore providing the host with more resistance to bleaching (Tchernov *et al.* 2004; Hennige *et al.* 2011; LaJeunesse *et al.* 2014; Hume *et al.* 2016). These thermally-tolerant algae can act as opportunists, where they replace the dominant symbiont type once its population numbers decline (Baker & Kelly 2004; Jones *et al.* 2008; LaJeunesse *et al.* 2009). *Symbiodinium* from clade D are the most common opportunists during times of thermal stress (Rowan 2004; LaJeunesse *et al.* 2009; Stat & Gates 2011). More specifically, *Symbiodinium* type D1a (*Symbiodinium trenchii*) is the most globally distributed symbiont type that commonly populates heat-stressed corals (LaJeunesse *et al.* 2014; Hoadley *et al.* 2016). The presence of opportunistic, thermally-tolerant algae has led to a theory that corals may adapt to climate

change by ‘shuffling’ or ‘switching’ their symbiont assemblages to accommodate clade D *Symbiodinium* (or other thermally tolerant symbiont types) as the dominant partner, thereby conferring a higher thermal tolerance on the entire holobiont (Baker *et al.* 2003; Berkelmans & van Oppen 2006; Baskett *et al.* 2009). Symbiont shuffling is described as a change in the relative abundance of existing symbiont types within a mixed assemblage of homologous (i.e. naturally occurring) symbionts, while symbiont switching is described as a complete change from the dominant homologous symbiont type to a heterologous (i.e. not naturally occurring) type acquired from the environment (Baker 2003). *S. trenchii* is thought to be a Pacific Ocean dinoflagellate that was introduced to the Atlantic and has since become invasive, as it is the only clade D symbiont found in the Caribbean (Pettay *et al.* 2015). In various Caribbean corals, *S. trenchii* exists as a background symbiont that becomes dominant when the host is under environmental stress (Correa *et al.* 2009; Grottoli *et al.* 2014; Kennedy *et al.* 2015). This demonstrates an interesting phenomenon that lies somewhere between the previously defined symbiont shuffling and switching, where a non-native symbiont colonizes heterologous hosts over time and can out-compete the homologous type under stress, but never completely replaces the homologous symbiont and returns to only minimal background populations once environmental conditions stabilize (Thornhill *et al.* 2006). This gives us evidence that heterologous symbioses can occur in nature, but it is unknown if they are capable of completely replacing the homologous type in the long-term.

Symbiotic interactions between cnidarians and *Symbiodinium* are thought to exist on a continuum from mutualism to parasitism (Lesser *et al.* 2013). Clades with thermally tolerant symbiont types can exhibit more parasitic qualities by impairing host metabolism and reproduction (Little *et al.* 2004; Stat *et al.* 2008; Jones & Berkelmans 2011; Pernice *et al.* 2014). For instance, both *Symbiodinium* clades A and D translocate less fixed carbon to their hosts than do other symbiont types (Stat *et al.* 2008; Pernice *et al.* 2014). Additionally, corals at the Keppel Islands infected with clade A were found to have the lowest survival and growth rates compared to corals infected with two other symbiont types (Mieog *et al.* 2009). Clade D also has an impact on growth rate, as seen by the two- to three-fold slower growth of juvenile corals infected with clade D compared to juveniles infected with Clade C (Little *et al.* 2004). Likewise, corals harbouring clade D contain less stored lipid, with smaller and less numerous eggs produced during spawning compared to counterparts harbouring clade C (Jones & Berkelmans 2011). However, while these previous studies provide evidence that clade D is a

less mutually beneficial symbiont, conferring reduced fitness even to its regular host species, the molecular effects of hosting this symbiont have never been investigated in a novel symbiosis. This therefore hinders our ability to understand the implications of hosting a heterologous, and potentially less beneficial, symbiont type. Indeed, cnidarians can be experimentally infected with a range of heterologous *Symbiodinium* types that can form long-term associations with the new host, though these are typically less successful than their homologous counterparts (Weis *et al.* 2001; Belda-Baillie *et al.* 2002; Dunn & Weis 2009). Examining the response of symbiotic cnidarians to infection by different symbiont types at the molecular, cellular and physiological levels, therefore provides a means of understanding the diverse, complex processes that undoubtedly underlie the formation of a successful cnidarian-dinoflagellate symbiosis, and which may dictate the capacity for partner switching and holobiont adaptation in the face of climate change.

Protein expression can be used to determine the effect of environmental conditions on an organism's cellular processes (Bradley *et al.* 2002). Therefore, proteomic analysis can be a powerful tool for elucidating the impacts of different symbiotic partners on a host cnidarian. Early research in this field reported differences in protein profiles between symbiotic and aposymbiotic host anemones (*Anthopleura elegantissima*) using Western blots, providing evidence that dinoflagellate symbionts directly affect host molecular biology (Weis & Levine 1996). Later, the cnidarian genes encoding for two of the symbiosis-upregulated proteins were identified as carbonic anhydrase (Weis & Reynolds 1999) and sym32, a cell adhesion protein (Reynolds *et al.* 2000). Investigations aimed at identifying additional host proteins involved in symbiosis have since begun using advanced quantitative methods such as liquid chromatography-nano electrospray-tandem mass spectrometry (LC-nano-ESI-MS/MS). Peng and co-workers (2010) conducted a proteomic analysis of isolated symbiosome membranes (i.e. host gastrodermal vesicles housing symbiont cells), identifying a small fraction of proteins derived from both host and symbiont (Peng *et al.* 2010). More recently, Oakley and co-workers (2016) identified host proteins of the model cnidarian *Aiptasia* that are associated with the symbiotic state, finding that host metabolism shifts to accommodate symbiotic nutrient exchange (Oakley *et al.* 2016). Furthermore, Oakley *et al.* (submitted) used the same methods to identify *Aiptasia* proteins associated with thermal stress, finding that heat shock induced a number of stress-related proteins in the host, while slower acclimation to a higher temperature had virtually no effect on the host proteome. While progress has been made on the

characterization of proteins involved in cnidarian-dinoflagellate cellular processes, there have yet to be any investigations on the impact of different symbiont types on the host proteome.

In this study, I compared the effect of a heterologous clade D *Symbiodinium versus* a homologous clade B *Symbiodinium* on the symbiotic cnidarian *Aiptasia* at the proteomic level. *Aiptasia* is an important, globally-adopted model system for the study of the cnidarian-dinoflagellate symbiosis (Weis *et al.* 2008). This approach provided a platform to elucidate the molecular processes and biological functions that determine the successful establishment and persistence of the cnidarian-dinoflagellate symbiosis, and the implications of harbouring a novel, thermally-tolerant but potentially less mutually beneficial symbiont type. Ultimately, this approach sheds light on the adaptive potential of the symbiosis by means of changing the dominant symbiont type, and informs subsequent, more specific examination of the coral-dinoflagellate symbiosis.

## 3.2 Methods

### *3.2.1 Experimental organisms*

Individuals of the symbiotic sea anemone *Aiptasia* sp. (= *ExAiptasia* sp.) (n ~ 750) were collected from a laboratory stock population, originating from an unknown Pacific location, and divided evenly into three 1.5 L beakers. Beakers were filled with 0.22 µm-filtered seawater (FSW) and aerated with Hailea® air pumps, and then placed in separate water baths maintained at 25$^{o}$C with WEIPRO® MX-1019 temperature controllers. Light was provided by AQUA-GLO T8 fluorescent lightbulbs at ~95 µmol photons $m^{-2}$ $s^{-1}$ on a 12 h:12 h light: dark cycle. These temperature and light conditions were maintained throughout the experiment.

Anemones were allowed to settle within beakers for 72 h, and then rendered aposymbiotic using the menthol treatment described in Matthews *et al.* (2016). At the end of treatment, a subset (n = 20) of anemones was checked for residual symbionts with a confocal microscope (Olympus Provis AX70, 40x magnification). Each anemone was placed into a glass-bottom FluoroDish™ (World Precision Instruments, FL, USA) and examined at 40x magnification

under a 543 nm laser with a 600-700 nm emission filter, exciting the chlorophyll autofluorescence from any remaining symbionts. Aposymbiotic individuals were divided amongst 15 containers with screw-top lids and placed into water baths designated for the three treatment groups: *Symbiodinium* B1 (*S. minutum*); *Symbiodinium* D1a (*S. trenchii*); and aposymbiotic.

*Symbiodinium* B1 and D1a were sub-cultured from laboratory stocks and grown in f/2 medium (Bigelow Laboratory, USA) at 25$^{o}$C under an irradiance of 100 µmol photons $m^{-2}$ $s^{-1}$ (OSRAM DULUX L 36W 4000K white fluorescent bulbs) on a 12 h:12 h light: dark cycle for six weeks prior to the infection experiment. A 1-mL aliquot from each culture was centrifuged for 1 min at 16,000 x g to pellet algae. The supernatant was then discarded and the pellet stored in 500 µL DMSO buffer [20% dimethyl sulfoxide and 0.5 M ethylene diaminetetraacetic acid (EDTA) in NaCl-saturated water] at 4$^{o}$C prior to genotyping (see below).

### *3.2.2 Infection of Aiptasia with Symbiodinium*

Prior to infection, anemones were starved for approximately one week to encourage the uptake of symbionts as a feeding response during the infection experiment. A subset of anemones from each treatment group (n ~ 20) were also examined with confocal microscopy (see above for details) one day prior to infection to ensure that they had maintained an aposymbiotic status.

*Symbiodinium* cells were harvested from the culture flasks and pipetted into 50 mL Falcon™ tubes. The tubes were centrifuged for 5 min at 1,000 x g to pellet algae, and then the supernatant was discarded. Algal cells were then re-suspended in 20 mL FSW, and these steps were repeated twice to wash the cells. After the final resuspension, cell density was quantified using an Improved Neubauer haemocytometer (six counts *per* sample). Cell densities of each *Symbiodinium* type were brought to a similar concentration (~ 3 x $10^{6}$ $mL^{-1}$) by dilution of the denser suspension with FSW.

Anemones were infected during the midpoint of the light cycle. A dilute suspension of freshly-hatched *Artemia* nauplii to induce phagocytosis was added to the *Symbiodinium* cultures and

gently mixed. Aerators were removed from the anemone containers 15 min before infection to encourage extension of tentacles, and a glass pipette then used to distribute the appropriate *Symbiodinium* suspension evenly onto the oral discs of all anemones in the corresponding treatment groups. Anemones in the aposymbiotic group were not infected with any *Symbiodinium* culture. After infection, all aerators were replaced and the FSW refreshed after two days. This infection process was repeated weekly for three weeks, and the anemones sampled at the fourth week.

### *3.2.3 Analysis of infection success*

Symbiont populations were assessed at the end of the experiment (four weeks post-infection). Individual anemones from the B1 and D1a treatment groups (n = 5 *per* treatment) were homogenized in 1 mL FSW, using Eppendorf micropestles followed by an IKA T-10 electric saw-tooth homogenizer to further break up animal tissue. The homogenate was separated into host and symbiont fractions by centrifugation for 5 min at 16,000 x g; the supernatant (host fraction) was removed and stored at -20$^{o}$C for protein analysis, and the pellet (symbiont fraction) re-suspended in 100 µL FSW with 1% formalin and stored at 4$^{o}$C for cell counts. Algal cells were counted with an Improved Neubaur haemocytometer at 100x magnification with a light microscope (six counts *per* sample). Cell counts were then normalized to host protein content as measured by the Bradford assay (Bradford, 1976). Anemones from the aposymbiotic treatment were observed under confocal microscopy as described previously, to determine if any background symbiont re-establishment may have affected experimental anemones. At the end of the experiment, three anemones each from the B1 and D1a treatments were processed to separate host and algal fractions as before. The algal fraction was stored in DMSO at 4$^{o}$C to use for *Symbiodinium* genotyping (see below).

*3.2.4 Symbiont verification*

DNA was extracted from the initial *Symbiodinium* cultures (n = 2) and the isolated symbiont fractions (n = 3 *per* symbiotic treatment) using the CTAB/phenol-chloroform protocol of Baker *et al.* (2004). Samples stored in DMSO were centrifuged at 16,000 x g for 5 min to pellet algal cells, and the DMSO then removed. Algal pellets were added to 1% SDS in DNA buffer (0.4 M NaCl, 50 mM EDTA, dd$H_2O$, pH = 8), vortexed, and then incubated for 60 min at 65ºC. After incubation, a 100 µL aliquot of the sample was added to 5 µL of Proteinase K and incubated overnight at 37ºC. Room temperature CTAB mix was added to twice the volume (210 µL), and then incubated for 30-60 min at 65ºC. After allowing samples to cool, 315 µL chloroform were added and left on a rotating mixer for 2-3 h. Samples were centrifuged at 10,000 x g for 10 min, and the supernatant (~250 µL) then transferred to a new tube. Twice the volume (500 µL) of chilled 100% ethanol was mixed into samples, which were then kept at -20ºC for 30 min to precipitate DNA. Next, samples were centrifuged for 10 min at 10,000 x g and the supernatant discarded. The samples were dried in an Eppendorf Concentrator 5301 for 30 min at 45ºC, after which 100 µL 0.3 M NaOAc were added to dissolve the pellet. Then, 200 µL 100% ethanol were added, and the sample mixed and stored at -20ºC for 2 h. After defrosting, samples were centrifuged for 10 min at 10,000 x g and the supernatant discarded. The pellets were dried thoroughly as before, and then re-suspended in 50 µL TE buffer and analysed with PCR.

Extracted DNA was used for PCR with the outer primers ITSintfor2 (forward; 5'-GAATTGCAGAACTCCGTG-3') and ITS2Rev2 (reverse; 5'-CCTCCGCTTACTTATATGCTT-3'). The thermal cycling regime had an initial denaturation step of 3 min at 95ºC, followed by 40 cycles of 15 s at 95ºC, 15 s at 56ºC, and 10 s at 72ºC (performed with an Applied Biosystems Veriti thermo-cycler). Each reaction contained 1 µL DNA template, 12.5 µL 1x MyTaq PCR reaction mix (Bioline, Randolph, MA, USA), 1.5 µL each primer, 2 µL 10 mg/mL bovine serum albumin (Sigma Alrich, Auckland, New Zealand), and 6.5 µL deionised sterile water to a final volume of 25 µL. PCR products were cleaned with ExoSAP-IT (USB Corporation, Cleveland, OH, USA) and sequenced by the Macrogen Sequencing Service (Macrogen Inc., Seoul, South Korea). Sequences were aligned with Geneious v. 7.0 (Biomatters Ltd., Auckland, New Zealand) and a BLAST search was carried

out against *Symbiodinium* ITS2 sequences in GenBank. Sequences of the initial infection cultures were compared with those extracted from anemones at the end of the experiment to confirm symbiont identities.

### *3.2.5 Protein extraction*

Three weeks post-infection, anemones (n = 6 *per* treatment) were harvested for proteomic analysis. Individuals were homogenized with an IKA T-10 electric saw-tooth homogenizer, and then separated into host and symbiont fractions by centrifugation as described in section 3.2.3. Eppendorf™ LoBind microcentrifuge tubes for protein research were used in all of the following extraction steps. For each sample, 15 µg protein were combined with a lysis buffer consisting of 5% sodium deoxycholate, 100 mM dithiothreitol and 50 mM triethylammonium bicarbonate. The samples were then incubated for 15 min at 90ºC, followed by 15 min at 60ºC. Next, samples were centrifuged at 16,000 x g for 5 min to pellet cell debris and the supernatant transferred to a new tube. Iodoacetamide was added to a final concentration of 50 mM and samples then incubated in the dark, at room temperature, for 30 min. Samples were subsequently diluted ten-fold with HPLC-grade water (Sigma-Aldrich, Auckland, NZ) and vortexed briefly to mix. Next, 1 µg trypsin was added to each tube followed by incubation at 37ºC for 18 h to allow enzyme digestion. After incubation, trifluoroacetic acid was added to a final concentration of 0.5% and vortexed to mix. Samples were then centrifuged for 10 min at 16,000 x g to pellet precipitate and the supernatant transferred to a new tube. Sample volumes were then concentrated to < 500 µL using an Eppendorf Concentrator 5301 set to 45ºC, for approximately 1 h. The resulting peptides were desalted with Millipore® Ziptips $C_{18}$ (Omix Bond Elut, Agilent Technologies) before resuspension in 0.1% formic acid. All materials were acquired from Sigma Aldrich (Auckland, New Zealand).

### *3.2.6 Identification of proteins using LC-MS/MS*

Peptides were analysed by liquid chromatography-tandem mass-spectrometry in a LTQ Orbitrap XL (Thermo Scientific) using settings based on those described in Oakley *et al.* (2016). Peptide separation was achieved using liquid chromatography (Ultimate 3000, Dionex)

with an Acclaim PepMap C18 column (#160321, Thermo Scientific), while the column oven was set to 35ºC. Chromeleon Xpress software (v2.11.0.2914, Dionex) was used to conduct a 300-min nonlinear gradient from 96% buffer A (0.1% formic acid) to 50% buffer B (80% acetonitrile, 0.1% formic acid) at a flow rate of 0.3 µL $min^{-1}$. GOAT software (version 1.0.1) (Trudgian *et al.* 2014) was used to optimize the gradient, based on the initial run, to yield maximal protein identifications.

Peptides were ionized with an electrospray needle source at 1.9 kV spray voltage and injected into an LTQ Orbitrap XL (Thermo Scientific), operated using Thermo Xcalibur (v2.1, Thermo Scientific) software. The Orbitrap analysed MS spectra at 30,000 resolution before collision fractionation, and the ion trap then analysed MS/MS spectra by taking the top eight MS peaks while rejecting +1 charge states. A dynamic exclusion of 180 s was used to minimize repetitious peptide analysis. Other instrument settings were based on those of Kalli and Hess (2012).

The resulting spectra were searched against a custom *Aiptasia* database of 320,798 total sequences, and were processed by MScDb software (Marx *et al.* 2013) to reduce peptide-level redundancy. The database was constructed from the *Aiptasia* genome (Baumgarten *et al.* 2015), all cnidarian sequences from UniProt (28/4/14 release, Swiss-Prot and TrEMBL), all open reading frames from the *Aiptasia* CC7 transcriptome (Lehnert *et al.* 2012), and a contaminant database (CRAPome v1.0) (Mellacheruvu *et al.* 2013). MS peaks were extracted by Proteome Discoverer (v2.1, Thermo Scientific) and analysed using Sequest (Thermo Fisher Scientific) and X! Tandem (The GPM, v CYCLONE (2010.12.01.1)). Both Sequest and X! Tandem searches assumed trypsin as the digestion enzyme, with a fragment ion mass tolerance of 0.60 Da and a parent ion tolerance of 10 PPM. Both searches also included carbamidomethyl of cysteine as a fixed modification. In Sequest, oxidation of methionine and carbamylation of the n-terminus were specified as variable modifications. In X! Tandem, Glu->pyro-Glu of the n-terminus, ammonia-loss of the n-terminus, gln->pyro-Glu of the n-terminus, oxidation of methionine, and carbamylation of the n-terminus were specified as variable modifications.

Scaffold (v4.4.8, Proteome Software, Inc.) was used to validate MS/MS based peptide and protein identifications. Peptide identifications were accepted if they were established at > 99% probability by the Scaffold Local FDR algorithm. Protein identifications were accepted if they were established at > 99% probability and contained a minimum of two identified peptides. Protein probabilities were assigned by the Protein Prophet algorithm (Nesvizhskii *et al.* 2003). Proteins that contained similar peptides and could not be differentiated based on MS/MS analysis alone were grouped together to satisfy the principles of parsimony. Proteins sharing significant peptide evidence were grouped into clusters.

### *3.2.7 Statistical analysis*

Symbiont cell density and P:R values were tested for significant differences between B1 and D1a groups using a t-test in SPSS statistical software (v. 20, IBM Corporation).

Proteins were quantified by Precursor Intensity (PI) in Scaffold and statistical analyses were conducted in R v. 3.3.1 (www.r-project.org). To identify protein clusters with significant differences between treatments, a custom R script (developed by S.P. Wilkinson, Victoria University of Wellington) for multivariate analysis with *post hoc* identifications was used, according to the parameters described in Oakley *et al.* (submitted). First, a scaling factor was applied to correct for any differences in protein loading between samples. This was done by calculating a pairwise matrix of the scaling factors as each sample (x) against each other sample (y), as the median of the vector:

$$\frac{x_i}{y_i}\ i = \ 1, 2, 3, \ldots, m$$

Where *m* is the total number of proteins that were detected in the total number (18) of samples. The sample with the lowest protein loading depth from the reference treatment, cell type B1, was identified as the matrix column with the lowest average scaling factor. All other samples were then normalized using the reference sample column. To fit the model to parametric assumptions, PI values were assigned for low-abundance protein clusters where concentrations were below the detection limit of the instrument ('non-detects'). Protein clusters consisting of > 75% non-detects were removed from the dataset, and any non-detects in the remaining clusters were imputed by robust regression on order statistics (assuming a log-normal distribution) using the R package 'NADA'. Next, protein clusters that were significantly

different between treatments were identified. For multivariate analysis of treatment effects, the dataset was log transformed and Bray-Curtis dissimilarities calculated for each pairwise sample comparison. Analysis of variance by permutation of dissimilarities was carried out using the 'adonis' function in the 'vegan' R package (v2.2-1). To test for differences in individual protein clusters between treatments, a generalized linear model (GLM) with treatment effects was fitted and compared against an intercept-only null model using an analysis of deviance $X^2$ test, where $\alpha = 0.05$. Protein clusters with significantly different concentrations between treatments were identified with the false discovery rate (FDR) correction method of Benjamini & Hochberg (1995), at a *q*-threshold of 0.05. The procedure was repeated 100 times, with randomization of imputed values to prevent the regression on order statistics imputation from skewing the results.

Proteins that were significantly different between treatments were retrieved from the database and BLAST searched against the UniProtKB database using Geneious v.10.0.2. The top reviewed hit for each protein with an E value $\leq 1 \times 10^{-5}$ was used to assign an annotation, and any without a match under this threshold were designated as hypothetical proteins. Blast2GO Basic v 4.0.7 (Conesa *et al.* 2005) was used to map gene ontology (GO) terms to significantly different proteins.

## 3.3 Results

### *3.3.1 Infection success*

Examination of anemones in the aposymbiotic control treatment at the end of the experiment revealed no re-establishment of background symbionts. Additionally, *Symbiodinium* genotyping confirmed symbionts at the end of the experiments matched the *Symbiodinium* B1 and *Symbiodinium* D1a cultures originally used for infection. Symbiont cell densities in anemones infected with *Symbiodinium* B1 (average of $1.12 \times 10^{+7} \pm 1.16 \times 10^{+6}$ std. error) were 1.5-fold higher (d.f. = 1, $t = 2.36$, $p = 0.04$) than those in anemones infected with *Symbiodinium* D1a (average of $7.29 \times 10^{+6} \pm 1.19 \times 10^{+6}$).

### *3.3.2 Proteins unique to treatment groups*

A total of 1,608 protein clusters (from here on referred to solely as "proteins") were identified between all treatments, while 31 decoy sequences were discarded and 276 sequences were not analysed further due to having more than 75% non-detects. From the remaining 1,301 proteins, 966 had at least one value imputed. Across all 100 iterations, multivariate *p*-values for the differentially-expressed proteins in the GLM analysis were < 0.05. Overall, 142 identified proteins were significantly different between the three treatments (i.e. aposymbiotic; *Symbiodinium* B1; *Symbiodinium* D1a). After accounting for hypothetical proteins, 128 sequences were annotated using sequence similarities from the UniProtKB database. Between the B1 and aposymbiotic treatments, 105 significantly different proteins were found (Table 3.1); between the D1a and aposymbiotic treatments, 108 significantly different proteins were found (Table 3.2); and between the B1 and D1a treatments, 22 significantly different proteins were found (Table 3.3). While 124 of these proteins were found in all treatment groups, 18 were exclusive to only one or two of the treatments (Fig. 3.1).

**Table 3.1**. Proteins significantly different between *Symbiodinium* B1 and aposymbiotic treatments, in order of fold-change from B1 to Apo. Colour scale in first column indicates degree of protein upregulation in B1 (green) to aposymbiotic (red) anemones. Green and pink shaded rows are those proteins previously found to be significantly different between symbiotic and aposymbiotic anemones, respectively, in Oakley *et al.* (2016).

| B1-Apo Fold Change | Sequence ID | Proteins in Cluster | Best Annotation Match | Accession | Matched Species | E value | % Pairwise Identity |
|---|---|---|---|---|---|---|---|
| 1175.53 | AIPGENE22527 | 1 | Protein NPC2 homolog | Q9VQ62 | *Drosophila melanogaster* | 2.98E-26 | 37.9% |
| 383.67 | AIPGENE22473 | 1 | Niemann Pick type C2 protein homolog | P79345 | *Bos taurus* | 1.80E-19 | 29.9% |
| 62.28 | AIPGENE3015 | 1 | DELTA-alicitoxin-Pse2a | P58911 | *Phyllodiscus semoni* | 4.56E-151 | 63.7% |
| 49.27 | AIPGENE1278 | 1 | Unconventional myosin-XVIIIa | Q92614 | *Homo sapiens* | 0 | 33.1% |
| 30.12 | Q6S3M2 | 1 | Glutamine synthetase | P09606 | *Rattus norvegicus* | 0 | 68.4% |
| 28.59 | AIPGENE6975 | 2 | Fibronectin type III domain-containing protein | B8VIW9 | *Acropora millepora* | 5.65E-165 | 33.3% |
| 28.15 | BAB83090.1 | 1 | Carbonic anhydrase 2 | Q8UWA5 | *Tribolodon hakonensis* | 4.18E-41 | 44.7% |
| 21.90 | AIPGENE2901 | 1 | Carbonic anhydrase 2 | Q8UWA5 | *Tribolodon hakonensis* | 1.90E-56 | 38.0% |
| 21.87 | AIPGENE13275 | 1 | Circumsporozoite protein | P06915 | Plasmodium berghei | 4.20E-17 | 37.0% |
| 21.73 | AIPGENE9787 | 2 | Tropomyosin-1 | P39921 | *Hydra vulgaris* | 3.50E-17 | 32.1% |
| 21.70 | AIPGENE1237 | 1 | Hypothetical protein | KXJ28962.1 | *ExAiptasia pallida* | 1.20E-15 | 100% |
| 21.19 | AIPGENE27968 | 1 | Hypothetical protein | KXJ18477.1 | *ExAiptasia pallida* | 3.18E-77 | 100% |
| 20.27 | AIPGENE21668 | 1 | EGF and laminin G domain-containing protein | B8UU78 | *Acropora millepora* | 0 | 36.5% |
| 18.96 | BAB89358.1 | 2 | Calcyphosin-like protein | Q6P8Y1 | *Mus musculus* | 6.70E-69 | 47.8% |
| 16.41 | AIPGENE11024 | 2 | Hemicentin-2 | A2AJ76 | *Mus musculus* | 9.61E-17 | 24.5% |
| 16.33 | AIPGENE22517 | 4 | Isoform 4 of Golgin subfamily B member 1 | Q14789-4 | *Homo sapiens* | 2.60E-87 | 20.9% |
| 15.94 | EDO34868.1 | 1 | 40S ribosomal protein S19 | Q8T5Z4 | *Branchiostoma belcheri* | 4.38E-70 | 69.1% |
| 13.31 | AIPGENE9034 | 1 | Serine/arginine-rich splicing factor 4 | Q8VE97 | *Mus musculus* | 2.31E-64 | 56.7% |
| 12.90 | EDO49557.1 | 1 | Muscle M-line assembly protein unc-89 | KXJ27993.1 | *ExAiptasia pallida* | 1.25E-35 | 68% |
| 12.73 | EDO46723.1 | 1 | Calponin-1 | P26932 | *Gallus* | 1.24E-18 | 32.9% |
| 12.71 | EDO35342.1 | 1 | Hypothetical protein | KXJ25875.1 | *ExAiptasia pallida* | 8E-93 | 100% |
| 12.50 | A7S6S5 | 1 | Glutamine synthetase | P15103 | *Bos taurus* | 0 | 67.6% |
| 12.38 | EDO43201.1 | 1 | Actin-binding LIM protein 1 | O14639 | *Homo sapiens* | 1.58E-87 | 41.4% |
| 11.68 | Q09Y99 | 1 | Caspase-7 | P55214 | *Mesocricetus auratus* | 1.34E-67 | 45.6% |
| 10.55 | A7RP49 | 2 | Solute carrier family 8 member 1 | P48765 | *Bos taurus* | 0 | 54.0% |
| 9.93 | EDO40093.1 | 2 | von Willebrand factor D and EGF domain-containing protein | Q8N2E2 | *Homo sapiens* | 2.24E-25 | 32.6% |
| 9.76 | EDO39668.1 | 1 | Tropomyosin | Q8WR63 | *Trichinella pseudospiralis* | 7.34E-16 | 30.6% |

**Table 3.1** continued

| | | | | | | | |
|---|---|---|---|---|---|---|---|
| 9.30 | AIPGENE26879 | 1 | NADH dehydrogenase iron-sulfur protein 6, mitochondrial | P52503 | *Mus musculus* | 3.50E-39 | 56.1% |
| 9.16 | EDO41848.1 | 1 | Tropomodulin-1 | A0JNC0 | *Bos taurus* | 2.22E-74 | 40.4% |
| 8.28 | EDO29941.1 | 1 | Multifunctional protein ADE2 | P38024 | *Gallus gallus* | 1.15E-180 | 65.6% |
| 8.06 | AIPGENE7641 | 1 | Flotillin-2 | O61492 | *Drosophila melanogaster* | 0 | 65.0% |
| 7.87 | AIPGENE435 | 2 | Succinate--CoA ligasesubunit alpha, mitochondrial | P13086 | *Rattus norvegicus* | 4.58E-154 | 72.1% |
| 7.83 | AIPGENE6089 | 2 | Ras-like protein RAS2 | P38976 | *Hydra vulgaris* | 1.01E-89 | 74.1% |
| 7.78 | A7SGL1 | 1 | Protein disulfide-isomerase A6 | Q922R8 | *Mus musculus* | 0 | 60.0% |
| 7.50 | AIPGENE21644 | 1 | Muscle M-line assembly protein unc-89 | O01761 | *Caenorhabditis elegans* | 0.00E+00 | 26.5% |
| 7.34 | EDO43005.1 | 1 | Aprataxin and PNK-like factor | Q8IW19 | *Homo sapiens* | 4.33E-21 | 32.0% |
| 7.28 | AIPGENE3143 | 1 | DELTA-thalatoxin-Avl2a | Q76DT2 | *Actineria villosa* | 0.00E+00 | 59.7% |
| 6.67 | KXJ26680.1 | 1 | Rootletin | Q5TZA2 | *Homo sapiens* | 0 | 40.6% |
| 6.57 | A7RZ15 | 6 | Erythrocyte band 7 integral membrane protein | P27105 | *Homo sapiens* | 2.40E-129 | 72.3% |
| 6.44 | AIPGENE20022 | 3 | Hypothetical protein | KXJ13090.1 | *ExAiptasia pallida* | 0 | 99% |
| 6.10 | AIPGENE6448 | 2 | cGMP-dependent protein kinase 1 | O77676 | *Oryctolagus cuniculus* | 0 | 63.6% |
| 5.89 | EDO43151.1 | 1 | Hypothetical protein | KXJ24863.1 | *ExAiptasia pallida* | 3.48E-23 | 100% |
| 5.71 | AIPGENE7839 | 1 | Hypothetical protein | KXJ11047.1 | *ExAiptasia pallida* | 0 | 99% |
| 5.48 | AIPGENE13174 | 1 | Hypothetical protein | KXJ30118.1 | *Terebra subulata* | 4.05E-91 | 99% |
| 4.92 | AIPGENE19216 | 1 | Acid ceramidase | A5A6P2 | *Pan troglodytes* | 1.18E-102 | 41.6% |
| 4.61 | AIPGENE2351 | 1 | Peroxiredoxin-6 | Q9TSX9 | *Sus scrofa* | 1.01E-69 | 66.9% |
| 4.41 | AAR24460.1 | 2 | Tropomyosin | Q95VA8 | *Trichinella spiralis* | 2.53E-53 | 46.8% |
| 4.05 | A7STP5 | 1 | GTPase Kras | P79800 | *Meleagris gallopavo* | 4.80E-105 | 86.7% |
| 3.66 | EDO48626.1 | 2 | Heat shock protein HSP 90-beta | O57521 | *Danio rerio* | 0 | 78.5% |
| 3.63 | AIPGENE28926 | 1 | Myotrophin | Q91955 | *Gallus gallus* | 4.07E-19 | 38.6% |
| 3.49 | AIPGENE29213 | 3 | Gelsolin-like protein 1 | Q7JQD3 | *Lumbricus terrestris* | 1.56E-122 | 51.2% |
| 3.00 | AIPGENE13249 | 1 | Microtubule-associated protein RP/EB family member 1 | Q6V291 | *Coturnix coturnix* | 4.74E-94 | 51.7% |
| 2.85 | AIPGENE3056 | 1 | Calpain-9 | O35920 | *Rattus norvegicus* | 0 | 46.0% |
| 2.69 | AIPGENE700 | 1 | Tubulin polymerization-promoting protein family member 2 | Q3T077 | *Bos taurus* | 2.42E-42 | 50.6% |
| 2.62 | AIPGENE23774 | 4 | Myosin-like antigen | P21249 | Onchocerca volvulus | 4.91E-07 | 50.6% |
| 2.55 | AIPGENE16749 | 1 | Talin-2 | Q9Y4G6 | *Homo sapiens* | 0 | 49.2% |
| 2.38 | EEN66183.1 | 1 | Protein NPC2 homolog | Q9VQ62 | *Drosophila melanogaster* | 6.57E-24 | 49.4% |

**Table 3.1** continued

| | | | | | | | |
|---|---|---|---|---|---|---|---|
| 2.01 | AIPGENE27021 | 1 | U-actitoxin-Avd8a | P0DMZ3 | *Anemonia viridis* | 5.43E-19 | 45.8% |
| 1.96 | AIPGENE19130 | 1 | Myophilin | Q24799 | *Echinococcus granulosus* | 6.57E-36 | 41.4% |
| 1.85 | EDO46722.1 | 2 | Myophilin | Q24799 | *Echinococcus granulosus* | 2.96E-31 | 37.9% |
| 1.84 | EDO36481.1 | 2 | ZP domain-containing protein | G8HTB6 | *Acropora millepora* | 4.01E-75 | 39.3% |
| 1.75 | EDO45013.1 | 37 | Actin | P12716 | *Pisaster ochraceus* | 3.25E-113 | 89.4% |
| 1.69 | AAH90759.1 | 2 | 14-3-3 protein epsilon; Short=14-3-3E | P62258 | *Homo sapiens* | 8.35E-109 | 65.6% |
| 1.63 | AIPGENE28714 | 3 | Hypothetical protein | KXJ10810.1 | *ExAiptasia pallida* | 0 | 99% |
| 1.50 | KXJ18065.1 | 3 | Catalase | P04040 | *Homo sapiens* | 0 | 71.9% |
| 0.75 | A7SHH5 | 1 | Protein disulfide-isomerase | P05307 | *Bos taurus* | 0 | 59.5% |
| 0.56 | EDO37116.1 | 1 | Putative aminopeptidase W07G4.4 | Q27245 | *Caenorhabditis elegans* | 5.84E-26 | 44.7% |
| 0.56 | EDO42526.1 | 2 | Hydroxysteroid dehydrogenase-like protein 2 | A4FUZ6 | *Bos taurus* | 0 | 62.3% |
| 0.55 | EDO49845.1 | 1 | Beta-hexosaminidase subunit alpha | P06865 | *Homo sapiens* | 2.85E-158 | 47.6% |
| 0.52 | AIPGENE12299 | 4 | Glyceraldehyde-3-phosphate dehydrogenase | O57479 | *Columba livia* | 0.00E+00 | 73.2% |
| 0.50 | EDO44966.1 | 6 | Abscisic-aldehyde oxidase | Q7G9P4 | *Arabidopsis thaliana* | 0 | 35.6% |
| 0.50 | KXJ18065.1 | 3 | Catalase | P04040 | *Homo sapiens* | 0 | 71.9% |
| 0.50 | AIPGENE26156 | 2 | Cathepsin L | Q26636 | *Sarcophaga peregrina* | 1.54E-125 | 55.3% |
| 0.46 | AIPGENE26035 | 1 | Lysine-specific demethylase 8 | B2GUS6 | *Xenopus tropicalis* | 8.26E-18 | 27.3% |
| 0.42 | AIPGENE4246 | 4 | Cholinesterase | P21927 | *Oryctolagus cuniculus* | 1.20E-107 | 35.7% |
| 0.41 | AIPGENE13554 | 2 | Creatinase | P38487 | *Bacillus sp. (strain B-0618)* | 7.61E-134 | 66.6% |
| 0.41 | AIPGENE27013 | 1 | Hypothetical protein | KXJ29487.1 | *ExAiptasia pallida* | 1.27E-154 | 99% |
| 0.40 | EDO48107.1 | 2 | Dipeptidyl peptidase 2 | Q9EPB1 | *Rattus norvegicus* | 1.99E-112 | 51.9% |
| 0.37 | EEN57628.1 | 2 | Alpha-aminoadipic semialdehyde dehydrogenase | Q2KJC9 | *Bos taurus* | 0 | 67.2% |
| 0.35 | AIPGENE2301 | 2 | Carbonyl reductase [NADPH] 1 | P48758 | *Mus musculus* | 5.66E-84 | 50.8% |
| 0.30 | AIPGENE473 | 3 | Cathepsin Z | P05689 | *Bos taurus* | 3.04E-129 | 64.3% |
| 0.29 | EDO47653.1 | 2 | Aldehyde dehydrogenase, mitochondrial | P11884 | *Rattus norvegicus* | 0 | 72.7% |
| 0.28 | AIPGENE22562 | 1 | Inosine-uridine preferring nucleoside hydrolase | P83851 | *Leishmania major* | 2.64E-19 | 31.3% |
| 0.27 | AIPGENE7506 | 2 | Pirin-like protein | Q9SEE4 | *Solanum lycopersicum* | 1.10E-74 | 43.6% |
| 0.27 | AIPGENE6148 | 1 | Lysosomal alpha-mannosidase | Q60HE9 | *Macaca fascicularis* | 0 | 49.1% |
| 0.24 | EDO36900.1 | 1 | Nematocyst expressed protein 6 | K7Z9Q9 | *Nematostella vectensis* | 2.55E-74 | 58.8% |

**Table 3.1** continued

| | | | | | | | |
|---|---|---|---|---|---|---|---|
| 0.24 | EDO40873.1 | 3 | Creatinase | P19213 | *Flavobacterium sp. (strain U-188)* | 0 | 61.8% |
| 0.20 | EDO44805.1 | 1 | Universal stress protein A-like protein | Q8LGG8 | *Arabidopsis thaliana* | 1.10E-18 | 28.3% |
| 0.16 | EDO46736.1 | 1 | Homogentisate 1,2-dioxygenase | O09173 | *Mus musculus* | 0 | 67.6% |
| 0.15 | EDO31703.1 | 4 | Transmembrane protease serine 3 | Q8K1T0 | *Mus musculus* | 7.08E-53 | 40.9% |
| 0.14 | AIPGENE13027 | 2 | Alpha-N-acetylgalactosaminidase | Q90744 | *Gallus gallus* | 8.01E-158 | 55.0% |
| 0.13 | AIPGENE10977 | 1 | Betaine--homocysteine S-methyltransferase 1 (BHMT1) | Q5M8Z0 | *Xenopus tropicalis* | 0 | 61.9% |
| 0.13 | AIPGENE5163 | 1 | Urocanate hydratase | Q96N76 | *Homo sapiens* | 0 | 65.8% |
| 0.11 | KXJ15780.1 | 1 | Mesencephalic astrocyte-derived neurotrophic factor homolog | B4QX46 | *Drosophila simulans* | 2.01E-60 | 57.8% |
| 0.10 | EDO45852.1 | 1 | Cathepsin L | Q95029 | *Drosophila melanogaster* | 9.41E-132 | 59.7% |
| 0.08 | A7RLS5 | 1 | Aldehyde dehydrogenase, mitochondrial | P05091 | *Rattus norvegicus* | 0 | 71.8% |
| 0.08 | A7RIN6 | 1 | S-methylmethionine--homocysteine S-methyltransferase (BHMT2) | Q5RF32 | *Pongo abelii* | 7.54E-137 | 57.6% |
| 0.07 | EDO39870.1 | 1 | Beta-galactosidase | Q58D55 | *Bos taurus* | 1.22E-147 | 45.8% |
| 0.06 | 52902 | 1 | Heat shock 70 kDa protein A | P09446 | *Caenorhabditis elegans* | 5.94E-44 | 88.5% |
| 0.06 | AIPGENE28006 | 2 | Alpha-N-acetylglucosaminidase | P54802 | *Homo sapiens* | 0 | 47.7% |
| 0.04 | AIPGENE12842 | 1 | Hypothetical protein | KXJ12770.1 | *ExAiptasia pallida* | 0 | 99% |
| 0.04 | AIPGENE25444 | 1 | Oxidoreductase HTATIP2 | Q9Z2G9 | *Mus musculus* | 1.28E-30 | 37.5% |
| 0.03 | 12437 | 1 | Calmodulin-like protein 1 | Q9ZQE6 | *Arabidopsis thaliana* | 2.45E-04 | 33.8% |
| 0.00 | AIPGENE8259 | 1 | Persulfide dioxygenase ETHE1, mitochondrial | O95571 | *Homo sapiens* | 5.54E-90 | 56.0% |
| 0.00 | EDO47743.1 | 3 | Betaine--homocysteine S-methyltransferase 1 (BHMT1) | Q95332 | *Sus scrofa* | 6.96E-120 | 72.4% |

**Table 3.2** Proteins significantly different between *Symbiodinium* D1a and aposymbiotic treatments, in order of fold-change from D1a to Apo. Colour scale in first column indicates degree of protein upregulation in D1a (yellow) to aposymbiotic (red) anemones. Green and pink shaded rows were also found to be significantly different proteins between symbiotic and aposymbiotic anemones, respectively, in Oakley *et al.* (2016).

| D1a-Apo Fold Change | Sequence ID | Proteins in Cluster | Best Annotation Match | Accession | Matched Species | E value | % Pairwise Identity |
|---|---|---|---|---|---|---|---|
| 199.95 | EDO34868.1 | 1 | 40S ribosomal protein S19 | Q8T5Z4 | *Branchiostoma belcheri* | 4.38E-70 | 69.1% |
| 184.64 | AIPGENE3015 | 1 | DELTA-alicitoxin-Pse2a | P58911 | *Phyllodiscus semoni* | 4.56E-151 | 63.7% |
| 89.17 | AIPGENE6975 | 2 | Fibronectin type III domain-containing protein | B8VIW9 | *Acropora millepora* | 5.65E-165 | 33.3% |
| 50.82 | AIPGENE9787 | 2 | Tropomyosin-1 | P39921 | *Hydra vulgaris* | 3.50E-17 | 32.1% |
| 47.21 | AIPGENE27968 | 1 | Hypothetical protein | KXJ18477.1 | *ExAiptasia pallida* | 3.18E-77 | 100% |
| 45.25 | AIPGENE21668 | 1 | EGF and laminin G domain-containing protein | B8UU78 | *Acropora millepora* | 0 | 36.5% |
| 40.13 | BAB89358.1 | 2 | Calcyphosin-like protein | Q6P8Y1 | *Mus musculus* | 6.70E-69 | 47.8% |
| 39.74 | EDO42416.1 | 2 | Cell surface glycoprotein 1 | Q06852 | *Clostridium thermocellum* | 1.26E-10 | 45.2% |
| 35.61 | A7RIX7 | 2 | Proteasome subunit alpha type-6 | Q9QUM9 | *Mus musculus* | 7.65E-160 | 84.1% |
| 35.42 | EDO37221.1 | 1 | 40S ribosomal protein S6 | P62755 | *Rattus norvegicus* | 6.46E-123 | 84.8% |
| 32.46 | AIPGENE1237 | 1 | Hypothetical protein | KXJ28962.1 | *ExAiptasia pallida* | 1.20E-15 | 100% |
| 23.85 | EDO39668.1 | 1 | Tropomyosin | Q8WR63 | *Xenopus laevis* | 7.34E-16 | 30.6% |
| 22.19 | AIPGENE16941 | 1 | 60S acidic ribosomal protein P0 | Q9DG68 | *Rana sylvatica* | 2.59E-153 | 70.5% |
| 21.86 | EDO43151.1 | 1 | Hypothetical protein | KXJ24863.1 | *ExAiptasia pallida* | 3.48E-23 | 100% |
| 21.85 | EDO36394.1 | 1 | Predicted protein | XP_001628457.1 | *Nematostella vectensis* | 1.14E-105 | 63.0% |
| 21.26 | EDO43201.1 | 1 | Actin-binding LIM protein 1 | O14639 | *Homo sapiens* | 1.58E-87 | 41.4% |
| 19.68 | AIPGENE22517 | 4 | Isoform 4 of Golgin subfamily B member 1 | Q14789-4 | *Homo sapiens* | 2.60E-87 | 20.9% |
| 19.14 | AIPGENE3128 | 1 | DELTA-alicitoxin-Pse2a | P58911 | *Phyllodiscus semoni* | 0.00E+00 | 59.6% |
| 17.09 | BAB83090.1 | 1 | Carbonic anhydrase 2 | Q8UWA5 | *Tribolodon hakonensis* | 4.18E-41 | 44.7% |
| 16.71 | EDO45498.1 | 2 | Beta-hexosaminidase | Q04786 | *Vibrio vulnificus* | 1.04E-171 | 37.6% |
| 16.38 | AIPGENE2901 | 1 | Carbonic anhydrase 2 | Q8UWA5 | *Tribolodon hakonensis* | 1.90E-56 | 38.0% |
| 16.08 | EDO41848.1 | 1 | Tropomodulin-1 | A0JNC0 | *Bos taurus* | 2.22E-74 | 40.4% |
| 15.30 | AIPGENE1278 | 1 | Unconventional myosin-XVIIIa | Q92614 | *Homo sapiens* | 0 | 33.1% |
| 14.32 | EDO29941.1 | 1 | Multifunctional protein ADE2 | P38024 | *Gallus gallus* | 1.15E-180 | 65.6% |
| 13.93 | A7SGL1 | 1 | Protein disulfide-isomerase A6 | Q922R8 | *Mus musculus* | 0 | 60.0% |
| 13.37 | EDO39721.1 | 1 | Guanine nucleotide-binding protein subunit beta-2-like 1 | O42248 | *Danio rerio* | 0 | 80.8% |
| 13.26 | AIPGENE7641 | 1 | Flotillin-2 | O61492 | *Drosophila melanogaster* | 0 | 65.0% |

**Table 3.2** continued

| | | | | | | | |
|---|---|---|---|---|---|---|---|
| 13.24 | AIPGENE3067 | 2 | DELTA-thalatoxin-Avl2a | Q76DT2 | *Actineria villosa* | 0 | 62.5% |
| 13.15 | 47580 | 2 | Rootletin | Q5TZA2 | *Homo sapiens* | 0 | 40.6% |
| 12.86 | EDO26161.1 | 1 | Hypothetical protein | KXJ12230.1 | *ExAiptasia pallida* | 7.80E-147 | 100% |
| 12.32 | AIPGENE9796 | 1 | SH3 domain-binding glutamic acid-rich-like protein 3 | Q91VW3 | *Mus musculus* | 6.15E-20 | 43.3% |
| 10.89 | AIPGENE20022 | 3 | Hypothetical protein | KXJ13090.1 | *ExAiptasia pallida* | 0 | 99% |
| 10.65 | A7RZ15 | 6 | Erythrocyte band 7 integral membrane protein | P27105 | *Homo sapiens* | 2.40E-129 | 72.3% |
| 10.38 | AAR24460.1 | 2 | Tropomyosin | Q95VA8 | *Trichinella spiralis* | 2.53E-53 | 46.8% |
| 9.43 | AIPGENE435 | 2 | Succinate--CoA ligase [ADP/GDP-forming] subunit alpha, mitochondrial | P13086 | *Rattus norvegicus* | 4.58E-154 | 72.1% |
| 9.37 | AIPGENE16099 | 1 | Collagen alpha-3(VI) chain | P15989 | *Gallus gallus* | 5.61E-15 | 26.1% |
| 9.33 | AIPGENE26879 | 1 | NADH dehydrogenase [ubiquinone] iron-sulfur protein 6, mitochondrial | P52503 | *Mus musculus* | 3.50E-39 | 56.1% |
| 9.28 | AIPGENE3143 | 1 | DELTA-thalatoxin-Avl2a | Q76DT2 | *Actineria villosa* | 0.00E+00 | 59.7% |
| 9.00 | EDO46723.1 | 1 | Calponin-1 | P26932 | *Gallus gallus* | 1.24E-18 | 32.9% |
| 8.73 | AIPGENE19216 | 1 | Acid ceramidase | A5A6P2 | *Pan troglodytes* | 1.18E-102 | 41.6% |
| 8.72 | AIPGENE21644 | 1 | Muscle M-line assembly protein unc-89 | O01761 | *Caenorhabditis elegans* | 0.00E+00 | 26.5% |
| 8.58 | AIPGENE23527 | 1 | Universal stress protein Slr1101 | P72745 | *Synechocystis sp. (strain PCC 6803)* | 2.67E-10 | 36.6% |
| 8.58 | AIPGENE17132 | 1 | Spindle assembly abnormal protein 6 homolog | Q5ZMV2 | *Gallus gallus* | 1.55E-137 | 41.4% |
| 8.37 | EDO37155.1 | 2 | Protein disulfide-isomerase A6 | Q63081 | *Rattus norvegicus* | 4.49E-178 | 56.5% |
| 8.13 | Q09Y99 | 1 | Caspase-7 | P55214 | *Mesocricetus auratus* | 1.34E-67 | 45.6% |
| 8.09 | EDO40200.1 | 1 | Pleckstrin homology domain-containing family B member 2 | Q5F3S2 | *Gallus gallus* | 2.95E-18 | 33.7% |
| 7.74 | AIPGENE6448 | 2 | cGMP-dependent protein kinase 1 | O77676 | *Oryctolagus cuniculus* | 0 | 63.6% |
| 7.41 | AIPGENE20759 | 1 | Amiloride-sensitive amine oxidase | P36633 | *Rattus norvegicus* | 1.97E-171 | 36.7% |
| 7.10 | AIPGENE13174 | 1 | Hypothetical protein | KXJ30118.1 | *ExAiptasia pallida* | 4.05E-91 | 99% |
| 7.01 | EDO40093.1 | 2 | von Willebrand factor D and EGF domain-containing protein | Q8N2E2 | *Homo sapiens* | 2.24E-25 | 32.6% |
| 6.94 | AIPGENE6089 | 2 | Ras-like protein RAS2 | P38976 | *Hydra vulgaris* | 1.01E-89 | 74.1% |
| 6.93 | AIPGENE4457 | 1 | Matrilin-3 | O42401 | *Gallus gallus* | 1.17E-20 | 35.4% |
| 6.45 | EDO38232.1 | 1 | Delta(3,5)-Delta(2,4)-dienoyl-CoA isomerase, mitochondrial | O35459 | *Mus musculus* | 1.04E-127 | 58.5% |
| 5.44 | EDO39405.1 | 1 | Actin-related protein 2/3 complex subunit 3 | Q9JM76 | *Mus musculus* | 1.44E-84 | 67.6% |

**Table 3.2** continued

| | | | | | | | |
|---|---|---|---|---|---|---|---|
| 5.05 | AIPGENE29213 | 3 | Gelsolin-like protein 1 | Q7JQD3 | *Lumbricus terrestris* | 1.56E-122 | 51.2% |
| 5.00 | 9270 | 1 | Vitelline membrane outer layer protein 1 homolog | Q7Z5L0 | *Homo sapiens* | 1.10E-25 | 34.4% |
| 4.52 | AIPGENE3056 | 1 | Calpain-9 | O35920 | *Rattus norvegicus* | 0 | 46.0% |
| 4.24 | AIPGENE1342 | 1 | Aflatoxin B1 aldehyde reductase member 2 | Q8CG45 | *Rattus norvegicus* | 6.08E-119 | 53.3% |
| 4.20 | EDO48626.1 | 2 | Heat shock protein HSP 90-beta | O57521 | *Danio rerio* | 0 | 78.5% |
| 3.63 | AIPGENE7839 | 1 | Hypothetical protein | KXJ11047.1 | *ExAiptasia pallida* | 0 | 100% |
| 3.61 | AIPGENE2351 | 1 | Peroxiredoxin-6 | Q9TSX9 | *Sus scrofa* | 1.01E-69 | 66.9% |
| 3.57 | AIPGENE28926 | 1 | Myotrophin | Q91955 | *Gallus gallus* | 4.07E-19 | 38.6% |
| 3.42 | EDO42442.1 | 1 | Death-associated protein kinase 3 | O43293 | *Homo sapiens* | 7.62E-51 | 33.3% |
| 3.33 | AIPGENE29242 | 2 | Gelsolin-like protein 2 | Q8MPM1 | *Lumbricus terrestris* | 7.76E-123 | 53.3% |
| 3.32 | AIPGENE23774 | 4 | Isoform 4 of Golgin subfamily B member 1 | Q14789-4 | *Homo sapiens* | 1.50E-104 | 20.1% |
| 3.13 | AIPGENE12489 | 1 | Actin-depolymerizing factor 1 | Q39250 | *Arabidopsis thaliana* | 1.33E-15 | 31.0% |
| 2.93 | AIPGENE13249 | 1 | Microtubule-associated protein RP/EB family member 1 | Q6V291 | *Coturnix coturnix* | 4.74E-94 | 51.7% |
| 2.68 | EDO45013.1 | 37 | Actin | P12716 | *Pisaster ochraceus* | 3.25E-113 | 89.4% |
| 2.58 | AIPGENE27021 | 1 | U-actitoxin-Avd8a | P0DMZ3 | *Anemonia viridis* | 5.43E-19 | 45.8% |
| 2.21 | AIPGENE700 | 1 | Tubulin polymerization-promoting protein family member 2 | Q3T077 | *Bos taurus* | 2.42E-42 | 50.6% |
| 1.82 | AIPGENE19130 | 1 | Myophilin | Q24799 | *Echinococcus granulosus* | 6.57E-36 | 41.4% |
| 1.66 | AAH90759.1 | 2 | 14-3-3 protein epsilon | P62258 | *Homo sapiens* | 8.35E-109 | 65.6% |
| 1.63 | AIPGENE28714 | 3 | Hypothetical protein | KXJ10810.1 | *ExAiptasia pallida* | 0 | 99% |
| 1.43 | EDO46722.1 | 2 | Myophilin | Q24799 | *Echinococcus granulosus* | 2.96E-31 | 37.9% |
| 0.61 | AIPGENE13749 | 2 | Selenium-binding protein 1 | Q569D5 | *Xenopus tropicalis* | 0 | 65.7% |
| 0.58 | EDO42526.1 | 2 | Hydroxysteroid dehydrogenase-like protein 2 | A4FUZ6 | *Bos taurus* | 0 | 62.3% |
| 0.57 | EDO37116.1 | 1 | Putative aminopeptidase W07G4.4 | Q27245 | *Caenorhabditis elegans* | 5.84E-26 | 44.7% |
| 0.53 | $47926 | 3 | Catalase | P04040 | *Homo sapiens* | 0 | 71.9% |
| 0.51 | EDO44966.1 | 6 | Abscisic-aldehyde oxidase | Q7G9P4 | *Arabidopsis thaliana* | 0 | 35.6% |
| 0.51 | EDO48107.1 | 2 | Dipeptidyl peptidase 2 | Q9EPB1 | *Rattus norvegicus* | 1.99E-112 | 51.9% |
| 0.50 | AIPGENE27853 | 2 | Fumarylacetoacetate hydrolase domain-containing protein 2 | Q6GLT8 | *Xenopus laevis* | 2.77E-135 | 62.8% |
| 0.47 | AIPGENE4246 | 4 | Cholinesterase | P21927 | *Oryctolagus cuniculus* | 1.20E-107 | 35.7% |
| 0.43 | EDO49845.1 | 1 | Beta-hexosaminidase subunit alpha | P06865 | *Homo sapiens* | 2.85E-158 | 47.6% |

**Table 3.2** continued

| | | | | | | | |
|---|---|---|---|---|---|---|---|
| 0.43 | AIPGENE2301 | 2 | Carbonyl reductase [NADPH] 1 | P48758 | *Mus musculus* | 5.66E-84 | 50.8% |
| 0.42 | AIPGENE473 | 3 | Cathepsin Z | P05689 | *Bos taurus* | 3.04E-129 | 64.3% |
| 0.39 | EDO49709.1 | 2 | N(4)-(Beta-N-acetylglucosaminyl)-L-asparaginase | O02467 | *Spodoptera frugiperda* | 2.24E-132 | 57.6% |
| 0.38 | AIPGENE26156 | 2 | Cathepsin L | Q26636 | *Sarcophaga peregrina* | 1.54E-125 | 55.3% |
| 0.34 | EEN57628.1 | 2 | Alpha-aminoadipic semialdehyde dehydrogenase | Q2KJC9 | *Bos taurus* | 0 | 67.2% |
| 0.33 | AIPGENE7184 | 1 | Transmembrane protease serine 3 | Q8K1T0 | *Mus musculus* | 1.59E-57 | 41.7% |
| 0.32 | EDO40873.1 | 3 | Creatinase | P19213 | *Flavobacterium sp. (strain U-188)* | 0 | 61.8% |
| 0.29 | AIPGENE8932 | 1 | Heterogeneous nuclear ribonucleoprotein U-like protein 1 | Q8VDM6 | *Mus musculus* | 1.16E-108 | 35.4% |
| 0.27 | AIPGENE27013 | 1 | Hypothetical protein | KXJ29487.1 | *ExAiptasia pallida* | 1.27E-154 | 99% |
| 0.26 | EDO47653.1 | 2 | Aldehyde dehydrogenase, mitochondrial | P11884 | *Rattus norvegicus* | 0 | 72.7% |
| 0.25 | EDO37584.1 | 1 | Lysosomal alpha-mannosidase | O00754 | *Homo sapiens* | 0 | 51.2% |
| 0.23 | AIPGENE6148 | 1 | Lysosomal alpha-mannosidase | Q60HE9 | *Macaca fascicularis* | 0 | 49.1% |
| 0.18 | AIPGENE13027 | 2 | Alpha-N-acetylgalactosaminidase | Q90744 | *Gallus gallus* | 8.01E-158 | 55.0% |
| 0.17 | EDO46736.1 | 1 | Homogentisate 1,2-dioxygenase | O09173 | *Mus musculus* | 0 | 67.6% |
| 0.16 | AIPGENE7223 | 1 | Transmembrane protease serine 6 | Q9DBI0 | *Mus musculus* | 1.80E-56 | 41.8% |
| 0.14 | AIPGENE1156 | 1 | Guanylate-binding protein 4 | Q96PP9 | *Homo sapiens* | 1.89E-19 | 36.8% |
| 0.11 | AIPGENE7506 | 2 | Pirin-like protein | Q9SEE4 | *Solanum lycopersicum* | 1.10E-74 | 43.6% |
| 0.10 | AIPGENE12842 | 1 | Hypothetical protein | KXJ12770.1 | *ExAiptasia pallida* | 0 | 99% |
| 0.08 | AIPGENE25444 | 1 | Oxidoreductase HTATIP2 | Q9Z2G9 | *Mus musculus* | 1.28E-30 | 37.5% |
| 0.08 | AIPGENE27740 | 1 | Insoluble matrix shell protein 1 | P86982 | *Ruditapes philippinarum* | 1.44E-14 | 37.8% |
| 0.06 | AIPGENE28006 | 2 | Alpha-N-acetylglucosaminidase | P54802 | *Homo sapiens* | 0 | 47.7% |
| 0.04 | EDO45852.1 | 1 | Cathepsin L | Q95029 | *Drosophila melanogaster* | 9.41E-132 | 59.7% |
| 0.03 | 52902 | 1 | Heat shock 70 kDa protein A (hsp-1) | P09446 | *Caenorhabditis elegans* | 5.94E-44 | 88.5% |
| 0.03 | AIPGENE12842 | 1 | Hypothetical protein | KXJ12770.1 | *ExAiptasia pallida* | 1.32E-39 | 57% |
| 0.01 | AIPGENE8259 | 1 | Persulfide dioxygenase ETHE1, mitochondrial | O95571 | *Homo sapiens* | 5.54E-90 | 56.0% |

**Table 3.3** Proteins significantly different between *Symbiodinium* B1 and D1a treatments, in order of fold-change from B1 to D1a. Colour scale in first column indicates degree of protein upregulation in B1 (green) to D1a (yellow) anemones. Green and pink highlighted rows were also found to be significantly different proteins between symbiotic and aposymbiotic anemones, respectively, in Oakley *et al.* (2016).

| B1-D1a Fold Change | Sequence ID | Proteins in Cluster | Best Annotation Match | Accession | Matched Species | E value | % Pairwise Identity |
|---|---|---|---|---|---|---|---|
| 4384.86 | AIPGENE22527 | 1 | Protein NPC2 homolog | Q9VQ62 | *Drosophila melanogaster* | 2.98E-26 | 37.9% |
| 526.93 | AIPGENE22473 | 1 | Epididymal secretory protein E1 (NPC2) | P79345 | *Bos taurus* | 1.80E-19 | 29.9% |
| 26.04 | Q6S3M2 | 1 | Glutamine synthetase | P09606 | *Rattus norvegicus* | 0 | 67.2% |
| 25.61 | AIPGENE23106 | 2 | Legumain | Q95M12 | *Bos taurus* | 8.61E-54 | 41.4% |
| 23.25 | A7S6S5 | 1 | Glutamine synthetase | P15103 | *Bos taurus* | 0 | 67.6% |
| 15.27 | AIPGENE9034 | 1 | Serine/arginine-rich splicing factor 4 | Q8VE97 | *Mus musculus* | 2.31E-64 | 56.7% |
| 15.21 | AIPGENE13275 | 1 | Circumsporozoite protein | P06915 | *Plasmodium berghei* | 4.20E-17 | 37.0% |
| 10.29 | EDO43005.1 | 1 | Aprataxin and PNK-like factor | Q8IW19 | *Homo sapiens* | 4.33E-21 | 32.0% |
| 8.24 | AIPGENE14763 | 1 | Neurolysin | Q5R9V6 | *Pongo abelii* | 8.60E-66 | 55.9% |
| 2.49 | AIPGENE7506 | 2 | Pirin-like protein | Q9SEE4 | *Solanum lycopersicum* | 1.10E-74 | 43.6% |
| 2.47 | AIPGENE8932 | 1 | Heterogeneous nuclear ribonucleoprotein U-like protein 1 | Q8VDM6 | *Mus musculus* | 1.16E-108 | 35.4% |
| 1.61 | AIPGENE13749 | 2 | Selenium-binding protein 1 | Q569D5 | *Xenopus tropicalis* | 0 | 68.2% |
| 0.76 | AIPGENE12496 | 1 | 78 kDa glucose-regulated protein (GRP-78, Hsp70, BiP) | P07823 | *Mesocricetus auratus* | 0 | 79.2% |
| 0.66 | EDO45013.1 | 37 | Actin | P12716 | *Pisaster ochraceus* | 3.25E-113 | 89.4% |
| 0.31 | AIPGENE1342 | 1 | Aflatoxin B1 aldehyde reductase member 2 (rAFAR2) | Q8CG45 | *Rattus norvegicus* | 6.08E-119 | 53.3% |
| 0.26 | AIPGENE22562 | 1 | Inosine-uridine preferring nucleoside hydrolase (NSNH) | P83851 | *Leishmania major* | 2.64E-19 | 31.3% |
| 0.22 | AIPGENE10977 | 1 | Betaine--homocysteine S-methyltransferase 1 (BHMT1) | Q5M8Z0 | *Xenopus tropicalis* | 0 | 61.9% |
| 0.14 | A7RIN6 | 1 | Betaine--homocysteine S-methyltransferase 2 (BHMT2) | Q5RF32 | *Pongo abelii* | 7.54E-137 | 57.6% |
| 0.10 | ARMET | 1 | Mesencephalic astrocyte-derived neurotrophic factor homolog | B4QX46 | *Drosophila simulans* | 2.01E-60 | 57.8% |
| 0.09 | EDO26161.1 | 1 | Hypothetical | KXJ12230.1 | *ExAiptasia pallida* | 7.80E-147 | 100% |
| 0.08 | EDO34868.1 | 1 | 40S ribosomal protein S19 | Q8T5Z4 | *Branchiostoma belcheri* | 4.38E-70 | 69.1% |
| 0.01 | EDO47743.1 | 3 | Betaine--homocysteine S-methyltransferase 1 (BHMT1) | Q95332 | *Sus scrofa* | 6.96E-120 | 72.4% |

Non-metric multidimensional scaling (NMDS) of the proteins resulted in an excellent representation of protein patterns reduced to two dimensions (stress = 0.051). Grouping patterns can be seen between the three treatment groups, with most differences occurring along the NMDS2 axis (Fig. 3.1). The aposymbiotic group is skewed negatively away from the two symbiotic groups on NMDS2, while the D1a group has a smaller range along NMDS2 than the B1 group.

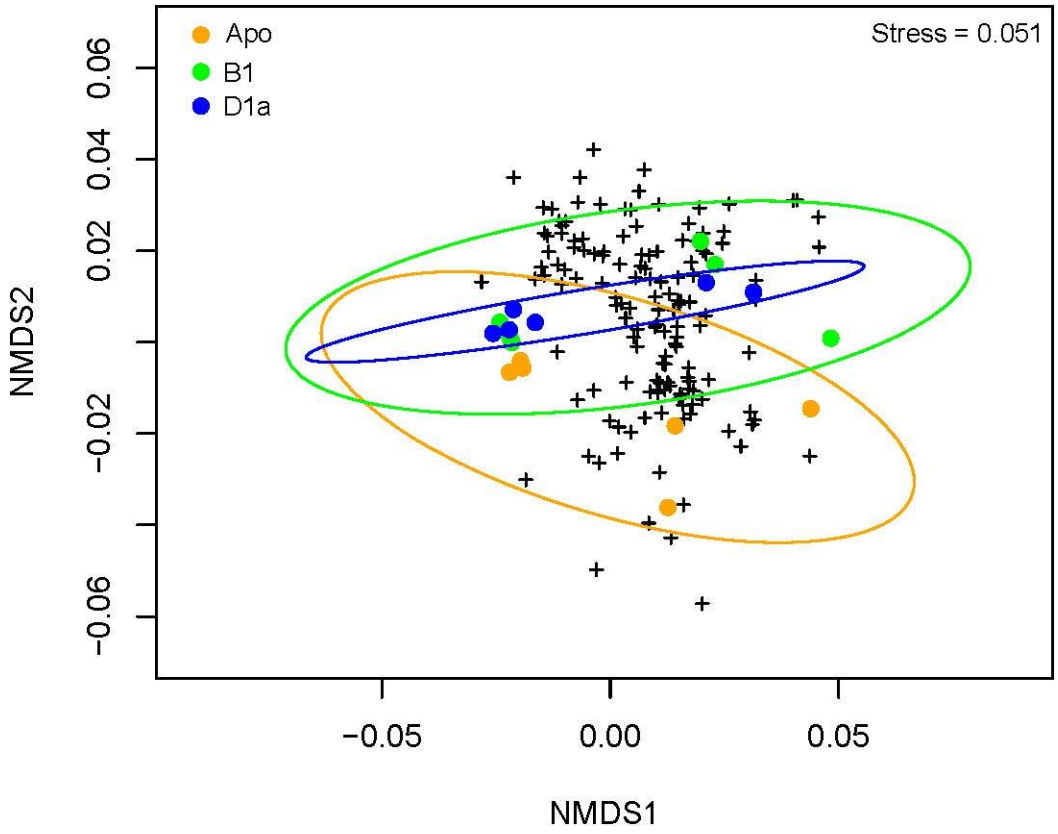


**Figure 3.1** NMDS plot showing grouping of *Aiptasia* protein samples (based on precursor intensity). Black crosses represent individual proteins, while coloured dots represent the protein profile of each replicate anemone in a particular treatment. Grouping patterns are encompassed by coloured ellipses according to treatment.

Eight annotated proteins were found in both the B1 and D1a treatments but not in aposymbiotic anemones, while the D1a and aposymbiotic treatments shared three proteins that were absent from the B1 treatment, and the B1 and aposymbiotic treatments shared just one protein that was absent from the D1a treatment (Fig. 3.2). The proteins unique to the two symbiotic treatments included two that are necessary for basic cell functioning: 40S ribosomal protein S19, which is required for ribosome biosynthesis (Danilova *et al.* 2008), and the muscle M-line assembly protein unc-89, which is necessary for proper anchoring of myosin filaments *via*

muscle M lines (Benian *et al.* 1996). Also included in the symbiotic-only proteins are two cell-signalling proteins: acid ceramidase and a guanine nucleotide-binding protein (GNBP aka G protein) (Vetter and Whitinghofler 2001; Bernardo *et al.* 1995). Additional proteins specific to the symbiotic state are involved in lipid and nitrogen metabolism, mRNA splicing, and cell adhesion. The three proteins shared exclusively by the D1a and aposymbiotic groups are all enzymes involved in the breakdown of ATP, amino acids, and aldehydes, while the protein shared exclusively by the B1 and aposymbiotic groups, cathepsin L, is an enzyme involved in the degradation of lysosomal proteins (Homma *et al.* 1994).

Two Neimann pick C2 protein (NPC2) homologs and a serine/arginine-rich splicing factor were discovered only in anemones infected with *Symbiodinium* B1, while a third NPC2 homolog was found in all treatments but was only significantly different between the B1 and aposymbiotic groups, with upregulation (2.38-fold) in the B1 treatment (Table 3.1). A persulfide dioxygenase ETHE1 protein was found only in aposymbiotic anemones, while no proteins were found uniquely in anemones infected with *Symbiodinium* D1a.

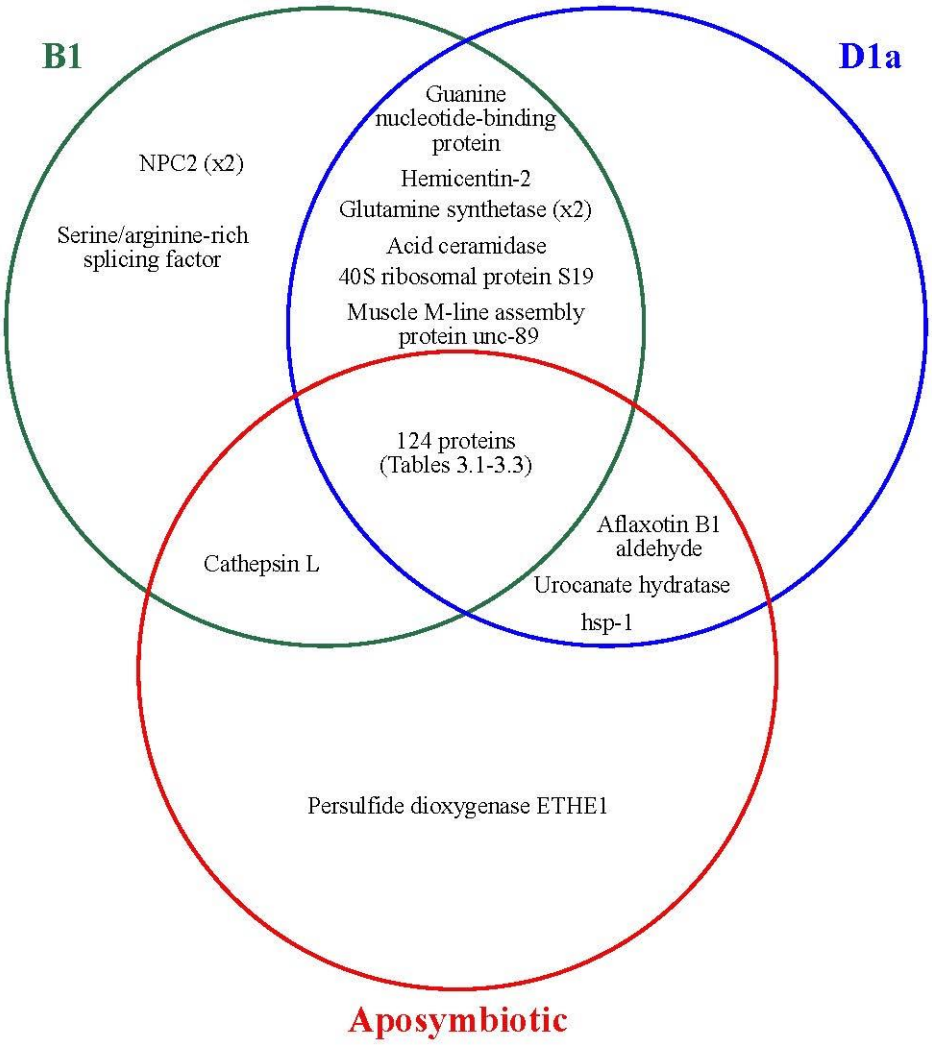


**Figure 3.2** Venn diagram comparison of annotated proteins exclusive to only one or two treatment groups.

Of the 22 proteins that were significantly different between B1- and D1a-colonised anemones, 18 were successfully mapped to at least one GO term (Fig. 3.3). The majority of these proteins are involved in cellular and metabolic processes, and mostly function in binding and catalytic activity (Fig. 3.3). While the majority of GO terms are mapped to a similar proportion of upregulated proteins from each symbiotic treatment, only proteins upregulated in D1a-colonised anemones were linked to multi-cellular organismal processes, immune system process, locomotion, and structural molecule activity (Fig. 3.3).

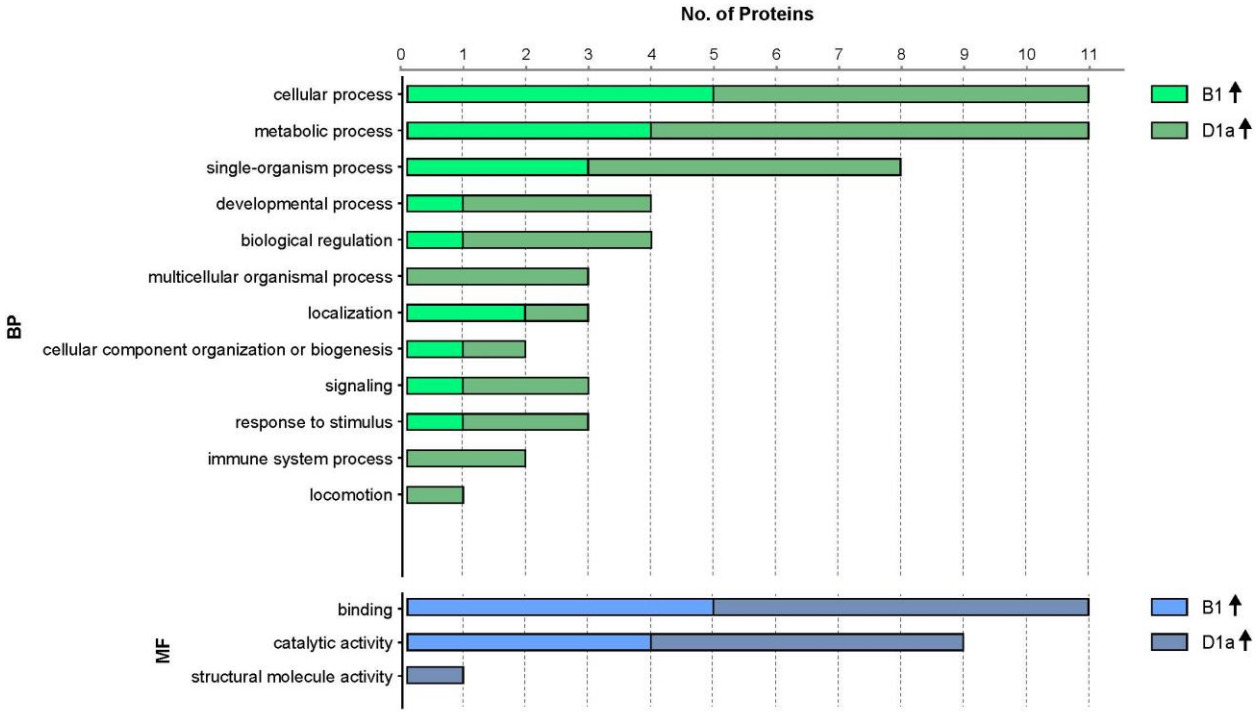


**Figure 3.3** Biological process (BP) and molecular function (MF) GO terms for successfully mapped proteins that were significantly different between B1- and D1a-colonised anemones, illustrating the proportions of each that were upregulated in either treatment.

## 3.4 Discussion

This study aimed to determine the molecular impact of a heterologous, thermally-tolerant opportunist symbiont type on a model cnidarian host, under normal environmental conditions. The results describe here expand on previous findings that reported a number of proteins to be unique to the symbiotic and aposymbiotic states, by identifying proteins that are enhanced by a native *versus* non-native symbiotic association. My findings confirmed the importance of some proteins to the symbiotic state, such as glutamine synthetase and G-proteins, while differentiating others as indicative of either an optimal or sub-optimal association. Most notably, I found that NPC2-like proteins are integral components of a successful homologous symbiosis. Additionally, I found that BHMT, which was previously only detected in aposymbiotic anemones, is expressed at high levels in the heterologous symbiosis with *Symbiodinium* D1a and therefore may indicate incompatibilities in the association. Overall, my findings suggest that *Symbiodinium* D1a is indeed a less mutually beneficial symbiont to *Aiptasia* hosts under normal environmental conditions.

### *3.4.1 Impact of symbiont density*

The density of *Symbiodinium* B1 was 1.5-fold higher than that of D1a, and it is unclear whether this may have affected differences in protein expression between treatments. Three proteins in particular exhibited fold-changes that approximately corresponded to the difference in symbiont density. These were the selenium-binding protein, 78kDa glucose-regulated protein, and actin. While it is noted here that the observed differences of the former two proteins may potentially be driven by cell density, there is also a possibility that the expression of these proteins is actually affected by symbiont type, and this is discussed in more detail below. As for actin, the fold-change from B1-D1a almost exactly matched the symbiont density difference, so it is either a unique coincidence or the two parameters are related. Actin is found ubiquitously throughout life and is most commonly known for its role as the thick filament in eukaryote muscle fibres (Cooper 2000; Gunning *et al.* 2015). In *Aiptasia*, it is an important component for maintaining structural integrity of the tissues, and inhibition of the protein can lead to animal mortality (Dunn *et al.* 2007a). Ultimately, the probable link between actin expression levels and symbiont density would need further investigation to confirm this.

### *3.4.2 Proteins associated with symbiotic and aposymbiotic states*

While six annotated proteins were found solely in the two symbiotic treatments, only one protein was found to be unique to aposymbiotic anemones. The two symbiotic proteins known to be involved in cell signalling are the G-protein and acid ceramidase. G-proteins act as a molecular switch to regulate processes such as cell growth, differentiation, and transport (Vetter & Wittinghofer 2001). Of particular relevance, in the cnidarian *Renilla koellikeri*, G-proteins were found to stimulate the enzyme adenylate cyclase, suggesting that a receptor-dependent G-protein signal transduction system operates in cnidarians (Awad & Anctil 1993). Furthermore, a proteomics study by Peng *et al.* (2010) discovered a G-protein-coupled receptor in symbiosome fractions of *Aiptasia*, indicating that G-protein signal transduction likely plays a role in symbiont recognition and/or regulation at the symbiotic interface. The other signalling protein found in symbiotic anemones, acid ceramidase, is a lysosomal enzyme that catalyses the hydrolysis of ceramide to free fatty acids and sphingosine (Bernardo *et al.* 1995).

*Symbiodinium* produces a unique ceramide, symbioramide-C16 (Nakamura *et al.* 1998), which could be translocated to the host as a substrate for this reaction. While free fatty acids are a major component of each partner's metabolism and are predicted to play a critical role in the success of the symbiosis (Dunn *et al.* 2012; Wang *et al.* 2013a), sphingosine acts in cell signalling and apoptosis (Cuvillier 2002). The sphingosine rheostat pathway has been identified as the homeostatic pathway triggered by the immune response for inter-partner communication of regulatory signals (Rodriguez-Lanetty *et al.* 2006; Detournay & Weis 2011). This pathway includes two complementary molecular signals: one which promotes apoptosis of the symbiotic cells and one that inhibits it; these pathways act in concert as a mechanism for the host to control proliferation of the symbiont population (Detournay & Weis 2011). The presence of these two proteins only in symbiotic *Aiptasia* confirms their importance in communication between the partners of the symbiosis.

Three of the proteins found only in symbiotic anemones function primarily in maintaining cell structure. Hemicentin-2 acts as an extracellular adhesive, holding cells together to preserve the integrity of tissues (Vogel *et al.* 2006; Xu *et al.* 2013). Hemicentins have previously been found in cnidarians and may also have a secondary role in immunity or cell signalling (Schwarz *et al.* 2008; Barshis *et al.* 2013; Brekhman *et al.* 2015; Oakley *et al.* 2016). Protein unc-89 is required for proper anchoring of myosin filaments *via* muscle M lines (Benian *et al.* 1996), while the 40S ribosomal protein S19 is necessary for ribosome biosynthesis (Danilova *et al.* 2008). The downregulation of these proteins in aposymbiotic anemones could lead to developmental defects of tissues, but more research on this would be necessary. One protein specific to the symbiotic treatments, glutamine synthetase, is involved in nitrogen metabolism and has previously been reported to be characteristic of symbiotic *Aiptasia* (Oakley *et al.* 2016). Ammonium can be assimilated by both the host and symbiont separately, through the glutamine synthetase/glutamine oxoglutarate aminotransferase cycle (Pernice *et al.* 2012). The expression of this enzyme only in symbiotic anemones indicates that aposymbiotic anemones assimilate less nitrogen when they no longer need to control symbiont population numbers through nitrogen limitation (Miller and Yellowlees 1989; Wang & Douglas 1998; Yellowlees *et al.* 2008).

The only protein expressed solely in aposymbiotic anemones was sulphur deoxygenase ETHE1 (aka persulphide deoxygenase). This protein is involved in the mitochondrial oxidation pathway, acting as a catalyst for the oxidation of a persulphide molecule to sulphite (Hildebrandt & Grieshaber 2008). Sulphite is an important intermediate in sulphur metabolism pathways, however sulphite on its own is toxic to both plant and animal cells (Hänsch & Mendel 2005; Niknahad & O'Brien 2008). When sulphite is not readily metabolized into sulphate or other products, it can inhibit certain enzymes and attack various substrates (Heber & Hueve 1997). Furthermore, it can lead to an increase in oxygen consumption and production of reactive oxygen species (ROS) (Niknahad & O'Brien 2008); the accumulation of ROS in symbiotic cnidarians is known to induce host cell apoptosis and is linked to symbiotic breakdown (Lesser 2006; Weis 2008). The upregulation of sulphur deoxygenase could therefore cause an accumulation of toxic sulphite in aposymbiotic *Aiptasia* cells, especially if any substrates used for sulphite metabolism are usually obtained from the symbionts. This finding suggests that the aposymbiotic state could be physiologically detrimental to *Aiptasia* and could possibly explain, in part, why they do not occur in an aposymbiotic state in nature.

### *3.4.3 Proteins upregulated in symbiotic versus aposymbiotic anemones*

#### ***3.4.3.1 Previously identified proteins in symbiotic* Aiptasia**

Only one previous study has identified differences in the host proteome between symbiotic and aposymbiotic *Aiptasia* (Oakley *et al.* 2016). The present study confirmed many of the findings of this previous work, including the elevated expression of NPC2 proteins, glutamine synthetase and flotillin-2 in symbiotic anemones. All three of these proteins enhance host metabolism by acting in lipid or nitrogen processing, indicating the metabolic benefit of the symbiosis to the host. Additionally, the current study showed the upregulation of catalase, creatinase, transmembrane protease serine, betaine-homocysteine S-methyltransferase (BHMT), and fumarylacetoacetase in aposymbiotic anemones relative to symbiotic ones. Many of these proteins aid in the breakdown of proteins and other products, and are thought to be more highly expressed in aposymbiotic anemones due to their higher reliance on heterotrophy (Oakley *et al.* 2016). Interestingly, however, when comparing the host proteome of anemones infected with *Symbiodinium* D1a to that of aposymbiotic anemones, some results differ from

the previous study of Oakley *et al.* (2016), where the anemones containing homologous *Symbiodinium* B1 were compared with the aposymbiotic state. In particular, these authors reported selenium-binding proteins to be upregulated 10-fold in symbiotic *vs.* aposymbiotic anemones, while here the same proteins were downregulated 0.6-fold in D1a-colonised anemones. Additionally, amine oxidase, which Oakley *et al.* (2016) found to be downregulated in B1-colonised anemones, was upregulated 7.41-fold in D1a-colonised anemones. These two proteins are involved in intra-Golgi protein transport and histamine breakdown, respectively (Porat *et al.* 2000; Mcgrath *et al.* 2009). This means that D1a symbionts may induce inhibition of proper protein synthesis by the Golgi, while also breaking down histamine at an increased rate. Histamine is an important molecule in the immune response of vertebrates, mainly being associated with the deleterious effects of allergic reactions, and also having other potentially beneficial roles (Schneider *et al.* 2002). While research on invertebrate histamine is scarce, it is known to act as a major neurotransmitter, as in vertebrates (Roeder *et al.* 2003). The enhanced breakdown of histamine in D1a-colonised anemones could be a way for the symbionts to evade a host immune response that may attack the foreign symbionts. This evidence illustrates how *Symbiodinium* D1a affects the host proteome differently than *Symbiodinium* B1, possibly impairing cellular function in *Aiptasia* more than the aposymbiotic state, while simultaneously protecting the foreign symbiont.

Two carbonic anhydrase proteins were found to be highly upregulated (16-29 fold) in both symbiotic treatments when compared to the aposymbiotic state. Carbonic anhydrase is an integral part of the carbon concentrating mechanism used by symbiotic cnidarians to transport DIC from seawater to the symbiont's chloroplast (Weis 1991; Bertucci *et al.* 2013). Oakley *et al.* (2016) found upregulation of an H+-ATPase in symbiotic anemones, which is a protein that commonly works in conjunction with carbonic anhydrase to transport protons across the symbiosome and allow the conversion of $HCO_3$ to $CO_2$; the $CO_2$ can then be utilized by the symbiont (Furla *et al.* 2000; Barott *et al.* 2015). Anemones in the present study were sampled just four weeks after establishing a symbiont population, whereas Oakley *et al.* (2016) used anemones involved in a lifelong symbiosis, so it is clear that cellular processes that are critical to the long-term success of the symbiosis, such as those involved with DIC delivery, operate even during the early stages of symbiont colonisation of the host.

### *3.4.3.2 Redox and breakdown processes*

Many previously unreported proteins were likewise found to be upregulated in both symbiotic treatments, and may also be indicative of processes that are important during the earlier stages of symbiosis establishment. Only two proteins involved in oxidative stress were found: mitochondrial complex I (NADH: Ubiquinone Oxidoreductase), which is the major site of ROS generation within mitochondria (Galkin & Brandt 2005); and peroxiredoxin 6 which acts in antioxidant defence by repairing damaged cell membranes (Manevich & Fisher 2005). This might indicate the expression of normally functioning cellular redox systems, where ROS are produced at low levels and can act in cell signalling (Circu & Aw 2010), however it is difficult to make this assumption since these proteins only make up a small part of the overall respiratory electron transport system. A number of proteins involved in cytolytic and proteolytic activity were also found. These include two novel anemone toxins, PsTX-60A and AvTX-60A, that are nematocyst components serving to attack and kill foreign cells (Nagai *et al.* 2002; Oshiro *et al.* 2004). The presence of these toxins indicates the development of an effective defence system and method of food capture, *via* nematocysts, in symbiotic anemones. The caspase-7 protease, which can induce cell apoptosis (Marcelli *et al.* 1998), and the calpain-9 protease, which is activated second to caspase during apoptosis (Wood & Newcomb 1999), were both up-regulated in symbiotic anemones. Cnidarians can control their symbiont populations by inducing either apoptosis or autophagy of their symbiont-colonised gastrodermal cells, with caspase as a participant in the former (Dunn *et al.* 2007b; Dunn & Weis 2009). As these two mechanisms are known to work in tandem, our findings may implicate calpain as an additional component of the autophagy mechanism in symbiotic cnidarians.

### *3.4.3.3 Cell signalling*

Signalling molecules are necessary for cnidarian hosts to communicate with their dinoflagellate symbionts. Here, a number of proteins associated with signalling pathways were upregulated in the symbiotic treatments. This included two signalling proteins from the Ras superfamily, RAS2, which acts in plasma membrane signalling and responses to nutrient limitation (Tatchell *et al.* 1985), and GTPase KRas, which acts in regulation of cell proliferation (Yang *et al.* 2012; Zimmermann *et al.* 2013). Also upregulated in the symbiotic state were a protein kinase central

to the nitric oxide/cGMP signalling pathway (Hofmann *et al.* 2000), the 14-3-3 epsilon protein responsible for regulation of signalling pathways (Fu *et al.* 2000), and a calcyphosin-like protein that acts in calcium-dependent signalling cascades (Dong *et al.* 2008). Future investigations on host-symbiont signalling should include these pathways for further study, as they could be key to successful symbiosis establishment.

#### *3.4.3.4 Tissue structure and muscle functioning*

Structural changes to host gastrodermal cells occur during symbiosis establishment, by the formation of specialized vesicles called symbiosomes that house symbiont cells (Fitt & Trench 1983; Wakefield & Kempf 2001). The structural proteins upregulated in symbiotic anemones could reflect proteins which aid in the creation of symbiosomes from late endosomes and their subsequent maintenance. These include fibronectin type III proteins, which are cell-surface glycoproteins that act in cell adhesion and have been previously reported as a component of cnidarian mesoglea (Zhang *et al.* 1994; Koide *et al.* 1998). Also found were the cytoskeletal rootletin protein (Yang *et al.* 2002) and the microtubule-binding protein EB1 that aids in cell division and migration (Juwana *et al.* 1999). A number of muscle proteins were also upregulated, including calponin-1 and myophilin, which are involved in actin- and protein-binding (Gimona *et al.* 1990; Martin *et al.* 1995), tropomyosin and tropomodulin, which play critical roles in muscle contraction and filament organization (Weber *et al.* 1994), a gelsolin-like protein that promotes filament assembly (Sun *et al.* 1999), and myotrophin, which promotes muscle cell-growth and -assembly (Sen *et al.* 1990). These findings suggest that both cell structural integrity and muscle development are enhanced by the symbiotic state.

#### *3.4.3.5 Cellular and metabolic processes*

The majority of upregulated proteins in the symbiotic anemones are involved in cellular and metabolic processes. A number of these were involved in transport systems, including a golgin protein responsible for vesicle transport to the Golgi apparatus (Malsam 2005), a sodium/calcium antiporter protein in the plasma membrane (Komuro *et al.* 1992), and the transmembrane stomatin protein, which regulates ion channel transport (Price *et al.* 2004).

Additionally, a succinyl-coA synthetase involved in the TCA cycle (Fraser *et al.* 1999) was also upregulated in symbiotic anemones, illustrating the role of symbionts in host carbohydrate metabolism. Inter-partner transport mechanisms are especially important when considering the high percentage of photosynthetic carbon products that need to be transported to the host for use in its metabolism. Previously, a host-derived proton pump was localized to the symbiosome membrane in two coral species, and was predicted to act in host regulation of symbiont physiology by acidifying the internal environment (Barott *et al.* 2015). It is therefore possible that the transporter proteins identified in this study may also be components of the symbiosome membrane, acting similarly on symbiont physiology by regulating the symbiont's access to other molecules.

### *3.4.4 Homologous (B1) versus heterologous (D1a) symbiont effects on host proteome*

By comparing the host proteome of anemones infected with two different symbiont types that differ in infection success, one homologous and one heterologous, we gain new insights into the processes involved in the establishment of a successful symbiosis. Our results suggest that the protein most indicative of a successful symbiosis is NPC2, which was found to be highly upregulated in B1-colonised anemones when compared to D1a-colonised anemones (4384.86- and 526.93-fold upregulation, respectively). The present study therefore confirms the presence of NPC2 in cnidarians and its close association with the symbiotic state (Kuo *et al.* 2004; Ganot *et al.* 2011; Dani *et al.* 2014; Lehnert *et al.* 2014; Oakley *et al.* 2016), while also providing evidence that its activity is linked to the ultimate colonisation success of the invading symbiont type. Here, we found that two of three identified NPC2 homologs are exclusive to anemones infected with homologous symbionts, while the third NPC2 homolog was upregulated only in the homologous association compared to the aposymbiotic treatment. NPC2 works in conjunction with the integral membrane protein NPC1 in the binding and export of cholesterol from lysosomes and late endosomes (Xu *et al.* 2008). Four NPC2 genes have been found in the cnidarian, *Anemonia viridis*, with the protein product of one gene being localized to the host gastrodermal cells (Dani *et al.* 2014). Because of its general role and localization, it has been suggested that it may be associated with the symbiosome membrane, where it could play a role in sterol transport from symbiont to host (Dani *et al.* 2014; Oakley *et al.* 2016). Additionally, it has been speculated that the cnidarian NPC2 protein might act in symbiont recognition and

persistence due to its role in immune signalling pathways of other invertebrates (Shi *et al.* 2012; Dani *et al.* 2014). If this is the case, our results might indicate the inefficiency of heterologous symbionts when transporting essential lipids to the host, or the inefficiency of heterologous symbionts when initiating the adequate signalling pathway for host-symbiont compatibility.

#### *3.4.4.1 Metabolic processes*

Other proteins that were upregulated in B1- *versus* D1a-colonised anemones include two isoforms of glutamine synthetase (26- and 23-fold upregulation). Glutamine synthetase is the enzyme used by microalgae to catalyse the conversion of ammonia and glutamate into the amino acid glutamine (Syrett & Peplinska 1988). It is also thought to be the primary enzyme responsible for inorganic nitrogen incorporation and host protein synthesis in algal-invertebrate symbioses (Pernice *et al.* 2012), due to its presence in host tissues of symbiotic corals, sea anemones, giant clams, and freshwater hydra (Miller & Yellowlees 1989; Rees *et al.* 1994; Wang & Douglas 1998; Smith *et al.* 2004). Interestingly, previous studies have consistently found glutamine synthetase to be upregulated in symbiotic host tissues compared to aposymbiotic ones (Lipschultz & Cook 2002), so the upregulation of this enzyme in the homologous infection only, suggests that hosting the heterologous D1a may result in slower nitrogen incorporation into host tissues. Alternatively, it may indicate that D1a symbionts in the experiment have not yet triggered the host population control mechanism of nitrogen limitation (Miller & Yellowlees 1989; Wang & Douglas 1998; Yellowlees *et al.* 2008).

#### *3.4.4.2 Proteolysis and gene processing*

The proteases neurolysin and legumain were also only upregulated in B1-infected anemones. These proteins act in the regulation of cell proliferation pathways by metabolizing bioactive compounds (Paschoalin *et al.* 2007; Dall & Brandstetter 2013). Neurolysin is an enzyme secreted by melanoma tumours that regulates tumour proliferation by triggering an angiogenic switch (Paschoalin *et al.* 2007). Legumain, which mainly acts in lysosomal compartments, is overexpressed in the majority of human cancer tumours and is linked to enhancing tissue invasion and promoting tumour growth (reviewed in Dall and Brandstetter 2016). The presence

of these enzymes could indicate that B1-colonised anemones may have more control over the growth and proliferation of their symbiont population than when colonised by D1a. B1-colonised anemones may also have more efficient RNA and DNA processing mechanisms, as illustrated by the upregulation of a heterogeneous ribonucleoprotein and a serine/arginine-rich splicing factor (Kohtz *et al.* 1994; Kzhyshkowska *et al.* 2003), and the PALF nuclease responsible for DNA repair (Kanno *et al.* 2007), all in only B1-colonised anemones. This could mean that D1a-colonised anemones are more susceptible to mutations and transcription errors. Overall, these results point to better integration of host-symbiont metabolism and gene processing in the B1- *versus* D1a-colonised anemones.

#### *3.4.4.3 Immune responses*

Proteins involved in immune responses were also upregulated in B1- *versus* D1a-colonised anemones. One highly upregulated protein (15-fold increase) was identified as the circumsporozoite (CS) protein. The CS protein is the main surface antigen produced by the mature sporozoite of the malaria parasite, *Plasmodium berghei*, and is highly upregulated in the infective stage of the parasite compared to non-infective stages (Aikawa *et al.* 1981; Yoshida *et al.* 1981; Nardin *et al.* 1982). The CS protein is important to the parasite as it is thought to play a critical role in invasion of host cells by binding to regions of the host cell's plasma membrane that are exposed to circulating blood (Aikawa *et al.* 1981; Cerami *et al.* 1992). The *Aiptasia* CS protein homolog identified here could similarly function to promote infectivity of host cells, and its upregulation in B1-colonised hosts might help explain why *Symbiodinium* B1 infects *Aiptasia* more rapidly than *Symbiodinium* D1a. The cnidarian CS protein should be studied further for its potentially pivotal role as a *Symbiodinium* surface ligand that binds to host cells to aid in infectivity.

Also upregulated in B1- *versus* D1a-colonised anemones was a pirin-like protein. The human pirin protein functions in cell migration and is upregulated during cell death (Gelbman *et al.* 2007; Miyazaki *et al.* 2010). Pirin proteins are highly conserved between all kingdoms of life (Dunwell *et al.* 2001), however their functions differ between organisms, and range from roles in programmed cell death to seed germination (Orzaez *et al.* 2001; Lapik & Kaufman 2003; Adams & Jia 2005). Because of the versatility of this protein, a specific role in symbiotic

cnidarians is difficult to determine, though it could very likely be involved apoptosis pathways given the number of other apoptosis-associated proteins that were found here.

#### *3.4.4.4 Multifunctional cellular processes*

Proteins upregulated in D1a-colonised anemones are involved in a number of important cell processes. These include aflatoxin B1 aldehyde reductase (AKR7A2), a nucleoside hydrolase, and betaine-homocysteine S-methyltransferases 1 and 2 (BHMT1 and BHMT2). AKR7A2 in humans is involved in the production of neurotransmitters and may play a role in detoxification, tumour resistance, and regulation of osmolarity in the kidneys (O'Connor *et al.* 1999; Lyon *et al.* 2007). Nucleoside hydrolase is an enzyme used by protozoan parasites for purine salvaging and *A. thaliana* for pyrimidine breakdown (Parkin *et al.* 1991; Shi *et al.* 1999; Jung *et al.* 2009). The function in *Aiptasia* is most likely similar to that of *A. thaliana* since neither have a parasitic role, potentially showing an upregulation of pyrimidine breakdown in D1a-colonised anemones. Upregulation of this breakdown could explain the downregulation in gene processing proteins described above, and together may indicate a reduced ability for RNA and DNA synthesis.

Three BHMT proteins were highly upregulated (up to 100-fold) in D1a-colonised anemones when compared to the B1-colonised anemones, which is interesting considering that they are typically characteristic of the aposymbiotic state (Rodriguez-Lanetty *et al.* 2006; Oakley *et al.* 2016). Indeed, BHMT levels were the same in D1a-colonised and aposymbiotic anemones. BHMT converts homocysteine to methionine *via* a methyl donor from betaine, therefore acting in both the regulation of homocysteine levels and in methionine metabolism (Finkelstein & Martin 1984). Other than being a critical component in methionine metabolism, protein 'moonlighting' is possible for BHMT; though other functions have only been speculated upon, and range from associations with tubulin to lysosomal membranes (Pajares & Pérez-Sala 2006). In mammals, feeding restrictions and folate-deficient diets were linked with increased BHMT activity (Park & Garrow 1999; Halsted *et al.* 2002). It is possible that the increased BHMT in aposymbiotic and D1a-colonised *Aiptasia* is linked to a lack of carbon energy, since they would usually obtain this from the symbionts. On the other hand, the upregulation of BHMT could signify that compatible symbionts are required for methionine metabolism in the symbiosis.

Consistent with this, it was previously found that bleached *Aiptasia* could only synthesize two of the essential amino acids - threonine and methionine - leading to the conclusion that these two amino acids were synthesized by the host while the others were translocated from the symbionts (Wang & Douglas 1998). A host methionine pathway would explain the presence of BHMT in all treatments in the present study, however the upregulation of this protein in D1a-colonised and aposymbiotic anemones requires further explanation. Of particular note in this regard, a transcriptomic study of a coral holobiont (*Porites australiensis*) found that half of the enzymes for the methionine synthesis pathway were expressed by the host while the other half were expressed by the symbiont, suggesting that the methionine pathway in the cnidarian-dinoflagellate symbiosis involves intimate cooperation between the partners (Shinzato *et al.* 2014). Additionally, *Symbiodinium* cells are known to synthesize their own two betaine compounds, zooxanthellabetaine-A and –B (Nakamura *et al.* 1998), and these compounds are potentially substrates in the host methionine reaction. Given this, an inability to obtain these compounds from less compatible symbionts might result in an accumulation of methionine-production enzymes, such as BHMT, in the host.

#### *3.4.4.5 Protein assembly*

Two upregulated proteins in D1a-colonised anemones may indicate problems with protein assembly. A neurotropic factor protein called Armet was upregulated 10-fold in these anemones. Armet is a protein that is secreted in response to an accumulation of misfolded proteins in the endoplasmic reticulum (ER), to protect against ER stress-induced cell death (Apostolou *et al.* 2008; Tadimalla *et al.* 2008; Hellman *et al.* 2011). Armet has been localized to both the ER and Golgi apparatus, and found to protect against apoptosis while also inhibiting cell proliferation (Apostolou *et al.* 2008). Concurrently, a 78 kDa glucose-regulating protein (aka BiP) that also plays a role in the ER protein folding stress-response (Bertolotti *et al.* 2000; Oka *et al.* 2013) and is upregulated in heat-shocked anemones (Oakley *et al.* unpublished data) was slightly more abundant in D1a-colonised anemones. The upregulation of these proteins suggests that *Aiptasia* host cells are stressed when infected with *Symbiodinium* D1a, and this may, in part, be due to defects in protein folding in the ER. Additionally, the presence of Armet as an immune response to *Symbiodinium* D1a may be another explanation for the lesser success of this heterologous symbiont type.

Finally, the 40S ribosomal protein S19 (Rps19), which is necessary for the maturation of the 40S ribosomal subunit (Flygare *et al.* 2007), was also upregulated in D1a-colonised anemones. Rps19 is essential for ribosome construction and was present in anemones within all treatment groups, however it may have been upregulated in the presence of D1a due to its secondary role in immunity. In particular, Rps19 dimers are able to activate a phagocytosis pathway that eliminates invasive organisms (Revollo *et al.* 2005; Mollnes *et al.* 2013), once again highlighting a lack of compatibility between *Symbiodinium* D1a and *Aiptasia*.

### *3.4.5 Conclusions*

The results of this study improve our understanding of how different symbiont types affect the host cnidarian proteome, with major implications for symbiosis function and the potential for the establishment of novel host-symbiont pairings. Furthermore, the identification of host proteins that exhibit changed levels only four weeks after infection provide insight into the cellular processes important in the early stages of symbiosis establishment and symbiont proliferation (Fig. 3.4). My findings confirm NPC2 and glutamate synthetase as integral components of a successful symbiosis, and emphasize the importance of cell signalling pathways and structural proteins to symbiosis success. Significant differences were found between B1- and D1a-colonised anemones, leading me to conclude that heterologous infections with *Symbiodinium* D1a may cause reduced fitness of the host.

Indeed, D1a-colonised anemones upregulated proteins indicative of stress or aposymbiosis. Conversely, when colonised by the homologous *Symbiodinium* B1, the host anemone exhibits better function of carbon, nitrogen and lipid metabolism, as well as more active pathways for the regulation of symbiont cell proliferation (Fig. 3.4).

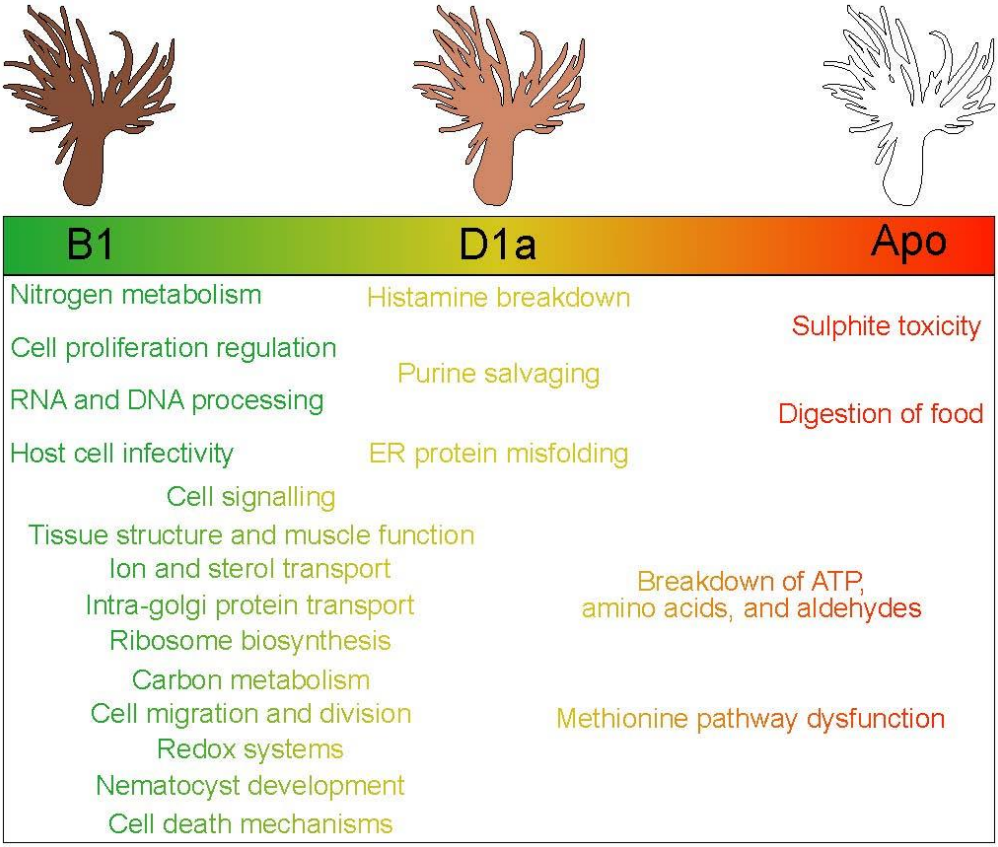


**Figure 3.4** Functional implications of upregulated proteins in *Aiptasia*, along a continuum of symbiotic success. The continuum ranges from aposymbiotic anemones (no symbiont population; red) to B1-colonised anemones (homologous symbiont population; green), with D1a-colonised anemones (heterologous symbiont population; yellow) falling in between the two. Functional descriptions are coloured according to their placement along the scale. Image credit: A. Sproles.

Furthermore, only those anemones colonised by *Symbiodinium* B1 possessed elevated levels of NPC2 proteins, for which there is increasing evidence of a major role in the establishment of a successful cnidarian-dinoflagellate association. Given these numerous patterns, relating both to the structural and functional integrity of the symbiosis, it seems likely that a heterologous symbiosis between *Symbiodinium* D1a and *Aiptasia* would not be optimal in the long-term under normal environmental conditions. This finding is especially significant in light of the widespread interest in the biogeographical spread and thermal resilience of this symbiont type, as if similar effects are induced in corals, then this would help to explain why this *Symbiodinium* type rarely dominates in the field. Even in its regular, homologous associations, *Symbiodinium* D1a is known to trade functional efficiency for thermal tolerance (Stat & Gates 2011), and the discoveries presented here suggest that it affects proper functioning of host cellular processes in heterologous associations. This raises substantial doubts about whether this symbiont type could be a 'nugget of hope' for coral reefs, as previously suggested

(Berkelmans & van Oppen 2006), though whether these same traits persist over longer periods of symbiosis establishment warrants study, so that we can better determine the adaptive capacity of reef corals in the face of climate change.

# Chapter 4: *Symbiodinium* type effects nutrient exchange and symbiont success in *Aiptasia*

## 4.1 Introduction

The exchange of carbon and nitrogen are essential aspects of the mutualistic relationship between cnidarians and dinoflagellate algae of the genus *Symbiodinium* (Muscatine 1990; Lipschultz & Cook 2002). Photosynthetic products from the algal symbionts can meet up to 100% of the cnidarian's metabolic energy demand, thereby supporting important processes such as respiration, growth, reproduction and coral calcification (Vandermeulen *et al.* 1972; Falkowski *et al.* 1984; Muscatine 1984). Fixed carbon from photosynthesis is translocated mostly as the sugar glucose (Burriesci *et al.* 2012; Hillyer *et al.* 2016). Glucose is a necessary metabolite as it is utilized in glycolysis to produce TCA cycle intermediates for the ultimate production of ATP energy (Fernie *et al.* 2004). The translocation of adequate fixed carbon is essential for host survival, as it is incorporated into all cnidarian tissue layers (Tremblay *et al.* 2012; Kopp *et al.* 2015; Freeman *et al.* 2016). The symbionts act as important primary producers in coral reef ecosystems where waters are typically nutrient-limited (Mustatine & Porter 1977; Hatcher 1988). This high productivity is due to efficient nitrogen cycling, and symbionts have the ability to take up dissolved nitrate, ammonium, and urea from the seawater along with excretory ammonium translocated from the host (Rahav *et al.* 1989; Grover *et al.* 2002, 2003, 2006, 2008). The symbionts use these nitrogenous compounds to synthesise amino acids that are used in the algae's cellular processes or provided back to the host (Lewis & Smith 1971; Tanaka *et al.* 2006).

The genus *Symbiodinium* contains high genetic diversity, being separated into nine distinct clades (A-I) which are further divided into 'types' or species (Trench & Blank 1987; Coffroth & Santos 2005; Pochon & Gates 2010; Lajeunesse *et al.* 2012; LaJeunesse *et al.* 2015; Lee *et al.* 2015). Functional characteristics vary greatly between the different algal clades (and types) in a variety of respects, including thermal sensitivity, host infectivity and metabolite production (Rowan *et al.* 1997; van Oppen *et al.* 2001; Santos *et al.* 2004; Starzak *et al.* 2014). Some of these symbionts act as generalists, being able to form associations with a wide range of different host species across multiple oceans, while others are specific to only a small handful of hosts (LaJeunesse 2005; Frade *et al.* 2008; Fabina *et al.* 2012, 2013). Additionally, hosts can display

this type of selectivity for symbionts (Baker 2003). This phenomenon is called host-symbiont specificity, and the mechanisms underpinning its existence are not yet entirely clear (Hambleton *et al.* 2014). It is of particular interest in the realm of coral adaptability to climate change, because some *Symbiodinium* types are more thermally tolerant, and therefore more resistant to symbiotic breakdown *via* bleaching (Tchernov *et al.* 2004; Jones & Berkelmans 2011; Hume *et al.* 2016). However, these thermally tolerant symbiont types do not naturally associate with all coral species, and usually only exist in low background populations under normal environmental conditions. Of particular note is *Symbiodinium* from clade D, particularly type D1a (*Symbiodinium trenchii*), which can overrun a host's dominant symbiont population when seawater temperatures become thermally stressful (Jones *et al.* 2008; LaJeunesse *et al.* 2009). A major benefit of hosting D1a is the enhanced thermal tolerance of the entire holobiont, and its ability to remain metabolically active under very high seawater temperatures (Baker *et al.* 2013). However, under normal environmental conditions, D1a presents major drawbacks, as the host may suffer decreased growth, reproduction and metabolite exchange (Jones & Berkelmans 2010, 2011; Baker *et al.* 2013; Starzak *et al.* 2014; Pernice *et al.* 2014). This makes *Symbiodinium* D1a an especially interesting candidate for studying the implications of a change in the dominant member of the symbiont population, and ultimately the functional attributes that lead, in part, to host-symbiont specificity.

*Symbiodinium* types vary in the amount of fixed carbon they contribute to the host (Starzak *et al.* 2014; Pernice *et al.* 2014), and nitrogen assimilation rates differ between symbiont types (Baker *et al.* 2013, Pernice *et al.* 2014). However, few have investigated whether similar patterns exist with respect to the amount of host-derived nitrogen translocated to the symbionts. Carbon and nitrogen assimilation may be important during the initial establishment of a symbiosis, as illustrated by the green *Hydra – Chlorella* symbiosis, where excreted symbiont metabolites signal nutritional potential to the host (Hohman *et al.* 1982; McAuley & Smith 1982). This system of signalling may be linked to symbiont specificity in cnidarian-dinoflagellate associations, however symbiont specificities often change at some point between initial symbiont uptake and cell proliferation (Starzak *et al.* 2014; Little *et al.* 2004; Bay *et al.* 2011; Weis *et al.* 2001).

In this study, I investigated the exchange of carbon and nitrogen metabolites between different host-symbiont pairs to uncover the functional dynamics triggered by different symbiont types. Using nanoscale secondary ion mass-spectrometry (nanoSIMS), I was able to image symbiont cells within host tissues directly, and provide precise quantifications of the carbon and nitrogen enrichment derived from the assimilation and inter-partner translocation of isotope tracers. To address the possible link to host-symbiont specificity, I examined these interactions both in the presence of a homologous (i.e. native) and heterologous (i.e. non-native) symbiont type during the earlier phases of symbiosis establishment, with particular focus on the opportunistic but thermally tolerant *Symbiodinium* D1a. I then considered the patterns observed in light of the potential long-term persistence of these host-symbiont pairings.

## 4.2 Methods

### *4.2.1 Experimental organisms*

Individuals of the sea anemone *Aiptasia* sp. (n = 300), originating from an unknown Pacific location, were divided evenly into three 1.5-L beakers filled with 0.22 µm-filtered seawater (FSW). Beakers were placed in three separate water baths maintained at 25ºC with WEIPRO® MX-1019 temperature controllers and the water was aerated with Hailea® air pumps. Illumination by AQUA-GLO T8 fluorescent lightbulbs at ~95 µmol photons $m^{-2}$ $s^{-1}$ was provided on a 12 h:12 h light: dark cycle. Anemones were rendered aposymbiotic using menthol incubations over a period of four weeks (Matthews *et al.* 2016), and then kept in the described experimental set-up for the duration of the experiment. *Symbiodinium minutum* (type B1) and *Symbiodinium trenchii* (D1a) cultures were prepared according to the methods in section 3.2.1.

### *4.2.2 Infection of* Aiptasia *with* Symbiodinium

All seawater used in the experiments was 0.22-µm filtered. Anemones were starved for one week following recovery from menthol treatment to increase the eventual uptake of introduced symbionts. *Symbiodinium* f/2 culture medium (NCMA Bigelow Laboratory, USA) was

refreshed two days before infection, and *Artemia* sp. nauplii were hatched one day before infection. All anemones were examined under the confocal microscope (Olympus Provis AX70, 40x magnification) to check for background symbionts. This was achieved by placing anemones into a glass-bottom FluoroDish™ (World Precision Instruments, FL, USA) and examining them under a 543 nm laser with a 600-700 nm emission filter, exciting the chlorophyll autofluorescence from symbionts. Any anemones found to be harbouring symbionts were removed from the experimental population.

Because replicate anemones needed to be kept separate from their source populations during sampling (isotopic labelling), a system using six-well plates was adopted prior to infection. Anemones intended for sampling at the first time point (2 days) were removed from their stock populations and allowed to settle individually in plate wells prior to inoculation with *Symbiodinium*, to avoid the risk of mechanical detachment affecting symbiosis establishment at this early stage in the colonisation process. In total, four six-well plates containing a subset of anemones (n = 5) were prepared 24 h before infection, and labelled as follows: *Symbiodinium* B1 autotrophy; *Symbiodinium* D1a autotrophy; *Symbiodinium* B1 heterotrophy; and *Symbiodinium* D1a heterotrophy. Inoculation with *Symbiodinium* was carried out in the plates, along with the rest of the anemone stock populations from each treatment, as described below.

*Symbiodinium* cultures were prepared for inoculation according to the methods outlined in section 3.2.2. Aerators were removed to encourage tentacle extension. A glass pipette was used to drop the corresponding *Symbiodinium* culture suspension onto the oral disc of each anemone in the re-infected treatments, while no culture suspension was added to the aposymbiotic treatment. FSW in all treatments was replaced after 24 h, and samples for the first time point (TP1) were collected after 2 days. Anemones remained in the experimental setup for two weeks following inoculation, at which point another set of anemones was transferred to the six-well plates for sampling at the second time point (TP2). The first time-point was chosen as 2 days after infection to observe the nutritional interactions occurring during the earlier phases (i.e. recognition, engulfment, and sorting) of symbiont establishment. The second time-point was chosen as two-weeks after infection, to observe interactions likely to be in the 'proliferation' phase of symbiosis establishment.

*4.2.3 Analysis of colonisation success*

Colonisation success was evaluated at 2 days after inoculation (TP1) and 14 days after inoculation (TP2) by quantifying symbiont populations using haemocytometer counts and mean fluorescence index (MFI). For cell counts, anemones (n = 5 *per* treatment) were homogenized in 1 mL FSW with an IKA T-10 electric saw-tooth homogenizer and separated into host and symbiont fractions, by centrifuging for 5 min at 16,000 x g. The host protein in the supernatant was quantified using the Bradford Assay (Bradford 1976), and the algal pellet was re-suspended in 100 µL FSW with 1% formalin. Symbiont cells were counted with an Improved Neubaur haemocytometer at 100x magnification under a light microscope (six counts *per* sample) and normalised to host protein. To measure infection success using MFI, whole anemones from each treatment were examined by confocal microscopy (Olympus Provis AX70, at 100× magnification) to detect the chlorophyll autofluorescence of any dinoflagellates. Anemones (n = 5) were selected at random from each treatment, and placed in a "relaxation solution" [50% FSW, 50% 0.37 M magnesium chloride ($MgCl_2$)] for 15 min before being moved to a FluoroDish$^{TM}$ glass-bottom confocal dish (World Precision Instruments, Florida USA). Anemone tissues were viewed under TD1 (transmitted detector 1) set to the 473 nm laser, and symbiont chlorophyll autofluorescence was detected using 543 nm excitation and a 600–700 nm emission filter. Ten images were acquired in the *z*-plane for three tentacles of each replicate anemone ($n$ = 5/treatment) and cell fluorescence was quantified as a proxy for symbiont density by measuring the mean 600-700 nm fluorescence intensity of tentacle gastrodermis using ImageJ software (National Institutes of Health, Bethesda, MD, USA). Chlorophyll autofluorescence intensity for each pixel was measured against a threshold value for the background, determined by measuring the MFI at 600 nm of an aposymbiotic gastrodermal section.

Maximum photosynthetic and dark respiratory $O_2$ fluxes were also measured at the end of the experiment (TP2), to assess photosynthetic function of each symbiotic treatment. A single anemone (n = 3 *per* symbiotic treatment) was placed on top of a piece of nylon mesh inside a 10-mL glass chamber filled with FSW, and left to settle on the mesh for 1 – 2 h. A magnetic stir bar was placed underneath the mesh floor to circulate the water inside the chamber, and was set to the lowest setting to avoid disturbing the anemone. The chamber was then sealed with a glass lid and rubber O-ring. Oxygen and temperature probes (FIBOX 3; PreSens GmbH,

Germany) were inserted into the lid to measure oxygen % air saturation in the chamber. The chamber was placed inside a 500 mL beaker filled with FSW heated to 25ºC within the experimental water bath to regulate the chamber's temperature. The respiration rate (mL $O_2$ $h^{-1}$) was measured for 30 min in the dark or until a constant rate was attained, after which time the rate of net photosynthesis was measured for 30 min or until constant, at a saturating irradiance of 400 µmol photons $m^{-2}$ $s^{-1}$. The water in the chamber was refreshed with each change of anemone. A FSW-only control was also measured for 30 min in the dark and light in order to account for oxygen fluctuations associated with microbial contamination. Gross photosynthesis was calculated by the addition of net photosynthesis to dark respiration (Muscatine *et al.* 1981). The average ratio of hourly gross photosynthesis to respiration (P:R) was calculated to determine the potential productivity of each anemone.

*4.2.4 Confirmation of symbiont genotype*

DNA was extracted from *Symbiodinium* cultures and algae isolated from anemones TP2, using a method adapted from Logan *et al.* (2010). Samples in DMSO were centrifuged at 16,000 x g for 5 min to pellet algae, and the DMSO then removed. Algal pellets were re-suspended in 300 µL guanidinium buffer (50% w/v guanidinium isothiocyanate; 50 mM Tris pH 7.6; 10 µM EDTA; 4.2% w/v sarkosyl; 2.1% v/v β-mercaptoethanol), before being incubated for 7 d at 4ºC to gently break open algal cells. Following incubation, samples were heated for 10 min at 72ºC, and then centrifuged at 16,000 x g for 5 min. The supernatant was combined with an equal volume of cold isopropanol in a new tube, and samples then chilled at -20ºC overnight to precipitate DNA. Following DNA precipitation, samples were centrifuged at 16,000 x g for 10 min at 4ºC and the supernatant discarded. The pellet was washed by adding 200 µL 70% ethanol, vortexing, and centrifuging at 16,000 x g for 10 min at 4ºC. Samples were then dried in a laminar flow hood for 1 h before re-suspension in 50 µL 10 mM TE buffer by milling without beads at 30 Hz for 1 min. DNA extractions were then used for qPCR.

To provide immediate verification of symbiont identities, qPCR with clade-specific primers was used (Yamashita *et al.* 2011). The clade D primers SymD28S-1F (forward; 5'-AAT GCT TGT GAG CCC TGG TC-3') and SymD28S-1R (reverse; 5'-AAG GCA ATC CTC ATG CGT ATG-3'), and the clade B primers SymB28S-1F (forward; 5'-CAC ATG TCG TGC TGA GAT TGC-3') and SymbB28S-1R (reverse; 5'-CTC GCA TGC TGA GAA ACA CTG-3') were used. The thermal cycling regime had an initial denaturation step of 10 min at 95ºC followed

by 40 cycles of 15 s at 95ºC and 1 min at 60ºC (performed with Applied Biosystems StepOne system). Each reaction contained 2 µL DNA template, 5 µL SYBR Green Mastermix (Life Technologies), 0.5 µL bovine serum albumin (Sigma Alrich, Auckland, New Zealand), 1.7 µL PCR grade $H_2O$, 0.4 µL forward primer, and 0.4 µL reverse primer. Samples where the clade-specific primer matched the clade of *Symbiodinium* present showed amplification, and were used to compare the identity of the inoculation cultures with the TP2 symbionts.

*4.2.5 Isotopic labelling of carbon and nitrogen compounds*

At each sampling time point, the anemones in six-well plates (see section 4.2.2) were labelled with $^{13}C$ and $^{15}N$. The anemones in the "heterotrophy" plates were each fed $^{13}C$- and $^{15}N$-labelled *Artemia*, in order to track these nutrients as they were incorporated into host tissues and translocated to symbiont cells. The anemones in the "autotrophy" plates were incubated in $^{13}C$-and $^{15}N$-labelled seawater to track the nutrients as they were assimilated by the symbionts and translocated to host tissues. All incubations were conducted under the conditions described in section 4.2.1, with light provided by AQUA-GLO T8 fluorescent lightbulbs at ~95 µmol photons $m^{-2}$ $s^{-1}$, and lids were placed loosely over the plates to prevent evaporation while maintaining oxygen exchange.

***4.2.5.1 Preparation of isotope solutions***

$^{13}C$-labelled FSW was obtained by adding 5 mL 1 M HCl to 2 L autoclaved 0.22 µm FSW, to convert the existing $^{12}C$ in the water to $CO_2$, and then aerating the water under a fume hood for 3 h to remove the $CO_2$. The carbon in the medium was then replaced by adding 2 mM $NaH^{13}CO_3$ and the pH was balanced to ~ 7.8 using 1 M NaOH. $^{15}N$- and $^{13}C$-labelled f/2 culture medium was then prepared by adding the components of an f/2 medium kit (Bigelow Laboratory, MA) to the $^{13}C$-labelled FSW, while replacing the $NaNO_3$ component with $Na^{15}NO_3$. An unlabelled f/2 medium was also prepared for reference samples in the same manner, except using $NaHCO_3$ and the $NaNO_3$ included with the f/2 medium kit. Isotopically-labelled FSW for the autotrophy experiment was prepared by adding $K^{15}NO_3$ to a final concentration of 30 µM into the $^{13}C$-labelled FSW. $K^{15}NO_3$ was used *in lieu* of $K^{15}NH_4$, since the goal was to observe only symbiont assimilated nitrogen, and the host is also able to

assimilate ammonium (Kopp *et al.* 2013). Unlabelled FSW for the reference sample containing 2 mM $NaHCO_3$ and 30 µM $KNO_3$ was also prepared. All reagents were obtained from Sigma Alrich (Auckland, New Zealand).

#### *4.2.5.1 Heterotrophic nitrogen translocation*

Cultures of the green alga *Tetraselmis* were grown in $^{15}N$- and $^{13}C$- labelled f/2 medium for 5 months, with sub-culturing every 2 weeks, to yield highly-enriched algae. *Tetraselmis* in unlabelled f/2 medium was also cultured for the same time-period, to use as reference samples. *Artemia* nauplii were hatched and divided into two groups, with one group being fed labelled *Tetraselmis* and the other fed unlabelled *Tetraselmis* for reference samples, for 10 days before harvesting. At TP1 and TP2, anemones from the B1 and D1a treatments were fed three labelled shrimp each (determined from preliminary trials of host labelling intensity). Six hours post-feeding, anemones were placed in an EM fixative (2% paraformaldehyde, 2.5% glutaraldehyde, 0.1 M sodium cacodylate) and stored at 4$^{o}$C for 24 h. Anemone tentacles were excised and returned to the same fixative solution. The unlabelled *Tetraselmis* and *Artemia* were each collected in a 50 mL Falcon tube and centrifuged for 10 min at 4,000 x g to pellet. The supernatant was discarded and the pellets were frozen at -80$^{o}$C and freeze-dried for later enrichment analysis with the nanoSIMS.

#### *4.2.5.1 Autotrophic C and N fixation and translocation*

The FSW in each well (15 mL) containing an anemone (n = 5) was replaced with $^{13}C$- and $^{15}N$-labelled FSW, and incubated for 6 h (determined from preliminary trials of symbiont labelling intensity). One anemone from the B1 treatment was also incubated in unlabelled FSW as a control. After incubation, anemones were placed into EM fixative as above and stored at 4$^{o}$C for 24 h. Anemone tentacles were then excised as before and returned to the fixative.

*4.2.6 NanoSIMS sample preparation and enrichment measurements*

Fixative was removed from anemone tentacles and they were post-fixed for 1 h in 1% $OsO_4$. Next, the samples were dehydrated through an ethanol series (15%, 30%, 50%, 70%, 90%, 3 x 100%), followed by 10 min in propylene oxide (10 min in each solution). Samples were incubated in a 1:1 propylene oxide: resin mixture for ~ 18 h before embedding in Procure 812 resin (ProSciTech, Australia). Semi-thin sections (500 nm) of each resin block were cut with a Diatome Ultra 45º Diamond Knife. Sections were stretched using a Max Wax heated pen and transferred to 10 mm round glass coverslips using a Perfect Loop (Electron Microscopy Sciences, USA). Both *Tetraselmis* and *Artemia* lyophilized samples were smeared onto a 10 mm round glass cover slip.

Regions of interest (ROIs) on each cover slip were identified under a light microscope (40x magnification) as those containing *Symbiodinium* cells within host tissue and were photographed to use as image maps in subsequent analysis. Cover slips were then coated with 7 nm gold and ROIs were imaged with a NanoSIMS ion probe (conducted at École Polytechnique Fédérale de Lausanne, Switzerland). About 10 *Symbiodinium* cells were imaged *per* anemone at TP1, while around 20-40 *Symbiodinium* cells were imaged *per* anemone at TP2, reflecting the increase in symbiont density and hence ease of locating cells over time. In the autotrophy experiment, a reduced number of replicates ($n = 4$ anemones; $n \geq 12$ symbionts total/treatment) was obtained at TP1 due to the inability of the instrument to detect much carbon translocation from symbiont to host at such cell densities. Samples were bombarded with a 16 keV primary ion beam of (1-2 pA) $Cs^+$ focused to a spot size between 100 – 150 nm on the sample surface. Secondary molecular ions $^{12}C^{14}N^-$, $^{12}C^{15}N^-$, $^{12}C^{12}C^-$ and $^{12}C^{13}C^-$ were simultaneously collected in electron multipliers at a mass resolution ($M/\Delta M$) of ~ 9000, enough to resolve the $^{12}C^{15}N^-$ and $^{13}C^{14}N^-$ ions from possibly problematic interferences, while charge compensation was not necessary. Images of 40 x 40 µm with 256 x 256 pixels were obtained for $^{12}C^{14}N^-$, $^{12}C^{15}N^-$, $^{12}C^{12}C^-$ and $^{12}C^{13}C^-$ by rastering the primary ion beam across the sample with a dwell-time of 5 ms. A drift correction was applied, and the $^{15}N/^{14}N$ and $^{13}C/^{14}C$ maps obtained by taking the ratio between $^{12}C^{15}N^-$ and $^{12}C^{14}N^-$ images or $^{12}C^{13}C^-$ and $^{12}C^{12}C^-$ images. $^{15}N$ and $^{13}C$ enrichments were expressed in the delta notation ($\delta^{15}N$ and $\delta^{13}C$ in ‰) as calculated by:

$$\delta^{15}N = (\frac{N_{mes}}{N_{nat}} - 1) \text{ x } 10^3$$

Where $N_{mes}$ is the measured $^{15}N/^{14}N$ ratio and $N_{nat}$ is the natural $^{15}N/^{14}N$ ratio measured in unlabelled control anemone samples.

$$\delta^{13}C = (\frac{C_{mes}}{C_{nat}} - 1) \text{ x } 10^3$$

Where $C_{mes}$ is the measured $^{13}C/^{12}C$ ratio and $C_{nat}$ is the natural $^{13}C/^{12}C$ ratio measured in unlabelled control anemone samples from the autotrophy experiment. Both $N_{nat}$ and $C_{nat}$ were measured on sections of unlabelled anemone tissue each day of NanoSIMS analysis to correct for any potential instrument drift. Measured enrichments from NanoSIMS images were considered significant when above the natural fluctuations of the $^{15}N/^{14}N$ and $^{13}C/^{12}C$ ratios from different images of unlabelled tissue, defined as the average of $\delta^{15}N$ or $\delta^{13}C \pm 3\sigma$.

### *4.2.7 NanoSIMS image analysis*

L'IMAGE® software was used to analyse NanoSIMS images. ROIs were defined within the images by first tracing the outline of dinoflagellate cells, and then separately tracing the gastrodermal tissue (avoiding intercellular space and mesoglea) and subtracting the dinoflagellate ROIs, i.e. to gather enrichment data for the symbiont and host, respectively. ROI enrichment values were averaged between replicates for each sample. For *Tetraselmis* and *Artemia* samples, the entire area containing lyophilized sample was selected as an ROI.

### *4.2.8 Statistical analysis*

Symbiont cell density values could not be transformed to fit normality assumptions, so the non-parametric Kruskal-Wallis test was used to test for differences (quantified using MFI) between symbiont types at the two time-points. The hourly ratios of gross photosynthesis to dark respiration (P:R) at TP2 were tested for differences between symbiont types using a one-way ANOVA.

Nitrogen enrichment from the heterotrophy experiment and carbon enrichment from the autotrophy experiment were compared between anemones infected with *Symbiodinium* type B1 *versus* D1a. Any negative enrichment values were changed to zero and included in mean calculations. Average host and symbiont enrichment values for each anemone were used, since raw data could not be normalized through transformations and did not have equal sample sizes. Nitrogen enrichment values (in $\delta^{15}N$ ‰) were $\log_{10}$ transformed to meet normality assumptions. For the heterotrophy experiment, a two-way ANOVA was conducted to test whether nitrogen enrichment was significantly influenced by symbiont type or time point. Separate tests were conducted for enrichment values of the host tissues and symbiont cells. For the autotrophy experiment, a two-way ANOVA was similarly used to determine if carbon enrichment in the host tissues and symbiont cells was influenced by either symbiont type or time point.

## 4.3 Results

### *4.3.1 Infection success*

*Symbiodinium* genotyping confirmed successful colonisation by *Symbiodinium* B1 and D1a in their respective experimental treatments. A significant difference in cell density between B1 and D1a was seen at both time points (Fig. 4.1), where B1 was approximately 13x more dense than D1a at TP1 (d.f. = 1, $\chi^2 = 6.82$, $p < 0.01$), and approximately 3x more dense at TP2 (d.f. = 1, $\chi^2 = 6.82$, $p < 0.01$). Furthermore, at 2 days post-infection, B1 symbionts had successfully colonised all anemone tentacles, while D1a symbionts had left many tentacles un-colonised. There were no differences between symbiont types with respect to gross photosynthesis (One-way ANOVA; F (1, 4) = 0.533, $p = 0.51$), photosynthesis *per* symbiont cell (One-way ANOVA; F (1, 4) = 1.38, $p = 0.31$) or P:R ratio (One-way ANOVA; F (1, 4) = 4.98, p = 0.09). The average hourly P:R ratio of B1-colonised anemones was 2.6 and D1a-colonised anemones was 1.8.

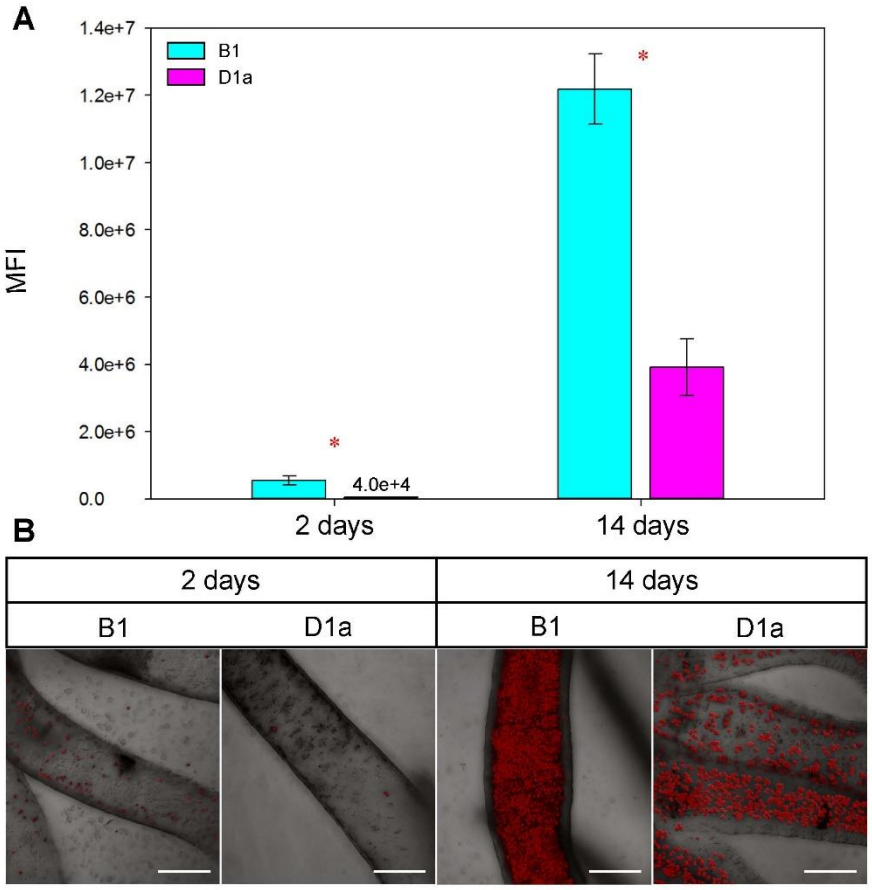


**Figure 4.1** Infection success of *Symbiodinium* types B1 and D1a in the cnidarian host *Aiptasia*. **A**) Symbiont population density within anemone tentacles as assessed by mean fluorescence index (MFI) at 2 days [TP1] and 14 days [TP2] post infection, shown with +/- standard error of the mean. Significant differences between symbiont types are indicated by a red asterisk (*$p < 0.05$). **B**) Confocal images of anemone tentacles infected with both symbiont types at the two time points, showing red autofluorescence of symbiont cells. Scale bars are 100 µm.

### *4.3.2 Heterotrophy experiment*

*Tetraselmis* cells successfully incorporated $^{15}$N-nitrate and $^{13}$C-bicarbonate ($\delta^{13}$C: 4885 ‰ and $\delta^{15}$N: 1,170,772 ‰), while *Artemia* successfully incorporated the labelled algae ($\delta^{13}$C: 4266 ‰ and $\delta^{15}$N: 113,031 ‰). Carbon enrichment values ($\delta^{13}$C ‰) for both the host tissues and symbiont cells were mostly negative or lower than the window of error, so were excluded from further analysis (Appendix B, Table B1). Nitrogen enrichment ($\delta^{15}$N ‰) in host tissues of B1-colonised anemones was 74% lower, while in D1a-colonised anemones it was 60% lower, at 14 days post-inoculation than at 2 days (two-way ANOVA; $F(3, 19) = 12.81$, $p = 0.003$). Between the same time points, B1 symbiont cell enrichment was 90% lower and D1 symbiont

cell enrichment was 28% lower (two-way ANOVA; F (3, 19) = 44.67, $p < 0.0001$) (Fig. 4.2; Table 4.1).

At 2 days post inoculation, no differences in $^{15}N$ enrichment were observed between symbiont types (Fig. 4.3A, B). However, at 14 days post-inoculation, *Symbiodinium* D1a cells appeared more enriched with $^{15}N$ than *Symbiodinium* B1 cells (Fig.4.3C, D). While host nitrogen enrichment was not affected by symbiont type during this time (two-way ANOVA; F (3, 19) = 0.391, $p = 0.541$), nitrogen enrichment of the dinoflagellate cells was significant (two-way ANOVA; F (1, 19) = 6.88, $p = 0.018$). Ultimately, B1 cells were only an average of 20% as enriched with nitrogen as D1a cells. Particles highly enriched in nitrogen (up to $\delta^{15}N$ 215,000 ‰; Table 1) were also noted within the host gastrodermal tissues, which were likely phagocytosed *Artemia* particles (Fig. 4.3A-D).

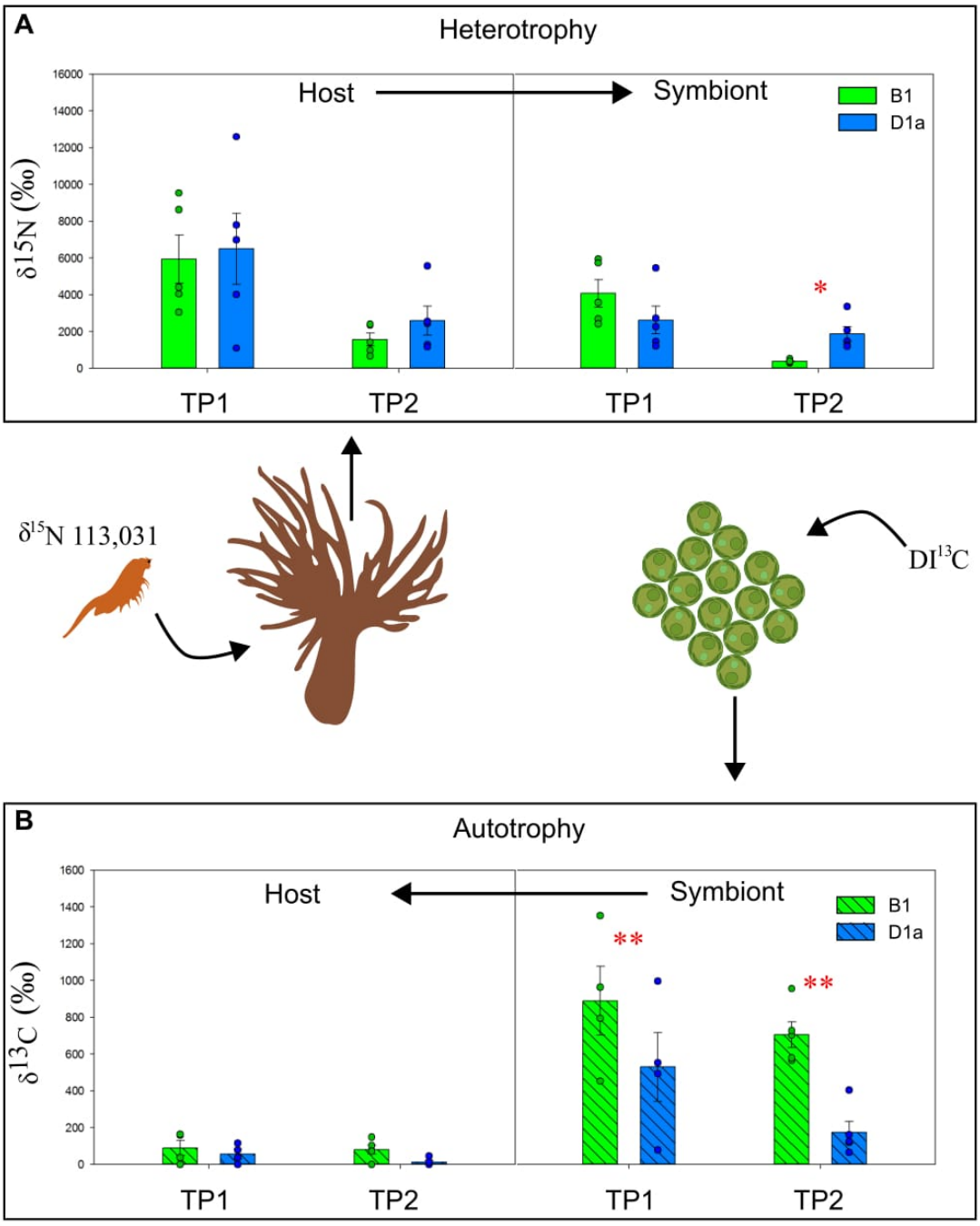


**Figure 4.2** Nitrogen and carbon enrichment of host tissues and symbiont cells. Arrows indicate flow of labelled compounds in the system. **A**) In the heterotrophy experiment, labelled *Artemia* was fed to symbiotic *Aiptasia* and the nitrogen was incorporated into host tissues, then translocated to the symbionts. **B**) In the autotrophy experiment, symbiotic *Aiptasia* were incubated in labelled seawater and the carbon was fixed by the symbionts, and then translocated to the host tissues. Bars represent the mean delta values across all replicate anemones, while plotted points over each bar show the mean delta value for each replicate anemone (n = 5). Bars are shown with +/- standard error of the mean. Significant differences between symbiont types are indicated by a red asterisk (*$p < 0.05$; **$p < 0.01$).

*4.3.3 Autotrophy Experiment*

*Symbiodinium* cells successfully utilized dissolved $^{13}$C-bicarbonate in the seawater for carbon fixation. While some symbiont incorporation of dissolved $^{15}$N-nitrate was detectable, $\delta^{15}$N enrichment values were mostly below the window-of-error and were therefore excluded from further analysis (Appendix B, Table B2). Carbon enrichment ($\delta^{13}$C) of dinoflagellate cells was significantly affected by symbiont type during both time points (two-way ANOVA; $F(3, 17) = 9.934$, $p < 0.01$). At 2 days post-inoculation (Fig. 4.3E, F), *Symbiodinium* D1a cells were an average of 41% less enriched in carbon than *Symbiodinium* B1 cells (Fig. 4.2). At 14 days post-inoculation (Fig. 4.3G, H), *Symbiodinium* B1 cells were clearly more enriched with carbon than *Symbiodinium* D1a cells, where D1a symbionts were an average of 75% less enriched than B1 symbionts (Fig. 4.2). Values for carbon enrichment in host tissues were low and there was no effect of symbiont type (two-way ANOVA; $F(3, 17) = 3.75$, $p = 0.073$).

Negative or zero $\delta^{13}$C values were interpreted as symbionts that were not fixing carbon (Fig. 4.3H; Table 4.1). At TP1, 100% of type B1 symbionts analysed (n = 12) were fixing carbon, while 85% of type D1a symbionts analysed (n = 13) were fixing carbon. At TP2, 89% of type B1 symbionts (n = 205) surveyed were fixing carbon, while nearly 50% of D1a symbionts surveyed (n = 132) were fixing carbon.

**Table 4.1** Range of nitrogen and carbon enrichment values between the time points and symbiont types, as measured using nanoSIMS image analyses.

| **TP1** | | | | |
|---|---|---|---|---|
| | **B1** | | **D1a** | |
| | **Heterotrophy** | **Autotrophy** | **Heterotrophy** | **Autotrophy** |
| **Host** | $\delta^{15}$N 1,845 - 1,6077 | $\delta^{13}$C 0 - 184 | $\delta^{15}$N 497 - 44,131 | $\delta^{13}$C 0 - 132 |
| **Symbiont** | $\delta^{15}$N 132 - 11,371 | $\delta^{13}$C 382 - 1,660 | $\delta^{15}$N 71 - 7,821 | $\delta^{13}$C 0 - 2,728 |
| **Phagocytosed food** | $\delta^{15}$N 14,395 - 215,286 | N/A | $\delta^{15}$N 1,787 - 194,186 | N/A |
| **TP2** | | | | |
| | **B1** | | **D1a** | |
| | **Heterotrophy** | **Autotrophy** | **Heterotrophy** | **Autotrophy** |
| **Host** | $\delta^{15}$N 616 - 2,575 | $\delta^{13}$C 0 - 659 | $\delta^{15}$N 783 - 6,585 | $\delta^{13}$C 0 - 182 |
| **Symbiont** | $\delta^{15}$N 27 - 1,915 | $\delta^{13}$C 0 - 3,579 | $\delta^{15}$N 264 - 5,279 | $\delta^{13}$C 0 - 1,510 |
| **Phagocytosed food** | $\delta^{15}$N 5,221 - 98,634 | N/A | $\delta^{15}$N 13,568 - 137,195 | N/A |

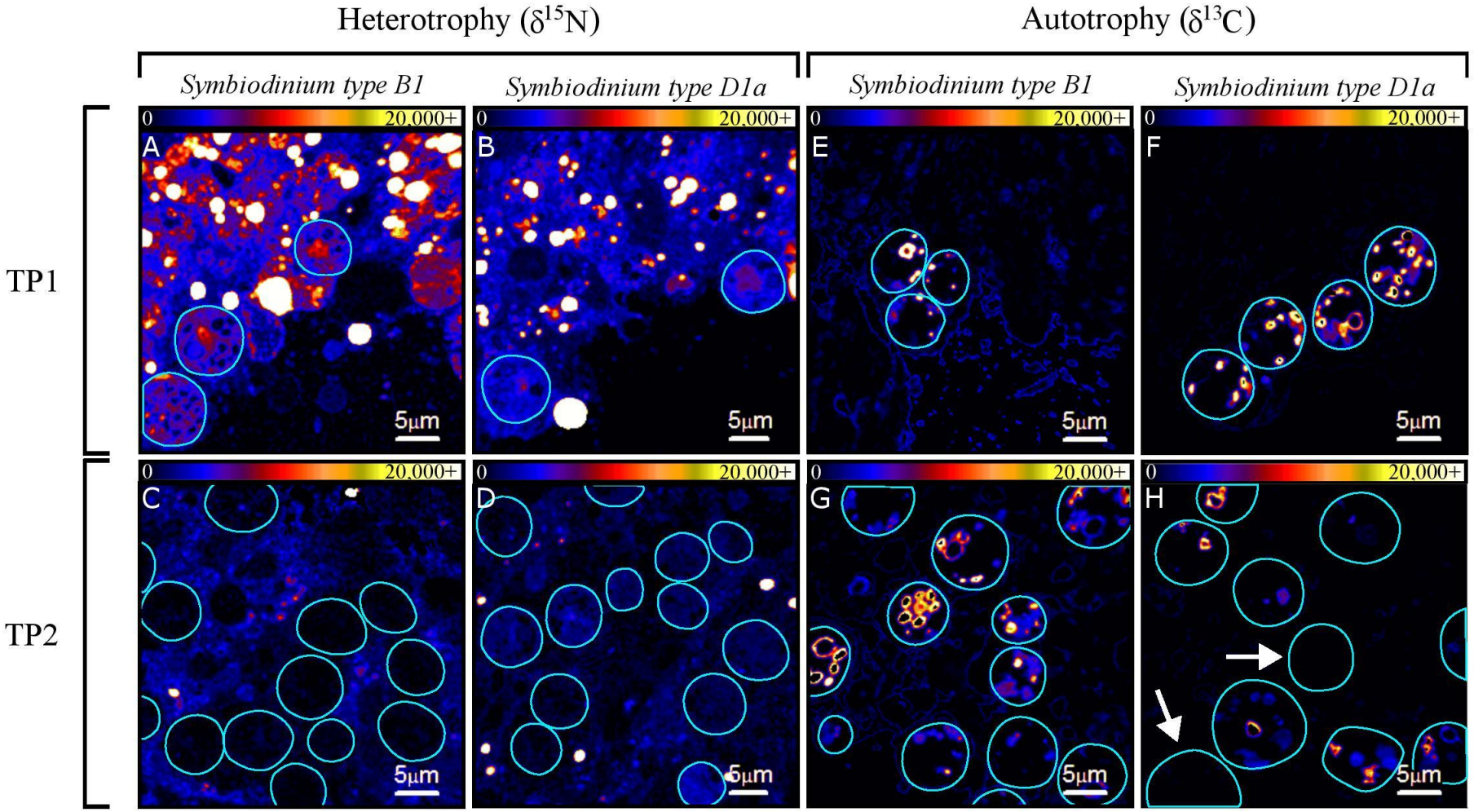


**Figure 4.3** Imaging of $^{15}N$ and $^{13}C$ carbon enrichment within symbiotic *Aiptasia* tissue between 2 days post-inoculation [TP1] and 14 days post-inoculation [TP2] with *Symbiodinium* B1 and *Symbiodinium* D1a. Colour scale indicates values in delta notation, where black signifies no enrichment and white signifies enrichment higher than δ 20,000. Symbiont cells are outlined in cyan, with remaining enriched areas being anemone gastrodermal tissue. (A-D) $^{15}N$ enrichment of *Symbiodinium* B1-colonised *Aiptasia* (A, C) and *Symbiodinium* D1a-colonised *Aiptasia* (B, D) at TP1 (A-B) and TP2 (C-D). (E-H) $^{13}C$ enrichment of *Symbiodinium* B1-colonised *Aiptasia* (E, G) and *Symbiodinium* D1a-colonised *Aiptasia* (F, G) at TP1 (E, F) and TP2 (G, H). White arrows point to symbiont cells that are not fixing any carbon.

## 4.4 Discussion

This study assessed the dynamics of carbon and nitrogen metabolism during two phases of symbiosis establishment, while comparing the differences between a homologous (*Symbiodinium* B1) and heterologous symbiont type (*Symbiodinium* D1a). The reduced translocation of photosynthetic carbon to the host by D1a is consistent with its inability to colonise hosts as readily as the homologous symbionts. In fact, the lack of carbon fixation by a little over half of D1a cells in the longer-term raises questions about the likelihood of its ultimate success in providing energy to the host; however, D1a appears to adequately receive host-derived nitrogen throughout symbiosis establishment, indicating that the heterologous symbiosis is a less mutually beneficial symbiont.

### *4.4.1 Infection dynamics of* Symbiodinium *B1 versus* Symbiodinium *D1a*

Quantification of symbiont population density at two time points during the infection process allowed for a comparison of the rate of symbiosis establishment between the algal types. Not surprisingly, the homologous type (B1) was able to fully colonise the anemones at a greater rate and reached higher symbiont densities than the heterologous type (D1a). MFI was used to assess infection success throughout the experiment because this method provides visual corroboration of symbiont population densities within *Aiptasia* tentacles, which were also the site of nanoSIMS measurements. *Symbiodinium* B1 was able to quickly establish symbiont populations in all host tentacles by TP1, while *Symbiodinium* D1a was slower to establish symbiont populations in host tentacles, leaving many un-colonised at TP1. Oxygen fluxes after two weeks of infection, determined by P:R ratios, indicated that both symbiont types were producing enough carbon to sustain animal respiratory needs in the light (P:R > 1). Previous studies are unanimous in finding a similar result with respect to colonisation by homologous *versus* heterologous symbionts, where both can successfully invade the host, but with the heterologous symbiont doing so more slowly and often achieving lower cell densities (Weis *et al.* 2001; Belda-Baillie *et al.* 2002; Dunn & Weis 2009; Starzak *et al.* 2014). The reasons for this pattern are uncertain, but could be related to complementary glycans on the cell surface of the homologous symbiont (Koike *et al.* 2004; Logan *et al.* 2010; Bay *et al.* 2011), important inter-partner signalling processes (Schwarz & Weis 2003; Wood-Charlson *et al.* 2006;

Detournay *et al.* 2012) or up- or down-regulation of the host's immune defences (Davy *et al.* 2012). Although densities of B1 were more than 10-fold higher than those of D1a at TP1, this gap had narrowed to ~3-fold by TP2. This may be due to B1 populations reaching maximum capacity while D1a populations were still in the proliferation phase. The results presented here suggest that most D1a cells are rejected during the recognition and sorting phases, but those few that do become successfully established as symbionts are able to proliferate to some degree. The colonisation patterns seen here are therefore representative of the establishment process for an optimal symbiosis (*Symbiodinium* B1) and a sub-optimal symbiosis (*Symbiodinium* D1a).

### *4.4.2 The effect of symbiont type on heterotrophic metabolic translocation*

Anemones in the two treatments incorporated similar levels of $^{15}N$ into host tissues. However, a difference in the translocation of labelled nitrogen to symbionts during TP2 was observed, where D1a symbionts were enriched about four times as much as B1 symbionts (Fig. 4.3). Differences in symbiont density between the two *Symbiodinium* types may have contributed to this outcome, since the population density of B1 was three-fold more than that of D1a at TP2, and hence D1a may have had less competition from neighbouring cells if N was a limited resource (Cook & D'Elia 1987; Falkowski *et al.* 1993). However, despite the population of B1 being 13-fold more dense than that of D1a at TP1, no difference in symbiont $^{15}N$ enrichment was seen at this earlier time point. This could simply be because N was not limiting at this earlier stage, though an alternative explanation would be that B1 is more efficient at taking up nitrogen from the host in the initial stages of colonisation, so countering any increased inter-cellular competition for resources. Furthermore, it is also possible that D1a is less 'metabolically adept' during these early stages. Consistent with this, previous studies have reported that members of *Symbiodinium* clade D assimilate less DIN than do their clade C counterparts under normal seawater temperatures (Baker *et al.* 2013; Pernice *et al.* 2014), though this trend reverses once temperatures become thermally stressful (30$^{o}$C) (Baker *et al.* 2013). The possible reasons for the differential N-uptake are therefore unclear, as both type-specific differences and density-dependent effects could be involved, and the contributions of these towards the patterns seen could shift during host colonisation. Further experiments when the anemones contain equal densities of different symbiont types would help to shed some light

on this issue. Nevertheless, these findings contribute further to our understanding of heterotrophic N metabolism in the cnidarian-dinoflagellate symbiosis and its role in symbiont population regulation.

While *Artemia* were highly enriched with $^{13}C$ ($\delta^{13}C$: 4885 ‰) when fed to anemones, the enrichment values for both host tissues and symbiont cells were very low or undetectable, which may reflect the sensitivity limits of the instrument. Cnidarians use carbon derived from heterotrophy for building proteins and membranes throughout their body, where it tends to reside for a long time (Bachar *et al.* 2007). This heterotrophy-derived carbon is also a potential factor for enhancing coral bleaching resistance by prohibiting intercellular $CO_2$ limitation (Wooldridge 2014). Therefore, the quantification of heterotrophic carbon between symbiont treatment types does present an interesting topic for further investigations, but studies should focus on using more sensitive techniques such as bulk isotope ratio-mass spectrometry.

*4.4.3 The effect of symbiont type on autotrophic metabolite translocation*

*Symbiodinium* B1 fixed 41-75% more carbon than *Symbiodinium* D1a while in symbiosis with *Aiptasia* throughout symbiosis establishment. However, no differences in translocation to the host (indicated by levels of host tissue $^{13}C$-enrichment) were found. Enrichment in host tissues was very low, and at times undetectable in anemone tissues hosting both symbiont types. It is unknown if this is again attributable to the sensitivity threshold of the instrument, or if neither symbiont was releasing much carbon during the experiment. Furthermore, 11% of D1a cells showed no evidence of carbon fixation at the first time point, with this proportion increasing to more than 50% of the population by the later time point; this compared to 100 and 89% of functional B1 cells at the first and later time points, respectively. The small decline in the photosynthetic performance of the homologous symbionts can potentially be explained by regular senescence and degradation processes that occur in a steady-state population (Trench 1974; Titlyanov *et al.* 1996; Jones & Yellowlees 1997). However, the high portion of D1a cells that ceased to fix carbon, and the sharp decline over time, suggests symbiont dysfunction; further studies on cellular viability will help to clarify this issue.

The lower capacity for clade D *Symbiodinium* to assimilate carbon and nitrogen in comparison to the more dominant clade C symbiont has been demonstrated previously (Baker *et al.* 2013;

Pernice *et al.* 2014). This ultimately is a disadvantage to the host, which would have to rely on other carbon sources to meet its daily energy demands. Translocation of photosynthetic products from symbiont to host can be regulated by putative host release factors (HRFs) that may vary widely between host species and exhibit different host-symbiont specificities (Sutton & Hoegh-Guldberg 1990; Gates *et al.* 1995, 1999; Cook & Davy 2001), while cell signalling molecules can also regulate photosynthetic performance and even completely inhibit it (Wang & Douglas 1997; Grant *et al.* 2001). It is therefore possible that, in addition to enhanced cellular dysfunction, the reduced photosynthesis of D1a could be due to incompatibilities with unknown *Aiptasia* signalling molecules that usually enhance photosynthesis and translocation by its symbionts.

Nitrate from the seawater can only be utilized by the symbionts, since the coral host lacks the reductase enzymes necessary for assimilation (Tanaka *et al.* 2006). Symbionts convert nitrate to ammonium using nitrate reductase, which is the assimilated into amino acids for use in building both host and symbiont proteins (Crossland & Barnes 1977; Swanson *et al.* 1998). Here, enrichment resulting from nitrate uptake from the seawater, in both symbiont cells and host tissues, was limited. Other studies have similarly found that dissolved nitrate is taken up at a much slower rate (up to 23-times) than is DIC by the symbionts (Tanaka *et al.* 2006). If ammonium had been used in place of nitrate, higher uptake values would have likely been obtained, since ammonium is the primary nitrogen source for symbionts (Kopp *et al.* 2013).

### *4.4.4 Conclusions*

NanoSIMS is a powerful analytical tool for investigating C and N metabolism in the cnidarian-dinoflagellate symbiosis. Recently, studies have successfully used the technique to visualize intracellular sites of C and N assimilation within symbiotic tissues using incubations in $^{13}C$ and $^{15}N$ isotope solutions (Clode *et al.* 2007; Pernice *et al.* 2012, 2014, Kopp *et al.* 2013, 2015). Chemical fixation techniques are suitable for investigations involving elements bound to macromolecules (Grovenor *et al.* 2006), such as photosynthetically fixed carbon and assimilated nitrogen. However, fixation chemicals and resin may introduce C and N with natural isotope ratios that may slightly dilute the $^{13}C$ and $^{15}N$ tracers (Stadermann *et al.* 2005, Musat *et al.* 2014), which could have contributed to the almost undetectable enrichment values

obtained for $^{15}N$ in the autotrophy experiment and $^{13}C$ in the heterotrophy experiment. Freeze-substitution methods could be used in future investigations to avoid dilution of the tracers by fixation chemicals, and to track any diffusible ions in the symbiosis since this method prevents the redistribution of such elements within the cell (Grovenor *et al.* 2006, Feng *et al.* 2015).

The results presented here are the first to use nanoSIMS to investigate metabolite fluxes during symbiosis establishment, as well as the influence of symbiont genotype on these fluxes. Additionally, this study is one of the first to assess the translocation of heterotrophically-derived compounds from host to symbiont. The results demonstrate how *Symbiodinium* D1a acts as a less mutually beneficial symbiont for *Aiptasia* when compared with the homologous *Symbiodinium* B1 under normal temperatures, during the early and late stages of symbiosis establishment. Overall, *Symbiodinium* D1a was less effective at fixing and hence translocating carbon (at the population level) to the host during both early and late stages of symbiosis establishment. These interactions occur alongside a less successful colonisation of the host, raising the possibility that infection success and metabolic exchange are linked in determining symbiont colonisation success. However, more information would be needed to determine if the nutritional patterns seen are cause or consequence of host-symbiont compatibility.

Clade D symbionts can cause reduced coral holobiont fitness by impairing growth rates and reproduction (Little *et al.* 2004; Jones & Berkelmans 2010, 2011; Lesser *et al.* 2013). The results from my experiment support the previous findings of clade D symbionts being less efficient at certain cellular processes. While over half of the D1a symbionts neglected to provide any fixed carbon to the host in the latter stages of host colonisation, all were receiving nitrogen from the host. Parasitism is defined by one partner living inside another, obtaining beneficial nutrients while the host gains no benefit from the relationship (Park & Allaby 2013). The D1a symbiosis does continue to provide carbon to the host, albeit at lesser quantities, and therefore is merely a sub-optimal symbiont rather than truly parasitic. These findings reinforce the conclusions from Chapter 3, that a symbiosis between *Aiptasia* and *Symbiodinium* D1a may not be sustainable long-term under normal environmental conditions. *Aiptasia* represents a model organism for the cnidarian-dinoflagellate system (Weis 2008; Lehnert *et al.* 2012; Wolfowicz *et al.* 2016), and interactions between other cnidarian species and *Symbiodinium* D1a could well experience similar inadequacy in metabolic exchange.

# Chapter 5: General Discussion

## 5.1 Summary

The exchange of carbon and nitrogen is a central feature driving the persistence of the cnidarian-dinoflagellate symbiosis (Muscatine & Porter 1977; Tremblay *et al.* 2012; Pernice *et al.* 2014). Therefore, the aim of this thesis was to characterize the cellular mechanisms essential for inter-partner nutritional exchange in this symbiosis, and to determine the effects of hosting a thermally-tolerant, but putatively less mutually beneficial symbiont type. This information is necessary to assess the possibility of symbiont switching as a means of adapting to climate change, since the successful establishment of a symbiosis may be linked to the nutritional potential between host-symbiont pairs. First, bioinformatics was used to elucidate, for the first time, protein sequences of membrane transporters likely to act in the exchange of metabolites between host and symbiont (**Chapter 2**). These sequences consisted primarily of glucose, glycerol, nitrogen, and ammonium transporters, and were found to be conserved among a diversity of species, while patterns between different *Symbiodinium* clades were also evident. Next, proteomic and isotopic-labelling experiments were conducted to examine the effects of hosting the thermally tolerant symbiont type, *Symbiodinium* D1a, on cellular processes within a symbiotic association (**Chapter 3 and 4**). My findings corroborated the importance of carbon and nitrogen translocation to the successful establishment and persistence of the symbiosis, and showed that *Symbiodinium* D1a was a less successful partner than the normal symbiont type (*Symbiodinium* B1). The results presented here demonstrate that, under non-stressful environmental conditions, *Symbiodinium* D1a provides less benefits to the host when engaged in a heterologous association with the model cnidarian *Aiptasia* than that of a homologous association. These findings raise the following important questions: How has the integration of cellular processes allowed for adaptation to a symbiotic life-style? Does the degree of compatibility between host and symbiont cell processes determine where partnerships fall on the mutualism – parasitism continuum? And, what are the implications of thermally-tolerant heterologous symbionts for the adaptability of coral reefs to climate change? These questions will be considered further here, with reference to Fig. 5.1, summarising the important cellular interactions and how they are affected by the different symbiotic associations.

## 5.2 Host-symbiont integration determines functionality of symbiosis

### *5.2.1 How has the integration of cellular processes allowed for adaptation to a symbiotic life-style?*

The establishment of symbiotic associations can cause co-evolution of the partners as they adapt to conditions experienced while in symbiosis (Kawaida *et al.* 2013; Guerrero *et al.* 2013). Symbiotic corals first evolved within the mid-to-late Triassic period (225-199 mya; Stanley Jr., 1981), allowing for a long history of natural selection on the partners as a cohesive unit. Thus, selection pressures likely drove the integration of host and symbiont cellular processes seen within modern cnidarian-dinoflagellate relationships. Most remarkable is the integration of carbon metabolism (Fig. 5.1). Uptake of DIC is achieved through a carbon concentrating mechanism (CCM) involving host carbonic anhydrase (CA), that converts seawater carbon to a form that can be utilized in host calcification and symbiont photosynthesis (Furla *et al.* 2000). This integrated mechanism likely evolved to satiate both partners' carbon demands using just one process, but it is unable to function efficiently when the partners are separated (**Chapter 3**). The downregulation of important CCM proteins in aposymbiotic individuals is due to their location in the symbiosome (Barott *et al.* 2015; Oakley *et al.* 2016). The membrane protein VHA (vacuolar $H^+$ -ATPase) pumps $H^+$ into the symbiosome where it reacts with carbonic anhydrase in the conversion of $HCO_3^-$ to $CO_2$, that is then used for symbiont photosynthesis and translocation of the resulting sugars to the host (Barott *et al.* 2015). The primary sugar translocated to the host is glucose, while glycerol is released by the dinoflagellates largely as a stress response (Burriesci *et al.* 2012; Suescun-Bolivar *et al.* 2016). The mechanism of glucose transport to the host is likely through GLUT transporters in the symbiosome membrane (**Chapter 2**), with GLUT8 suggested as a likely candidate for the marking of isolated symbiosome vesicles (Ling *et al.* 2016). Overall, the integration of carbon metabolism between host and symbiont enhances the nutritional potential of each partner and provides benefits that neither would achieve on their own.

Inositol has not been highly studied in the symbiosis, but its roles in host-symbiont pathways are now becoming clearer. The phosphatidylinositol signalling system (PtdIns) and the inositol phosphate metabolism pathway (InsP) are common to at least four different *Symbiodinium*

clades, and may to be critical to the foundation of the symbiosis (Rosic *et al.* 2014). *Myo*-inositol is a central reactant to both of these pathways, which produce metabolites used in signal transduction, such as vesicular trafficking, secretion, actin assembly, and nuclear messaging (Anderson *et al.* 1999; Abel *et al.* 2001). Cnidarians likely transport *myo*-inositol across the symbiosome membrane (**Chapter 2**), so that symbionts can use it as a critical building block in these pathways. In a similarly integrated association, the legume-rhizobia symbiosis, signalling between host and symbiont is mediated *via* phosphatidylinositide-regulated endocytosis (Peleg-Grossman *et al.* 2007). Therefore, inositol in the cnidarian-dinoflagellate symbiosis may can be considered a putative means of communication between host and symbiont. Along these lines are potential glycosylphosphatidylinositol (GPI) anchors on the symbiont cell surface that may be important for recognition by cnidarian hosts (Davy *et al.* 2012). More research should be conducted on the role of inositol in host-symbiont interactions, as it could be a multifaceted molecule important to the establishment and persistence of compatible associations.

The exchange of ions across the symbiotic interface is another important feature of host-symbiont integration. Ion transport is important to the symbiosis as it regulates pH of the symbiosome space (Gibbin *et al.* 2014; Barott *et al.* 2015) and drives the transport of *myo*-inositol, as well as other molecules, through membrane co-transporters (Pao *et al.* 1998). The symbiotic state is necessary for adequate expression of sodium/calcium antiporters and other transmembrane ion regulators, and possibly upregulates the production of free fatty acids (**Chapter 3)**. Fatty acids are other important products coupled with ion transport from host to symbiont (Imbs *et al.* 2014), likely though either SMCT or OCTN proteins in the symbiosome membrane (**Chapter 2**).

Integrated host-symbiont nitrogen metabolism is a further major adaptation to a symbiotic life-style, as symbionts are provided with host-derived nitrogen from heterotrophic feeding (**Chapter 4**). Ammonium is the primary nitrogen source for symbiotic corals, as it can be assimilated by both the host and symbiont (Pernice *et al.* 2012; Kopp *et al.* 2013). Nitrate and urea dissolved in the seawater are also nitrogen products that can be important nutrients for symbiotic corals, with urea being preferred over nitrate (Grover *et al.* 2003, 2006). Other than water and glycerol, aquaporin channel proteins can also likely transport urea, purines, and

pyrimidines through the symbiosome (**Chapter 2**). Aquaporins are protein channels in both cnidarian and *Symbiodinium* cell membranes (Fig. 5.1), so these solutes would be able to flow freely between the partners (Lin *et al.* 2015). When nitrogen availability is high, symbionts store the nutrient as uric acid crystals to use as reserves for when conditions are nitrogen limited (Clode *et al.* 2007; Kopp *et al.* 2013). This may account for increased translocation of host nitrogen to symbionts during early stages of symbiosis when nitrogen is freely available, so that they can rely on these nitrogen stores in later phases of symbiosis when high symbiont densities cause nitrogen limitation (**Chapter 4**). Formation of these uric acid crystals is also important to the host, since the crystals contain purine rings that may be used for host purine salvaging, facilitated by host nucleoside hydrolase (NH) and aquaporin channels in the symbiosome (**Chapter 2 & 3**).

One apparent adaptation to a shared nitrogen metabolism is the upregulation of AMT proteins seen in *Symbiodinium*. A previous genomic study found an expansion of ammonium transporter genes in the dinoflagellates that showed species-specific patterns between *Symbiodinium minutum, Symbiodinium kawagutii,* and *Symbiodinium microadriaticum* genomes (Aranda *et al.* 2016). However, examination of *Symbiodinium* transcripts was better able to show how adaptation to integrated nitrogen metabolism may differ between clades, as more transcriptomes are publicly available (**Chapter 2)**. The most ancestral clade, *Symbiodinium* A may have retained some of its reliance on seawater nitrate over host ammonium, while the more derived clades have lost the need to transcribe a nitrate transporter repertoire due to an increasing reliance on host-derived ammonium (**Chapter 2**). Interestingly, the more typically free-living *Symbiodinium* clade F (*Symbiodinium kawagutii*) transcribed few ammonium and nitrate transporting proteins, despite having the genes for them (Lin *et al.* 2015). *Symbiodinium* C expressed the greatest diversity of ammonium uptake proteins, which is likely an adaptation to its qualities as a host-generalist and ability to thrive in a diversity of environments (LaJeunesse 2005; Lin *et al.* 2015).

Mechanisms of ammonium transport in the symbiosis further illustrate the congruent evolutionary paths leading to host-symbiont integration. Both *Symbiodinium* and cnidarians possess ammonium channel proteins (**Chapter 2**), and their expression in the host is downregulated when not engaged in symbiosis (Lehnert *et al.* 2014; Oakley *et al.* 2016).

Therefore, these channels likely work in tandem to allow the flow of ammonium molecules between partners. Co-evolution of the host and symbiont ammonium channels is evident by the amino acid conservation seen between *Aiptasia* AMT sequences and *Symbiodinium* AMT sequences from clades A, B, C that cluster together in phylogenetic analysis (**Chapter 2**). Interestingly, *Aiptasia* is able to form associations with symbionts from all of these clades (Chen *et al.* 2016; Wolfowicz *et al.* 2016), demonstrating that evolutionary adaptations may be key to successful associations. Additionally, the protein sequence for *Symbiodinium* adenylate cyclase is closely related to a metazoan-like clade of *Symbiodinium* ammonium transporters. Although this result initially seemed inexplicable, it may also be related to the co-evolution of cnidarian and *Symbiodinium* proteins, since G-proteins induced by the symbiosis are known to stimulate adenylate cyclase (**Chapter 3**). Therefore, these cnidarian G-proteins could be stimulating *Symbiodinium* adenylate cyclase as part of a signalling pathway.

The integration of cell-signalling pathways is responsible for successful recognition and regulation of symbiont populations. Apoptosis and autophagy pathways are one of the primary ways that hosts can regulate symbiont proliferation and remove damaged or unwanted symbionts (Dunn *et al.* 2007b; Dunn & Weis 2009). Host proteins expressed at the symbiotic interface are likely to help facilitate this pathway by transporting apoptosis-inducing products into the symbiosome space (**Chapter 2**). The presence of a properly integrated symbiosome is critical to the host's abilities to remove unwanted symbiont cells, as apoptosis pathways are highly downregulated without the presence of a symbiotic relationship (**Chapter 3**).

Animal cell adhesion proteins evolved new roles under the selection pressures of symbiosis, by gaining the ability to mediate cell-to-cell interactions in the symbiosome membrane. The Sym32 protein is usually expressed on the apical edges of cnidarian gastrodermal cells, but becomes part of the symbiosome upon establishment of symbiosis (Reynolds *et al.* 2000; Schwarz & Weis 2003). Additional cell adhesion proteins that may act similarly are the cnidarian AQP0 protein (**Chapter 2**), and the glycoproteins hemicentin and fibronectin (**Chapter 3**). Glycoproteins on the *Symbiodinium* cell surface are known to act in symbiont recognition by the host (Lin *et al.* 2000; Bay *et al.* 2011). This recognition process is executed by the glycoproteins binding to lectins on the foreign symbiont cell's outer surface, consequently activating phagocytosis of the cell (McGuinness *et al.* 2003). Glycan-lectin

signalling ultimately determines whether cells are accepted as symbionts or rejected (Koike *et al.* 2004; Wood-Charlson *et al.* 2006; Logan *et al.* 2010; Bay *et al.* 2011). The presence of these symbiosis-enhanced host proteins could indicate that *Symbiodinium* cell surface glycoproteins are incorporated into the symbiosome membrane after phagocytosis.

The cnidarian animal seems to have evolved a dependence on *Symbiodinium* metabolites to maintain its overall health and physiology. The symbionts trigger more efficient production of nematocyst toxins, which allow the animal to more efficiently defend itself against predators and capture food (**Chapter 3**). Additionally, the symbionts promote muscle fibre assembly (**Chapter 3**), while the absence of symbionts can cause toxic reactants to build up in host tissues when the solutes needed to complete the reaction pathway are usually provided by the symbiont (**Chapter 3**).

### *5.2.2 Does the degree of cellular compatibility determine where host-symbiont pairs fall on the mutualism-parasitism continuum?*

Corals must adapt to elevated seawater temperatures in order to survive the imminent effects of climate change. Many think that this will happen according to the Adaptive Bleaching Hypothesis (ABH), with more thermally-tolerant symbionts becoming dominant in corals (Buddemeier & Fautin 1993; Fautin & Buddemeier 2004; Berkelmans & van Oppen 2006). However, the functional diversity among *Symbiodinium* types poses the question of whether the more tolerant symbionts will be wholly compatible with all host species on a cellular level. While integration of host and symbiont cells must occur for a relationship to be established, my results suggest that there are varying degrees of cellular compatibility and that these are linked to where the association falls on a scale from mutualism – parasitism – complete dysfunction (Fig. 5.1).

A previously described continuum for symbiotic corals categorized *Symbiodinium* from clades A and D as being more towards the parasitism end of the scale, due to the reduced fitness they impart on hosts under normal environmental conditions (Stat *et al.* 2008; Lesser *et al.* 2013). This is problematic since these two clades are also the most tolerant to environmental stress

(Loram *et al.* 2007; Yuyama *et al.* 2016; Silverstein *et al.* 2017). *Symbiodinium* from clade A is likely to be the most parasitic since it is the most ancient, and therefore it may be less physiologically integrated with the host than are more derived clades of *Symbiodinium* (**Chapter 2**). This lower compatibility has been highlighted by background populations of *Symbiodinium* A, that exhibited lower rates of carbon fixation and translocation than did the dominant symbionts from clade C *Symbiodinium* (Stat *et al.* 2008). In homologous infections, clade D *Symbiodinium* has also been observed as less efficient at nutrient assimilation and translocation than clade C counterparts (Baker *et al.* 2013; Pernice *et al.* 2014). Consistent with these previous observations, in the current study more than half of the symbiont cells from *Symbiodinium* clade D did not photosynthesize at all in *Aiptasia*, but were still able to receive host-derived nitrogen (**Chapter 4**). This demonstrates how less-than-optimal host-symbiont nitrogen and carbon pathways are characteristic of symbioses involving clade D *Symbiodinium*. This could be related to incompatible cellular aspects such as host release factors (HRFs). *Symbiodinium* types incubated with HRFs from the same host species fix and release different quantities of photosynthetic carbon (Stat *et al.* 2008). HRFs can consist of different compounds such as amino acids (Gates *et al.* 1995, 1999; Wang & Douglas 1997; Stat *et al.* 2008), but they differ greatly in their symbiont-specificity (Sutton & Hoegh-Guldberg 1990). However, it should be recognised that HRFs are now widely regarded as artefact of experiments with isolated symbionts and homogenized host tissues (Davy *et al.* 2012). The reduced ability of *Symbiodinium* D cells to fix carbon could also be related to incompatibilities within the carbon concentrating mechanism, which would ultimately provide less carbon for photosynthesis (Fig. 5.1).

## Homologous

High symbiont infection
High carbon fixation
Ave. nitrogen assimilation

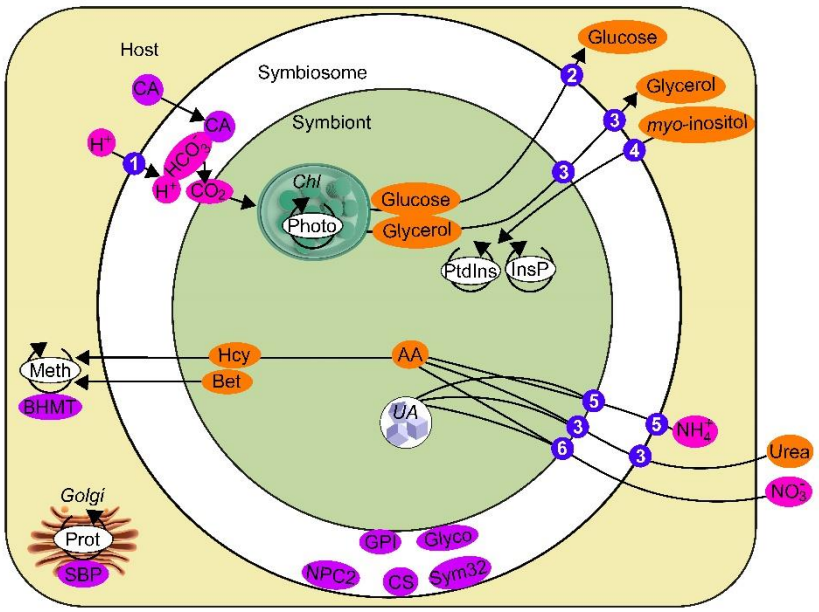


## Heterologous

Low symbiont infection
~ 50% carbon fixation
Ave. nitrogen assimilation

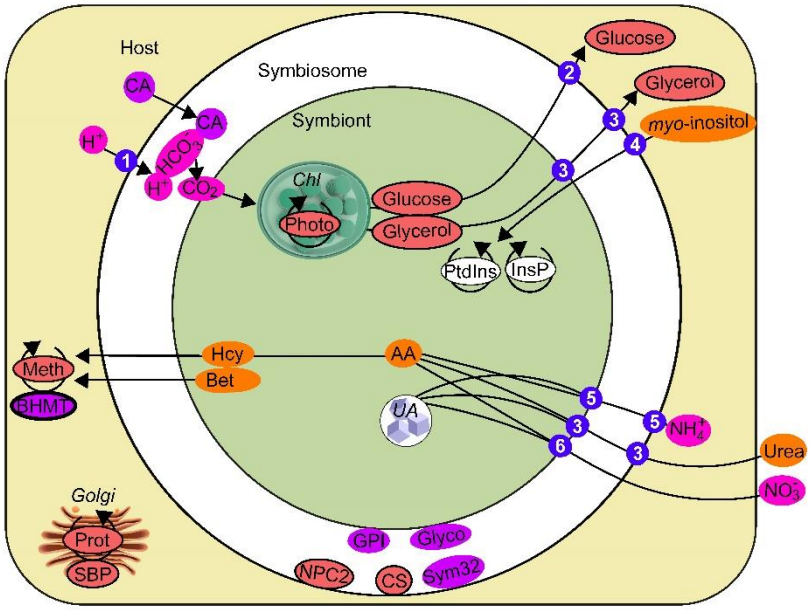


## Aposymbiotic

No symbiont infection
No carbon fixation
No nitrogen assimilation

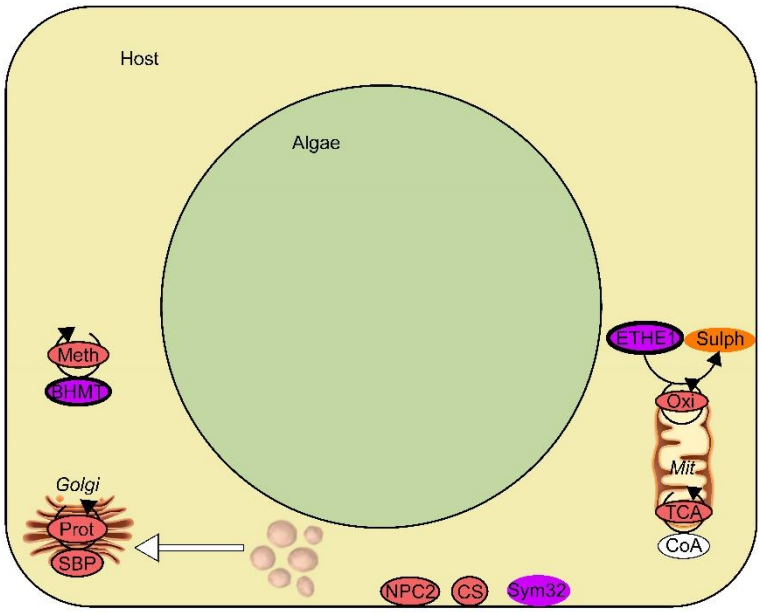

◂ **Figure 5.1** Conceptual diagram of the cellular processes during varying degrees of symbiont compatibility. Purple = proteins; pink = charged molecules; blue = transporters; orange = organic compounds. Molecules and processes downregulated in comparison to the homologous association are filled in red; upregulated molecules are outlined in bold. In a homologous association, H+ ions are pumped through the symbiosomes by vATPase (1), where they react with carbonic anhydrase (CA) to convert bicarbonate ions to $CO_2$ to be used in symbiont photosynthesis. Photosynthesis (Photo) produces sugars, mainly glucose, that are translocated to the host through GLUT proteins (2). Glycerol is released by the symbiont and potentially translocated to the host through AQP proteins (3). Myo-inositol from the host is transported to the symbiont through HMIT and SMIT proteins (4) where it acts in the symbiont's phosphatidylinositol signalling system (PtdIns) and inositol phosphate metabolism (InsP). Nitrogen is taken up by the symbiont from the host in the form of ammonium by AMT transporters (5) in the symbiosome and symbiont cell membrane, and is also taken up from the seawater in the form of nitrate, through NRT2 transporters (6), and urea, through AQP proteins (3). The nitrogen compounds are used for amino acid assimilation or stored as uric acid crystals (UA). Symbiont betaine (Bet) and homocysteine (Hcy) are translocated to the host to be used in the methionine pathway (Meth), catalysed by BHMT. Selenium binding proteins (SBP) act in protein transport (Prot) within the Golgi apparatus. GPI-anchors and glycoproteins (Glyco) on the symbiont cell surface, as well as NPC2, the circumsporozoite protein (CS), and the cell adhesion protein Sym32 all act in recognition processes.

In a heterologous association, CA is downregulated, which further impairs photosynthesis and reduces translocation of sugars to the host, and NPC2 and CS are downregulated. BHMT is upregulated, indicating dysfunction of methionine metabolism, and selenium binding proteins are downregulated indicating dysfunction in protein transport of the Golgi.

In aposymbiotic anemones, ETHE1 is upregulated indicating dysfunction in the mitochondrial (Mit) oxidation pathway, and succinyl coA is downregulated indicating dysfunction in the TCA cycle. NPC2 and CS are downregulated, as are vesicle transport to the Golgi and inter-Golgi protein transport.

Regulation of symbiont cell proliferation is a prime feature of mutualistic associations, used to ensure that nutritional resources do not become unevenly allocated to the symbionts (Muscatine & Pool 1979; Detournay & Weis 2011). However, heterologous clade D *Symbiodinium* can suppress many of the constituents of these pathways in the host, meaning that cell proliferation is not able to be adequately regulated (**Chapter 3**). This could provide an opportunity for the symbionts to have uncontrolled growth that may deprive the host of nutrients. This was potentially the case in another infection experiment, where heterologous symbionts were able to reach population densities much higher than the homologous symbionts (Starzak *et al.* 2014). Clade D *Symbiodinium* also induces the breakdown of molecules involved in the animal's immune response, possibly making it more susceptible to diseases (**Chapter 3**). This may have been the case for *Symbiodinium* A, which was found to have a significant association with diseased or abnormal corals over healthy corals (Stat *et al.* 2008). Additionally, *Symbiodinium* D impairs protein and DNA synthesis, which could be a side-effect of elevated pyrimidine breakdown (**Chapter 3**). Overall, clade D *Symbiodinium* has many negative effects on host cellular processes despite its ability to form an association.

In *Aiptasia* - *Symbiodinium* D associations, central enzymes of the nitrogen assimilation pathway in the host were downregulated (**Chapter 3**), yet nitrogen from heterotrophy was still

easily incorporated and provided to the symbiont (**Chapter 4**). This indicates that the symbionts may impair the host's ability to assimilate dissolved ammonium in the seawater, but not their ability to utilize nutrients from feeding. The most notable incompatibility is within the methionine assimilation pathway, which relies on solutes from each partner for proper functioning (Nakamura *et al.* 1998; Wang & Douglas 1998). Dysfunction of the pathway is apparent in both aposymbiotic anemones and in *Symbiodinium* D-colonised anemones by accumulation of the intermediate, BHMT, which is generally consumed in the functioning reaction (**Chapter 3**). The decreased nutritional potential for *Symbiodinium* D associations may also be due to missing putative recognition molecules from the onset of symbiosis, such as the NPC2 and CS proteins (Fig. 5.1), which could be important for the development of successful mutualistic relationships (**Chapter 3**). Overall, the degree of cellular compatibility between host and symbiont can reveal the type of symbiotic relationship being observed, which ultimately determines symbiont success.

### 5.3 Implications for coral adaptability *via* thermally tolerant symbionts

Opportunistic, thermally tolerant symbiont types are less beneficial, and sometimes harmful, to cnidarian hosts at non-stressful temperatures (Little *et al.* 2004; Jones & Berkelmans 2011; Pernice *et al.* 2014), especially when the host is not well-adapted to their presence (**Chapters 3 & 4**). However, when in symbiosis with their native host species, these symbiont types are able to retain high nutritional potential under the conditions provided by a warming climate (Jones & Berkelmans 2010; Baker *et al.* 2013; Silverstein *et al.* 2017). Therefore, symbiont shuffling to thermally tolerant *Symbiodinium* types is a viable option for corals already harbouring one of these types in background populations. The caveat to this adaptation process would be reduced growth of the corals as temperatures fluctuate between stressful and tolerable across seasons (Brown *et al.* 1999; Warner *et al.* 2002). However, as ocean temperatures warm, to be consistently near the current tolerance limits of corals, associations with homologous *Symbiodinium* A and D will become more globally dominant to improve coral survival (Howells *et al.* 2016; Sampayo *et al.* 2016). Unfortunately, coral species that have not previously adapted to these symbiont types are unlikely to survive due to the negative effects that will be induced by the symbionts under fluctuating temperatures (**Chapter 3 & 4**). Seawater temperatures are rising at an alarming rate, much faster than the

environmental pressures that have shaped host-symbiont specificities (Hoegh-Guldberg *et al.* 2007; Heron *et al.* 2016). Therefore, novel associations with heterologous symbiont types will likely not have enough time to evolve compatible cellular mechanisms (**Chapter 2**).

This scenario would cause an overall decrease in genetic diversity on coral reefs, as only coral species with previously existing populations of thermally-tolerant symbionts would survive. Moreover, there would be a shift in dominance to mostly *Symbiodinium* A and D. Genetic diversity in plant and animal populations allows for population growth and resistance to disease (Williams 2001; Tarpy 2002; Hughes & Boomsa 2004). A lesser resistance to disease in coral populations may be further amplified by the ability of some thermally-tolerant symbiont types to suppress host immune processes (**Chapter 3**). Coral diseases such as black band disease and white syndrome are accelerated under thermal stress, further complicating the situation (Jones *et al.* 2004; Bruno *et al.* 2007). Ultimately, if the rate of ocean warming was reduced, then corals might have a better chance to adapt to changing conditions, *via* the ABH or by developing compatible symbioses with novel symbiont types, and so avoid a reduction in genetic diversity and coral cover.

### 5.4 Limitations and future work

While data mining is an extremely useful tool for bioinformatic analyses of the symbiosis, investigations are limited to those of cnidarian species and *Symbiodinium* types with transcriptomes and genomes that have already been reliably sequenced (**Chapter 2**). While new resources are being released frequently, bioinformatic analysis will also have to take into consideration that the organisms were sampled under different conditions. Therefore, future work examining protein sequences would benefit from a comparative transcriptomics approach of hosts infected with different symbiont types under controlled conditions. This method has been used to show genetic differences between symbiotic and aposymbiotic individuals, and has identified some transmembrane sequences (Lehnert *et al.* 2014; Aranda *et al.* 2016). This method could help elucidate whether integration of transporter proteins in the symbiosome is successful between different symbiotic associations, and whether this led to some of the patterns observed in my research.

Proteomic analysis using LC-MS/MS has allowed the discovery of host proteins important to the symbiotic state (Peng *et al.* 2010; Oakley *et al.* 2016). However, methods for analysis of the symbiont fraction have yet to be developed, and could be vital to future projects aimed at understanding the cellular changes undergone by symbionts integrating into host cells. Many of the proteins I discovered seemed to be symbiosome membrane proteins (**Chapter 2 & 3**). Immunolabelling would be useful to further investigate the location of these proteins and confirm whether they are components of the symbiotic interface, as this technique has previously been successful in localizing NPC2 and vATPase to the symbiosome (Dani *et al.* 2014; Barott *et al.* 2015). While nanoSIMS has provided novel imaging of the nutrient exchange between cnidarians and their symbiotic dinoflagellates, the instrument was not able to obtain many values for carbon enrichment in host tissues. I was unable to tell if these low values indicate the absence of translocation or if the levels were beyond the sensitivity threshold of the instrument. Future studies should couple nanoSIMS translocation experiments with bulk isotope-ratio mass spectrometry (IRMS) measurements to offset the potential problems of instrument sensitivity (Tanaka *et al.* 2006; Popa *et al.* 2007; Grover *et al.* 2008).

Establishing a baseline is important before attempting to observe the impacts of temperature manipulations on a system. Due to this, and the complexity of experimental analyses, all of my experiments were conducted under normal seawater conditions (**Chapters 3 & 4**). However, the functioning of thermally-tolerant symbiont types changes with temperature (Baker *et al.* 2013; Silverstein *et al.* 2017). Therefore, further information on the functionality of heterologous *Symbiodinium* D1a as a suboptimal symbiont would benefit from repeating these experiments at various elevated temperatures.

## 5.5 Conclusions

Overall, my work has shown that the exchange of carbon and nitrogen products is a process shaped by the compatibility of host and symbiont, and that this partly determines the success of a symbiotic relationship. My findings further the work of Oakley *et al.* (2016), who identified proteins that were upregulated in the symbiotic *versus* aposymbiotic state, by

differentiating proteins upregulated by mutualistic *versus* parasitic, or less beneficial, symbiosis. My findings have also furthered the work of Pernice *et al.* (2014), by observing the fluxes of carbon and nitrogen in symbiotic tissues during the earlier phases of symbiosis establishment, and observing the effect of heterologous clade D *Symbiodinium* on these fluxes compared to the homologous *Symbiodinium* type. An understanding of the mechanisms driving host-symbiont specificity are important for determining how corals may adapt to climate change (LaJeunesse *et al.* 2010; Stat & Gates 2011; Davy *et al.* 2012; Silverstein *et al.* 2012), especially if the only hope for coral survival is symbiont community change to a thermally tolerant symbiont type.

## References


Abel K, Anderson RA, Shears SB (2001) Phosphatidylinositol and inositol phosphate metabolism. *Journal of Cell Science*, **114**, 2207–2208.

Abrego D, van Oppen MJH, Willis BL (2009) Onset of algal endosymbiont specificity varies among closely related species of *Acropora* corals during early ontogeny. *Molecular Ecology*, **18**, 3532–43.

Abrego D, Ulstrup K (2008) Species–specific interactions between algal endosymbionts and coral hosts define their bleaching response to heat and light stress. *Proceedings of the Royal Society B: Biological Sciences*, **275**, 2273–82.

Adams M, Jia Z (2005) Structural and biochemical analysis reveal pirins to possess quercetinase activity. *Journal of Biological Chemistry*, **280**, 28675–28682.

Adl SM, Simpson AG, Lane CE, Lukeš J, Bass D, Bowser SS, Brown MW, Burki F, Dunthorn M, Hampl V, Heiss A (2012) The revised classification of eukaryotes. *Journal of Eukaryote Microbiology*, **59**, 429–493.

Agre P, King LS, Yasui M, Guggino WB, Ottersen OP, Fujiyoshi Y, Engel A, Nielsen S (2002) Aquaporin water channels--from atomic structure to clinical medicine. *The Journal of Physiology*, **542**, 3–16.

Aikawa M, Yoshida N, Nussenzweig RS, Nussenzweig V (1981) The protective antigen of malarial sporozoites (*Plasmodium berghei*) is a differentiation antigen. *The Journal of Immunology*, **126**, 2494–2495.

Ainsworth TD, Kvennefors EC, Blackall LL, Fine M, Hoegh-Guldberg O (2007) Disease and cell death in white syndrome of Acroporid corals on the Great Barrier Reef. *Marine Biology*, **151**, 19–29.

Allemand D, Furla P, Benazet-Tambutte S (1998) Mechanisms of carbon acquisition for endosymbiont photosynthesis in Anthozoa. *Canadian Journal of Botany*, **76**, 925–941.

Anderson RA, Boronenkov IV, Doughman SD, Kunz J, Loijens JC (1999) Phosphatidylinositol phosphate kinases, a multifaceted family of signaling enzymes. *The Journal of Biological Chemistry*, **274**, 9907–9910.

Anthony K, Fabricius K (2000) Shifting roles of heterotrophy and autotrophy in coral energetics under varying turbidity. *Journal of Experimental Marine Biology and Ecology*, **252**, 221–253.

Apostolou A, Shen Y, Liang Y, Luo J, Fang S (2008) Armet, a UPR-upregulated protein, inhibits cell proliferation and ER stress-induced cell death. *Experimental Cell Research*, **314**, 2454–2467.

Aranda M, Li Y, Liew YJ, Baumgarten S, Simakov O, Wilson MC, Piel J, Ashoor H, Bougouffa S, Bajic VB, Ryu T (2016) Genomes of coral dinoflagellate symbionts highlight evolutionary adaptations conducive to a symbiotic lifestyle. *Scientific Reports*, **6**, 1–15.

Ashkenazy H, Erez E, Martz E, Pupko T, Ben-Tal N (2010) ConSurf 2010: Calculating evolutionary conservation in sequence and structure of proteins and nucleic acids. *Nucleic Acids Research*, **38**, 529–533.

Augustin R, Riley J, Moley KH (2005) GLUT8 contains [DE]XXXL[LI] sorting motif and localizes to a late endomosal/lysosomal compartment. *Traffic*, **6**, 1196–1212.

Awad EW, Anctil M (1993) Positive coupling of beta-like adrenergic receptors with adenylate cyclase in the cnidarian *Renilla koellikeri*. *The Journal of Experimental Biology*, **182**, 131–46.

Babcock RC, Heyward AJ (1986) Larval development of certain gamete-spawning scleractinian corals. *Coral Reefs*, **5**, 111–116.

Bachar A, Achituv Y, Pasternak Z, Dubinsky Z (2007) Autotrophy versus heterotrophy: The origin of carbon determines its fate in a symbiotic sea anemone. *Journal of Experimental Marine Biology and Ecology*, **349**, 295–298.

Baker AC (2003) Flexibility and specificity in coral-algal symbiosis: diversity, ecology, and biogeography of *Symbiodinium*. *Annual Review of Ecology, Evolution, and Systematics*, **34**, 661–689.

Baker DM, Andras JP, Jordan-Garza AG, Fogel ML (2013) Nitrate competition in a coral symbiosis varies with temperature among *Symbiodinium* clades. *The ISME journal*, **7**, 1248–1251.

Baker DA, Kelly JM (2004) Structure, function and evolution of microbial adenylyl and guanylyl cyclases. *Molecular Microbiology*, **52**, 1229–1242.

Barneah O, Weis VM, Perez S, Benayahu Y (2004) Diversity of dinoflagellate symbionts in Red Sea soft corals: Mode of symbiont acquisition matters. *Marine Ecology Progress Series*, **275**, 89–95.

Barott KL, Venn AA, Perez SO, Tambutté S, Tresguerres M (2015) Coral host cells acidify symbiotic algal microenvironment to promote photosynthesis. *Proceedings of the National Academy of Sciences of the United States of America*, **112**, 607–12.

Barshis DJ, Ladner JT, Oliver TA, Seneca FO, Traylor-Knowles N, Palumbi SR (2013) Genomic basis for coral resilience to climate change. *Proceedings of the National Academy of Sciences*, **110**, 1387–92.

Barshis DJ, Ladner JT, Oliver TA, Palumbi SR (2014) Lineage-specific transcriptional profiles of *Symbiodinium* spp. unaltered by heat stress in a coral host. *Molecular Biology and Evolution*, **31**, 1343–1352.

Baskett ML, Gaines SD, Nisbet RM (2009) Symbiont diversity may help coral reefs survive moderate climate change. *Ecological Applications*, **19**, 3–17.

Battey JF, Patton JS (1984) A reevaluation of the role of glycerol in carbon translocation in zooxanthellae-coelenterate symbiosis. *Marine Biology*, **79**, 27–38.

Baumgarten S, Simakov O, Esherick LY, Liew YJ, Lehnert EM, Michell CT, Li Y,

Hambleton EA, Guse A, Oates ME, Gough J (2015) The genome of *Aiptasia*, a sea anemone model for coral symbiosis. *Proceedings of the National Academy of Sciences*, **112**, 201513318.

Bay LK, Cumbo VR, Abrego D, Kool JT, Ainsworth TD, Willis BL (2011) Infection dynamics vary between *Symbiodinium* types and cell surface treatments during establishment of endosymbiosis with coral larvae. *Diversity*, **3**, 356–374.

Bay LK, Doyle J, Logan M, Berkelmans R (2016) Recovery from bleaching is mediated by threshold densities of background thermo-tolerant symbiont types in a reef-building coral. *Royal Society Open Science*, **3**, 160322.

Belda-Baillie C, Baillie B, Maruyama T (2002) Specificity of a model cnidarian-dinoflagellate symbiosis. *The Biological Bulletin*, **202**, 74–85.

Bellis ES, Howe DK, Denver DR (2016) Genome-wide polymorphism and signatures of selection in the symbiotic sea anemone *Aiptasia*. *BMC Genomics*, **17**, 160.

Benian GM, Tinley TL, Tang X, Borodovsky M (1996) The *Caenorhabditis elegans* gene unc-89, required for muscle M-line assembly, encodes a giant modular protein composed of Ig and signal transduction domains. *The Journal of Cell Biology*, **132**, 835–848.

Benjamini Y, Hochberg Y (1995) Controlling the false discovery rate: A practical and powerful approach to multiple testing. *Journal of the Royal Statistical Society: Series B*, 289-300.

Berg J, Tymoczko J, Stryer L (2002) Complex carbohydrates are formed by linkage of monosaccharides. In: *Biochemistry* (ed Freeman W), New York.

Berkelmans R, van Oppen MJ (2006) The role of zooxanthellae in the thermal tolerance of corals: a "nugget of hope" for coral reefs in an era of climate change. *Proceedings of the Royal Society of London B: Biological Sciences*, **273**, 2305–12.

Bernardo K, Hurwitz R, Zenk T, Desnick RJ, Ferlinz K, Schuchman EH, Sandhoff K (1995) Purification, characterization, and biosynthesis of human acid ceramidase. *The Journal of Biological Chemistry*, **270**, 11098–11102.

Bertolotti A, Zhang Y, Hendershot LM, Harding HP, Ron D (2000) Dynamic interaction of BiP and ER stress transducers in the unfolded-protein response. *Nature Cell Biology*, **2**, 326–332.

Bertucci A, Forêt S, Ball EE, Miller DJ (2015) Transcriptomic differences between day and night in *Acropora millepora* provide new insights into metabolite exchange and light-enhanced calcification in corals. *Molecular Ecology*, **24**, 4489–4504.

Bertucci A, Moya A, Tambutté S, Allemand D, Supuran CT, Zoccola D (2013) Carbonic anhydrases in anthozoan corals - A review. *Bioorganic and Medicinal Chemistry*, **21**, 1437–1450.

Bieri T, Onishi M, Xiang T, Grossman AR, Pringle JR (2016) Relative contributions of various cellular mechanisms to loss of algae during cnidarian bleaching. *PLoS One*, **11**,

1–24.

Boulotte NM, Dalton SJ, Carroll AG, Harrison PL, Putnam HM, Peplow LM, van Oppen MJ (2016) Exploring the *Symbiodinium* rare biosphere provides evidence for symbiont switching in reef-building corals. *The ISME Journal*, **10**, 1–9.

Bourgeois F, Coady MJ, Lapointe JY (2005) Determination of transport stoichiometry for two cation-coupled myo-inositol cotransporters: SMIT2 and HMIT. *The Journal of Physiology*, **563**, 333–343.

Bradford MM (1976) A rapid and sensitive method for the quantitation of microgram quantities of protein utilizing the principle of protein-dye binding. *Analytical Biochemistry*, **72**, 248–54.

Bradley BP, Shrader EA, Kimmel DG, Meiller JC (2002) Protein expression signatures: An application of proteomics. *Marine Environmental Research*, **54**, 373–377.

Brekhman V, Malik A, Haas B, Sher N, Lotan T (2015) Transcriptome profiling of the dynamic life cycle of the scypohozoan jellyfish *Aurelia aurita*. *BMC Genomics*, **16**, 74-88.

Brown T, Coffroth MA, Lasker H, Brazeau D (2011) Differential gene expression of a putative ammonium transporter in the algal symbiont, *Symbiodinium*. *Submitted to the EMBL/GenBank/DDBJ databases*.

Brown BE, Dunne RP, Ambarsari I, Le Tissier MDA, Satapoomin U (1999) Seasonal fluctuations in environmental factors and variations in symbiotic algae and chlorophyll pigments in four Indo-Pacific coral species. *Marine Ecology Progress Series*, **191**, 53–69.

Bruno JF, Selig ER, Casey KS, Page CA, Willis BL, Harvell CD, Sweatman H, Melendy AM (2007) Thermal stress and coral cover as drivers of coral disease outbreaks. *PLoS Biology*, **5**, 1220–1227.

Bucher M, Wolfowicz I, Voss PA, Hambleton EA, Guse A (2016) Development and symbiosis establishment in the cnidarian endosymbiosis model *Aiptasia* sp. *Scientific Reports*, **6**, 19867.

Bucka-Lassen K, Caprani O, Hein J (1999) Combining many multiple alignments in one improved alignment. *Bioinformatics*, **15**, 122–130.

Buddemeier RW, Fautin D (1993) Coral bleaching as an adaptive mechanism. *Bioscience*, **43**, 320–326.

Burriesci MS, Raab TK, Pringle JR (2012) Evidence that glucose is the major transferred metabolite in dinoflagellate–cnidarian symbiosis. *The Journal of Experimental Biology*, **215**, 3467–77.

Carlos A, Baillie B, Kawachi M, Maruyama T (1999) Phylogenetic position of *Symbiodinium* (Dinophyceae) isolates from tridacnids (Bivalvia), cardiids (Bivalvia), a sponge (Porifera), a soft coral (Anthozoa), and a free-living strain. *Journal of Phycology*, **35**, 1054–1062.

Cates N, McLaughlin J (1979) Nutrient availability for zooxanthellae derived from physiological activities of *Condylactus* spp. *Journal of Experimental Marine Biology and Ecology*, **37**, 31–41.

Cavanaugh CM (1994) Microbial symbiosis: patterns of diversity in the marine environment. *American Zoologist*, **34**, 79–89.

Cerami C, Frevert U, Sinnis P, Takacs B, Clavijo P, Santos MJ, Nussenzweig V (1992) The basolateral domain of the hepatocyte plasma membrane bears receptors for the circumsporozoite protein of *Plasmodium falciparum* sporozoites. *Cell*, **70**, 1021–1033.

Cernichiari E, Muscatine L, Smith DC (1969) Maltose excretion by the symbiotic algae of *Hydra viridis*. *Proceedings of the Royal Society of London B: Biological Sciences*, **173**, 557–576.

Chen WN, Hsiao YJ, Mayfield AB, Young R, Hsu LL, Peng SE (2016) Transmission of a heterologous clade C *Symbiodinium* in a model anemone infection system via asexual reproduction. *PeerJ*, **4**, e2358.

Ciarimboli G (2008) Organic cation transporters. *Xenobiotica*, **38** (7-8), 936–971.

Circu M, Aw TY (2010) Reactive oxygen species, cellular redox systems and apoptosis. *Free Radical Biology and Medicine*, **48**, 749–762.

Clode PL, Saunders M, Maker G, Ludwig M, Atkins CA (2009) Uric acid deposits in symbiotic marine algae. *Plant, Cell, and Environment*, **32**, 170–177.

Clode PL, Stern RA, Marshall AT (2007) Subcellular imaging of isotopically labeled carbon compounds in a biological sample by ion microprobe (NanoSIMS). *Microscopy Research and Technique*, **229**, 220–229.

Coady MJ, Wallendorff B, Gagnon DG, Lapointe JY (2002) Identification of a novel $Na^+$/myo-inositol cotransporter. *Journal of Biological Chemistry*, **277**, 35219–35224.

Coffroth MA, Santos SR (2005) Genetic diversity of symbiotic dinoflagellates in the genus *Symbiodinium*. *Protist*, **156**, 19–34.

Colombo-Pallotta MF, Rodríguez-Román A, Iglesias-Prieto R (2010) Calcification in bleached and unbleached *Montastraea faveolata*: evaluating the role of oxygen and glycerol. *Coral Reefs*, **29**, 899–907.

Conesa A, Götz S, García-Gómez JM, Terol J, Talón M, Robles M (2005) Blast2GO: A universal tool for annotation, visualization and analysis in functional genomics research. *Bioinformatics*, **21**, 3674-3676.

Cook CB (1972) Benefit to symbiotic zoochlorellae from feeding by green hydra. *The Biological Bulletin*, **142**, 236–242.

Cook CB, D'Elia CF (1987) Are natural populations of zooxanthellae ever nutrient-limited? *Symbiosis*, **4**, 199–211.

Cook C, D'Elia C, Muller-Parker G (1988) Host feeding and nutrient sufficiency for

zooxanthellae in the sea anemone *Aiptasia pallida*. *Marine Biology*, **98**, 253–262.

Cook CB, Davy SK (2001) Are free amino acids responsible for the " host factor " effects on symbiotic zooxanthellae in extracts of host tissue? *Hydrobiologia*, **461**, 71–78.

Cooper G (2000) Actin, Myosin, and Cell Movement. In: *The Cell: A Molecular Approach*, Available from: https://www.ncbi.nlm.nih.gov/books. Sinauer Associates, Sunderland (MA).

Cooper TF, Lai M, Ulstrup KE, Saunders SM, Flematti GR, Radford B, van Oppen MJ (2011) *Symbiodinium* genotypic and environmental controls on lipids in reef building corals. *PloS One*, **6**, e20434.

Correa AMS, Brandt ME, Smith TB, Thornhill DJ, Baker AC (2009) *Symbiodinium* associations with diseased and healthy scleractinian corals. *Coral Reefs*, **28**, 437–448.

Crossland CJ, Barnes DJ (1977) Nitrate assimilation enzymes from two hard corals, *Acropora acuminata* and *Goniastrea australensis*. *Comparative Biochemistry and Physiology*, **57**, 151–157.

Cuvillier O (2002) Sphingosine in apoptosis signaling. *Biochimica Et Biophysica Acta*, **1585**, 153–162.

D'Elia C, Domotor S, Webb K (1983) Nutrient uptake kinetics of freshly isolated zooxanthellae. *Marine Biology*, **167**, 157–167.

Dall E, Brandstetter H (2013) Mechanistic and structural studies on legumain explain its zymogenicity, distinct activation pathways, and regulation. *Proceedings of the National Academy of Sciences*, **110**, 10940–5.

Dani V, Ganot P, Priouzeau F, Furla P, Sabourault C (2014) Are Niemann-Pick type C proteins key players in cnidarian-dinoflagellate endosymbioses? *Molecular Ecology*, **23**, 4527–4540.

Dani V, Priouzeau F, Pagnotta S, Carette D, Laugier JP, Sabourault C (2016) Thermal and menthol stress induce different cellular events during sea anemone bleaching. *Symbiosis*, **69**, 175–192.

Danilova N, Sakamoto KM, Lin S (2008) Ribosomal protein S19 deficiency in zebrafish leads to developmental abnormalities and defective erythropoiesis through activation of p53 protein family. *Blood*, **112**, 5228–5237.

Davies P (1984) The role of zooxanthellae in the nutritional energy requirements of *Pocillopora eydouxi*. *Coral Reefs*, **2**, 181–186.

Davies PS (1991) Effect of daylight variations on the energy budgets of shallow-water corals. *Marine Biology*, **108**, 137–144.

Davy SK, Allemand D, Weis VM (2012) Cell biology of cnidarian-dinoflagellate symbiosis. *Microbiology and Molecular Biology Reviews*, **76**, 229–61.

Davy SK, Turner JR (2003) Early development and acquisition of zooxanthellae in the

temperate symbiotic sea anemone *Anthopleura ballii* (Cocks). *Biological Bulletin*, **205**, 66–72.

Deane E, O'Brien R (1981) Uptake of phosphate by symbiotic and free-living dinoflagellates. *Archives of Microbiology*, **128**, 307–310.

Deboer M, Krupp D, Weis VM (2007) Proteomic and transcriptional analyses of coral larvae newly engaged in symbiosis with dinoflagellates. *Comparative Biochemistry and Physiology Part D*, **2**, 63–73.

Detournay O, Schnitzler C, Poole A, Weis VM (2012) Regulation of cnidarian–dinoflagellate mutualisms: evidence that activation of a host TGFβ innate immune pathway promotes tolerance of the symbiont. *Developmental & Comparative Immunology*, **38**, 525-537.

Detournay O, Weis VM (2011) Role of the sphingosine rheostat in the regulation of cnidarian-dinoflagellate symbioses. *The Biological Bulletin*, **221**, 261–269.

Doege H, Bocianski A, Scheepers A, Hubertus AX, Eckel J, Joost HG, Schurmann A (2001) Characterization of human glucose transporter (GLUT) 11 (encoded by SLC2A11), a novel sugar-transport facilitator specifically expressed in heart and skeletal muscle. *Biochemical Journal*, **449**, 443–449.

Doege H, Schürmann A, Bahrenberg G, Brauers A, Joost HG (2000) GLUT8, a novel member of the sugar transport facilitator family with glucose transport activity. *Journal of Biological Chemistry*, **275**, 16275–16280.

Dong H, Li X, Lou Z, Xu X, Su D, Zhou X, Zhou W, Bartlam M, Rao Z (2008) Crystal-structure and biochemical characterization of recombinant human calcyphosine delineates a novel EF-hand-containing protein family. *Journal of Molecular Biology*, **383**, 455–464.

Douglas A (1998) Host benefit and the evolution of specialization in symbiosis. *Heredity*, **81**, 599–603.

Dunn SR, Phillips WS, Green DR, Weis VM (2007a) Knockdown of actin and caspase gene expression by RNA interference in the symbiotic anemone *Aiptasia pallida*. *Biological Bulletin*, **212**, 250–258.

Dunn SR, Schnitzler CE, Weis VM (2007b) Apoptosis and autophagy as mechanisms of dinoflagellate symbiont release during cnidarian bleaching: Every which way you lose. *Proceedings of the Royal Society of London B: Biological Sciences*, **274**, 3079–3085.

Dunn SR, Thomas MC, Nette GW, Dove SG (2012) A lipidomic approach to understanding free fatty acid lipogenesis derived from dissolved inorganic carbon within cnidarian-dinoflagellate symbiosis. *PLoS One*, **7**, e46801.

Dunn SR, Thomason JC, Le Tissier MD, Bythell JC (2004) Heat stress induces different forms of cell death in sea anemones and their endosymbiotic algae depending on temperature and duration. *Cell Death and Differentiation*, **11**, 1213–1222.

Dunn SR, Weis VM (2009) Apoptosis as a post-phagocytic winnowing mechanism in a coral–dinoflagellate mutualism. *Environmental Microbiology*, **11**, 268–276.

Dunwell JM, Culham A, Carter CE, Sosa-Aguirre CR, Goodenough PW (2001) Evolution of functional diversity in the cupin superfamily. *Trends in Biochemical Sciences*, **26**, 740–746.

Edmunds P, Davies P (1986) An energy budget for *Porites porites* (Scleractinia). *Marine Biology*, **92**, 339–347.

Eisen JA (1998) Phylogenomics: Improving functional predictions for uncharacterized genes by evolutionary analysis. *Genome Research*, **8**, 163–167.

Eisen JA, Kaiser D, Myers RM (1997) Gastrogenomic delights: a movable feast. *Nature medicine*, **3**, 1076–1078.

Eraly SA, Monte JC, Nigam SK (2004) Novel slc22 transporter homologs in fly, worm, and human clarify the phylogeny of organic anion and cation transporters. *Physiological Genomics*, **18**, 12–24.

Escher SA, Rasmuson-Lestander A (1999) The *Drosophila* glucose transporter gene: cDNA sequence, phylogenetic comparisons, analysis of functional sites and secondary structures. *Hereditas*, **130**, 95–103.

Fabina NS, Putnam HM, Franklin EC, Stat M, Gates RD (2012) Transmission mode predicts specificity and interaction patterns in coral-*Symbiodinium* networks. *PloS one*, **7**, e44970.

Fabina NS, Putnam HM, Franklin EC, Stat M, Gates RD (2013) Symbiotic specificity, association patterns, and function determine community responses to global changes: Defining critical research areas for coral-*Symbiodinium* symbioses. *Global Change Biology*, **19**, 3306–16.

Falkowski PGP, Dubinsky Z, Muscatine L, Mccloskey L (1993) Population control in symbiotic corals. *Bioscience*, **43**, 606–611.

Falkowski PG, Dubinsky Z, Muscatine L, Porter JW (1984) Light and the bioenergetics of a symbiotic coral. *Bioscience*, **34**, 705–709.

Fautin D, Buddemeier RW (2004) Adaptive bleaching: A general phenomenon. *Coelenterate Biology*, **530**, 459–467.

Feng Y, Williams BG, Koumanov F, Wolstenholme AJ, Holman GD (2013) FGT-1 is the major glucose transporter in *C. elegans* and is central to aging pathways. *The Biochemical Journal*, **456**, 219–29.

Feng ZT, Deng YQ, Zhang SC, Liang X, Yuan F, Hao JL, Zhang JC, Sun SF, Wang BS (2015) K+ accumulation in the cytoplasm and nucleus of the salt gland cells of Limonium bicolor accompanies increased rates of salt secretion under NaCl treatment using NanoSIMS. *Plant Science*, **238**, 286–296.

Finkelstein JD, Martin JJ (1984) Methionine metabolism in mammals. *The Journal of Biological Chemistry*, **259**, 9508–9513.

Finney JC, Pettay DT, Sampayo EM, Warner ME, Oxenford HA, LaJeunesse TC (2010) The

relative significance of host-habitat, depth, and geography on the ecology, endemism, and speciation of coral endosymbionts in the genus *Symbiodinium*. *Microbial Ecology*, **60**, 250–263.

Fitt WK (1984) The role of chemosensory behavior of *Symbiodinium microadriaticum*, intermediate hosts, and host behavior in the infection of coelenterates and molluscs with zooxanthellae. *Marine Biology*, **81**, 9–17.

Fitt WK, Trench RK (1983) Endocytosis of the symbiotic dinoflagellate *Symbiodinium microadriaticum* Freudenthal by endodermal cells of the scyphistomae of *Cassiopeia xamachana* and resistance of the algae to host digestion. *Journal of Cell Science*, **64**, 195–212.

Flygare J, Aspesi A, Bailey JC, Miyake K, Caffrey JM, Karlsson S, Ellis SR (2007) Human RPS19, the gene mutated in Diamond-Blackfan anemia, encodes a ribosomal protein required for the maturation of 40S ribosomal subunits. *Blood*, **109**, 980–986.

Forde BG (2000) Nitrate transporters in plants: Structure, function and regulation. *Biochimica Et Biophysica Acta*, **1465**, 219–35.

Fortin MG, Morrison NA, Verma DPS (1986) Nodulin-26, a peribacteroid membrane nodulin is expressed independently of the development of the peribacteroid compartment. *Nucleic Acids Research*, **15**, 8513–8533.

Fotiadis D, Hasler L, MuÈller DJ, Stahlberg H, Kistler J, Engel A (2000) Surface tongue-and-groove contours on lens MIP facilitate cell-to-cell adherence. *Journal of Molecular Biology*, **300**, 779–789.

Frade PR, De Jongh F, Vermeulen F, van Bleijswijk J, Bak RP (2008) Variation in symbiont distribution between closely related coral species over large depth ranges. *Molecular Ecology*, **17**, 691–703.

Fransolet D, Roberty S, Herman AC, Tonk L, Hoegh-Guldberg O, Plumier JC (2013) Increased cell proliferation and mucocyte density in the sea anemone *Aiptasia pallida* recovering from bleaching. *PloS One*, **8**, e65015.

Fraser ME, James MN, Bridger WA, Wolodko WT (1999) A detailed structural description of *Escherichia coli* succinyl-CoA synthetase. *Journal of Molecular Biology*, **285**, 1633–1653.

Freedman B (2014) Symbiosis. In: *The Gale Encyclopedia of Science* (eds Lerner KL, Lerner BW), Gale.

Freeman CJ, Stoner EW, Easson CG, Matterson KO, Baker DM (2016) Symbiont carbon and nitrogen assimilation in the *Cassiopea – Symbiodinium* mutualism. *Marine Ecology Progress Series*, **544**, 281–286.

Freudenthal H (1962) *Symbiodinium* gen. nov. and *Symbiodinium microadriaticum* sp. nov., a zooxanthella: Taxonomy, life cycle, and morphology. *The Journal of Protozoology*, **9**, 45–52.

Fu H, Subramanian RR, Masters SC (2000) 14-3-3 Proteins: Structure, function, and

regulation. *Annual Review of Pharmacology and Toxicology*, **40**, 617–647.

Furla P, Galgani I, Durand I, Allemand D (2000) Sources and mechanisms of inorganic carbon transport for coral calcification and photosynthesis. *The Journal of Experimental Biology*, **203**, 3445–3457.

Galkin A, Brandt U (2005) Superoxide radical formation by pure complex I (NADH:ubiquinone oxidoreductase) from *Yarrowia lipolytica*. *Journal of Biological Chemistry*, **280**, 30129–30135.

Ganapathy V, Thangaraju M, Gopal E, Martin PM, Itagaki S, Miyauchi S, Prasad PD (2008) Sodium-coupled monocarboxylate transporters in normal tissues and in cancer. *The AAPS journal*, **10**, 193–199.

Ganot P, Moya A, Magnone V, Allemand D, Furla P, Sabourault C (2011) Adaptations to endosymbiosis in a cnidarian-dinoflagellate association: differential gene expression and specific gene duplications. *PLoS Genetics*, **7**, e1002187.

Garcia GD, Santos ED, Sousa GV, Zingali RB, Thompson CC, Thompson FL (2016) Metaproteomics reveals metabolic transitions between healthy and diseased stony coral *Mussismilia braziliensis*. *Molecular Ecology*, **25**, 4632–4644.

Gates RD, Bil KY, Muscatine L (1999) The influence of an anthozoan "'host factor'" on the physiology of a symbiotic dinoflagellate. *Journal of Experimental Marine Biology and Ecology*, **232**, 241–259.

Gates RD, Hoegh-Guldberg O, Mcfall-Ngai MJ, Bil KY, Muscatine L (1995) Free amino acids exhibit anthozoan "host factor" activity: They induce the release of photosynthate from symbiotic dinoflagellates in vitro. *Proceedings of the National Academy of Sciences*, **92**, 7430–7434.

Gazzarrini S, Lejay L, Gojon A, Ninnemann O, Frommer WB, von Wirén N (1999) Three functional transporters for constitutive, diurnally regulated, and starvation-induced uptake of ammonium into *Arabidopsis* roots. *The Plant Cell*, **11**, 937–948.

Gelbman BD, Heguy A, O'Connor TP, Zabner J, Crystal RG (2007) Upregulation of pirin expression by chronic cigarette smoking is associated with bronchial epithelial cell apoptosis. *Respiratory Research*, **8**, 10-23.

Gibbin EM, Davy SK (2014) The photo-physiological response of a model cnidarian – dinoflagellate symbiosis to $CO_2$-induced acidification at the cellular level. *Journal of Experimental Marine Biology and Ecology*, **457**, 1–7.

Gibbin EM, Putnam HM, Davy SK, Gates RD (2014) Intracellular pH and its response to $CO_2$-driven seawater acidification in symbiotic versus non-symbiotic coral cells. *The Journal of Experimental Biology*, **217**, 1963–1969.

Gimona M, Herzog M, Vandekerckhove J, Small J V (1990) Smooth-muscle specific expression of calponin. *FEBS Letters*, **274**, 159–162.

González-Ballester D, Camargo A, Fernández E (2004) Ammonium transporter genes in *Chlamydomonas*: The nitrate-specific regulatory gene Nit2 is involved in Amt1;1

expression. *Plant Molecular Biology*, **56**, 863–878.

Gordon BBR, Leggat W (2010) *Symbiodinium*-invertebrate symbioses and the role of metabolomics. *Marine Drugs*, **8**, 2546–2568.

Gorin MB, Yancey SB, Cline J, Revel JP, Horwitz J (1984) The major intrinsic protein (MIP) of the bovine lens fiber membrane: Characterization and structure based on cDNA cloning. *Cell*, **39**, 49–59.

Grant AJ, Remond M, Withers KJT, Hinde R (2001) Inhibition of algal photosynthesis by a symbiotic coral. *Hydrobiologia*, **461**, 63–69.

Griffiths DJ (1970) The Pyrenoid. *Botanical Review*, **36**, 29–58.

Grottoli G, Warner ME, Levas SJ, Matthew D (2014) The cumulative impact of annual coral bleaching can turn some coral species winners into losers. *Global Change Biology*, **20**, 3823–3833.

Grovenor CR, Smart KE, Kilburn MR, Shore B, Dilworth JR, Martin B, Hawes C, Rickaby RE (2006) Specimen preparation for NanoSIMS analysis of biological materials. *Applied Surface Science*, 252, 6917–6924.

Grover R, Maguer JF, Allemand D, Ferrier-Pages C (2003) Nitrate uptake in the scleractinian coral *Stylophora pistillata*. *Limnology and Oceanography*, **48**, 2266–2274.

Grover R, Maguer JF, Allemand D, Ferrier-Pages C (2006) Urea uptake by the scleractinian coral *Stylophora pistillata*. *Journal of Experimental Marine Biology and Ecology*, **48**, 216–225.

Grover R, Maguer JF, Allemand D, Ferrier-Pagès C (2008) Uptake of dissolved free amino acids by the scleractinian coral *Stylophora pistillata*. *The Journal of Experimental Biology*, **211**, 860–865.

Grover R, Maguer JF, Reynaud-vaganay S, Ferrier-Pagès C, Ferrier-page C (2002) Uptake of ammonium by the scleractinian coral *Stylophora pistillata*: Effect of feeding, light, and ammonium concentrations. *Limnology and Oceanography*, **47**, 782–790.

Guerrero R, Margulis L, Berlanga M (2013) Symbiogenesis: The holobiont as a unit of evolution. *International Microbiology*, **16**, 133–143.

Guillard RL (1975) Culture of phytoplankton for feeding marine invertebrates. In: *Culture of Marine Invertebrate Animals* (eds Smith WL, Chanley MH), pp. 29–60. Springer US, Boston, MA.

Gunning PW, Ghoshdastider U, Whitaker S, Popp D, Robinson RC (2015) The evolution of compositionally and functionally distinct actin filaments. *Journal of Cell Science*, **128**, 2009–2019.

Gupta N, Martin PM, Prasad PD, Ganapathy V (2006) SLC5A8 (SMCT1)-mediated transport of butyrate forms the basis for the tumor suppressive function of the transporter. *Life Sciences*, **78**, 2419–2425.

Halsted CH, Villanueva JA, Devlin AM, Niemelä O, Parkkila S, Garrow TA, Wallock LM, Shigenaga MK, Melnyk S, James SJ (2002) Folate deficiency disturbs hepatic methionine metabolism and promotes liver injury in the ethanol-fed micropig. *Proceedings of the National Academy of Sciences*, **99**, 10072–10077.

Hambleton EA, Guse A, Pringle JR (2014) Similar specificities of symbiont uptake by adults and larvae in an anemone model system for coral biology. *The Journal of Experimental Biology*, **217**, 1613–1619.

Hanes SD, Kempf SC (2013) Host autophagic degradation and associated symbiont loss in response to heat stress in the symbiotic anemone, *Aiptasia pallida*. *Invertebrate Biology*, **132**, 95–107.

Hänsch R, Mendel RR (2005) Sulfite oxidation in plant peroxisomes. *Photosynthesis Research*, **86**, 337–343.

Hara-Chikuma M, Verkman AS (2006) Physiological roles of glycerol-transporting aquaporins: The aquaglyceroporins. *Cellular and Molecular Life Sciences*, **63**, 1386–1392.

Hatcher BG (1988) Coral reef primary productivity: a beggar's banquet. *TREE*, **3**, 106–111.

Hawkins TD, Bradley BJ, Davy SK (2013) Nitric oxide mediates coral bleaching through an apoptotic-like cell death pathway: evidence from a model sea anemone-dinoflagellate symbiosis. *FASEB Journal*, **27**, 4790–8.

Hawkins TD, Davy SK (2012) Nitric oxide production and tolerance differ among *Symbiodinium* types exposed to heat stress. *Plant & Cell Physiology*, **53**, 1889–1898.

Hawkins TD, Hagemeyer JC, Hoadley KD, Marsh AG, Warner ME (2016) Partitioning of respiration in an animal-algal symbiosis: Implications for different aerobic capacity between *Symbiodinium* spp. *Frontiers in Physiology*, **7**.

Hawkins TD, Krueger T, Becker S, Fisher PL, Davy SK (2014) Differential nitric oxide synthesis and host apoptotic events correlate with bleaching susceptibility in reef corals. *Coral Reefs*, **33**, 141–153.

Heber U, Hueve K (1997) Action of $SO_2$ on plants and metabolic detoxification of $SO_2$. *International Review of Cytology*, **177**, 255–286.

Hellman M, Arumäe U, Yu LY, Lindholm P, Peränen J, Saarma M, Permi P (2011) Mesencephalic astrocyte-derived neurotrophic factor (MANF) has a unique mechanism to rescue apoptotic neurons. *Journal of Biological Chemistry*, **286**, 2675–2680.

Hennige SJ, McGinley MP, Grottoli AG, Warner ME (2011) Photoinhibition of *Symbiodinium* spp. within the reef corals *Montastraea faveolata* and *Porites astreoides*: Implications for coral bleaching. *Marine Biology*, **158**, 2515–2526.

Hennige SJ, Suggett DJ, Warner ME, McDougall KE, Smith DJ (2008) Photobiology of *Symbiodinium* revisited: Bio-physical and bio-optical signatures. *Coral Reefs*, **28**, 179–195.

Heron SF, Maynard JA, van Hooidonk R, Eakin CM (2016) Warming trends and bleaching stress of the world's coral reefs 1985–2012. *Scientific Reports*, **6**, 38402.

Hildebrandt TM, Grieshaber MK (2008) Three enzymatic activities catalyze the oxidation of sulfide to thiosulfate in mammalian and invertebrate mitochondria. *FEBS Journal*, **275**, 3352–3361.

Hillyer KE, Tumanov S, Villas-Bôas S, Davy SK (2016) Metabolite profiling of symbiont and host during thermal stress and bleaching in a model cnidarian-dinoflagellate symbiosis. *The Journal of Experimental Biology*, **219**, 516–527.

Hirose M, Reimer JD, Hidaka M, Suda S (2008) Phylogenetic analyses of potentially free-living *Symbiodinium* spp. isolated from coral reef sand in Okinawa, Japan. *Marine Biology*, **155**, 105–112.

Hoadley KD, Pettay DT, Grottoli AG, Cai WJ, Melman TF, Levas S, Schoepf V, Ding Q, Yuan X, Wang Y, Matsui Y (2016) High-temperature acclimation strategies within the thermally tolerant endosymbiont *Symbiodinium trenchii* and its coral host, *Turbinaria reniformis*, differ with changing $pCO_2$ and nutrients. *Marine Biology*, **163**, 1–13.

Hoegh-Guldberg O (1999) Climate change, coral bleaching and the future of the world's coral reefs. *Marine and Freshwater Research*, **50**, 839–866.

Hoegh-Guldberg O, Mumby PJ, Hooten AJ, Steneck RS, Greenfield P, Gomez E, Harvell CD, Sale PF, Edwards AJ, Caldeira K, Knowlton N (2007) Coral reefs under rapid climate change and ocean acidification. *Science*, **318**, 1737–1742.

Hofmann F, Ammendola A, Schlossmann J (2000) Rising behind NO: cGMP-dependent protein kinases. *Journal of Cell Science*, **113**, 1671–1676.

Hofmann D, Kremer B (1981) Carbon metabolism and strobilation in *Cassiopea andromedea* (Cnidaria: Scyphozoa): Significance of endosymbiotic dinoflagellates. *Marine Biology*, **33**, 25–33.

Hohman TC, McNeil PL, Muscatine L (1982) Phagosome-lysosome fusion inhibited by algal symbionts of *Hydra viridis*. *Journal of Cell Biology*, **94**, 56–63.

Holcomb M, Tambutté E, Allemand D, Tambutté S (2014) Light enhanced calcification in *Stylophora pistillata*: Effects of glucose, glycerol and oxygen. *PeerJ*, **2**, e375.

Holub BJ (1986) Metabolism and function of myo-inositol and inositol phospholipids. *Annual Review of Nutrition*, **32**, 59–74.

Homma KI, Kurata S, Natori S (1994) Purification, characterization, and cDNA cloning of procathepsin L from the culture medium of NIH-Sape-4, an embryonic cell line of *Sarcophaga peregrina* (flesh fly), and its involvement in the differentiation of imaginal discs. *Journal of Biological Chemistry*, **269**, 15258-15264.

Hong MC, Huang YS, Song PC, Lin WW, Fang LS, Chen MC (2009) Cloning and characterization of ApRab4, a recycling Rab protein of *Aiptasia pulchella*, and its implication in the symbiosome biogenesis. *Marine Biotechnology*, **11**, 771–85.

Houlbrèque F, Tambutté E, Richard C, Ferrier-Pagès C (2004) Importance of a micro-diet for scleractinian corals. *Marine Ecology Progress Series*, **282**, 151–160.

Howells EJ, Abrego D, Meyer E, Kirk NL, Burt JA (2016) Host adaptation and unexpected symbiont partners enable reef-building corals to tolerate extreme temperatures. *Global Change Biology*, **22**, 2702–2714.

Hughes WO, Boomsa JJ (2004) Genetic diversity and disease resistance in leaf-cutting ant societies. *Evolution*, **58**, 1251–1260.

Hume BC, D'Angelo C, Smith EG, Stevens JR, Burt J, Wiedenmann J (2015) *Symbiodinium thermophilum* sp. nov., a thermotolerant symbiotic alga prevalent in corals of the world's hottest sea, the Persian/Arabian Gulf. *Scientific Reports*, **5**, 8562.

Hume BC, Voolstra CR, Arif C, D'Angelo C, Burt JA, Eyal G, Loya Y, Wiedenmann J (2016) Ancestral genetic diversity associated with the rapid spread of stress-tolerant coral symbionts in response to Holocene climate change. *Proceedings of the National Academy of Sciences*, **113**, 4416-4421.

Imbs AB, Yakovleva IM, Dautova TN, Bui LH, Jones P (2014) Diversity of fatty acid composition of symbiotic dinoflagellates in corals: Evidence for the transfer of host PUFAs to the symbionts. *Phytochemistry*, **101**, 76–82.

Ishibashi K, Kondo S, Hara S, Morishita Y (2011) The evolutionary aspects of aquaporin family. *American Journal of Physiology-Regulatory, Integrative and Comparative Physiology*, **300**, R566–R576.

Ishikura M, Adachi K, Maruyama T (1999) Zooxanthellae release glucose in the tissue of a giant clam, *Tridacna crocea*. *Marine Biology*, **133**, 665–673.

Jackson A, Yellowlees D (1990) Phosphate uptake by zooxanthellae isolated from corals. *Proceedings of the Royal Society of London B: Biological Sciences*, **242**, 201–204.

Jeong H, Lee S, Kang N (2014) Genetics and morphology characterize the dinoflagellate *Symbiodinium voratum*, n. sp.,(Dinophyceae) as the sole representative of *Symbiodinium* Clade E. *Journal of Eukaryotic Microbiology*, **61**, 75-94.

Jiang PL, Pasaribu B, Chen CS (2014) Nitrogen-deprivation elevates lipid levels in *Symbiodinium* spp. by lipid droplet accumulation: Morphological and compositional analyses. *PLoS One*, **9**, 1–10.

Jokiel PL (2004) Temperature Stress and Coral Bleaching. In: *Coral Health and Disease* (eds Rosenberg E, Loya Y), pp. 401–425.

Jones A, Berkelmans R (2010) Potential costs of acclimatization to a warmer climate: Growth of a reef coral with heat tolerant vs. sensitive symbiont types. *PloS One*, **5**, e10437–e10437.

Jones AM, Berkelmans R (2011) Tradeoffs to thermal acclimation: Energetics and reproduction of a reef coral with heat tolerant *Symbiodinium* type-D. *Journal of Marine Biology*, **2011**, 1–12.

Jones AM, Berkelmans R, Van Oppen MJ, Mieog JC, Sinclair W (2008) A community change in the algal endosymbionts of a scleractinian coral following a natural bleaching event: Field evidence of acclimatization. *Proceedings of the Royal Society of London B: Biological Sciences*, **275**, 1359–1365.

Jones RJ, Bowyer J, Hoegh-guldberg O, Blackall LL (2004) Dynamics of a temperature-related coral disease outbreak. *Marine Ecology Progress Series*, **281**, 63–77.

Jones R, Yellowlees D (1997) Regulation and control of intracellular algae (= zooxanthellae) in hard corals. *Proceedings of the Royal Society of London B: Biological Sciences*, **352**, 457–468.

Joost HG, Bell GI, Best JD, Birnbaum MJ, Charron MJ, Chen YT, Doege H, James DE, Lodish HF, Moley KH, Moley JF (2002) Nomenclature of the GLUT/SLC2A family of sugar/polyol transport facilitators. *American Journal of Physiology-Endocrinology and Metabolism*, **282**, E974–E976.

Joost HG, Thorens B (2001) The extended GLUT-family of sugar/polyol transporter facilitators: Nomenclature, sequence characteristics, and potential function of its novel members (Review). *Molecular Membrane Biology*, **18**, 247–256.

Juwana JP, Henderikx P, Mischo A, Wadle A, Fadle N, Gerlach K, Arends JW, Hoogenboom H, Pfreundschuh M, Renner C (1999) EB/RP gene family encodes tubulin binding proteins. *International Journal of Cancer*, **81**, 275–284.

Kanno SI, Kuzuoka H, Sasao S, Hong Z, Lan L, Nakajima S, Yasui A (2007) A novel human AP endonuclease with conserved zinc-finger-like motifs involved in DNA strand break responses. *The EMBO Journal*, **26**, 2094–2103.

Katoh K, Standley DM (2013) MAFFT multiple sequence alignment software version 7: Improvements in performance and usability. *Molecular Biology and Evolution*, **30**, 772–780.

Kawaida H, Ohba K, Koutake Y, Shimizu H, Tachida H, Kobayakawa Y (2013) Symbiosis between hydra and chlorella: Molecular phylogenetic analysis and experimental study provide insight into its origin and evolution. *Molecular Phylogenetics and Evolution*, **66**, 906–914.

Kazandjian A, Shepherd VA, Rodriguez-Lanetty M, Nordemeier W, Larkum AW, Quinnell RG (2008) Isolation of symbiosomes and the symbiosome membrane complex from the zoanthid *Zoanthus robustus*. *Phycologia*, **47**, 294–306.

Kellogg R, Patton J (1983) Lipid droplets, medium of energy exchange in the symbiotic anemone *Condylactis gigantea*: A model coral polyp. *Marine Biology*, **75**, 137–149.

Kemp DW, Hernandez-Pech X, Iglesias-Prieto R, Fitt WK, Schmidt GW (2014) Community dynamics and physiology of *Symbiodinium* spp. before, during, and after a coral beaching event. *Limnology and Oceanography*, **59**, 788–797.

Kennedy E V, Foster NL, Mumby PJ, Stevens JR (2015) Widespread prevalence of cryptic *Symbiodinium* D in the key Caribbean reef builder, *Orbicella annularis*. *Coral Reefs*, **34**, 519–531.

Kinzie R (1974) Experimental infection of aposymbiotic gorgonian polyps with zooxanthellae. *Journal of Experimental Marine Biology and Ecology*, **15**, 335–345.

Kinzie R, Chee G (1979) The effect of different zooxanthellae on the growth of experimentally reinfected hosts. *The Biological Bulletin*, **156**, 315–327.

Kinzie RA, Chee GS (1982) Strain-specific differences in surface antigens of symbiotic algae. *Applied and Environmental Microbiology*, **44**, 1238–1240.

Kitchen SA, Crowder CM, Poole AZ, Weis VM, Meyer E (2015) De novo assembly and characterization of four anthozoan (Phylum Cnidaria) transcriptomes. *G3: Genes, Genomes, Genetics*, **5**, 2441–2452.

Knowlton N (2001) The future of coral reefs. *Proceedings of the National Academy of Sciences*, **98**, 5419–5425.

Kohtz JD, Jamison SF, Will CL, Zuo P, Lührmann R, Garcia-Blanco MA, Manley JL (1994) Protein-protein interactions and 5'-splice-site recognition in mammalian mRNA precursors. *Nature*, **368**, 119–124.

Koide A, Bailey CW, Huang X, Koide S (1998) The fibronectin type III domain as a scaffold for novel binding proteins. *Journal of Molecular Biology*, **284**, 1141–1151.

Koike K, Jimbo M, Sakai R, Kaeriyama M (2004) Octocoral chemical signaling selects and controls dinoflagellate symbionts. *The Biological Bulletin*, **207**, 80–86.

Komuro I, Wenninger KE, Philipson KD, Izumo S (1992) Molecular cloning and characterization of the human cardiac $Na^+$ /$Ca_2^+$ exchanger cDNA. *Proceedings of the National Academy of Sciences*, **89**, 4769–4773.

Kopp C, Domart-Coulon I, Escrig S, Humbel BM, Hignette M, Meibom A (2015) Subcellular investigation of photosynthesis-driven carbon and nitrogen assimilation and utilization in the symbiotic reef coral *Pocillopora damicornis*. *MBio*, **6**, 1–9.

Kopp C, Pernice M, Domart-Coulon I, Djediat C, Spangenberg JE, Alexander DT, Hignette M, Meziane T, Meibom A (2013) Highly dynamic cellular-level response of symbiotic coral to a sudden increase in environmental nitrogen. *MBio*, **4**, S1–S8.

Kopp C, Wisztorski M, Revel J, Mehiri M, Dani V, Capron L, Carette D, Fournier I, Massi L, Mouajjah D, Pagnotta S (2014) MALDI-MS and NanoSIMS imaging techniques to study cnidarian–dinoflagellate symbioses. *Zoology*, **118**(2), 1–7.

Kovačević G, Franjevic D, Jelencic B, Kalafatić M (2010) Isolation and cultivation of endosymbiotic algae from green hydra and phylogenetic analysis of 18S rDNA sequences. *Folia Biologica*, **58**, 135–143.

Krueger T (2016) Concerning the cohabitation of animals and algae – an English translation of K. Brandt's 1881 presentation "Ueber das Zusammenleben von Thieren und Algen." *Symbiosis*, **71**(3), 1–8.

Krueger T, Fisher PL, Becker S, Pontasch S, Dove S, Hoegh-Guldberg O, Leggat W, Davy SK (2015) Transcriptomic characterization of the enzymatic antioxidants FeSOD,

MnSOD, APX and KatG in the dinoflagellate genus *Symbiodinium*. *BMC Evolutionary Biology*, **15**, 1–20.

Kuo J, Chen MC, Lin CH, Fang LS (2004) Comparative gene expression in the symbiotic and aposymbiotic *Aiptasia pulchella* by expressed sequence tag analysis. *Biochemical and Biophysical Research Communications*, **318**, 176–186.

Kzhyshkowska J, Rusch A, Wolf H, Dobner T (2003) Regulation of transcription by the heterogeneous nuclear ribonucleoprotein E1B-AP5 is mediated by complex formation with the novel bromodomain-containing protein BRD7. *Biochemical Journal*, **371**, 385–393.

Ladner JT, Barshis DJ, Palumbi SR (2012) Protein evolution in two co-occurring types of *Symbiodinium*: an exploration into the genetic basis of thermal tolerance in *Symbiodinium* clade D. *BMC Evolutionary Biology*, **12**, 217-230.

LaJeunesse TC (2001) Investigating the biodiversity, ecology, and phylogeny of endosymbiotic dinoflagellates in the genus *Symbiodinium* using the its region: In search of a "species" level marker. *Journal of Phycology*, **37**, 866–880.

LaJeunesse TC (2005) "Species" radiations of symbiotic dinoflagellates in the Atlantic and Indo-Pacific since the Miocene-Pliocene transition. *Molecular Biology and Evolution*, **22**, 570–581.

LaJeunesse TC, Lee SY, Gil-Agudelo DL, Knowlton N, Jeong HJ (2015) *Symbiodinium necroappetens* sp. nov. (Dinophyceae): an opportunist "zooxanthella" found in bleached and diseased tissues of Caribbean reef corals. *European Journal of Phycology*, **50**, 223–238.

Lajeunesse TC, Parkinson JE, Reimer JD (2012) A genetics-based description of *Symbiodinium minutum* sp. nov. and *S. psygmophilum* sp. nov. (Dinophyceae), two dinoflagellates symbiotic with cnidaria. *Journal of Phycology*, **48**, 1380–1391.

LaJeunesse TC, Smith RT, Finney J, Oxenford H (2009) Outbreak and persistence of opportunistic symbiotic dinoflagellates during the 2005 Caribbean mass coral "bleaching" event. *Proceedings of the Royal Society of London B: Biological Sciences*, **276**, 4139–4148.

LaJeunesse TC, Smith R, Walther M, Pinzón J, Pettay DT, McGinley M, Aschaffenburg M, Medina-Rosas P, Cupul-Magaña AL, Pérez AL, Reyes-Bonilla H (2010) Host-symbiont recombination versus natural selection in the response of coral-dinoflagellate symbioses to environmental disturbance. *Proceedings of the Royal Society of London B: Biological Sciences*, **277**, 2925–2934.

LaJeunesse TC (2002) Diversity and community structure of symbiotic dinoflagellates from Caribbean coral reefs. *Marine Biology*, **141**, 387–400.

LaJeunesse TC, Thornhill DJ, Cox EF, Stanton FG, Fitt WK, Schmidt GW (2004) High diversity and host specificity observed among symbiotic dinoflagellates in reef coral communities from Hawaii. *Coral Reefs*, **23**, 596–603.

LaJeunesse TC, Wham DC, Pettay DT, Parkinson JE, Keshavmurthy S, Chen CA (2014)

Ecologically differentiated stress-tolerant endosymbionts in the dinoflagellate genus *Symbiodinium* (Dinophyceae) Clade D are different species. *Phycologia*, **53**, 305–319.

Lapik YR, Kaufman LS (2003) The *Arabidopsis* cupin domain protein AtPirin1 interacts with the G protein α-subunit GPA1 and regulates seed germination and early seedling development. *The Plant Cell*, **15**, 1578–1590.

Larsson A (2014) AliView: A fast and lightweight alignment viewer and editor for large datasets. *Bioinformatics*, **30**, 3276–3278.

Lasker H (1981) Phenotypic variation in the coral *Montastrea cavernosa* and its effects on colony energetics. *The Biological Bulletin*, **160**, 292–302.

Law CJ, Maloney PC, Wang D (2008) Ins and outs of major facilitator superfamily antiporters. *Annual Review of Microbiology*, **62**, 289–305.

Lee SY, Jeong HJ, Kang NS, Jang TY, Jang SH, Lajeunesse TC (2015) *Symbiodinium tridacnidorum* sp. nov., a dinoflagellate common to Indo-Pacific giant clams, and a revised morphological description of *Symbiodinium microadriaticum* Freudenthal, emended Trench & Blank. *European Journal of Phycology*, **50**, 155–172.

Leggat W, Hoegh-Guldberg O, Dove S, Yellowlees D (2007) Analysis of an EST library from the dinoflagellate (*Symbiodinium* sp.) symbiont of reef-building corals. *Journal of Phycology*, **43**, 1010–1021.

Lehnert EM, Burriesci MS, Pringle JR (2012) Developing the anemone *Aiptasia* as a tractable model for cnidarian-dinoflagellate symbiosis: the transcriptome of aposymbiotic *A. pallida*. *BMC Genomics*, **13**, 271-281.

Lehnert EM, Mouchka ME, Burriesci MS, Gallo ND, Schwarz JA, Pringle JR (2014) Extensive differences in gene expression between symbiotic and aposymbiotic cnidarians. *G3: Genes, Genomes, Genetics*, **4**, 277–295.

Leletkin VA (2000) Trophic status and population density of zooxanthellae in hermatypic corals. *Russian Journal of Marine Biology*, **26**, 231–240.

Lesser MP (2006) Oxidative stress in marine environments: biochemistry and physiological ecology. *Annual Review of Physiology*, **68**, 253–278.

Lesser MP, Falcón LI, Rodríguez-Román A, Enríquez S, Hoegh-Guldberg O, Iglesias-Prieto R (2007) Nitrogen fixation by symbiotic cyanobacteria provides a source of nitrogen for the scleractinian coral *Montastraea cavernosa*. *Marine Ecology Progress Series*, **346**, 143–152.

Lesser M, Stat M, Gates RD (2013) The endosymbiotic dinoflagellates (*Symbiodinium* sp.) of corals are parasites and mutualists. *Coral Reefs*, **32**, 603–611.

Levin RA, Beltran VH, Hill R, Kjelleberg S, McDougald D, Steinberg PD, van Oppen MJ (2016) Sex, scavengers, and chaperones: Transcriptome secrets of divergent *Symbiodinium* thermal tolerances. *Molecular Biology and Evolution*, **33**, 2201–2215.

Lewis D, Smith D (1971) The autotrophic nutrition of symbiotic marine coelenterates with

special reference to hermatypic corals. I. Movement of photosynthetic products between the symbionts. *Proceedings of the Royal Society of London B: Biological Sciences*, **178**, 111–129.

Lezhneva L, Kiba T, Feria-Bourrellier AB, Lafouge F, Boutet-Mercey S, Zoufan P, Sakakibara H, Daniel-Vedele F, Krapp A (2014) The *Arabidopsis* nitrate transporter NRT2.5 plays a role in nitrate acquisition and remobilization in nitrogen-starved plants. *The Plant Journal*, **80**, 230–241.

Lin S, Cheng S, Song B, Zhong X, Lin X, Li W, Li L, Zhang Y, Zhang H, Ji Z, Cai M (2015) The *Symbiodinium kawagutii* genome illuminates dinoflagellate gene expression and coral symbiosis. *Science*, **350**, 691–694.

Lin K, Wang J, Fang L (2000) Participation of glycoproteins on zooxanthellal cell walls in the establishment of a symbiotic relationship with the sea anemone, *Aiptasia pulchella*. *Zoological Studies*, **39**, 172–178.

Ling L, Krediet CJ, Pringle JR (2016) Following proteomic changes in symbiotic *Aiptasia* cytosol and symbiosome membranes during thermal stress. *Presented at the 13th International Coral Reef Symposium, Honolulu, Hawaii.*

Lipschultz F, Cook CB (2002) Uptake and assimilation of $^{15}$N-ammonium by the symbiotic sea anemones *Bartholomea annulata* and *Aiptasia pallida*: Conservation versus recycling of nitrogen. *Marine Biology*, **140**, 489–502.

Little AF, Van Oppen MJH, Willis BL (2004) Flexibility in algal endosymbioses shapes growth in reef corals. *Science*, **304**, 1492–1494.

Lodish HF, Berk A, Zipursky S (2000) Overview of membrane transport proteins. In: *Molecular Cell Biology*, Vol. 3. New York: Scientific American Books.

Logan DK, LaFlamme AC, Weis VM, Davy SK (2010) Flow-cytometric characterization of the cell-surface glycans of symbiotic dinoflagellates (*Symbiodinium* spp.). *Journal of Phycology*, **46**, 525–533.

Loh WK, Loi T, Carter D, Hoegh-Guldberg O (2001) Genetic variability of the symbiotic dinoflagellates from the wide ranging coral species *Seriatopora hystrix* and *Acropora longicyathus* in the Indo-West Pacific. *Marine Ecology Progress Series*, **222**, 97–107.

Loram JE, Trapido-Rosenthal HG, Douglas AE (2007) Functional significance of genetically different symbiotic algae *Symbiodinium* in a coral reef symbiosis. *Molecular Ecology*, **16**, 4849–4857.

Lyon RC, Johnston SM, Watson DG, McGarvie G, Ellis EM (2007) Synthesis and catabolism of alpha-hydroxybutyrate in SH-SY5Y human neuroblastoma cells: Role of the aldo-keto reductase AKR7A2. *Journal of Biological Chemistry*, **282**, 25986–25992.

Malsam J (2005) Golgin tethers define subpopulations of COPI vesicles. *Science*, **307**, 1095–1098.

Manevich Y, Fisher AB (2005) Peroxiredoxin 6, a 1-Cys peroxiredoxin, functions in antioxidant defense and lung phospholipid metabolism. *Free Radical Biology and*

*Medicine*, **38**, 1422–1432.

Marcelli M, Cunningham GR, Haidacher SJ, Padayatty SJ, Sturgis L, Kagan C, Denner L (1998) Caspase-7 is activated during lovastatin-induced apoptosis of the prostate cancer cell line LNCaP. *Cancer Research*, **58**, 76–83.

Margulis L (1971) The origin of plant and animal cells. *American Scientist*, **59**, 230–235.

Marini AM, Boeckstaens M, Benjelloun F, Chérif-Zahar B, André B (2006) Structural involvement in substrate recognition of an essential aspartate residue conserved in Mep/Amt and Rh-type ammonium transporters. *Current Genetics*, **49**, 364–374.

Markell D, Trench R (1993) Macromolecules exuded by symbiotic dinoflagellates in culture: Amino acid and sugar composition. *Journal of Phycology*, **29**, 64–68.

Markell DA, Trench RK, Iglesias-Prieto R (1992) Macromolecules associated with the cell walls of symbiotic dinoflagellates. *Symbiosis*, **12**, 19–31.

Markell D, Wood-Charlson E (2010) Immunocytochemical evidence that symbiotic algae secrete potential recognition signal molecules in hospite. *Marine Biology*, **157**, 1105–1111.

Martin RM, Gasser RG, Jones MK, Lightowlers MW (1995) Identification and characterization of myophilin, a muscle specific antigen of *Echinococcus granulosus*. *Molecular and Biochemical Parasitology*, **70**, 139–148.

Marx H, Lemeer S, Klaeger S, Rattei T, Kuster B (2013) MScDB: A mass spectrometry-centric protein sequence database for proteomics. *Journal of Proteome Research*, **12**, 2386-98.

Matthews JL, Sproles AE, Oakley CA, Grossman AR, Weis VM, Davy SK (2016) Menthol-induced bleaching rapidly and effectively provides experimental aposymbiotic sea anemones (*Aiptasia* sp.) for symbiosis investigations. *Journal of Experimental Biology*, **219**, 306–310.

Mayfield AB, Hsiao Y, Fan TY, Chen C-S (2010) Investigating the impacts of episodic upwelling on the physiology of the common Indo-Pacific reef coral *Seriatopora hystrix*. *Submitted to the EMBL/GenBank/DDBJ databases*.

Mayrose I, Graur D, Ben-Tal N, Pupko T (2004) Comparison of site-specific rate-inference methods for protein sequences: Empirical Bayesian methods are superior. *Molecular Biology and Evolution*, **21**, 1781–1791.

McAuley PJ, Smith DC (1982) The green hydra symbiosis. V. Stages in the intracellular recognition of algal symbionts by digestive cells. *Proceedings of the Royal Society of London B: Biological Sciences*, **216**, 7–23.

McGrath AP, Hilmer KM, Collyer CA, Shepard EM, Elmore BO, Brown DE, Dooley DM, Guss JM (2009) The structure and inhibition of human diamine oxidase. *Biochemistry*, **48**, 9810–9822.

Mcguinness DH, Dehal PK, Pleass RJ (2003) Pattern recognition molecules and innate

immunity to parasites. *Trends in parasitology*, **19**, 312–319.

McIlroy SE, Gillette P, Cunning R, Klueter A, Capo T, Baker AC, Coffroth MA (2016) The effects of *Symbiodinium* (Pyrrhophyta) identity on growth, survivorship, and thermal tolerance of newly settled coral recruits. *Journal of Phycology*, **1124**, 1114–1124.

McNally K (1994) Small-subunit ribosomal DNA sequence analysis and a reconstruction of the inferred phylogeny amon symbiotic dinoflagellates (Pyrrophyta) 1. *Journal of Phycology*, **30**, 316–329.

Mellacheruvu D, Wright Z, Couzens AL, Lambert JP, St-Denis N, Li T, Miteva YV, Hauri S, Sardiu ME, Low TY, Halim VA (2013) The CRAPome: A contaminant repository for affinity purification mass spectrometry data. *Nature Methods*, **10**, 730.

Mieog JC, Olsen JL, Berkelmans R, Bleuler-Martinez SA, Willis BL, van Oppen MJ (2009) The roles and interactions of symbiont, host and environment in defining coral fitness. *PloS One*, **4**, e6364.

Miller D, Yellowlees D (1989) Inorganic nitrogen uptake by symbiotic marine cnidarians: A critical review. *Proceedings of the Royal Society of London B: Biological Sciences*, **237**, 109–125.

Miyazaki I, Simizu S, Okumura H, Takagi S, Osada H (2010) A small-molecule inhibitor shows that pirin regulates migration of melanoma cells. *Nature Chemical Biology*, **6**, 667–673.

Mohamed AR, Cumbo V, Harii S, Shinzato C, Chan CX, Ragan MA, Bourne DG, Willis BL, Ball EE, Satoh N, Miller DJ (2016) The transcriptomic response of the coral *Acropora digitifera* to a competent *Symbiodinium* strain: The symbiosome as an arrested early phagosome. *Molecular Ecology*, **25**, 3127–3141.

Mollnes TE, Brekke OL, Fung M, Fure H, Christiansen D, Bergseth G, Videm V, Lappegård KT, Köhl J, Lambris JD (2013) Essential role of the C5a receptor in *E. coli* − induced oxidative burst and phagocytosis revealed by a novel lepirudin-based human whole blood model of inflammation. *Blood*, **100**, 1869–1877.

Mulders SM, Preston GM, Deen PM, Guggino WB, van Os CH, Agre P (1995) Water channel properties of major intrinsic protein of lens. *The Journal of Biological Chemistry*, **270**, 9010–9016.

Muller-Parker G, Mccloskey LR, Hoegh-Guldberg O, McAuley PJ (1994) Effect of ammonium enrichment on animal and algal biomass of the coral *Pocillopora damicornis*. *Pacific Science*, **48**, 273–283.

Musat N, Stryhanyuk H, Bombach P, Adrian L, Audinot JN, Richnow HH (2014) The effect of FISH and CARD-FISH on the isotopic composition of 13 C-and 15 N-labeled *Pseudomonas putida* cells measured by nanoSIMS. *Systematic and Applied Microbiology*, **37**, 267-276.

Muscatine L (1965) Symbiosis of hydra and algae—III. Extracellular products of the algae. *Comparative Biochemistry and Physiology*, **16**, 77–92.

Muscatine L (1967) Glycerol excretion by symbiotic algae from corals and *Tridacna* and its control by the host. *Science*, **156**, 516–519.

Muscatine L (1984) Fate of photosynthetic fixed carbon in light-and shade-adapted colonies of the symbiotic coral *Stylophora pistillata*. *Proceedings of the Royal Society of London B: Biological Sciences*, **222**, 181–202.

Muscatine L (1990) The role of symbiotic algae in carbon and energy flux in reef corals. *Ecosystems of the World*, **25**, 75–89.

Muscatine L, Cernichiari E (1969) Assimilation of photosynthetic products of zooxanthellae by a reef coral. *The Biological Bulletin*, **137**, 506–523.

Muscatine L, Ferrier-Pages C, Blackburn A (1998) Cell-specific density of symbiotic dinoflagellates in tropical anthozoans. *Coral Reefs*, **17**, 329–337.

Muscatine L, Karakashian SJ, Karakashian MW (1967) Soluble extracellular products of algae symbiotic with a ciliate, a sponge, and a mutant hydra. *Comparative Biochemistry and Physiology*, **20**, 1IN17-6IN412.

Muscatine L, Lenhoff H (1965) Symbiosis of hydra and algae. II. Effects of limited food and starvation on growth of symbiotic and aposymbiotic hydra. *The Biological Bulletin*, **129**, 316–328.

Muscatine L, Mccloskey LR, Marian RE (1981) Estimating the daily contribution of carbon from zooxanthellae to coral animal respiration. *Limonology And Oceanography*, **26**, 601–611.

Muscatine L, Pool RR (1979) Regulation of number of intracellular algae. *Proceedings of the Royal Society of London B: Biological Sciences*, **204**, 131–139.

Muscatine AL, Porter JW (1977) Reef corals: Mutualistic symbioses adapted to nutrient-poor environments. *Bioscience*, **27**, 454–460.

Nagai H, Oshiro N, Takuwa-Kuroda K, Iwanaga S, Nozaki M, Nakajima T (2002) Novel proteinaceous toxins from the nematocyst venom of the Okinawan sea anemone *Phyllodiscus semoni* Kwietniewski. *Biochemical and Biophysical Research Communications*, **294**, 760–763.

Nakamura H, Kawase Y, Maruyama K, Murai A (1998) Polyketide metabolites of a symbiotic dinoflagellate, *Symbiodinium* sp.: A new C30 marine alkaloid, zooxanthellamine, a plausible precursor for zoanthid alkaloids. *Bulletin of the Chemical Society of Japan*, **71**, 781–787.

Nardin EH, Nussenzweig VI, Nussenzweig RS, Collins WE, Harinasuta KT, Tapchaisri P, Chomcharn Y (1982) Circumsporozoite proteins of human malaria parasites *Plasmodium falciparum* and *Plasmodium vivax*. *The Journal of Experimental Medicine*, **156**, 20–30.

Nesvizhskii AI, Keller A, Kolker E, Aebersold R (2003) A statistical model for identifying proteins by tandem mass spectrometry. *Analytical Chemistry*, **75**, 4646-4658.

Neubauer EF, Poole AZ, Weis VM, Davy SK (2016) The scavenger receptor repertoire in six cnidarian species and its putative role in cnidarian-dinoflagellate symbiosis. *PeerJ*, **4**, e2692.

Niknahad H, O'Brien PJ (2008) Mechanism of sulfite cytotoxicity in isolated rat hepatocytes. *Chemico-Biological Interactions*, **174**, 147–154.

O'Connor T, Ireland LS, Harrison DJ, Hayes JD (1999) Major differences exist in the function and tissue-specific expression of human aflatoxin B1 aldehyde reductase and the principal human aldo-keto reductase AKR1 family members. *Biochemical Journal*, **343**, 487–504.

O'Neil JM, Capone DG (2008) Nitrogen cycling in coral reef environments. *Nitrogen in the marine environment, Eds.: Capone, DG, Bronk, DA, Mulholland, MR, and Carpenter, EJ*, 949-989.

Oakley CA, Ameismeier MF, Peng L, Weis VM, Grossman AR, Davy SK (2016) Symbiosis induces widespread changes in the proteome of the model cnidarian *Aiptasia*. *Cellular Microbiology*, **18**, 1009–1023.

Oka OBV, Pringle MA, Schopp IM, Braakman I, Bulleid NJ (2013) ERdj5 Is the ER reductase that catalyzes the removal of non-native disulfides and correct folding of the LDL receptor. *Molecular Cell*, **50**, 793–804.

Okamoto M, Vidmar JJ, Glass ADM (2003) Regulation of NRT1 and NRT2 gene families of *Arabidopsis thaliana*: Responses to nitrate provision. *Plant and Cell Physiology*, **44**, 304–317.

Orzaez D, De Jong AJ, Woltering EJ (2001) A tomato homologue of the human protein PIRIN is induced during programmed cell death. *Plant Molecular Biology*, **46**, 459–468.

Oshiro N, Kobayashi C, Iwanaga S, Nozaki M, Namikoshi M, Spring J, Nagai H (2004) A new membrane-attack complex/perforin (MACPF) domain lethal toxin from the nematocyst venom of the Okinawan sea anemone *Actineria villosa*. *Toxicon*, **43**, 225–228.

Pajares MA, Pérez-Sala D (2006) Betaine homocysteine S-methyltransferase: Just a regulator of homocysteine metabolism? *Cellular and Molecular Life Sciences*, **63**, 2792–2803.

Palincsar JS, Jones WR, Palincsar EE (1988) Effects of isolation of the endosymbiont *Symbiodinium microadriaticum* (Dinophyceae) from its host *Aiptasia pallida* (Anthozoa) on cell wall ultrastructure and mitotic rate. *Transactions of the American Microscopical Society*, **107**, 53–66.

Palincsar EE, Jones WR, Palincsar JS, Glogowski MA, Mastro JL (1989) Bacterial aggregates within the epidermis of the sea anemone *Aiptasia pallida*. *Biological Bulletin*, **177**, 130–140.

Pao S, Paulsen I, Saier M (1998) Major facilitator superfamily. *Microbiology and Molecular Biology Reviews*, **62**, 1–34.

Park C, Allaby M (2013) Parasite. In: *A Dictionary of the Environment*, Oxford University

Press.

Park EI, Garrow TA (1999) Interaction between dietary methionine and methyl donor intake on rat liver betaine-homocysteine methyltransferase gene expression and organization of the human gene. *Journal of Biological Chemistry*, **274**, 7816–7824.

Pasaribu B, Li YS, Kuo PC, Lin IP, Tew KS, Tzen JT, Liao YK, Chen CS, Jiang PL (2016) The effect of temperature and nitrogen deprivation on cell morphology and physiology of *Symbiodinium*. *Oceanologia*, **58**, 272-278.

Pasaribu B, Lin IP, Tzen JT, Jauh GY, Fan TY, Ju YM, Cheng JO, Chen CS, Jiang PL (2014) SLDP: a novel protein related to caleosin is associated with the endosymbiotic *Symbiodinium* lipid droplets from *Euphyllia glabrescens*. *Marine Biotechnology*, **16**, 560–571.

Paschoalin T, Carmona AK, Rodrigues EG, Oliveira V, Monteiro HP, Juliano MA, Juliano L, Travassos LR (2007) Characterization of thimet oligopeptidase and neurolysin activities in B16F10-Nex2 tumor cells and their involvement in angiogenesis and tumor growth. *Molecular Cancer*, **6**, 44-58.

Patton J, Burris J (1983) Lipid synthesis and extrusion by freshly isolated zooxanthellae (symbiotic algae). *Marine Biology*, **136**, 131–136.

Paxton CW, Davy SK, Weis VM (2013) Stress and death of cnidarian host cells play a role in cnidarian bleaching. *The Journal of Experimental Biology*, **216**, 2813–2820.

Pearse VB, Muscatine L (1971) Role of symbiotic algae (zooxanthellae) in coral calcification. *Biological Bulletin*, **141**, 350–363.

Peleg-Grossman S, Volpin H, Levine A (2007) Root hair curling and *Rhizobium* infection in *Medicago truncatula* are mediated by phosphatidylinositide-regulated endocytosis and reactive oxygen species. *Journal of Experimental Botany*, **58**, 1637–1649.

Peng SE, Wang YB, Wang LH, Chen WN, Lu CY, Fang LS, Chen CS (2010) Proteomic analysis of symbiosome membranes in cnidaria-dinoflagellate endosymbiosis. *Proteomics*, **10**, 1002–1016.

Pernice M, Dunn SR, Tonk L, Dove S, Domart-Coulon I, Hoppe P, Schintlmeister A, Wagner M, Meibom A (2014) A nanoscale secondary ion mass spectrometry study of dinoflagellate functional diversity in reef-building corals. *Environmental Microbiology*, **17**, 3570-3580.

Pernice M, Meibom A, Van Den Heuvel A, Kopp C, Domart-Coulon I, Hoegh-Guldberg O, Dove S (2012) A single-cell view of ammonium assimilation in coral-dinoflagellate symbiosis. *The ISME Journal*, **6**, 1314–24.

Pettay DT, Wham DC, Smith RT, Iglesias-Prieto R, LaJeunesse TC (2015) Microbial invasion of the Caribbean by an Indo-Pacific coral zooxanthella. *Proceedings of the National Academy of Sciences*, **112**, 7513–7518.

Pierleoni A, Indio V, Savojardo C, Fariselli P, Martelli PL, Casadio R (2011) MemPype: A pipeline for the annotation of eukaryotic membrane proteins. *Nucleic Acids Research*,

**39**, 375–380.

Pochon X, Gates R (2010) A new *Symbiodinium* clade (Dinophyceae) from soritid foraminifera in Hawai'i. *Molecular Phylogenetics and Evolution*, **56**, 492–497.

Poole AZ, Kitchen SA, Weis VM (2016) The role of complement in cnidarian-dinoflagellate symbiosis and immune challenge in the sea anemone *Aiptasia pallida*. *Frontiers in Microbiology*, **7**.

Popa R, Weber PK, Pett-Ridge J, Finzi JA, Fallon SJ, Hutcheon ID, Nealson KH, Capone DG (2007) Carbon and nitrogen fixation and metabolite exchange in and between individual cells of *Anabaena oscillarioides*. *The ISME Journal*, **1**, 354–360.

Porat A, Sagiv Y, Elazar Z (2000) A 56-kDa selenium-binding protein participates in intra-Golgi protein transport. *Journal of Biological Chemistry*, **275**, 14457–14465.

Porollo A, Meller J (2007) Versatile annotation and publication quality visualization of protein complexes using POLYVIEW-3D. *BMC Bioinformatics*, **8**, 316.

Porter JW (1974) Zooplankton feeding by the caribbean reef-building coral *Montastrea cavernosa*. *Proceedings of the Second International Coral Reef Symposium*, **1**, 111–125.

Price MP, Thompson RJ, Eshcol JO, Wemmie JA, Benson CJ (2004) Stomatin modulates gating of acid-sensing ion channels. *Journal of Biological Chemistry*, **279**, 53886–53891.

Quevillon E, Silventoinen V, Pillai S, Harte N, Mulder N, Apweiler R, Lopez R (2005) InterProScan: Protein domains identifier. *Nucleic Acids Research*, **33**, 116–120.

Rahav O, Dubinsky Z, Achituv Y, Falkowski PG (1989) Ammonium metabolism in the zooxanthellate coral, *Stylophora pistillata*. *Proceedings of the Royal Society of London B: Biological Sciences*, **236**, 325–337.

Rands M, Loughman B, Douglas AE (1993) The symbiotic interface in an alga-invertebrate symbiosis. *Proceedings of the Royal Society of London B: Biological Sciences*, **253**, 161–165.

Reaka-Kudla ML (1997) The global biodiversity of coral reefs: a comparison with rain forests. In: *Biodiversity II: Understanding and Protecting Our Biological Resources*, pp. 83–108.

Reddy VS, Shlykov MA, Castillo R, Sun EI, Saier MH (2012) The major facilitator superfamily (MFS) revisited. *FEBS Journal*, **279**, 2022–2035.

Rees TA V, Fitt WK, Yellowlees D (1994) Host glutamine synthetase activities in the giant clam-zooxanthellae symbiosis: Effects of clam size, elevated ammonia and continuous darkness. *Marine Biology*, **118**, 681–685.

Reimer JD, Shah MR, Sinniger F, Yanagi K, Suda S (2010) Preliminary analyses of cultured *Symbiodinium* isolated from sand in the oceanic Ogasawara Islands, Japan. *Marine Biodiversity*, **40**, 237–247.

Revollo I, Nishiura H, Shibuya Y, Oda Y, Nishino N, Yamamoto T (2005) Agonist and antagonist dual effect of the cross-linked S19 ribosomal protein dimer in the C5a receptor-mediated respiratory burst reaction of phagocytic leukocytes. *Inflammation Research*, **54**, 82–90.

Reynolds JM, Bruns BU, Fitt WK, Schmidt GW (2008) Enhanced photoprotection pathways in symbiotic dinoflagellates of shallow-water corals and other cnidarians. *Proceedings of the National Academy of Sciences*, **105**, 13674–13678.

Reynolds WS, Schwarz JA, Weis VM (2000) Symbiosis-enhanced gene expression in cnidarian-algal associations: cloning and characterization of a cDNA, sym32, encoding a possible cell adhesion protein. *Comparative Biochemistry and Physiology. Part A, Molecular & Integrative Physiology*, **126**, 33–44.

Richmond RH (1993) Coral reefs: Present problems and future concerns resulting from anthropogenic disturbance. *Integrative and Comparative Biology*, **33**, 524–536.

Richmond R, Hunter C (1990) Reproduction and recruitment of corals: Comparisons among the Caribbean, the Tropical Pacific, and the Red Sea. *Marine Ecology Progress Series*, **60**, 185–203.

Rodriguez-Lanetty M (2003) Evolving lineages of *Symbiodinium*-like dinoflagellates based on ITS1 rDNA. *Molecular Phylogenetics and Evolution*, **28**, 152–168.

Rodriguez-Lanetty M, Phillips WS, Weis VM (2006) Transcriptome analysis of a cnidarian-dinoflagellate mutualism reveals complex modulation of host gene expression. *BMC genomics*, **7**, 23.

Roeder T (2003) Metabotropic histamine receptors—nothing for invertebrates? *European Journal of Pharmacology*, **466**, 85-90.

Rojek A, Praetorius J, Frøkiaer J, Nielsen S, Fenton RA (2008) A current view of the mammalian aquaglyceroporins. *Annual Review of Physiology*, **70**, 301–327.

Roossinck MJ (2005) Symbiosis versus competition in plant virus evolution. *Nature reviews. Microbiology*, **3**, 917–924.

Rosic N, Ling EY, Chan CK, Lee HC, Kaniewska P, Edwards D, Dove S, Hoegh-Guldberg O (2014) Unfolding the secrets of coral-algal symbiosis. *The ISME Journal*, **9**, 844-857.

Röthig T, Costa RM, Simona F, Baumgarten S, Torres AF, Radhakrishnan A, Aranda M, Voolstra CR (2016) Distinct bacterial communities associated with the coral model *Aiptasia* in aposymbiotic and symbiotic states with *Symbiodinium*. *Frontiers in Marine Science*, **3**, 234.

Rouzé H, Lecellier GJ, Saulnier D, Planes S, Gueguen Y, Wirshing HH, Berteaux-Lecellier V (2017) An updated assessment of *Symbiodinium* that associate with common scleractinian corals from Moorea (French Polynesia) reveals high diversity among background symbionts and a novel finding of clade B. *PeerJ*, **5**, e2856.

Rowan R (2004) Coral bleaching: Thermal adaptation in reef coral symbionts. *Nature*, **430**, 742-742.

Rowan R, Knowlton N, Baker AC, Jara J (1997) Landscape ecology of algal symbionts creates variation in episodes of coral bleaching. *Nature*, **388**, 265–269.

Rowan R, Powers DA (1991) Molecular genetic identification of symbiotic dinoflagellates (zooxanthellae). *Marine Ecology Progress Series*, **71**, 65–73.

Roy A, Kucukural A, Zhang Y (2010) I-TASSER: a unified platform for automated protein structure and function prediction. *Nature Protocols*, **5**, 725–738.

Saier M (1994) Computer-aided analyses of transport protein sequences: Gleaning evidence concerning function, structure, biogenesis, and evolution. *Microbiological Reviews*, **58**, 71–93.

Saier MH (2000) A functional-phylogenetic classification system for transmembrane solute transporters. *Microbiology and Molecular Biology Reviews*, **64**, 354–411.

Saier Jr MH, Beatty JT, Goffeau A, Harley KT, Heijne WH, Huang SC, Jack DL, Jahn PS, Lew K, Liu J, Pao SS (1999) The major facilitator superfamily. *Journal of Molecular Microbiology and Biotechnology*, **1**, 257–279.

Salemi M, Vandamme AM (2003) *The Phylogenetic Handbook: A Practical Guide to DNA and Protein Phylogeny*. Cambridge Univeristy Press.

Sampayo EM, Dove S, LaJeunesse TC (2009) Cohesive molecular genetic data delineate species diversity in the dinoflagellate genus *Symbiodinium*. *Molecular Ecology*, **18**, 500–519.

Sampayo EM, Ridgway T, Franceschinis L, Roff G, Hoegh-Guldberg O, Dove S (2016) Coral symbioses under prolonged environmental change: Living near tolerance range limits. *Scientific Reports*, **6**, 36271.

Santi C, Bogusz D, Franche C (2013) Biological nitrogen fixation in non-legume plants. *Annals of Botany*, **111**, 743–767.

Santos SR, Coffroth MA (2003) Molecular genetic evidence that dinoflagellates belonging to the genus *Symbiodinium* freudenthal are haploid. *Biological Bulletin*, **204**, 10–20.

Santos SR, Gutierrez-Rodriguez C, Coffroth MA (2003) Phylogenetic identification of symbiotic dinoflagellates via length heteroplasmy in domain V of chloroplast large subunit (cp23S)—ribosomal DNA sequences. *Marine Biotechnology*, **5**, 130–140.

Santos SR, Shearer TL, Hannes AR, Coffroth MA (2004) Fine-scale diversity and specificity in the most prevalent lineage of symbiotic dinoflagellates ( *Symbiodinium* , Dinophyceae) of the Caribbean. *Molecular Ecology*, **13**, 459–469.

Santos SR, Taylor DJ, Kinzie Iii RA, Hidaka M, Sakai K, Coffroth MA (2002) Molecular phylogeny of symbiotic dinoflagellates inferred from partial chloroplast large subunit (23S)-rDNA sequences. *Molecular Phylogenetics and Evolution*, **23**, 97–111.

Sapp J (2004) The dynamics of symbiosis: an historical overview. *Canadian Journal of Botany*, **82**, 1046–1056.

Sawyer SJ, Muscatine L (2001) Cellular mechanisms underlying temperature-induced bleaching in the tropical sea anemone *Aiptasia pulchella*. *The Journal of Experimental Biology*, **204**, 3443–3456.

Scheepers A, Joost HG, Schürmann A (2015) The glucose transporter families SGLT and GLUT: Molecular basis of normal and aberrant function. *Journal of Parenteral and Enteral Nutrition*, **28**, 364–371.

Schmitz K, Kremer B (1977) Carbon fixation and analysis of assimilates in a coral-dinoflagellate symbiosis. *Marine Biology*, **313**, 305–313.

Schneider E, Rolli-Derkinderen M, Arock M, Dy M (2002) Trends in histamine research: New functions during immune responses and hematopoiesis. *Trends in Immunology*, **23**, 255-263.

Schoenberg D, Trench R (1980) Genetic variation in *Symbiodinium* (=Gymnodinium) *microadriaticum* Freudenthal, and specificity in its symbionts with marine invertebrates. III. Specificity and infectivity of *Symbiodinium microadriaticum*. *Proceedings of the Royal Society of London B: Biological Sciences*, **1169**, 445–460.

Schwarz JA, Brokstein PB, Voolstra C, Terry AY, Miller DJ, Szmant AM, Coffroth MA, Medina M (2008) Coral life history and symbiosis: Functional genomic resources for two reef building Caribbean corals, *Acropora palmata* and *Montastraea faveolata*. *BMC Genomics*, **9**, 97.

Schwarz J, Krupp D, Weis VM (1999) Late larval development and onset of symbiosis in the scleractinian coral *Fungia scutaria*. *The Biological Bulletin*, **196**, 70–79.

Schwarz JA, Weis VM (2003) Localization of a symbiosis-related protein, Sym32, in the *Anthopleura elegantissima-Symbiodinium muscatinei* association. *The Biological Bulletin*, **205**, 339–350.

Sen S, Kundu G, Mekhail N, Castel J, Misono K, Healy B (1990) Myotrophin: Purification of a novel peptide from spontaneously hypertensive rat heart that influences myocardial growth. *Journal of Biological Chemistry*, **265**, 16635–16643.

Shi XZ, Zhong X, Yu XQ (2012) *Drosophila melanogaster* NPC2 proteins bind bacterial cell wall components and may function in immune signal pathways. *Insect Biochemistry and Molecular Biology*, **42**, 545-556.

Shinzato C, Inoue M, Kusakabe M (2014) A snapshot of a coral "holobiont": A transcriptome assembly of the scleractinian coral, *Porites*, captures a wide variety of genes from both the host and symbiotic zooxanthellae. *PLoS One*, **9**, e85182.

Silverstein RN, Correa AMS, Baker AC (2012) Specificity is rarely absolute in coral-algal symbiosis: Implications for coral response to climate change. *Proceedings of the Royal Society of London B: Biological Sciences*, **279**, 2609–2618.

Silverstein RN, Cunning R, Baker AC (2017) Tenacious D: *Symbiodinium* in clade D remain in reef corals at both high and low temperature extremes despite impairment. *Journal of Experimental Biology*, **220**, 1192-1196.

Sjölander K (2004) Phylogenomic inference of protein molecular function: Advances and challenges. *Bioinformatics*, **20**, 170–179.

Smith DC (1979) From extracellular to intracellular: The establishment of a symbiosis. *Proceedings of the Royal Society of London B: Biological Sciences*, **204**, 115–30.

Smith O, Marinov A, Chan K, Drew Ferrier M (2004) Cloning and sequencing of cDNA encoding glutamine synthetase from the sea anemone *Aiptasia pallida*. *Hydrobiologia*, **530**–**531**, 267–272.

Stadermann FJ, Croat TK, Bernatowicz TJ, Amari S, Messenger S, Walker RM, Zinner E (2005) Supernova graphite in the NanoSIMS: Carbon, oxygen and titanium isotopic compositions of a spherule and its TiC sub-components. *Geochimica et Cosmochimica Acta*, **69**, 177–188.

Stamatakis A (2014) RAxML version 8: A tool for phylogenetic analysis and post-analysis of large phylogenies. *Bioinformatics*, **30**, 1312–1313.

Stanley Jr. GD (1981) Early history of scleractinian corals and its geological consequences. *Geology*, **9**, 507–511.

Starzak DE (2012) The influence of symbiont diversity on the functional biology of a model sea anemone. *A Thesis Submitted to Victoria University of Wellington*.

Starzak DE, Quinnell RG, Nitschke MR, Davy SK (2014) The influence of symbiont type on photosynthetic carbon flux in a model cnidarian-dinoflagellate symbiosis. *Marine Biology*, **161**, 711–724.

Stat M, Carter D, Hoegh-Guldberg O (2006) The evolutionary history of *Symbiodinium* and scleractinian hosts—Symbiosis, diversity, and the effect of climate change. *Perspectives in Plant Ecology, Evolution and Systematics*, **8**, 23–43.

Stat M, Gates RD (2011) Clade D *Symbiodinium* in scleractinian corals: A "nugget" of hope, a selfish opportunist, an ominous sign, or all of the above? *Journal of Marine Biology*, **2011**, 1–9.

Stat M, Morris E, Gates RD (2008) Functional diversity in coral-dinoflagellate symbiosis. *Proceedings of the National Academy of Sciences*, **105**, 9256–9261.

Stat M, Pochon X, Cowie ROM, Gates RD (2009) Specificity in communities of *Symbiodinium* in corals from Johnston Atoll. *Marine Ecology Progress Series*, **386**, 83–96.

Steen RG (1986) Evidence for heterotrophy by zooxanthellae symbiosis with *Aiptasia pulchella*. *Biological Bulletin*, **170**, 267–278.

Suescún-Bolívar LP, Iglesias-Prieto R, Thomé PE (2012) Induction of glycerol synthesis and release in cultured *Symbiodinium*. *PloS One*, **7**, e47182.

Suescun-Bolivar LP, Traverse GMI, Thome PE (2016) Glycerol outflow in *Symbiodinium* under osmotic and nitrogen stress. *Marine Biology*, **163**, 128–140.

Sun HQ, Yamamoto M, Mejillano M, Yin HL (1999) Gelsolin, a multifunctional actin regulatory protein. *The Journal of Biological Chemistry*, **274**, 33179–33182.

Sutton D, Hoegh-Guldberg O (1990) Host-zooxanthella interactions in four temperate marine invertebrate symbioses: Assessment of effect of host extracts on symbionts. *The Biological Bulletin*, **178**, 175–186.

Suzuki Y, Nakashima N, Yoshida K, Casareto B, Taki M, Hiraga T, Okabayashi T, Ito H, Yamada K (1995) The important role of organic matter cycling for the biological fixation of $CO_2$ in coral reefs. *Energy Conservation and Management*, **36**, 737–740.

Swanson R, Hoegh O, Hoegh-Guldberg O (1998) Amino acid synthesis in the symbiotic sea anemone *Aiptasia pulchella*. *Marine Biology*, **131**, 83–93.

Syrett APJ, Peplinska AM (1988) Effects of nitrogen-deprivation, and recovery from it, on the metabolism of microalgae. *New Phytologist*, **109**, 289–296.

Tadimalla A, Belmont PJ, Thuerauf DJ, Glassy MS, Martindale JJ, Gude N, Sussman MA, Glembotski CC (2008) Mesencephalic astrocyte-derived neurotrophic factor is an ischemia-inducible secreted endoplasmic reticulum stress response protein in the heart. *Circulation Research*, **103**, 1249–1258.

Takabayashi M, Santos SR, Cook CB (2004) Mitochondrial DNA phylogeny of the symbiotic dinoflagellates (*Symbiodinium*, Dinophyta). *Journal of Phycology*, **40**, 160–164.

Tanaka Y, Miyajima T, Koike I, Hayashibara T, Ogawa H (2006) Translocation and conservation of organic nitrogen within the coral-zooxanthella symbiotic system of *Acropora pulchra*, as demonstrated by dual isotope-labeling techniques. *Journal of Experimental Marine Biology and Ecology*, **336**, 110–119.

Tarpy DR (2002) Genetic diversity within honeybee colonies prevents severe infections and promotes colony growth. *Proceedings of the Royal Society of London B: Biological Sciences*, **270**, 99–103.

Tatchell K, Robinson LC, Breitenbach M (1985) RAS2 of *Saccharomyces cerevisiae* is required for gluconeogenic growth and proper response to nutrient limitation. *Proceedings of the National Academy of Sciences*, **82**, 3785–3789.

Taylor D (1968) In situ studies on the cytochemistry and ultrastructure of a symbiotic marine dinoflagellate. *Journal of the Marine Biological Association of the United Kingdom*, **48**, 349–366.

Taylor D (1971) Ultrastructure of the "Zooxanthella" *Endodinium chattoni* in Situ. *Journal of the Marine Biological Association of the United Kingdom*, **51**, 227–234.

Tchernov D, Gorbunov MY, de Vargas C, Yadav SN, Milligan AJ, Häggblom M, Falkowski PG (2004) Membrane lipids of symbiotic algae are diagnostic of sensitivity to thermal bleaching in corals. *Proceedings of the National Academy of Sciences*, **101**, 13531–13535.

Telford MJ (2007) Phylogenomics. *Current Biology*, **17**, 945–946.

Thomas L, Kendrick GA, Kennington WJ, Richards ZT, Stat M (2014) Exploring *Symbiodinium* diversity and host specificity in *Acropora* corals from geographical extremes of Western Australia with 454 amplicon pyrosequencing. *Molecular Ecology*, **23**, 3113–3126.

Thomas GH, Mullins JGL (2000) Membrane topology of the Mep/Amt family of ammonium transporters. *Molecular Microbiology*, **37**, 331–344.

Thornhill DJ, Daniel MW, LaJeunesse TC, Schmidt GW, Fitt WK (2006) Natural infections of aposymbiotic *Cassiopea xamachana* scyphistomae from environmental pools of *Symbiodinium*. *Journal of Experimental Marine Biology and Ecology*, **338**, 50–56.

Thornhill DJ, Xiang Y, Fitt WK, Santos SR (2009) Reef endemism, host specificity and temporal stability in populations of symbiotic dinoflagellates from two ecologically dominant Caribbean corals. *PloS One*, **4**, e6262.

Titlyanov EA, Titlyanova TV, Leletkin VA, Tsukahara J, Van Woesik R, Yamazato K (1996) Degradation of zooxanthellae and regulation of their density in hermatypic corals. *Marine Ecology Progress Series*, **139**, 167–178.

Tolleter D, Seneca FO, DeNofrio JC, Krediet CJ, Palumbi SR, Pringle JR, Grossman AR (2013) Coral bleaching independent of photosynthetic activity. *Current Biology*, **23**, 1782–1786.

Tremblay P, Grover R, Maguer JF, Legendre L, Ferrier-Pagès C (2012) Autotrophic carbon budget in coral tissue: A new $^{13}$C-based model of photosynthate translocation. *The Journal of Experimental Biology*, **215**, 1384–1393.

Trench R (1971a) The physiology and biochemistry of zooxanthellae symbiotic with marine coelenterates II. Liberation of fixed $^{14}$C by zooxanthellae in vitro. *Proceedings of the Royal Society B: Biological Sciences*, **177**, 237–250.

Trench R (1971b) The physiology and biochemistry of zooxanthellae symbiotic with marine coelenterates III. The effect of homogenates of host tissues on the excretion of photosynthetic products in vitro by zooxanthellae from two marine coelenterates. *Proceedings of the Royal Society B: Biological Sciences*, **177**, 251–264.

Trench RK (1974) Nutritional potentials in *Zoanthus sociathus* (Coelenterata, Anthozoa). *Helgoländer Wissenschaftliche Meeresuntersuchungen*, **26**, 174–216.

Trench RK (1997) Diversity of symbiotic dinoflagellates and the evolution of microalgal-invertebrate symbiosis. *Proceedings of the 8th International Coral Reef Symposium*, **2**, 1275–1286.

Trench R, Blank R (1987) *Symbiodinium microadriaticum* Freudenthal, *S. goreau* sp. nov., *S. kawagutii* sp. nov. and *S. pilosum* sp. nov.: Gymnodinioid dinoflagellate symbionts of marine invertebrates. *Journal of Phycology*, **23**, 469–481.

Trench R, Winsor H (1987) Symbiosis with dinoflagellates in two pelagic flatworms, *Amphiscolops* sp. and *Haplodiscus* sp. *Symbiosis*, **3**, 1–21.

Trudgian DC, Fischer R, Guo X, Kessler BM, Mirzaei H (2014) GOAT–A simple LC-

MS/MS gradient optimization tool. *Proteomics*, **14**, 1467-1471.

Trueman LJ, Richardson A, Forde BG (1996) Molecular cloning of higher plant homologues of the high-affinity nitrate transporters of *Chlamydomonas reinhardtii* and *Aspergillus nidulans*. *Gene*, **175**, 223–231.

Udvardi MK, Day DA (1997) Metabolite transport across symbiotic membranes of legume nodules. *Annual Review of Plant Physiology and Plant Molecular Biology*, **48**, 493–523.

Uldry M, Thorens B (2004) The SLC2 family of facilitated hexose and polyol transporters. *Pflugers Archiv European Journal of Physiology*, **447**, 480–489.

Van Den Heuvel A (2012) The effects of exogenous nitrogen on the coral/dinoflagellate symbiosis: Effect of nitrogen on staghorn coral. *A Thesis Submitted to the University of Queensland*.

van Oppen MJ, Palstra FP, Piquet AM, Miller DJ (2001) Patterns of coral-dinoflagellate associations in *Acropora*: Significance of local availability and physiology of *Symbiodinium* strains and host-symbiont selectivity. *Proceedings of the Royal Society of London B: Biological Sciences*, **268**, 1759–1767.

Vander Heiden MG, Cantley LC, Thompson CB (2009) Understanding the Warburg effect: The metabolic requirements of cell proliferation. Science (New York, N.Y.), 324, 1029–1033.

Vandermeulen JH, Davis ND, Muscatine L (1972) The effect of inhibitors of photosynthesis on zooxanthellae in corals and other marine invertebrates. *Marine Biology*, **16**, 185–191.

Venn A, Loram J, Douglas A (2008) Photosynthetic symbioses in animals. *Journal of Experimental Botany*, **59**, 1069–1080.

Vetter IR, Wittinghofer A (2001) The guanine nucleotide – binding switch in three dimensions. *Science (New York, N.Y.)*, **294**, 1299–1305.

Vidal-Dupiol J, Adjeroud M, Roger E, Foure L, Duval D, Mone Y, Ferrier-Pages C, Tambutte E, Tambutte S, Zoccola D, Allemand D (2009) Coral bleaching under thermal stress: Putative involvement of host/symbiont recognition mechanisms. *BMC Physiology*, **9**, 14.

Vogel BE, Muriel JM, Dong C, Xu X (2006) Hemicentins: What have we learned from worms? *Cell Research*, **16**, 872–878.

von Holt C (1968) Uptake of glycine and release of nucleoside-polyphosphates by zooxanthellae. *Comparative Biochemistry and Physiology*, **26**, 1071–1079.

von Holt C, von Holt M (1968a) Transfer of photosynthetic products from zooxanthellae to coelenterate hosts. *Comparative Biochemistry and Physiology*, **24**, 73–81.

von Holt C, von Holt M (1968b) The secretion of organic compounds by zooxanthellae isolated from various types of *Zoanthus*. *Comparative Biochemistry and Physiology*, **24**, 83–92.

von Wiren N, Gazzarrini S, Gojon A, Frommer WB (2000) The molecular physiology of ammonium uptake and retrieval. *Current Opinion in Plant Biology*, **3**, 254–261.

Voolstra CR, Schwarz JA, Schnetzer J, Sunagawa S, Desalvo MK, Szmant AM, Coffroth MA, Medina M (2009) The host transcriptome remains unaltered during the establishment of coral-algal symbioses: FAST TRACK. *Molecular Ecology*, **18**, 1823–1833.

Voolstra CR, Sunagawa S, Matz MV, Bayer T, Aranda M, Buschiazzo E, DeSalvo MK, Lindquist E, Szmant AM, Coffroth MA, Medina M (2011) Rapid evolution of coral proteins responsible for interaction with the environment. *PloS One*, **6**, e20392.

Wakefield TS, Farmer M, Kempf SC (2000) Revised description of the fine structure of in situ "zooxanthellae" genus *Symbiodinium*. *Biological Bulletin*, **199**, 76–84.

Wakefield TS, Kempf SC (2001) Development of host- and symbiont-specific monoclonal antibodies and confirmation of the origin of the symbiosome membrane in a cnidarian-dinoflagellate symbiosis. *Biological Bulletin*, **200**, 127–143.

Wang J, Douglas AE (1997) Nutrients, signals, and photosynthate release by symbiotic algae. *Plant Physiology*, **114**, 631–636.

Wang J, Douglas AE (1998) Nitrogen recycling or nitrogen conservation in an alga-invertebrate symbiosis? *The Journal of Experimental Biology*, **201**, 2445–2453.

Wang J, Douglas A (1999) Essential amino acid synthesis and nitrogen recycling in an alga–invertebrate symbiosis. *Marine Biology*, **135**, 219–222.

Wang ZD, Jiang YR, Sun Y, Li Q, Li YP, Du ZJ, Liu YQ, Qin L (2013a) Molecular characterization of a phosphoserine aminotransferase gene in *Antheraea pernyi* and assessment of its value for phylogenetic inference. *Biochemical Systematics and Ecology*, **48**, 293–300.

Wang LH, Lee HH, Fang LS, Mayfield AB, Chen CS (2013b) Fatty acid and phospholipid syntheses are prerequisites for the cell cycle of *Symbiodinium* and their endosymbiosis within sea anemones. *PloS One*, **8**, e72486.

Warner ME, Chilcoat GC, Mcfarland IFK, Fitt WK (2002) Seasonal fluctuations in the photosynthetic capacity of photosystem II in symbiotic dinoflagellates in the Caribbean reef-building coral *Montastraea*. *Marine Biology*, **141**, 31–38.

Weaver CD, Shomer NH, Louis CF, Roberts DM (1994) Nodulin 26, a nodule-specific symbiosome membrane protein from soybean, is an ion channel. *Journal of Biological Chemistry*, **269**, 17858–17862.

Weber A, Pennise CR, Babcock GG, Fowler VM (1994) Tropomodulin caps the pointed ends of actin filaments. *Journal of Cell Biology*, **127**, 1627–1635.

Weis VM (1991) The induction of carbonic anhydrase in the symbiotic sea anemone *Aiptasia pulchella*. *Biological Bulletin*, **180**, 496–504.

Weis VM (2008) Cellular mechanisms of cnidarian bleaching: Stress causes the collapse of

symbiosis. *The Journal of Experimental Biology*, **211**, 3059–3066.

Weis VM, Levine R (1996) Differential protein profiles reflect the different lifestyles of symbiotic and aposymbiotic *Anthopleura elegantissima*, a sea anemone from temperate waters. *The Journal of Experimental Biology*, **199**, 883–892.

Weis VM, Reynolds W (1999) Carbonic anhydrase expression and synthesis in the sea anemone *Anthopleura elegantissima* are enhanced by the presence of dinoflagellate symbionts. *Physiological and Biochemical Zoology*, **72**, 307–316.

Weis VM, Reynolds WS, DeBoer MD, Krupp DA (2001) Host-symbiont specificity during onset of symbiosis between the dinoflagellates *Symbiodinium* spp. and planula larvae of the scleractinian coral *Fungia scutaria*. *Coral Reefs*, **20**, 301–308.

Werner D (1992) *Symbiosis of plants and microbes*. Chapman & Hall.

Whitehead LF, Douglas AE (2003) Metabolite comparisons and the identity of nutrients translocated from symbiotic algae to an animal host. *Journal of Experimental Biology*, **206**, 3149–3157.

Wilkerson FP, Kobayashi D, Muscatine L (1988) Mitotic index and size of symbiotic algae in caribbean reef corals. *Coral Reefs*, **7**, 29–36.

Wilkerson FP, Muller-Parker G, Muscatine L (1983) Temporal patterns of cell division in natural populations of endosymbiotic algae. *Limnology and Oceanography*, **28**, 1009–1014.

Williams SL (2001) Reduced genetic diversity in eelgrass transplantations affects both population growth and individual fitness. *Ecological Applications*, **11**, 1472–1488.

Wilson-O'Brien AL, Patron N, Rogers S (2010) Evolutionary ancestry and novel functions of the mammalian glucose transporter (GLUT) family. *BMC Evolutionary Biology*, **10**, 152.

Wolfowicz I, Baumgarten S, Voss PA, Hambleton EA, Voolstra CR, Hatta M, Guse A (2016) *Aiptasia* sp. larvae as a model to reveal mechanisms of symbiont selection in cnidarians. *Scientific reports*, **6**, 32366.

Wood-Charlson EM, Hollingsworth LL, Krupp DA, Weis VM (2006) Lectin/glycan interactions play a role in recognition in a coral/dinoflagellate symbiosis. *Cellular Microbiology*, **8**, 1985–1993.

Wood-Charlson EM, Weis VM (2009) The diversity of C-type lectins in the genome of a basal metazoan, *Nematostella vectensis*. *Developmental and Comparative Immunology*, **33**, 881–889.

Wood DE, Newcomb EW (1999) Caspase-dependent activation of calpain during drug-induced apoptosis. *Journal of Biological Chemistry*, **274**, 8309–8315.

Wood IS, Trayhurn P (2003) Glucose transporters (GLUT and SGLT): expanded families of sugar transport proteins. *The British Journal of Nutrition*, **89**, 3–9.

Wooldridge SA (2010) Is the coral-algae symbiosis really "mutually beneficial" for the partners? *BioEssays*, **32**, 615–625.

Wooldridge SA (2014) Formalising a mechanistic linkage between heterotrophic feeding and thermal bleaching resistance. *Coral Reefs*, **33**, 1131–1136.

Wright EM (2013) Glucose transport families SLC5 and SLC50. *Molecular Aspects of Medicine*, **34**, 183–196.

Wright EM, Turk E (2004) The sodium/glucose cotransport family SLC5. *Pflugers Archiv European Journal of Physiology*, **447**, 510–518.

Xiang T, Hambleton EA, DeNofrio JC, Pringle JR, Grossman AR (2013) Isolation of clonal axenic strains of the symbiotic dinoflagellate *Symbiodinium* and their growth and host specificity (S Lin, Ed,). *Journal of Phycology*, **49**, 447–458.

Xu Z, Farver W, Kodukula S, Storch J (2008) Regulation of sterol transport between membranes and NPC2. *Biochemistry*, **47**, 11134–11143.

Xu X, Xu M, Zhou X, Jones OB, Moharomd E, Pan Y, Yan G, Anthony DD, Isaacs WB (2013) Specific structure and unique function define the hemicentin. *Cell & Bioscience*, **3**, 27.

Yamashita H, Suzuki G, Hayashibara T, Koike K (2011) Do corals select zooxanthellae by alternative discharge? *Marine Biology*, **158**, 87-100.

Yamashiro H, Oku H, Higa H, Chinen I, Sakai K (1999) Composition of lipids, fatty acids and sterols in Okinawan corals. *Comparative Biochemistry and Physiology Part B: Biochemistry and Molecular Biology*, **122**, 397–407.

Yang J, Liu X, Yue G, Adamian M, Bulgakov O, Li T (2002) Rootletin, a novel coiled-coil protein, is a structural component of the ciliary rootlet. *Journal of Cell Biology*, **159**, 431–440.

Yang MH, Nickerson S, Kim ET, Liot C, Laurent G, Spang R, Philips MR, Shan Y, Shaw DE, Bar-Sagi D, Haigis MC (2012) Regulation of RAS oncogenicity by acetylation. *Proceedings of the National Academy of Sciences*, **109**, 10843–10848.

Yang J, Roy A, Zhang Y (2013) Protein-ligand binding site recognition using complementary binding-specific substructure comparison and sequence profile alignment. *Bioinformatics*, **29**, 2588–2595.

Yoshida N, Potocnjak P, Nussenzweig V, Nussenzweig RS (1981) Biosynthesis of Pb44, the protective antigen of sporozoites of *Plasmodium berghei*. *Journal of Experimental Medicine*, **154**, 1225–1236.

Yuyama I, Hayakawa H, Endo H, Iwao K, Takeyama H, Maruyama T, Watanabe T (2005) Identification of symbiotically expressed coral mRNAs using a model infection system. *Biochemical and Biophysical Research Communications*, **336**, 793–798.

Yuyama I, Nakamura T, Higuchi T, Hidaka M (2016) Different stress tolerances of juveniles of the coral *Acropora tenuis* associated with clades C1 and D *Symbiodinium*. *Zoological*

*Studies*, **55**, 1–9.

Yuyama I, Watanabe T (2008) Molecular characterization of coral sulfate transporter homolog that is up-regulated by the presence of symbiotic algae. *Fisheries Science*, **74**, 1269–1276.

Zhang Y (2008) I-TASSER server for protein 3D structure prediction. *BMC Bioinformatics*, **9**, 40.

Zhang X, Hudson BG, Sarras Jr. MP (1994) Hydra cell aggregate development is blocked by selective fragments of fibronectin and type IV collagen. *Developmental Biology*, **164**, 10–23.

Zhao FQ, Keating AF (2007) Functional properties and genomics of glucose transporters. *Current Genomics*, **8**, 113–128.

Ziegler M, Arif C, Burt JA, Dobretsov S, Roder C, LaJeunesse TC, Voolstra CR (2017) Biogeography and molecular diversity of coral symbionts in the genus *Symbiodinium* around the Arabian Peninsula. *Journal of Biogeography*, **44**, 674-686.

Zimmermann G, Papke B, Ismail S, Vartak N, Chandra A, Hoffmann M, Hahn SA, Triola G, Wittinghofer A, Bastiaens PI, Waldmann H (2013) Small molecule inhibition of the KRAS-PDEδ interaction impairs oncogenic KRAS signalling. *Nature*, **497**, 638–642.

Zmasek CM, Eddy SR (2001) ATV: Display and manipulation of annotated phylogenetic trees. *Bioinformatics*, **17**, 383–384.

# Appendix A: Protein sequences and genetic resources

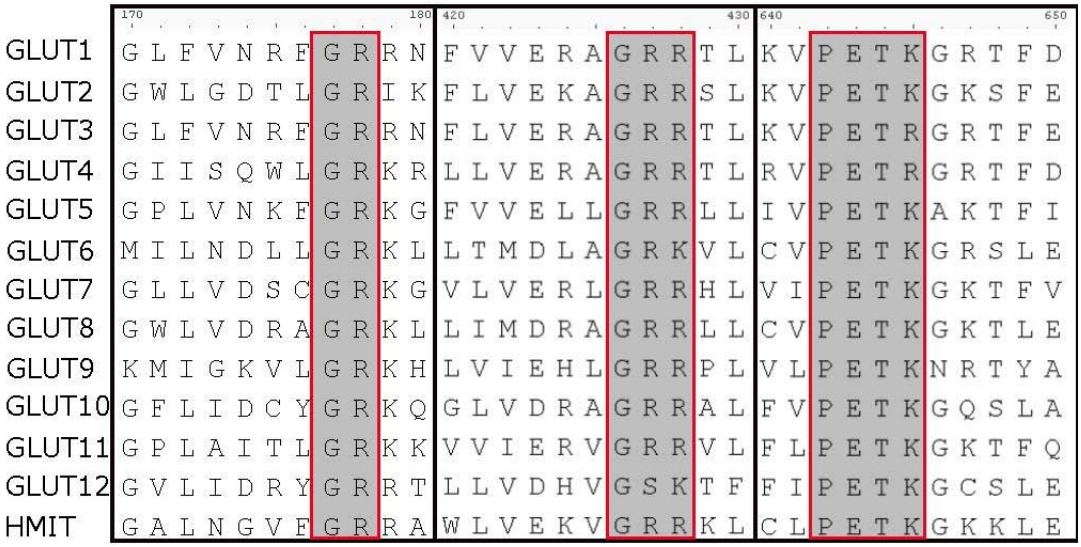


**Figure A1** Motifs used for manual editing of the GLUT alignment. Partial alignment of the *Homo sapiens* GLUT sequences, showing conserved domains with functional motifs used to screen identified protein sequences, outlined in red shaded boxes. Included are residues 170–180 with the GR motif, residues 420–430 with the GRR motif, and residues 640–650 with the PETK motif.

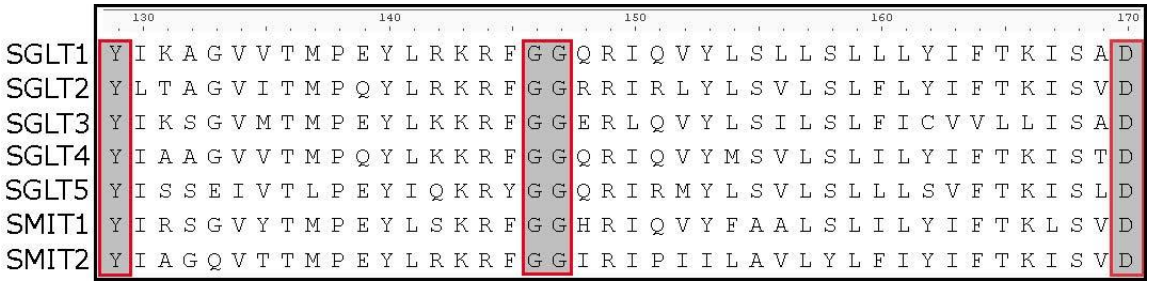


**Figure A2** Motifs used for manual editing of the SGLT alignment. Partial alignment of the *Homo sapiens* SGLT sequences, showing structural motifs used to screen identified protein sequences, outlined in red shaded boxes. Included are residues 129–170 with the Y, GG, and D motifs.

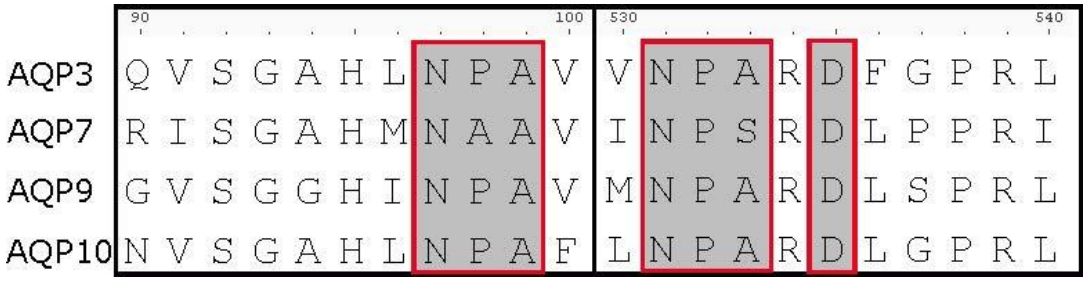


**Figure A3** Motifs used for manual editing of the AQP alignment. Partial alignment of the *Homo sapiens* aquaglyceroporin sequences, showing functional and structural motifs used to screen identified protein sequences, outlined in red shaded boxes. Included are residues 90–100 with the first NPA motif, and resides 530–540 with the second NPA motif and the D residue.

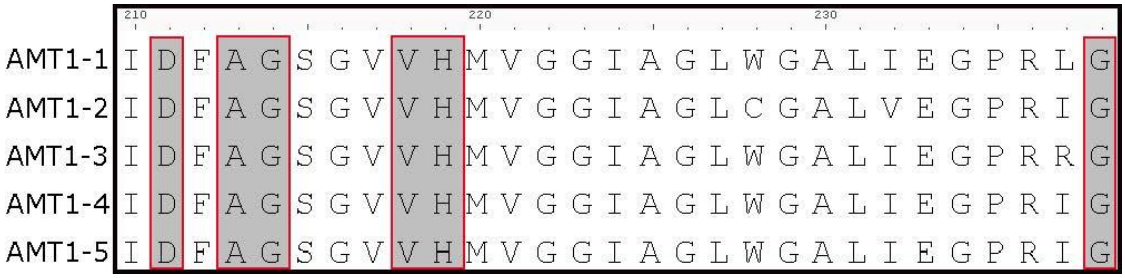


**Figure A4** Motifs used for manual editing of the AMT alignment. Partial alignment of the *Arabidopsis thaliana* AMT sequences, showing functional and structural motifs used to screen identified protein sequences, outlined in red shaded boxes. Included are residues 210–238 with the D, AG, VH, and G motifs responsible for ammonium recognition and transport function.

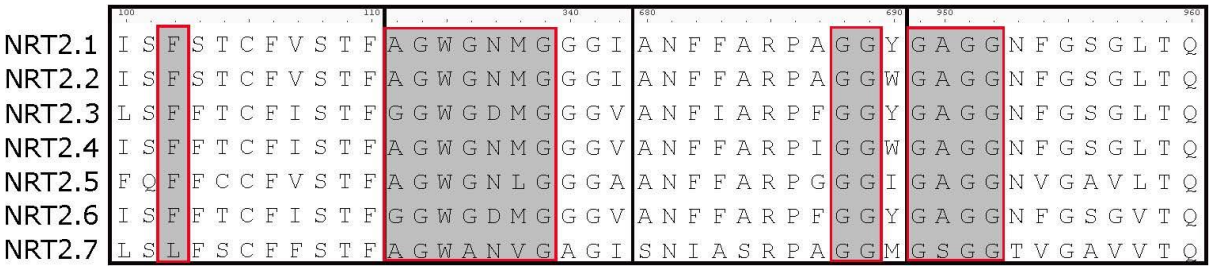


**Figure A5** Motifs used for manual editing of the NRT alignment. Partial alignment of the *Arabidopsis thaliana* NRT2 sequences, showing functional and structural motifs used to screen identified protein sequences, outlined in red shaded boxes. Included are residues 100–110 with a conserved F residue, 333–342 with a proposed NNP signature A/G-G-W-G/A-N/D-M/L-G, and 680–690 and 949–960 with structurally important conserved glycine residues GG and GAGG, respectively.

**Datasheet A1 (on disc)** Characterization data for newly identified cnidarian GLUT sequences. (Tab A) Summary of characteristics for each cnidarian GLUT sequence used in the phylogenetic analysis, with the sequence submitted to I-TASSER highlighted. (Tab B) Accession numbers for each homolog sequence from other species used in the GLUT phylogenetic tree. (Tab C) I-TASSER output for structural predictions of the *N. vectensis* GLUT8 sequence. (Tab D) MemPype results for the newly identified GLUT sequences.

**Datasheet A2 (on disc)** Characterization data for newly identified cnidarian SGLT sequences. (Tab A) Summary of characteristics for each cnidarian SGLT sequence used in the phylogenetic analysis, with the sequence submitted to I-TASSER highlighted. (Tab B) Accession numbers for each homolog sequence from other species used in the SGLT phylogenetic tree. (Tab C) I-TASSER output for structural predictions of the *N. vectensis* SMIT sequence. (Tab D) MemPype results for the newly identified SGLT sequences.

**Datasheet A3 (on disc)** Characterization data for newly identified cnidarian AQP sequences. (Tab A) Summary of characteristics for each cnidarian AQP sequence used in the phylogenetic analysis, with the sequence submitted to I-TASSER highlighted. (Tab B) Accession numbers for each homolog sequence from other species used in the AQP phylogenetic tree. (Tab C) I-TASSER output for structural predictions of the *N. vectensis*_4 AQP3 sequence. (Tab D) MemPype results for the newly identified AQP sequences.

**Datasheet A4 (on disc)** Characterization data for newly identified *Symbiodinium* AMT sequences. (Tab A) Summary of characteristics for each *Symbiodinium* AMT sequence used in the phylogenetic analysis, with the sequence submitted to I-TASSER highlighted. (Tab B) Accession numbers for each homolog sequence from other species used in the AMT phylogenetic tree. (Tab C) I-TASSER output for structural predictions of the *Symbiodinium*C1_25 sequence. (Tab D) MemPype results for the newly identified AMT sequences.

**Datasheet A5 (on disc)** Characterization data for newly identified *Symbiodinium* NRT2 sequences. (Tab A) Summary of characteristics for each *Symbiodinium* NRT2 sequence used in the phylogenetic analysis, with the sequence submitted to I-TASSER highlighted. (Tab B) Accession numbers for each homolog sequence from other species used in the AMT phylogenetic tree. (Tab C) I-TASSER output for structural predictions of the *Symbiodinium* A-24 sequence. (Tab D) MemPype results for the newly identified NRT2 sequences.

**Table A1** List of resources used in custom cnidarian and *Symbiodinium* BLAST databases, their origin, and publication if available. Species with an asterisk (*) after the name indicate those that were in symbiosis at the time of sampling.

| Cnidaria Resources | | | | | |
|---|---|---|---|---|---|
| **Species** | **Common name** | **Symbiotic?** | **Genome (G) or Transcriptome (T)** | **Source** | **Publication** |
| *Acropora digitifera* | Staghorn coral | Yes | G | OIST Marine Genomics Unit | Shinzato *et al.* 2011 |
| *Anthopleura elegantissima* | Aggregating anemone | Yes | T | Weis and Meyer lab | Kitchen *et al.* 2015 |
| *Acropora millepora* | Branching stony coral | Yes | T | Compagen | Brower *et al.* 1997 |
| *Acropora palmata** | Elkhorn coral | Yes | T | Compagen | Polato *et al.* 2011 |
| *Aiptasia pallida* | Pale anemone | Yes | T | personal comm. | Lehnert *et al.* 2012 |
| *Anemonia viridis** | Snakelocks anemone | Yes | T | Compagen | Sabourault *et al.* 2009 |
| *Aurelia aurita* | Moon jellyfish | No | T | Compagen | Fuchs *et al.* 2014 |
| *Clytia hemisphaerica* | Hydrozoan | No | T | Compagen | Lapebie *et al.* 2014 |
| *Edwardsiella lineata* | Lined sea anemone | No | T | EdwardsiellaBase | Stefanik *et al.* 2014 |
| *Fungia scutaria* | Mushroom coral | Yes | T | Weis and Meyer lab | Kitchen *et al.* 2015 |
| *Hydra magnapapillata* | Hydra | Yes | G | Compagen | Chapman *et al.* 2010 |
| *Hydra vulgaris** | Hydra | Yes | T | Compagen | Pan *et al.* 2014 |
| *Hydractinia symbiolongicarpus* | Hermit crab hydroid | No | T | Dryad Digital Repository | Plachetzki *et al.* 2014 |

| | | | | | |
|---|---|---|---|---|---|
| *Madracis auretenra** | Yellow pencil coral | Yes | T | Meyer lab | http://people.oregonstate.edu/~meyere/data.html |
| *Montastraea cavernosa** | Great star coral | Yes | T | Weis and Meyer lab | Kitchen *et al.* 2015 |
| *Metridium senile* | Plumose anemone | No | G | Compagen | Beagley *et al.* 1998 |
| *Montastrea (Orbicella) faveolata** | Mountain star coral | Yes | T | Compagen | Schwarz *et al.* 2008 |
| *Nematostella vectensis* | Starlet sea anemone | No | G | DOE Joint Genome Institute | Putnam *et al.* 2007 |
| *Pocillopora damicornis** | Cauliflower coral | Yes | T | PocillaporaBase | Traylor-Knowles *et al.* 2011 |
| *Pseudodiploria strigosa* | Symmetrical brain coral | Yes | T | Meyer lab | http://people.oregonstate.edu/~meyere/data.html |
| *Platygyra carnosus** | Brain coral | Yes | T | PcarnBase | Sun *et al.* 2013 |
| *Platygyra daedalea* | Brain coral | Yes | T | Meyer lab | http://people.oregonstate.edu/~meyere/data.html |
| *Tubastraea coccinea ** | Orange-cup coral | Yes | T | Meyer lab | Personal comm. |
| *Tubastraea micrantha** | Black sun coral | Yes | T | Meyer lab | Personal comm. |
| *Polypodium hydriforme* | Parasitic hydroid | No | T | European Nucleotide Archive | Shpirer *et al.* 2014 |
| *Porites compressa** | Finger coral | Yes | T | Meyer lab | Personal comm. |
| *Porities astreoides** | Mustard hill coral | Yes | T | Matz lab | Kenkel *et al.* 2013 |
| *Porites evermanni** | Finger coral | Yes | T | Meyer lab | Personal comm. |
| *Porites australiensis** | Finger coral | Yes | T | OIST Marine Genomics Unit | Shinzato *et al.* 2014 |
| *Porites lobata** | Lobe coral | Yes | T | Meyer lab | personal comm. |

| | | | | | |
|---|---|---|---|---|---|
| *Seriatopora hystrix** | Thin birdsnest coral | Yes | T | Weis and Meyer lab | Kitchen *et al.* 2015 |
| *Stylophora pistillata** | Smooth cauliflower coral | Yes | T | Centre Scientifique de Monaco | Karako-Lampert *et al.* 2014 |
| ***Symbiodinium* Resources** | | | | | |
| **Species or Type** | **Symbiotic?** | **Resource** | **Source** | | **Publication** |
| *Symbiodinium minutum* (B1) | Yes | G | OIST Marine Genomics Unit | | Shoguchi *et al.* 2013 |
| *Symbiodinium CassKB8* (A1) | Yes | T | iPlant Datastore | | Bayer *et al.* 2012 |
| *Symbiodinium kawagutii CCMP2468* (F) | No | T | iPlant Datastore | | Zhang *et al.* 2013 |
| *Symbiodinium* (C1) | Yes | T | iPlant Datastore | | Keeling *et al.* 2014 |
| *Symbiodinium* (C3)* | Yes | T | Palumbi Lab Website | | Ladner *et al.* 2012 |
| *Symbiodinium* (D2)* | Yes | T | Palumbi Lab Website | | Ladner *et al.* 2013 |

**Table A2** Reference proteins used as queries for homology searches of each protein group.

| Facilitated Glucose Transporters | | | |
|---|---|---|---|
| **UniProt ID** | **Protein** | **Tree ID** | **Species** |
| P11166 | Solute carrier family 2, facilitated glucose transporter 1 | GLUT1 | *Homo sapiens* |
| P11168 | Solute carrier family 2, facilitated glucose transporter 2 | GLUT2 | *Homo sapiens* |
| P11169 | Solute carrier family 2, facilitated glucose transporter 3 | GLUT3 | *Homo sapiens* |
| P14672 | Solute carrier family 2, facilitated glucose transporter 4 | GLUT4 | *Homo sapiens* |
| P22732 | Solute carrier family 2, facilitated glucose transporter 5 | GLUT5 | *Homo sapiens* |
| Q9UGQ3 | Solute carrier family 2, facilitated glucose transporter 6 | GLUT6 | *Homo sapiens* |
| Q6PXP3 | Solute carrier family 2, facilitated glucose transporter 7 | GLUT7 | *Homo sapiens* |
| Q9NY64 | Solute carrier family 2, facilitated glucose transporter 8 | GLUT8 | *Homo sapiens* |
| Q9NRM0 | Solute carrier family 2, facilitated glucose transporter 9 | GLUT9 | *Homo sapiens* |
| O95528 | Solute carrier family 2, facilitated glucose transporter 10 | GLUT10 | *Homo sapiens* |
| Q9BYW1 | Solute carrier family 2, facilitated glucose transporter 11 | GLUT11 | *Homo sapiens* |
| Q8TD20 | Solute carrier family 2, facilitated glucose transporter 12 | GLUT12 | *Homo sapiens* |
| Q96QE2 | Proton myo-inositol cotransporter | HMIT | *Homo sapiens* |
| **Sodium/Glucose Transporters** | | | |
| **UniProt ID** | **Protein** | **Tree ID** | **Species** |
| P13866 | Sodium/glucose cotransporter 1 | SGLT1 | *Homo sapiens* |
| P31639 | Sodium/glucose cotransporter 2 | SGLT2 | *Homo sapiens* |
| C7EWH7 | Sodium/glucose cotransporter 3 | SGLT3 | *Homo sapiens* |
| Q2M3M2 | Sodium/glucose cotransporter 4 | SGLT4 | *Homo sapiens* |
| A0PJK1 | Sodium/glucose cotransporter 5 | SGLT5 | *Homo sapiens* |
| **Aquaglyceroporins** | | | |
| **UniProt ID** | **Protein** | **Tree ID** | **Species** |

| | | | |
|---|---|---|---|
| Q92482 | Aquaporin-3 | AQP3 | *Homo sapiens* |
| O14520 | Aquaporin-7 | AQP7 | *Homo sapiens* |
| O43315 | Aquaporin-9 | AQP9 | *Homo sapiens* |
| Q96PS8 | Aquaporin-10 | AQP10 | *Homo sapiens* |
| **Ammonium Transporters** | | | |
| **UniProt ID** | **Protein** | **Tree ID** | **Species** |
| P54144 | Ammonium transporter 1 member 1 | AMT1-1 | *Arabidopsis thaliana* |
| Q9ZPJ8 | Ammonium transporter 1 member 2 | AMT1-2 | *Arabidopsis thaliana* |
| Q9SQH9 | Ammonium transporter 1 member 3 | AMT1-3 | *Arabidopsis thaliana* |
| Q9SVT8 | Ammonium transporter 1 member 4 | AMT1-4 | *Arabidopsis thaliana* |
| Q9LK16 | Ammonium transporter 1 member 5 | AMT1-5 | *Arabidopsis thaliana* |
| **Nitrate Transporters** | | | |
| **UniProt ID** | **Protein** | **Tree ID** | **Species** |
| O82811 | High affinity nitrate transporter 2.1 | NRT2.1 | *Arabidopsis thaliana* |
| Q9LMZ9 | High affinity nitrate transporter 2.2 | NRT2.2 | *Arabidopsis thaliana* |
| Q9FJH7 | High affinity nitrate transporter 2.3 | NRT2.3 | *Arabidopsis thaliana* |
| Q9FJH8 | High affinity nitrate transporter 2.4 | NRT2.4 | *Arabidopsis thaliana* |
| Q9LPV5 | High affinity nitrate transporter 2.5 | NRT2.5 | *Arabidopsis thaliana* |
| Q9LXH0 | High affinity nitrate transporter 2.6 | NRT2.6 | *Arabidopsis thaliana* |

# Appendix B: Carbon and nitrogen enrichment values

**Table B1** Carbon enrichment of host tissue and symbiont cells in the heterotrophy experiment.

| Time point | Tissue type | Symbiont type | Replicate anemone | Ave. C Enrichment ($\delta^{13}C$) | $\delta^{13}C$ std. error |
|---|---|---|---|---|---|
| 1 | Host | B1 | 1 | 38.64 | 5.30 |
| 1 | Host | B1 | 2 | 197.68 | 40.7 |
| 1 | Host | B1 | 3 | 41.59 | 15.03 |
| 1 | Host | B1 | 4 | 13.27 | 2.90 |
| 1 | Host | B1 | 5 | 11.63 | 1.91 |
| 1 | Host | D1a | 1 | 20.32 | 3.10 |
| 1 | Host | D1a | 2 | 4.91 | 3.23 |
| 1 | Host | D1a | 3 | 13.75 | 5.73 |
| 1 | Host | D1a | 4 | 38.12 | 11.06 |
| 1 | Host | D1a | 5 | 1.102 | 0.91 |
| 2 | Host | B1 | 1 | 9.76 | 0.37 |
| 2 | Host | B1 | 2 | 0 | 0 |
| 2 | Host | B1 | 3 | 7.49 | 5.30 |
| 2 | Host | B1 | 4 | 0 | 0 |
| 2 | Host | B1 | 5 | 0 | 0 |
| 2 | Host | D1a | 1 | 0.91 | 0.91 |
| 2 | Host | D1a | 2 | 3.14 | 2.48 |
| 2 | Host | D1a | 3 | 8.11 | 6.06 |
| 2 | Host | D1a | 4 | 5.19 | 5.19 |
| 2 | Host | D1a | 5 | 0 | 0 |
| 1 | Symbiont | B1 | 1 | 15.46 | 1.93 |
| 1 | Symbiont | B1 | 2 | 0 | 0 |
| 1 | Symbiont | B1 | 3 | 18.88 | 2.39 |
| 1 | Symbiont | B1 | 4 | 12.73 | 2.97 |
| 1 | Symbiont | B1 | 5 | 11.00 | 3.56 |
| 1 | Symbiont | D1a | 1 | 3.34 | 1.52 |
| 1 | Symbiont | D1a | 2 | 0 | 0 |
| 1 | Symbiont | D1a | 3 | 2.565 | 1.44 |
| 1 | Symbiont | D1a | 4 | 5.69 | 3.27 |
| 1 | Symbiont | D1a | 5 | 6.59 | 2.18 |
| 2 | Symbiont | B1 | 1 | 11.68 | 1.74 |
| 2 | Symbiont | B1 | 2 | 5.41 | 1.28 |
| 2 | Symbiont | B1 | 3 | 9.72 | 3.15 |
| 2 | Symbiont | B1 | 4 | 0.63 | 0.35 |
| 2 | Symbiont | B1 | 5 | 0.98 | 0.51 |
| 2 | Symbiont | D1a | 1 | 2.44 | 1.04 |
| 2 | Symbiont | D1a | 2 | 6.03 | 1.58 |
| 2 | Symbiont | D1a | 3 | 7.35 | 1.76 |
| 2 | Symbiont | D1a | 4 | 7.18 | 1.48 |
| 2 | Symbiont | D1a | 5 | 5.11 | 0.82 |

**Table B2** Nitrogen enrichment of host tissue and symbiont cells in the autotrophy experiment.

| Time point | Tissue type | Cell type | Replicate anemone | Ave. N Enrichment ($\delta^{15}N$) | $\delta^{15}N$ std. error |
|---|---|---|---|---|---|
| 1 | Host | B1 | 1 | 8.73 | 1.54 |
| 1 | Host | B1 | 2 | 0.73 | 0.73 |
| 1 | Host | B1 | 3 | 0 | 0 |
| 1 | Host | B1 | 4 | 7.48 | 2.25 |
| 1 | Host | D1a | 1 | 0 | 0 |
| 1 | Host | D1a | 2 | 0 | 0 |
| 1 | Host | D1a | 3 | 0 | 0 |
| 1 | Host | D1a | 4 | 0 | 0 |
| 2 | Host | B1 | 1 | 3.27 | 1.42 |
| 2 | Host | B1 | 2 | 5.44 | 0 |
| 2 | Host | B1 | 3 | 10.42 | 1.85 |
| 2 | Host | B1 | 4 | 10.51 | 1.86 |
| 2 | Host | B1 | 5 | 10.20 | 1.66 |
| 2 | Host | D1a | 1 | 2.21 | 0.60 |
| 2 | Host | D1a | 2 | 6.23 | 0.49 |
| 2 | Host | D1a | 3 | 6.12 | 3.12 |
| 2 | Host | D1a | 4 | 7.55 | 4.02 |
| 2 | Host | D1a | 5 | 9.17 | 2.31 |
| 1 | Symbiont | B1 | 1 | 202.77 | 12.40 |
| 1 | Symbiont | B1 | 2 | 130.29 | 51.14 |
| 1 | Symbiont | B1 | 3 | 13.01 | 13.01 |
| 1 | Symbiont | B1 | 4 | 115.01 | 20.35 |
| 1 | Symbiont | D1a | 1 | 0 | 0 |
| 1 | Symbiont | D1a | 2 | 0 | 0 |
| 1 | Symbiont | D1a | 3 | 3.86 | 1.97 |
| 1 | Symbiont | D1a | 4 | 12.22 | 10.33 |
| 2 | Symbiont | B1 | 1 | 16.67 | 1.70 |
| 2 | Symbiont | B1 | 2 | 55.03 | 3.74 |
| 2 | Symbiont | B1 | 3 | 30.81 | 2.74 |
| 2 | Symbiont | B1 | 4 | 61.55 | 3.98 |
| 2 | Symbiont | B1 | 5 | 71.59 | 5.37 |
| 2 | Symbiont | D1a | 1 | 14.29 | 2.08 |
| 2 | Symbiont | D1a | 2 | 24.37 | 1.79 |
| 2 | Symbiont | D1a | 3 | 36.34 | 3.02 |
| 2 | Symbiont | D1a | 4 | 17.58 | 3.39 |
| 2 | Symbiont | D1a | 5 | 42.86 | 7.03 |

## Appendix C: Additional Symbiosome Work

Optimization of the symbiosome isolation protocol from Kazandjian *et al.* (2008) and Starzak (2012) was attempted over a two-year period. I was able to identify membranes predicted to be symbiosomes, however they could not be isolated in concentrations high enough for accurate analysis. Isolation was first attempted using sucrose density gradients, as per the original protocol (Kazandjian *et al.* 2008), using 20 anemones. The predicted symbiosomes were stained with FM-143 and observed under the FITC filter of a fluorescence microscope (Figure C1). However, the top "golden layer" from where the resulting symbiosomes were harvested, was consistently found to contain many contaminants as well (Figure C2). I also attempted the method using Percoll® gradients and Ficoll® gradients, but again found that the gradients did not successfully isolate the symbiosome membranes from the rest of the host homogenate and intact *Symbiodinium* cells. I proceeded to test the FM-143 stain on *Symbiodinium* cultures, finding that it was able to stain the dinoflagellate cell membrane, rather than being specific to the symbiosome. I therefore concluded that FM-143 dye was not an accurate marker for the symbiosome, as was previously published. An appropriate marker for the symbiosome membrane is needed before isolation of the membranes is possible, which can be successfully accomplished using immunolabelling using an antibody for a known symbiosome protein (Dani *et al.* 2014; Barott *et al.* 2015). While other research groups have begun using immunocytochemistry techniques for this purpose, I carried out bioinformatic analysis of nutrient transporters in various cnidarian-dinoflagellate symbiosis to provide information on more protein candidates for the symbiosome.

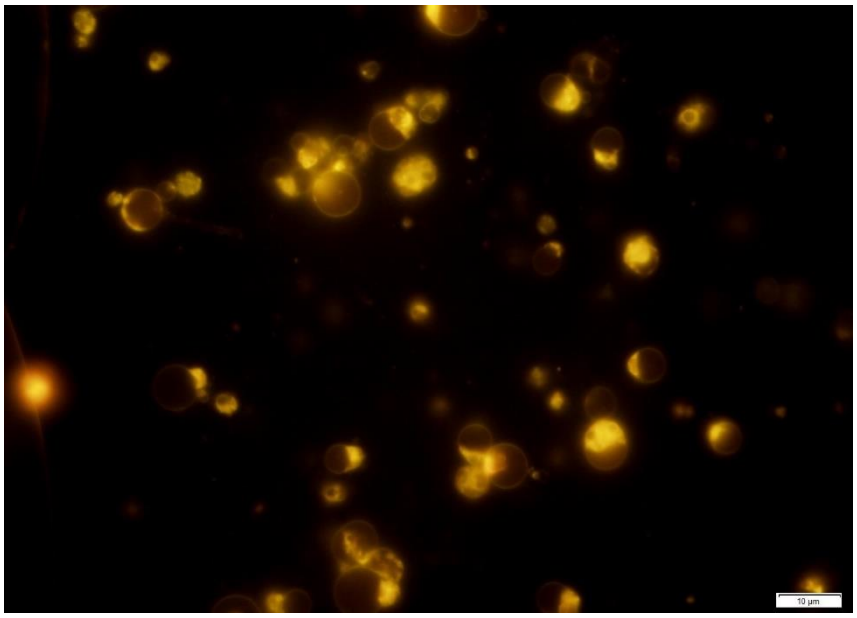


**Figure C1** Predicted symbiosome membranes, stained with FM-143, viewed under 40x magnification and the FITC filter. Scale bar is 10 µm.

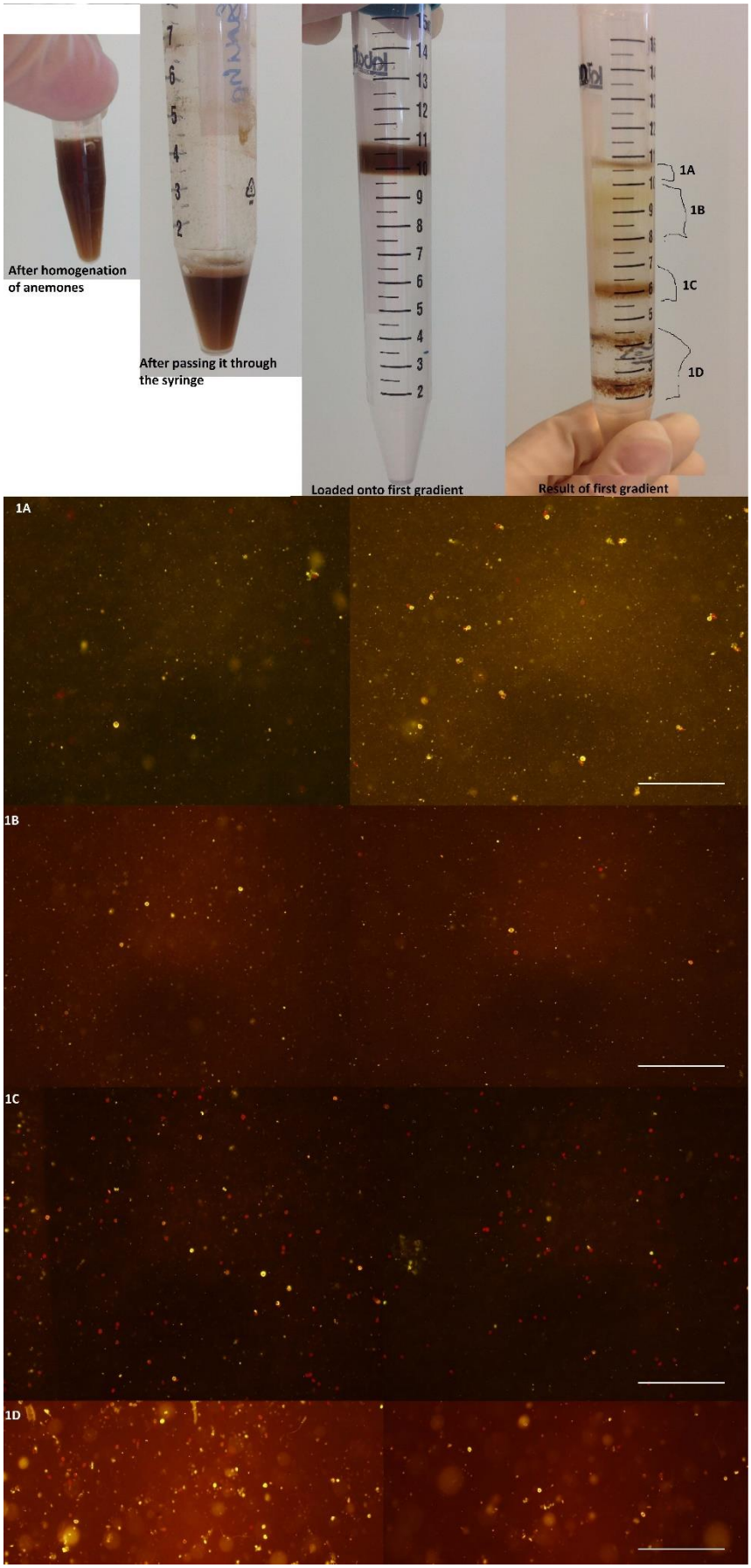


**Figure C2** Density gradient symbiosome isolation steps. Anemones were homogenised, then passed through a syringe and needle to strip membranes from intact algal cells. The homogenate was then loaded onto a density gradient (sucrose, Percoll®, or Ficoll®) and centrifuged at 4000 x g for 2 hours. Images 1A-1D correspond to the resolved layers, viewed under 20x magnification, scale bars are 100µm. The symbiosome membranes are meant to be resolved into the top "golden layer" in the loading zone (1A). However, other cellular debris was also found in this layer. Symbiosomes were also potentially visible in layers 1B-1D. Therefore, I concluded that this method was not successful in isolating symbiosomes from the rest of the anemone homogenate.

**Publications**

Matthews JL, Sproles AE, Oakley CA, Grossman AR, Weis VM, Davy SK (2016) Menthol-induced bleaching rapidly and effectively provides experimental aposymbiotic sea anemones (*Aiptasia* sp.) for symbiosis investigations. *Journal of Experimental Biology*, **219**, 306–310.

The following manuscript outlines the optimisation of a method for producing aposymbiotic individuals of the model cnidarian, *Aiptasia*. This work was carried out by myself and a fellow lab member, and was integral to chapters 2 and 3, which used this method to produce experimental animals for the infection studies. Since publication, this method has been utilized by other research groups investigating infection dynamics of the cnidarian-dinoflagellate symbiosis using *Aiptasia* as a model system, and will continue to allow these types of experiments to be more easily conducted.

© 2016. Published by The Company of Biologists Ltd | Journal of Experimental Biology (2016) 219, 306-310 doi:10.1242/jeb.128934

METHODS & TECHNIQUES

# Menthol-induced bleaching rapidly and effectively provides experimental aposymbiotic sea anemones (*Aiptasia* sp.) for symbiosis investigations

**Jennifer L. Matthews[1], Ashley E. Sproles[1], Clinton A. Oakley[1], Arthur R. Grossman[2], Virginia M. Weis[3] and Simon K. Davy[1,*]**

## ABSTRACT

Experimental manipulation of the symbiosis between cnidarians and photosynthetic dinoflagellates (*Symbiodinium* spp.) is crucial to advancing the understanding of the cellular mechanisms involved in host–symbiont interactions, and overall coral reef ecology. The anemone *Aiptasia* sp. is a model for cnidarian–dinoflagellate symbiosis, and notably it can be rendered aposymbiotic (i.e. dinoflagellate-free) and re-infected with a range of *Symbiodinium* types. Various methods exist for generating aposymbiotic hosts; however, they can be hugely time consuming and not wholly effective. Here, we optimise a method using menthol for production of aposymbiotic *Aiptasia*. The menthol treatment produced aposymbiotic hosts within just 4 weeks (97–100% symbiont loss), and the condition was maintained long after treatment when anemones were held under a standard light:dark cycle. The ability of *Aiptasia* to form a stable symbiosis appeared to be unaffected by menthol exposure, as demonstrated by successful re-establishment of the symbiosis when anemones were experimentally re-infected. Furthermore, there was no significant impact on photosynthetic or respiratory performance of re-infected anemones.

**KEY WORDS: Cnidarian–dinoflagellate symbiosis, *Symbiodinium*, Coral reefs**

## INTRODUCTION

The symbiosis between corals and dinoflagellate algae of the genus *Symbiodinium* promotes the success of coral reefs in nutrient-poor tropical seas. However, there are still large gaps in our knowledge about how this symbiosis is established and maintained (Davy et al., 2012; Weis and Allemand, 2009; Weis et al., 2008). Moreover, we do not fully understand how and why this symbiosis breaks down under stress (e.g. bleaching) (Weis, 2008). These knowledge gaps hinder our capacity to understand the function of coral reefs, and to predict how coral reefs might respond to our changing environment.

To elucidate the cellular basis of the coral–dinoflagellate relationship, the symbiotic sea anemone *Aiptasia* sp. has been widely adopted as a model system because of its robust nature and the ability to produce large populations easily in the laboratory (Weis et al., 2008). Furthermore, *Aiptasia* sp. can be cleared of symbionts, maintained in an aposymbiotic state for extended periods, and successfully re-infected with a variety of *Symbiodinium* types (Belda-Baillie et al., 2002; Schoenberg and Trench, 1980; Starzak et al., 2014). The ease of experimental manipulation, combined with the rapidly increasing resolution of genomic, proteomic and metabolic databases for *Aiptasia* sp., makes this symbiotic anthozoan an ideal candidate for biochemical and genetic experiments that will further our understanding of the cellular processes underlying the cnidarian–dinoflagellate symbiosis (Lehnert et al., 2012; Peng et al., 2010; Sunagawa et al., 2009; Weis et al., 2008).

Currently, the most commonly used method to render anemones (including *Aiptasia* sp.) aposymbiotic combines temperature stress (heat or cold shock) followed by dark treatment and/or chemical inhibition of photosynthesis with 3-(3,4-dichlorophenyl)-1,1-dimethylurea (DCMU) (e.g. Belda-Baillie et al., 2002; Lehnert et al., 2014; Xiang et al., 2013). This is a slow, laborious process that often requires months of preparation (Starzak et al., 2014; Xiang et al., 2013), and may not result in the full eradication of *in hospite* endosymbionts (Belda-Baillie et al., 2002; Schoenberg and Trench, 1980; Wang and Douglas, 1998).

Recently, Wang et al. (2012) described a method of menthol-induced bleaching in the corals *Isopora palifera* and *Stylophora pistillata*. Menthol is known to cause local anaesthetic effects in neuronal and skeletal muscles via blocking voltage-operated sodium channels (Haeseler et al., 2002). This cellular response has led to its use as a marine anaesthetic (Alexander, 1964; Lauretta et al., 2014). Menthol is known to act on a variety of different membrane receptors, including transient receptor potential (TRP) M8, which results in an increase in intracellular $Ca^{2+}$ concentrations and causes a cold sensation in vertebrates (Hans et al., 2012; McKemy et al., 2002; Okazawa et al., 2000; Peier et al., 2002). As proposed by Wang et al. (2012), the mechanism of menthol-induced bleaching might be attributable to $Ca^{2+}$-stimulated exocytosis (Pang and Südhof, 2010). Preliminary experiments conducted by Wang et al. (2012) also suggest that menthol inhibition of *Symbiodinium* photosystem II activity may play a role in the expulsion of the algal cells or the digestion of the *Symbiodinium* cells by the host. Although the exact mechanism by which menthol induces symbiont expulsion is not yet clear, the findings of Wang and co-authors provide a platform for developing the use of menthol to generate aposymbiotic *Aiptasia* sp.

We therefore tested the applicability of this approach to *Aiptasia* sp., in terms of its effectiveness and impact on the capacity for symbiosis re-establishment. In particular, we determined whether menthol can rapidly and effectively produce aposymbiotic anemones, and whether these anemones can be experimentally re-infected with symbiotic dinoflagellates at cell densities similar to

[1]School of Biological Sciences, Victoria University of Wellington, Wellington 6140, New Zealand. [2]Department of Plant Biology, The Carnegie Institution, Stanford, CA 94305, USA. [3]Oregon State University, Department of Integrative Biology, 3029 Cordley Hall, Corvallis, OR 97331, USA.

*Author for correspondence (Simon.Davy@vuw.ac.nz)

**Received 25 July 2015; Accepted 5 November 2015**



Journal of Experimental Biology

Journal of Experimental Biology (2016) 219, 306-310 doi:10.1242/jeb.128934

those of untreated and healthy symbiotic anemones. Ultimately, we describe a method to assist the many researchers around the world who use the *Aiptasia* model system to further our understanding of the coral–dinoflagellate symbiosis.

## MATERIALS AND METHODS

### Experimental organisms

Symbiotic individuals of *Aiptasia* sp. ($n$=300) were harvested from a long-term laboratory stock maintained in 1 µm filtered seawater (FSW) at 25°C, with light provided by AQUA-GLO T8 fluorescent bulbs at ∼95 µmol photons $m^{-2}$ $s^{-1}$ (12 h:12 h light:dark cycle). Anemones were maintained in 1 µm FSW aerated with a Hailea® aquarium air pump at 2 l $min^{-1}$ and at 25°C using the WEIPRO® Temperature Controller MX-1019. These lighting and aquarium conditions were maintained throughout the 19-week experiment. The anemones were evenly divided among the treatments (menthol, cold shock and untreated) and allowed to settle for 72 h before beginning a 4-week treatment period.

The *Symbiodinium* culture (ID: FLAp2) was grown at 25°C and an irradiance of 100 µmol photons $m^{-2}$ $s^{-1}$ on a 12 h:12 h light:dark cycle. *Symbiodinium* cells were sub-cultured from a laboratory stock and grown in silica-free f/2 medium (AusAqua Pty, SA, Australia) for 6 weeks before use in the infection study. To genotype the *Symbiodinium* cells, DNA was extracted as described by Hill et al. (2014) from an algal pellet derived from a 1 ml aliquot of the *Symbiodinium* suspension. Samples were immediately used for PCR, using the thermal cycling regime and reaction mixture of Hill et al. (2014), and the outer primers ITSintfor2 and ITS2Rev2. PCR products were cleaned with ExoSAP-IT (USB Corporation, OH, USA) and sequenced by the Macrogen Sequencing Service (Macrogen, Seoul, South Korea). Sequences were aligned with Geneious v. 7.0 (Biomatters, Auckland, NZ) and a BLAST search was carried out against *Symbiodinium* ITS2 sequences in GenBank. Using this approach, the *Symbiodinium* genotype was confirmed as B1.

### Menthol versus cold-shock treatment

Menthol (20% w/v in ethanol; Sigma-Aldrich, Auckland, NZ) was added to 1 µm FSW at a final concentration of 0.19 mmol $l^{-1}$. This concentration resulted in successful bleaching without causing mortality. A higher concentration of 0.38 mmol $l^{-1}$ as suggested by Wang et al. (2012) was trialled prior to this experiment, but caused mortality of over 50% of the anemones (J.L.M., unpublished data). The anemones were incubated in the menthol/FSW solution for 8 h, after which the menthol/FSW was removed and the anemones were incubated in 1 µm FSW for 16 h. DCMU (100 mmol $l^{-1}$ dissolved in EtOH, Sigma-Aldrich) was added to a final concentration of 5 µmol $l^{-1}$ to prevent nuisance algal blooms and to limit the re-establishment of any residual symbiont cells by inhibiting photosynthesis. This 24-h cycle was repeated for four consecutive days. The 8-h menthol/FSW incubation occurred during the 12-h light period. The 4-day treatment was repeated after a 3-day break, during which anemones were maintained under the lighting and temperature conditions stated above, with biweekly feeding with *Artemia* sp. nauplii.

For cold shock, the water was replaced with 4°C 1 µm FSW, and placed in a refrigerator at 4°C for 4 h. Afterwards, the water was replaced with 25°C 1 µm FSW containing a final concentration of 50 µmol $l^{-1}$ DCMU (100 mmol $l^{-1}$ dissolved in EtOH, Sigma-Aldrich) and held under the lighting and aquarium conditions

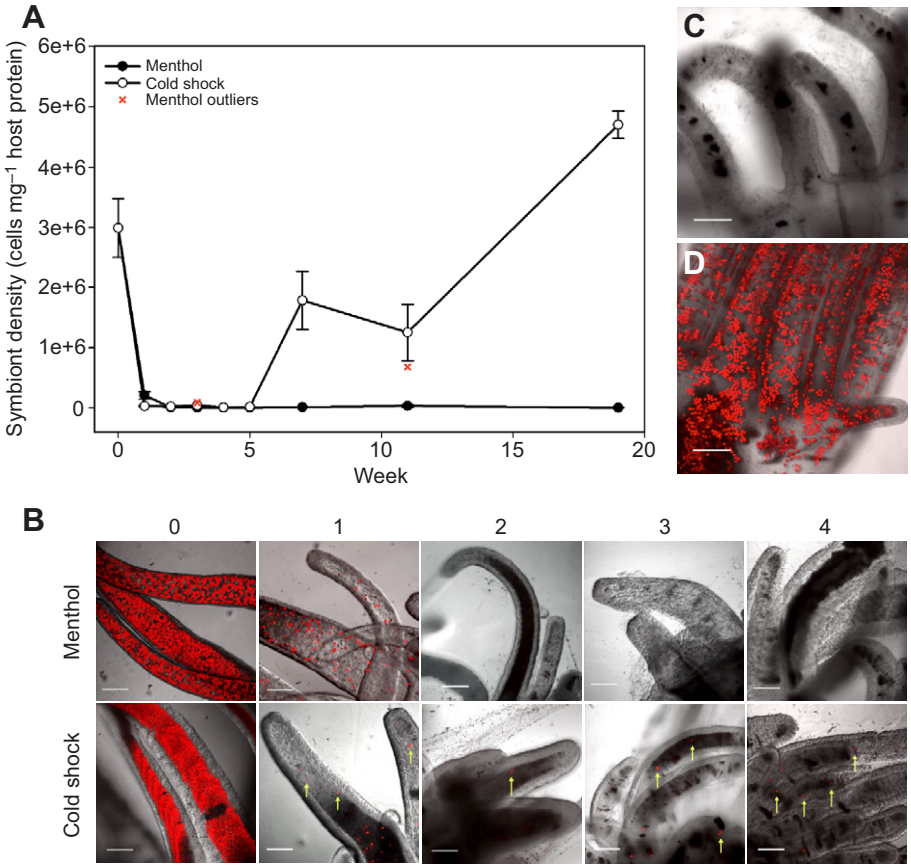


**Fig. 1. Effects of menthol and cold shock on algal cell density in *Aiptasia* sp.** (A) Density of *Symbiodinium* cells in menthol-treated (closed circles) and cold-shocked (open circles) anemones over a 19-week period. The anemones were treated for the first 4 weeks, then left to recover in regular filtered seawater for the remaining 15 weeks. Outliers (defined as exceeding 1.5× interquartile range) were detected in the menthol-treated anemones at weeks 4 and 11, and are indicated by a red cross. Values are mean±s.e.m.; $n$=5. (B) Confocal microscopy images of anemones during menthol treatment and cold shock (weeks 1–4). Yellow arrows indicate *Symbiodinium* cells in host tissues. (C,D) Confocal fluorescence images of menthol-treated and cold-shocked anemones, respectively, 15 weeks post-treatment (i.e. week 19). Scale bars are 100 µm.

Journal of Experimental Biology (2016) 219, 306-310 doi:10.1242/jeb.128934

described above. The anemones were incubated under these conditions for 3 days, and the treatment was then repeated. The anemones were unfed for the duration of the cold shock, as per the protocol described by Steen and Muscatine (1987). Anemones were cold shocked a total of eight times (twice per week) during the treatment period.

After the 4-week treatment period, all anemones were maintained in 1 µm FSW at 25°C under the irradiance regime described above, with biweekly feeding, for an additional 15 weeks. Their symbiotic status was assessed via confocal fluorescence microscopy and cell density estimates (described below) at weeks 1–5, 7, 9, 11 and 19.

The untreated group of anemones was kept under the same thermal and light regimes as the menthol-treated and cold-shocked anemones, with biweekly feeding throughout the entire 19-week experiment. They were assessed for symbiont density at the same time points as the experimental anemones, to obtain an average symbiont density of untreated, healthy anemones.

### Re-infection of aposymbiotic anemones

The capacity to re-infect menthol-treated anemones with algal symbionts was tested; this was not possible with cold-shocked anemones because they were not fully aposymbiotic. Anemones were infected with cultured homologous *Symbiodinium* type B1, i.e. symbionts originally isolated from *Aiptasia* sp. A drop of concentrated *Symbiodinium* suspension ($3\times10^6$ cells $ml^{-1}$) was pipetted onto the oral disc of each anemone, followed by a drop of *Artemia* sp. nauplii to invoke a feeding response and encourage *Symbiodinium* uptake (Davy et al., 1997). This process was repeated 4 h later, and the water was replaced with 1 µm FSW 8 h after the second infection.

### Confocal microscopy

Whole anemones from each treatment were examined at the same time points as cell density assessments by confocal microscopy (Olympus Provis AX70, at 100× magnification) to detect the chlorophyll autofluorescence of any dinoflagellates. Anemones were selected at random from each treatment, and placed in a 'relaxation solution' [50% FSW, 50% 0.37 mol $l^{-1}$ magnesium chloride ($MgCl_2$)] for 15 min before being moved to a FluoroDish™ glass-bottom confocal dish (World Precision Instruments, FL, USA). The autofluorescence emission of the *Symbiodinium* cells was excited using a 559 nm laser and captured at 647±10 nm. This was performed to check the rates of bleaching and re-infection, as well as to detect any background *Symbiodinium* populations in the post-treatment anemones.

### Symbiont density and protein content

*Symbiodinium* populations were quantified with a haemocytometer and light microscope (100× magnification; $n$=8 replicate counts per sample) using whole-anemone homogenate ($n$=5). Cell density was normalised to soluble protein content, measured via the Bradford assay (Bradford, 1976). Cell density was measured at weeks 1–5, 7, 9, 11 and 19.

### $O_2$ flux

Fifteen weeks after reinfection, maximum photosynthetic and dark respiratory $O_2$ fluxes were measured to compare re-infected menthol-treated anemones against untreated anemones ($n$=4). A FIBOX 3 fibre optic oxygen transmitter and oxygen probe (PreSens, Germany) were used as described by Starzak et al. (2014). The respiration rate (ml $O_2$ $h^{-1}$) was measured for 30 min in the dark, after which the rate of net photosynthesis was measured for 30 min at an irradiance of ~100 µmol photons $m^{-2}$ $s^{-1}$. Net photosynthesis and respiration were corrected for background levels using a FSW-only control, and gross photosynthesis was calculated by the addition of net photosynthesis to dark respiration (Muscatine et al., 1981). The average ratio of gross photosynthesis to respiration (P:R) for 24 h was calculated for each anemone, by assuming a 12 h:12 h light:dark cycle and that respiration was constant in the light and dark, and the average ratio for each treatment was calculated.

### Statistical tests

The non-parametric Mann–Whitney $U$-test was used to test for differences between treatments with respect to symbiont density (SPSS statistical software, v. 20, IBM Corporation). Separate analyses were run for the bleaching and post-bleaching periods.

A one-way ANOVA was performed on the photosynthetic rate, respiration rate and log-transformed P:R values to determine whether significant differences were present between the re-infected menthol-treated and untreated symbiotic anemones at the end of the 19-week experimental period.

## RESULTS AND DISCUSSION

Menthol treatment induced 97–100% symbiont loss within 14–28 days, with 60% of anemones losing all symbionts. In comparison, cold shock never induced 100% loss within the same

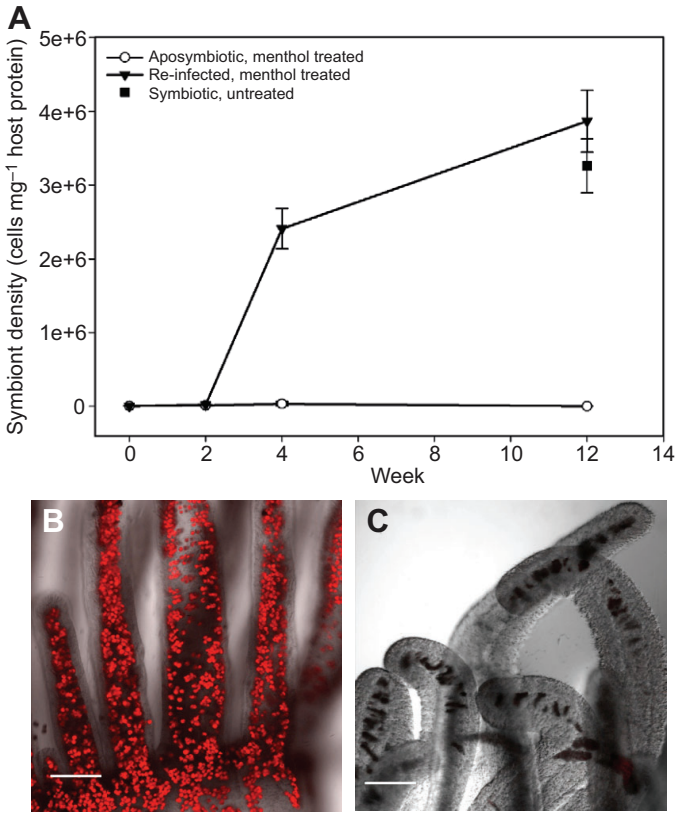


**Fig. 2. Repopulation of menthol-treated *Aiptasia* sp. with algal symbionts.** (A) Symbiont cell density over a 12-week period after anemones were experimentally re-infected with the homologous *Symbiodinium* type B1 (closed triangles). Also shown are symbiont densities in symbiotic, untreated anemones (closed square) and menthol-treated anemones that were not experimentally re-infected (open circles). Values are means±s.e.m.; $n$=5. (B,C) Confocal images showing, respectively, the re-established symbiont population 12 weeks after reinfection versus tissues in a non-infected aposymbiotic anemone. Scale bars are 100 µm.



Journal of Experimental Biology

Journal of Experimental Biology (2016) 219, 306-310 doi:10.1242/jeb.128934

time frame (Fig. 1A,B), and any residual symbionts in the menthol-treated anemones did not re-establish a full symbiosis once returned to normal seawater conditions over the course of our experiment (Fig. 1A,C).

Although statistically, the patterns of symbiont loss during weeks 1–4 were not different between the menthol and cold-shock treatments (Mann–Whitney $U$=113, d.f.=4, $P$=0.423, $n$=5; Fig. 1A), only the menthol-treated anemones successfully maintained aposymbiotic status in the longer term. In both treatments, symbiont density remained near zero during the first week of recovery (weeks 4–5; Fig. 1A); however, subsequently there was a significant difference between the cell densities of menthol- and cold-shock-treated anemones (Mann–Whitney $U$=35, d.f.=4, $P$<0.0005; $n$=5), with the menthol-treated anemones remaining mostly symbiont-free (0–0.05% of pre-bleaching density) and the cold-shocked anemones becoming fully re-populated (weeks 5–9; Fig. 1A). Confocal microscopy confirmed these measurements (Fig. 1C). Menthol treatment therefore has considerable potential for the rapid and effective generation of aposymbiotic *Aiptasia* sp.

One key use for aposymbiotic *Aiptasia* sp. is for experimental work that involves re-infection with symbiotic algae of different types and from different host species. It was therefore important to test the infectivity of the menthol-treated anemones, and establish whether there were any significant long-term impacts of menthol treatment versus no treatment on physiological performance (photosynthesis and respiration) of the re-infected anemones. When infected with *Symbiodinium* cells (ITS2 type B1), symbiont density increased slowly during the initial 2 weeks, followed by a rapid increase during weeks 2–12 (Fig. 2A). Confocal microscopy confirmed that menthol-treated anemones were fully repopulated after 12 weeks (Fig. 2B). The infection pattern and maximum cell density were similar to those of other re-infection studies using heat- and cold-shock bleached *Aiptasia* and type B1 *Symbiodinium*, where a steep increase in cell density was observed in the first 4 weeks, followed by stabilisation (Belda-Baillie et al., 2002; Schoenberg and Trench, 1980; Starzak et al., 2014). Additionally, the photosynthetic rate ($P$=0.432; $n$=4), respiration rate ($P$=0.347; $n$=4) and ratio of photosynthesis to respiration ($P$=0.368; $n$=4) in these anemones were similar to those of untreated symbiotic anemones. This indicates that their capacity to re-form a functional symbiosis was not compromised, further highlighting the value of this method.

As expected, given its anaesthetic properties (Alexander, 1964; Lauretta et al., 2014), menthol induced tentacle relaxation and unresponsiveness in anemones for the duration of the treatment. Once the seawater was replaced with regular FSW, the anemones were able to regain full movement and feeding capabilities within ~15 min. This is in stark contrast to the residual effects of cold shock on anemones, where long-lasting tentacle retraction and occasional mortality were observed.

In summary, we provide a rapid and effective method for the generation of aposymbiotic *Aiptasia* sp. that will facilitate studies of symbiosis establishment and maintenance, host–symbiont recognition, and symbiosis function with this model system. In particular, menthol treatment has the potential to rapidly create large stocks of aposymbiotic anemones without compromising their infectivity. Ultimately, this method will help to accelerate the rate of discovery as we try to better understand the function of coral reefs, and their response and adaptive capacity in the face of climate change.

**Acknowledgements**

We are grateful to Malindi Gammon and Josh Brian for laboratory assistance.

**Competing interests**

The authors declare no competing or financial interests.

**Author contributions**

J.L.M., A.E.S., C.A.O., A.R.G., V.M.W. and S.K.D. conceived and designed the experiments. J.L.M. and A.E.S. carried out the experiments and subsequent data analysis. J.L.M., A.E.S., C.A.O., A.R.G., V.M.W. and S.K.D. wrote the manuscript.

**Funding**

This work was supported by a grant from the Royal Society of New Zealand Marsden Fund (grant no. 1202 awarded to S.K.D., A.R.G. and V.M.W.).

**References**

**Alexander, R. M.** (1964). Visco-elastic properties of the mesogloea of jellyfish. *J. Exp. Biol.* **41**, 363-369.

**Belda-Baillie, C. A., Baillie, B. K. and Maruyama, T.** (2002). Specificity of a model cnidarian–dinoflagellate symbiosis. *Biol. Bull.* **202**, 74-85.

**Bradford, M. M.** (1976). A rapid and sensitive method for the quantitation of microgram quantities of protein utilizing the principle of protein-dye binding. *Anal. biochem.* **72**, 248-254.

**Davy, S., Turner, J. and Lucas, I.** (1997). The nature of temperate anthozoandinoflagellate symbioses. *In Proc. 7th Int. Coral Reef Symp.*, **vol. 2**, pp. 1307-1312.

**Davy, S., Turner, J. and Lucas, I.** (1997). The nature of temperate anthozoandinoflagellate symbioses. In *Proc. 7th Int. Coral Reef Symp.*, **vol. 2**, pp. 1307-1312.

**Davy, S. K., Allemand, D. and Weis, V. M.** (2012). Cell biology of cnidarian-dinoflagellate symbiosis. *Microbiol. Mol. Biol. Rev.* **76**, 229-261.

**Haeseler, G., Maue, D., Grosskreutz, J., Bufler, J., Nentwig, B., Piepenbrock, S., Dengler, R. and Leuwer, M.** (2002). Voltage-dependent block of neuronal and skeletal muscle sodium channels by thymol and menthol. *Eur. J. Anaesthesiol.* **19**, 571-579.

**Hans, M., Wilhelm, M. and Swandulla, D.** (2012). Menthol suppresses nicotinic acetylcholine receptor functioning in sensory neurons via allosteric modulation. *Chem. Senses* **37**, 463-469.

**Hill, R., Fernance, C., Wilkinson, S. P., Davy, S. K. and Scott, A.** (2014). Symbiont shuffling during thermal bleaching and recovery in the sea anemone *Entacmaea quadricolor*. *Mar. Biol.* **161**, 2931-2937.

**Lauretta, D., Häussermann, V., Brugler, M. R. and Rodríguez, E.** (2014). *Isoparactis fionae* sp. nov. (Cnidaria: Anthozoa: Actiniaria) from Southern Patagonia with a discussion of the family Isanthidae. *Organ. Divers. Evol.* **14**, 31-42.

**Lehnert, E. M., Burriesci, M. S. and Pringle, J. R.** (2012). Developing the anemone *Aiptasia* as a tractable model for cnidarian–dinoflagellate symbiosis: the transcriptome of aposymbiotic *A. pallida*. *BMC Genomics* **13**, 271.

**Lehnert, E. M., Mouchka, M. E., Burriesci, M. S., Gallo, N. D., Schwarz, J. A. and Pringle, J. R.** (2014). Extensive differences in gene expression between symbiotic and aposymbiotic cnidarians. *G3* **4**, 277-295.

**McKemy, D. D., Neuhausser, W. M. and Julius, D.** (2002). Identification of a cold receptor reveals a general role for TRP channels in thermosensation. *Nature* **416**, 52-58.

**Muscatine, L., McCloskey, L. and Marian, R.** (1981). Estimating the daily contribution of carbon from zooxanthellae to coral animal respiration. *Oceanography* **26**, 601-611.

**Okazawa, M., Terauchi, T., Shiraki, T., Matsumura, K. and Kobayashi, S.** (2000). l-Menthol-induced [$Ca^{2+}$]i increase and impulses in cultured sensory neurons. *Neuroreport* **11**, 2151-2155.

**Pang, Z. P. and Südhof, T. C.** (2010). Cell biology of $Ca^{2+}$-triggered exocytosis. *Curr. Opin. Cell Biol.* **22**, 496-505.

**Peier, A. M., Moqrich, A., Hergarden, A. C., Reeve, A. J., Andersson, D. A., Story, G. M., Earley, T. J., Dragoni, I., McIntyre, P. and Bevan, S.** (2002). A TRP channel that senses cold stimuli and menthol. *Cell* **108**, 705-715.

**Peng, S. E., Wang, Y. B., Wang, L. H., Chen, W. N. U., Lu, C. Y., Fang, L. S. and Chen, C. S.** (2010). Proteomic analysis of symbiosome membranes in Cnidaria–dinoflagellate endosymbiosis. *Proteomics* **10**, 1002-1016.

**Schoenberg, D. A. and Trench, R. K.** (1980). Genetic variation in *Symbiodinium* (= Gymnodinium) microadriaticum Freudenthal, and specificity in its symbiosis with marine invertebrates. III. Specificity and infectivity of *Symbiodinium microadriaticum*. *Proc. R. Soc. B Biol. Sci.* **207**, 445-460.

**Starzak, D. E., Quinnell, R. G., Nitschke, M. R. and Davy, S. K.** (2014). The influence of symbiont type on photosynthetic carbon flux in a model cnidarian–dinoflagellate symbiosis. *Mar. Biol.* **161**, 711-724.

**Steen, R. G. and Muscatine, L.** (1987). Low temperature evokes rapid exocytosis of symbiotic algae by a sea anemone. *Biol. Bull.* **172**, 246-263.

**Sunagawa, S., Wilson, E. C., Thaler, M., Smith, M. L., Caruso, C., Pringle, J. R., Weis, V. M., Medina, M. and Schwarz, J. A.** (2009). Generation and analysis of transcriptomic resources for a model system on the rise: the sea

Journal of Experimental Biology (2016) 219, 306-310 doi:10.1242/jeb.128934

anemone *Aiptasia pallida* and its dinoflagellate endosymbiont. *BMC Genomics* **10**, 258.

**Wang, J. and Douglas, A.** (1998). Nitrogen recycling or nitrogen conservation in an alga-invertebrate symbiosis? *J. Exp. Biol.* **201**, 2445-2453.

**Wang, J. T., Chen, Y. Y., Tew, K. S., Meng, P. J. and Chen, C. A.** (2012). Physiological and biochemical performances of menthol-induced aposymbiotic corals. *PLoS One* **7**, e46406.

**Weis, V. M.** (2008). Cellular mechanisms of Cnidarian bleaching: stress causes the collapse of symbiosis. *J. Exp. Biol.* **211**, 3059-3066.

**Weis, V. M. and Allemand, D.** (2009). Physiology. What determines coral health? *Science* **324**, 1153-1155.

**Weis, V. M., Davy, S. K., Hoegh-Guldberg, O., Rodriguez-Lanetty, M. and Pringle, J. R.** (2008). Cell biology in model systems as the key to understanding corals. *Trends Ecol. Evol.* **23**, 369-376.

**Xiang, T., Hambleton, E. A., DeNofrio, J. C., Pringle, J. R., Grossman, A. R. and Lin, S.** (2013). Isolation of clonal axenic strains of the symbiotic dinoflagellate *Symbiodinium* and their growth and host specificity. *J. Phycol.* **49**, 447-458.